Synthesis Design and Nuclear Medicine Applications For Radiometal, Beta and Gamma Emission, Chelated Complexes

---

A Dissertation

presented to

the Faculty of the Graduate School

at the University of Missouri-Columbia

In Partial Fulfillment

of the Requirements for the Degree

Doctor of Philosophy

---

by

Ashley N. Dame

Professor Silvia S. Jurisson, Dissertation Supervisor

May 2017

The undersigned, appointed by the dean of the Graduate School, have examined the dissertation entitled:

Synthesis Design and Nuclear Medicine Applications For Radio-metal, Beta and Gamma Emission, Chelated Complexes

presented by Ashley Nichole Dame,
a candidate for the degree of doctor of philosophy of chemistry,
and hereby certify that, in their opinion, it is worthy of acceptance.

_____
Professor Silvia S. Jurisson

_____
Professor Timothy J. Hoffman

_____
Professor Carol A. Deakyne

_____
Professor Heather M. Hennkens

ACKNOWLEDGMENTS

I would like to thank the NSF EPSCoR Track II award (IIA-1430428) for funding as well as the Department of Chemistry.

To my research advisor, you have pushed me in so many ways. Dr. Jurisson, is someone who is very confident in her skills as a mentor, and passes on knowledge for any student who is eager to take it. She doesn't hover over students, but let's us come to her when we have issues. She brings a professionalism to academics that can only come from years of experience and patience. I want to thank her for taking a chance on me. I have had my lazy days, I have hated synthesis, and I have cursed every machine in the lab. She has never once scoffed, and has taken the time to work with me until projects become bearable again. I am fortunate to have had her as my mentor and I hope with whatever new I face endeavors, we stay in touch.

To the mentors who helped me along the way, thank you. From research at the VA and animals studies with Dr. Hoffman and Tammy Rold, I got to experience another side of research. One that is a bit more structured than that in pure academic settings. I also was probed to think more about why we are doing the work we are doing. Taking a look at the bigger picture is something all scientists need to remember to do to be successful, not just when it's time to write a grant. Thank you to Dr. Galazzi and Dr. Wycoff for helping me sort through spectra and running instrumentation as well as you do. Lastly, in this portion, thank you Dr. Barnes (aka Grand High Poohbah) for not getting frustrated when my crystals weren't stellar. You taught me how to gently smooth out my data, and we have had our share of interesting meetings.

Now on to the people who have had to put up with me for more than my grad school years, and know how I really felt….

To my dad, you raised a little girl who grew up believing she could be anything she wanted. You let me get messy, and from that I was able to figure out the best way for me to learn was by doing it myself. If you ever wondered the reason I have never settled for less than the best, it's mostly because of you. I also gained the ability to approach people with a calm, collected way. A skill that has carried me this far, and earned me a favor because I can carry my own conversation in a field of study that gets awkward pretty quick. I know that if ever I need you, you will always be there for me. There are days I wish I could see the person I have become through your eyes so I would know that I really have come further than I think. There are only a few good people left in the world, and I am glad that I have one of them as my father.

To my mom, you set the example for being a smart and amazing woman. Having you for a mother, I knew I would have a lot to live up to. You pushed me hard, expected greatness from me, and I hope that I have made you proud. You work so hard, but you always try put your children first. Even in times where we have faltered, you never stopped showing love. I have your quick mouth (blessing and curse depending who you ask) and they say children get their brain from their mother, so I lucked out there. You are my best friend, and I don't think I would have made it this far without your gentle guidance. I could never replace you in a million years, nor would I try. I love you.

To my little brother, you are the freaking light of my life! We have not always seen eye to eye, but we have never not loved each other. I can't think of a brother and sister who are closer than we are. From the second you were a speck of a thought, I have loved you. No matter how frustrated I am, I always will. You believe in me, and I wish you would believe more in yourself. I'll never stop pushing you for greater things, and you'll never stop telling me I'm better than I think I am. No matter where life takes us, we always have each other.

To my best friends, HOLY CRAP! You all made it with me through graduate school. Congratulations to you, as I am well aware that I have not always been the calm collected person most of the population sees. Scott, we've been friends since day one of undergraduate. How you put up with me is a mystery. It's probably answered the same way I put up with you: sheer determination, love, and maybe a beer or two. Jim, you have stood by my side through the last couple of years and been a saving grace to have. I have had moments of being a complete mess and you have stuck it out, right next to me. I appreciate that more than you know. Mia, you are amazing. I want to put you in my pocket and take you with me on all my adventures. Our early days together, were no less adventurous than our later days. You have the ability to go out and make big things happen. If you ever don't have five million percent confidence in yourself to go out and shank the world's spleen, just call me. I will always tell you how awesome you really are. The friendship I have with you and Ali has made this process one of the biggest the reason I have stuck this one. I seriously would have quit fifty times, but with your help, all three musketeers are now doctors. Alison, my sister from another mister with the best hubby I could ever witness to, I love you. We instantly became best friends when we jumped on the ship of joining the same research group. That was quiet the interesting boat ride, to say the least. Then, knock knock, you were my neighbor and we spent about every weekend in sweatpants, yelling at the food network like we knew better than the professional cooks (we did most of the time). You have not just become my best friend over the last several years, you have become family. You are forced to all the holidays and you fit right in with the rowdy bunch I have. If I could give you anything, it would be to look in the future. Everyone knows you are going to do all these great and amazing things, you just have to wait. I mean, look where we were seven years ago? You've already stomped the people who doubted you, and I could not be more proud to be along for the

ride. If you were a friend or an acquaintance and we shared good times together, I thank you as well.

To the people who just didn't make it to the final stretch of this chapter, you gave me the love and drive to keep pushing myself. To my grandparents and greats who all played a part in shaping the woman I am today, I wish that whatever the next life brings me, I have you back by my side.

Thank you for a wonderful time here at the University of Missouri-Columbia. I will take these memories with me as I continue on to the next phase. I leave you with some lyrics that are a bit close to my heart, as they are the lyrics I heard so many times as I climbed in the vehicle with my grandpa on to the next stop.

"On the road again, just can't wait to get on the road again. The life I love is making music with my friends, and I can't wait to get on the road again. On the road again, goin' places that I've never been. Seein' things that I may never see again, and I can't wait to get on the road again." –Willie Nelson

TABLE OF CONTENTS

LIST OF FIGURES

Chapter 1:

Chapter 2:

Chapter 3:

Chapter 4:

Chapter 5:

TABLES AND SCHEMES

Chapter 2:

Chapter 3:

Chapter 4:

ACRRONYMS (alphabetically)

BBN- bombesin

$CHCl_3$- chloroform

DCM- dicholormethane

DIPEA- di-isoproplyethyl amine

EtOAc- ethyl acetate

EtOH- ethanol

GAS- 56.4 mM sodium glucoheptonate, 0.25 M HCl, 3.7 mM $SnCl_2$ solution (glucoheptonoate, acid, tin)

GRP- gastrin releasing peptide

H_2O- water

HBTU- *N,N,N′,N′*-tetramethyl-*O*-(1*H*-benzotriazol-1-yl)uronium hexafluorophosphate

HEDP- 1-hydroxy-ethylidene-1,1 diphosphonic acid

HPLC- high performance liquid chromatography

KBr- potassium bromide

MeCN- acetonitrile

MeOH- methanol

NaOH- sodium hydroxide

PBS- phosphate buffered saline

RB- round bottom

RT- room temperature

SPECT- Single-photon emission computed tomography

TAT- transactivator of transcription

TES- triethylsilane

TFA- trifluoroacetic acid

THF- tetrahydrofuran

TLC- thin layer chromatography

ACADEMIC ABSTRACT

Nuclear medicine covers a wide variety of radionuclides to meet demands of disease. In the current study, first we have looked at the application of mono-amine mono-amide ligands for Re(V), ^{99m}Tc(V), and ^{186}Re(V) with respect to bombesin for receptor targeting in the pancreas. While procedures for synthesizing ^{99m}Tc complexes is similar to other reported procedures, rhenium complexes were synthesized using $[ReO(citrate)_2]^-$ as the starting material, simplifying purification and isolation. Further studies for the 222-MAMA-BBN complex set included biodistribution studies, which determined that the ^{99m}Tc-BBN complex binds to GRP receptors in the pancreas, ~3% ID/g. The 323-MAMA complex and derivatives were investigated to determine if the 222- or the 323-MAMA backbone provide: an easier preparation, a better framework for chelating given metals, and better transport as a targeting receptor. It is found that, in comparative studies, the 222-MAMA derivates are more preferred in chelation. However, in either case, once the metal is chelated, there is no conversion of products upon the addition of a more preferred ligand system.

Another avenue of target therapy being pursued is the study of ^{105}Rh. We are specifically looking at the study of chelation with tetrathioether complexes, to rhodium(III) to translate to the radiotracer scale. Three product isomers are formed in the reaction of rhodium, using $SnCl_2$, with 222-S_4-diAcOH. The carboxylate arm can either be free dangling, one bound to the metal, or both (removing bound chlorides respectively); all of these isomers can be easily separated using HPLC. These three species will be avoided when translated to the ligand bombesin analog. Future research in this area will be done with the ^{105}Rh radiotracer for biological applications.

Chapter 1: Introduction to Radiopharmaceutical Chemistry: Diagnostic and Theranostic Tool Overviews

With the development of every drug comes a new problem, whether that be in a disease building resistance, or with a specific type of disease target becoming dated. As technology has grown, we have a better understanding of how the body reacts and the mechanics of how drugs are interacting within the body. The search for less harsh and more potent ways of discovering and treating body defects is a long road; specifically, looking at ways to detect and treat cancer is a billion dollar industry.[1] While numerous ways to treat cancer have been evaluated over the last 50 years, there are a few that predominate currently in practice. The most common treatments for aggressive cancers, such as breast, Non-Hodgkin's lymphoma and colorectal cancer, are chemotherapy and surgical removal, when applicable. [2] Issues associated with chemotherapy include a host of adverse side effects: anemia, vomiting, resistance to treatment, infertility, depletion of healthy cells, etc.[2]

Methods of treating cancer at earlier stages, thus increasing long term survival, is the overall goal in creating new agents. A more developed method at a targeted approach to cancer treatment has been the use of radioisotopes in a category known as radiopharmaceuticals. This broad scope of compounds covers radionuclides specifically for therapy, but also those that are very useful in imaging tumors and progression of cancers. One of the most frequently used radionuclides has been for therapy of thyroid cancer via ^{131}I, as the thyroid takes up iodine to produce hormones. [3] Other examples of radiotherapy that have been explored use chemical mimics that tumor sites take up such as $^{32}PO_4^-$ targeting ovarian cancer [4] and $^{89}Sr^{2+}$, which mimics Ca^{2+} and is used to treat bone pain.[5] These are considered as direct approaches to targeting, where the intended target takes up a given radioisotope based on chemical properties or

properties the isotope mimics. This can be performed by creating chemical equivalents of nutrients (as in the case with $^{89}Sr^{2+}$) or peptides that bind to a tumor, and are incorporated with a radionuclide. An example would be something such as ^{18}F-fluorodeoyglucose (^{18}F-FDG), which has been radiolabeled with ^{18}F and mimics glucose. [6] The more indirect approach uses targeting vectors, such as antibodies and peptides, bound to a bifunctional chelate containing a given radionuclide. The bifunctional chelate serves to provide stabile coordination between the radionuclide and the target vector. Most of the research with indirect tumor receptor targeting has been through the use of radiometals, such as ^{177}Lu, ^{99m}Tc, $^{186/188}$Re, ^{225}Ac, ^{64}Cu, ^{68}Ga. [7] The bifunctional chelate method for radiolabeling is a very developed, but ever growing area of study. Current research efforts are attempting to find more stable chelates for various metals. Once the chelate is identified, it is conjugated or linked to a targeting vector; this could be a peptide, antibody, or a direct delivery method, Figure 1-1. This provides for the incorporation of a given radionuclide and affinity toward targeting vector of interest. An understanding of how the targeting vector can be manipulated or the types of complexes that can bind to receptors is key in synthesizing complexes with high tumor receptor uptake. Potential complexes are screened for criteria such as charge, capacity size, and denticity. The radionuclide needs to stay bound to the chelate to avoid dose to non-target tissue or organs.[8] This has been accomplished by using multidentate chelates to increase stability of complexation. Multidentate ligands are those that bind at varied angles and occupy multiple coordination sites of a given metal. [9] Diethylenetriaminepentaacetic acid (DTPA) and 1,4,7,10-tetraazacyclododecanetetraacetic acid (DOTA), Figure 1-2, are examples of two commonly used multidentate chelates for several radiometals such as the radiolanthanides. Derivatives of these two chelates have been used as well.[10,11,12]

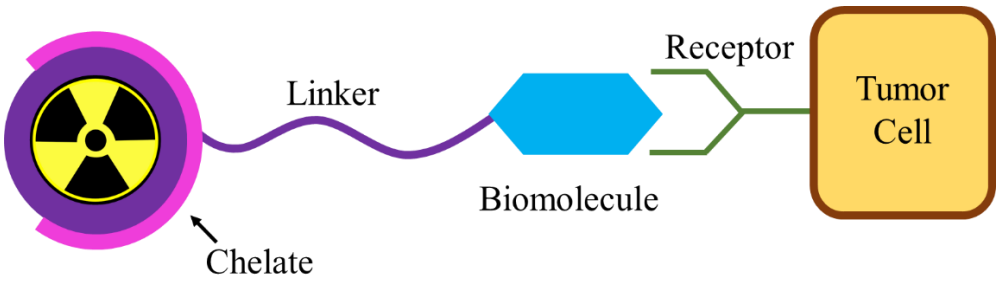

Figure 1-1. The bifunctional chelate approach uses a radiometal bound to a targeting vector via a linker and ligand framework that targets over expressed receptors on the tumor cells' surface.

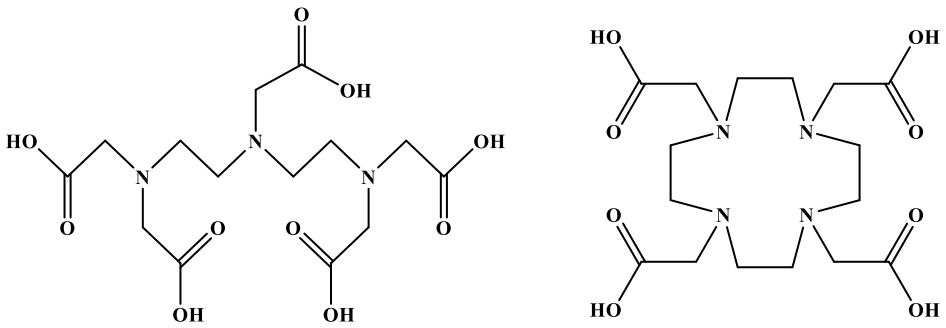

Figure 1-2. Structure representations of (a) DTPA and (b) DOTA

Radiopharmaceuticals can be separated into two area, namely: diagnostics and therapeutics. This distinction allows for the proper choice of radionuclide for each specific application. Modes of decay (α, β, γ, Auger e^-), half-life, chemical production, etc., must all be taken into consideration when looking into choices of proper radionuclide as well. For diagnostic imaging both gamma emitting and positron emission radionuclides are useful. For consideration of therapy, alpha, beta, and Auger electron emitting particles are of use. Currently the majority of radiopharmaceuticals are used for imaging purposes with about 95% used for

diagnostics and 5% for therapy purposes.[13] For theranostic use, radionuclides would be best suited with high specific activity, low abundance gamma emission (for dual purpose imaging if needed), and a short half-life decay to a stable isotope (to allow for clearance and eliminate radio recoil). It is also beneficial to compare the energy of a given nuclide with that of the tumor size and makeup (solid or more fluid) to choose the radionuclide with minimal effect to healthy tissue. Energy consideration needs to be adjusted with how the tumor takes up the radionuclide, whether it is via surface binding or internalization within a tumor. Consideration of these parameters would decrease the damage to nearby tissue.

A useful tool with radiomedicine is the ability to study or use "matched pair" isotopes. Matched pair isotopes are two radioisotopes that can be interchanged based on same or similar chemical properties in order to image or treat, depending on the intended purpose. Generally one radionuclide has the function of diagnostics and the other for therapy. Some matched pair isotopes include: ^{124}I/^{131}I, ^{86}Y/^{90}Y, ^{99m}Tc/$^{186/188}$Re, ^{72}As/^{77}As. ^{99m}Tc and $^{186/188}$Re are considered a matched pair, due to very similar chemical characteristics. [14] For example, Kim studies the duality of ^{99m}Tc and ^{188}Re for binding to folate receptors that are believed to be overexpressed in epithelia tumors. [15]

A large amount of research has been pursued with ^{99m}Tc, as it is one of the most readily available radioisotopes due to the use of the ^{99}Mo/^{99m}Tc generator. With a gamma energy of 140.5 keV, and a moderately short half-life (6.01 h) ^{99m}Tc is useful for Single-photon emission computed tomography (SPECT) imaging.[16] Various radiopharmaceuticals have been designed to chelate ^{99m}Tc for *in vivo* imaging, with FDA examples including Neurolite® (stroke detection), Ceretec™ (stroke detection), Myoview® (heart stress), ^{99m}Tc-MAG3™ (renal imaging), **Figure 1-3**.[17a-c] $^{186/188}$Re is available in both high and low specific activity, but

availability of isotopes poses the greatest hurdle to research (more specifically ^{186}Re). With a longer half-life (^{186}Re= 3.7 d, ^{188}Re= 17 h) ^{186}Rhenium is suited for radiolabeling antibodies or other longer circulating biomolecules that take much longer to accumulate at specific receptors.[18,19] ^{188}Re is available from a ^{188}W generator [20], while ^{186}Re is produced via cyclotron or reactor. [21a,b]

There are differences in chemistry between technetium and rhenium, namely redox chemistry and substitution kinetics. Reduction of rhenium is much more difficult, and oxidation occurs more easily than for technetium, meaning suitable complexes to chelate rhenium are needed in order to keep rhenium at the desired oxidation state. There are reports of Re(III) and Re(I) complexes investigated for therapeutic potential by investigators.[22,23] Rhenium does have stable non-radioactive isotopes unlike technetium, that aides in translational work. Some of the more recent work with rhenium includes: bisaminodithiols (BAT), monoamine-monoamide dithiols (MAMA), and diamide-dithiols (DADT) have all been shown to successfully chelate the oxorhenium(V) core and are used as chelators in potential radiopharmaceuticals that utilize Re(V), **Figure 1-4**.[22]

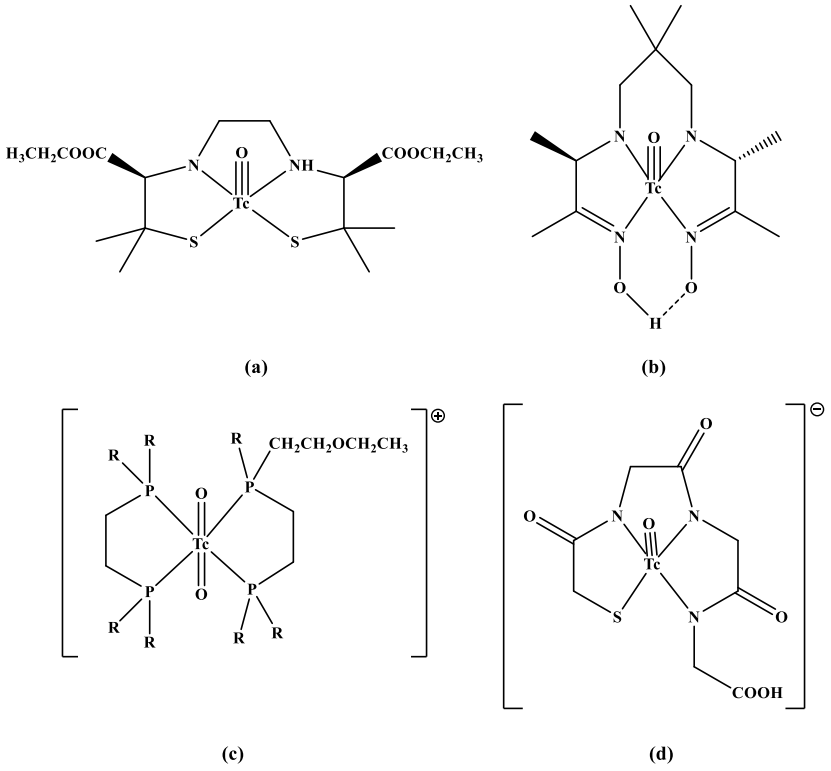

Figure 1-3. Examples of ^{99m}Tc FDA approved agents: a) Neurolite®, b) Ceretec™, c) Myoview®, d) ^{99m}Tc-MAG3™

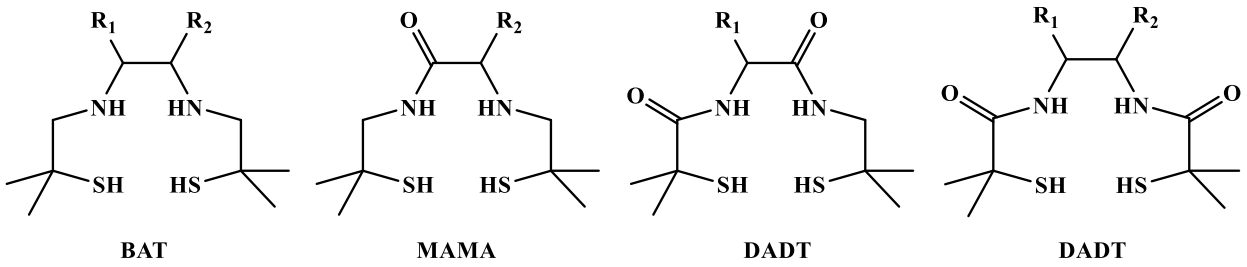

Figure 1-4. Possible chelator frameworks for rhenium(V).

Another radionuclide of interest is ^{105}Rh, which is useful for therapeutic purposes with a β^- emission, as well as a dual use of diagnostics with a low energy gamma emission. Rh(III), one

of the most commonly used oxidation states has an inert kinetic reactivity, making *in vivo* studies promising without the risk of redox chemistry. This is a unique feature over radionuclides such as ^{186}Re(V), which is prone to oxidation state changes in vivo if not properly chelated as previously mentioned. Macrocyclic ligand frameworks have been studied for Rh(III) bifunctional chelates methods of targeting. First in depth studies were by Troutner et al. in the late 1980's for radiotherapeutic purposes.[24] Troutner reported ^{nat}Rh(III) and ^{105}Rh oxime complexes in order to understand the octahedral binding of non-radioactive complexes before translating to the radioactive ^{105}Rh bidentate oximes to study dinging to human γ-globulin.[24] Radioisotopic complexes are limited in analysis to understand the chemistry of complexes, thus having a non-radioactive analog allows scientists to dealve deeper into understanding the coordination of the types of binding that work best for given metals. The half-life of ^{105}Rh is 36 h, with a 566 keV β^-_{max}, which is promising for future research with small solid tumors.[25] Several potential bifunctional chelates have been reported for analysis with ^{105}Rh and include a wide range of open, tetradentate frameworks with N, O, P, and S donor atoms[26a-e]; Rh(III), being a late d-block, soft metal, prefers to bind with soft donor atoms such as sulfur.

Two main areas of research that will be covered in this dissertation are: the bifunctional chelate approach of monoamine-monoamide frameworks with Re(V), ^{99m}Tc(V), and ^{186}Re(V), and the preliminary comparison investigation of tetrathioether frameworks to be applied to ^{105}Rh tracer studies. Both topics discussed share application to radiopharmaceutical research for future application to in vivo studies of GRP receptor binding in the prostate and pancreas, however both require separation based on radionuclide properties and characteristics of frameworks. Each chapter will go into further depth about the given radionuclide, mode of chelation, and application to other relevant research currently ongoing.

Chapter 2: Rhenium(V) and ^{99m}Technetium(V) complexes with 222-N_2S_2 MAMA ligands for bifunctional chelator agents: Syntheses and preliminary in vivo evaluation[1]

Introduction

Designing complexes that can perform both theranostic and diagnostic duties is a goal radiochemists and, in a broader picture, health scientists, aspire to accomplish. Radionuclides have the ability to contribute to this area of study, especially with respect to matched pairs. Matched pairs refers to radio isotopes that have chemically interchangeable properties. Some of the radionuclides that have been studied as potential matched pairs include $^{123/131}$I, $^{86/90}$Y[1], $^{149/152/155/161}$Tb[2,3], and for the current study ^{186}Re and ^{99m}Tc. Several examples of technetium complexes used as imaging agents in routine use include Cardiolite® (coronary artery disease), ^{99m}TcMAG3™ (renal imaging), and Ceretec™ (stroke detection) (**Figure 2-1)**. Many of these agents have been developed as kit formulations, where all the components are contained within one kits to be combined and administered to a given patient.[4] Rhenium, for this study specifically ^{186}Re, has the benefit of not only having an accessible radionuclide, with both high and low specific activity, but also a natural, non-radioactive isotope that can be easily manipulated. ^{186}Re is useful as a β^- emitting radionuclide for theranostic purposes with a penetrating tissue depth around 4.5 mm, making β^- radionuclides useful for studies with large tumors. With a half-life of 90 h, ^{186}Re-HEDP has shown promise for use in bone pain palliation.[5] Working with reactions on the macroscopic scale before working with radionuclides, allows for reactions to be better developed

[1] Dustin Wayne Demoin, Ashley N. Dame, *et* al., Monooxorhenium(V) complexes with 222-N_2S_2 MAMA ligands for bifunctional chelator agents: Syntheses and preliminary *in vivo* evaluation, Nuclear Medicine and Biology, 2016, *43*, 802-811.

and non-radioactive analogs are accessible for more institutions. The macroscopic synthesis provides the framework that can later be translated to the radiotracer scale. Technetium does have a longer lived, accessible radioisotope (^{99}Tc); however, research with the long-lived radionuclide ($t_{1/2}$= 2.11x10^5 y) has regulatory hurdles; ^{99}Tc is produced in ~6% fission yield from ^{235}U and ^{239}Pu. ^{99m}Tc ($t_{1/2}$= 6.01 h) is used in medically related studies, due to the availability of the ^{99}Mo/^{99m}Tc generator. Technetium-99m, the daughter of ^{99}Mo, is the most commonly used medical radioisotope globally. ^{99}Mo generators, which were brought into production for medical application in the 1960's, must generally be made on a weekly basis to give high specific activity ^{99m}Tc used for medical application.[6] It is estimated that over nine million medical procedures each year in the U.S. rely on ^{99m}Tc. This roughly accounts for, on average, 70% of all nuclear medicine procedures.[7] Most ^{99}Mo ($t_{1/2}$=65.98 h) is produced in reactors by the irradiation of targets containing enriched uranium and is separated in hot cells.[8] When looking at the chemistry of technetium and rhenium, there are chemical variances between the two metals. An example of this is the redox chemistry of both elements. Rhenium is much more difficult to reduce and is much more readily oxidized than technetium, which makes stability of rhenium complexes *in vivo* more problematic and chelates containing more reducing donors are required, such as thiols and/or phosphines. Greater amounts of reducing agent are also required in solution to inhibit oxidation of rhenium to perrhenate. One also has to put in place a free radical scavenger, such as gentisic or abscorbic acid, for rhenium complexes to prevent radiolysis from ionizing radiation cause by beta decay; however, many scientists still consider Tc/Re a matched pair.[9] Both technetium and rhenium have a wide range of oxidation states, and this research has chosen to focus on rhenium(V) and technetium(V) for their accessibility from perrhenate and pertechnetate. From an availability stand point, access to these materials in the 7+ oxidation state is easily obtained as starting

materials from chemical distributors (ReO_4^- salts) and reducing these to the 5+ oxidation state is readily achieved, and much easier to maintain than lower oxidation states.

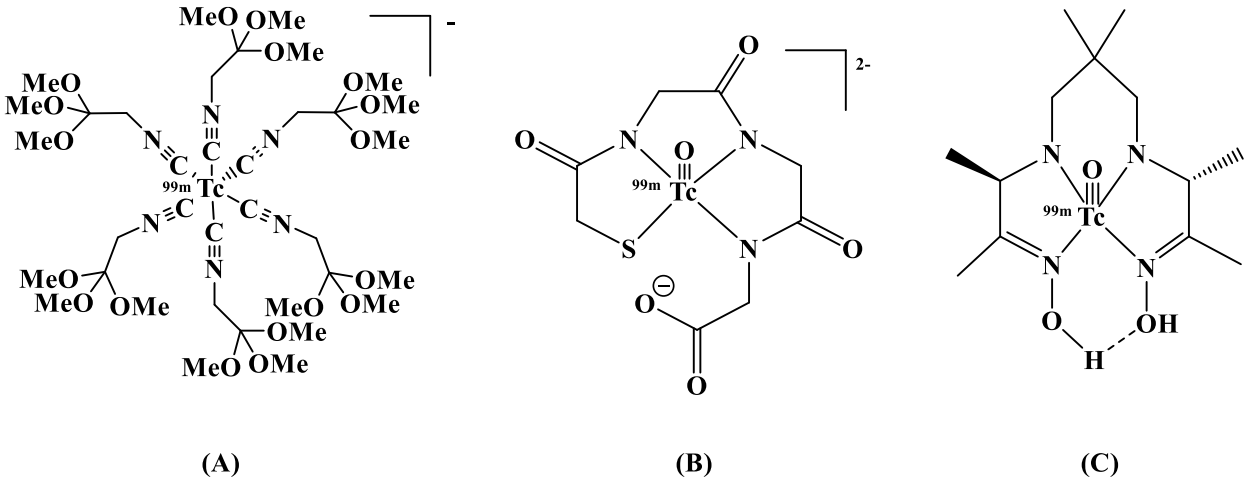

Figure 2-1. Schematics of (A) Cardiolite®, (B) ^{99m}TcMAG3™, and (C) Ceretec™

The ligand framework developed in these studies is based on dithiol anchors. A number of N_xS_{4-x} ligand systems have been reported for Tc(V) and Re(V) [10,11,12], with the N_2S_2-based monoamine-monoamide dithiol (MAMA) chelators of particular interest since the single amine allows for conjugation of a single targeting vector.[13,14] The 222 in the naming system used in reference to the complexes in this chapter are in relation to the number of carbon linkers between coordinating atoms (N_2S_2) to the metal center, or the ethylene bridges between coordinating atoms in this case. Kung et al. compared the 222-MAMA ligands for chelating oxotechnetium(V) with the bis(aminoethanethiol) (BAT) ligands and showed that the 222-MAMA chelators were more stable over time, **Figure 2-2**. The MAMA-based complexes were found to be more hydrophilic than their BAT analogues.[16] Computational studies performed by Demoin concur with synthetic results shown by Kung, with the thermodynamic stability of 222-MAMA chelate complexes

greater than that of BAT ligand frameworks.[16][22] This result is especially important when determining modes of delivery in biological systems. Subsequently, studies have demonstrated *N*-alkylated 222-MAMA derivatives complexed with monooxotechnetium(V) or monooxorhenium(V) to be stable under biological conditions.[17a-b] ^{188}Re-succinimidyl-3,6-diaza-5-oxo-3-[2-(triphenylmethyl)thio)ethyl]-8-[(triphenylmethyl)thio]octanoate (SOCTA)–trastuzumab, a N_2S_2 chelating framework, has been synthesized by Luo et al with significant tumor uptake ratio in the study of antibody bifunctional chelates for breast cancer treatments, with 7.28 ± 1.19 %ID/g at 48 h.[18]

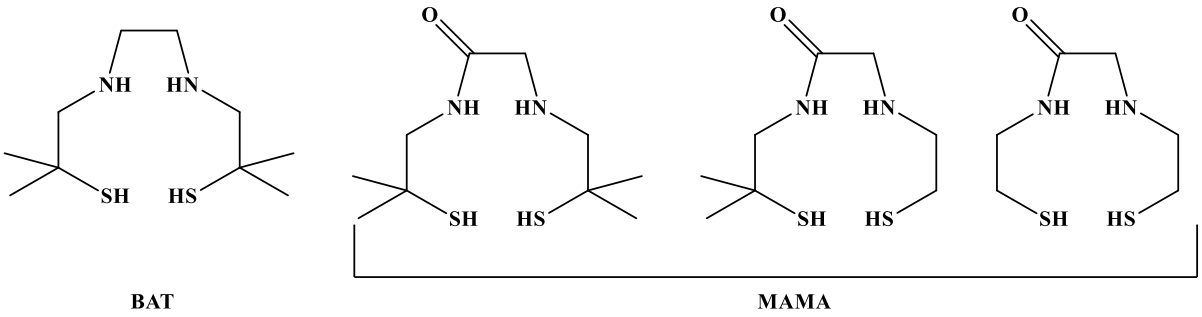

Figure 2-2. BAT and MAMA complexes used in competition studies by Kung et al.[20]

The 222-MAMA-based bifunctional chelating agents were evaluated for forming stable ^{99m}Tc and ^{186}Re complexes for targeted peptide-based nuclear imaging and therapy agents, using the seventh through fourteenth amino acids (BBN[7-14]$COONH_2$) of the bombesin peptide sequence as a potential bombesin receptor (BB2r) targeting vector.[19] Bombesin containing complexes have been investigated for their affinity to target the gastrin releasing peptide receptor (GRP). GRP receptors regulate numerous functions of the gastrointestinal and central nervous systems and have been shown to play a role in the formation of cancers such as lung, colon, and prostate.[20] The BBN(7-14)$COONH_2$ sequence, coupled to a variety of bifunctional chelating

agents has been shown to specifically target the BB2r both *in vitro* and *in vivo*, which is related to the GRP receptor.[21a-d] Thus further investigation was pursued to study the 222-MAMA bifunctional chelate as a primary framework choice in the *in vivo* receptor binding of $^{186}ReO(N_2S_2)$BBN[7-14]$COONH_2$ for translation to targeting prostate cancer cells.

Previous studies performed by Demoin initially found, according to cysteine studies, that ^{99m}TcO-222-MAMA-BBN[7-14]$COONH_2$ remained 92 ± 5 % intact at 1 h in 1 mM cysteine in phosphate buffered saline (PBS), and approximately 48 ± 7 % of the original complexed material was still intact at 24h.[16] Prior literature reports of ^{99m}Tc(V), without a bombesin targeting vector chelated, reported 70 ± 4% of ^{99m}TcO-222-MAMA complex was still intact after incubation in rat serum at 37 °C for 30 min[22] and 87.1 % of ^{99m}TcO-222-MAMAhexacid (^{99m}Tc-222-MAMAhexanote) remained intact after 1 h in 10 μM cysteine in 0.05 M phosphate buffer (pH 7.0) at 37 °C.[23] When biodistribution studies were performed by Demoin to study the receptor binding using ^{99m}TcO-222-MAMA-BBN[7-14]$COONH_2$, almost no uptake in the pancreas was observed. This was contradictory to results of *in vitro* cell binding studies using the Re(V) 222-MAMA-BBN[7-14]$COONH_2$ analog.[14] With modification, herein, the synthesis results of 222-MAMA chelated ligands with rhenium and technetium, as well as the *in vivo* results of ^{99m}TcO-222-MAMA-BBN[7-14]$COONH_2$ are repeated and improved.

Experimental

Methods

All chemicals, unless otherwise indicated, were commercially available and used without further purification. Technetium-99m pertechnetate was available from saline elution of a ^{99}Mo/^{99m}Tc generator (Mallinckrodt Medical, St. Louis, MO). No-carrier added ^{186}Re was produced at the Los Alamos National Laboratory Isotope Production Facility (LANL-IPF) using an encapsulated target

of enriched $^{186}WO_3$ Powder (99.9%; Isoflex USA) in a 40 MeV incident proton beam. The ^{186}Re was recovered as previously reported with a slight modification [16]: the anion exchange column was eluted with 8 M HNO_3 (2 x 50 mL) for $^{186}ReO_4^-$ desorption. The nitric acid was removed by evaporation and the residue reconstituted in 0.1 M HCl. The specific activity was determined to be 790 ± 90 TBq/g (21 ± 2 kCi/g).[24,25] Trityl protected 222-MAMA was synthesized using prior reported methods. CF-1 mice were obtained from Charles River Labratories. NMR studies were performed with a Bruker DRX 300 or 500 MHz Spectrometer (as noted). HPLC analysis was performed with a Shimadzu HPLC system outfitted with both UV-vis and radioisotope detectors. HPLC columns included either a Betabasic-18 column (Thermo Scientific, Waltham, MA, 150 mm × 4.6 mm, 5 μm) or a Jupiter C-18 column (Phenomenex, Torrance, CA, 250 mm × 4.60 mm, 5 μm, 300 Å pore size). All HPLC mobile phases used acetonitrile (MeCN) in water with 0.1% trifluoroacetic acid (TFA); the specific conditions (i.e., column, gradient, flow rate) are indicated below for purifications and analyses. Radio-TLC strips (Saturation pads, Analtech, Newark, DE) were counted using a Bioscan 200 Imaging Scanner (gas ionization detector), or by cutting the TLC strips and counting them in a NaI(Tl) well detector (Harshaw Chemical Company, Serial Number EX-53, with Ortec electronics and a Canberra high-voltage supply) or a Tri-Carb 2900TR Liquid Scintillation Analyzer (PerkinElmer, Waltham, MA). A Beckman Coulter HPLC system in series with an ion trap mass analyzer (a LCQ FLEET instrument, Thermo Fisher Scientific, with positive ion ionization) was used to obtain LC/ESI-MS results (Betabasic-18, 10-50% MeCN over 30 min, 1 mL/min). MS analysis was performed using the XCalibur software (Thermo Fisher Scientific). A Thermo Nicolet AEM FT-IR instrument was used for IR analysis (KBr pellets). UV-Vis analysis was performed with an OceanOptics USB2000 USB-ISS-UV/VIS spectrometer. All elemental analyses were performed by Atlantic Microlabs, Inc (Norcross, GA). Complexes 2-

(tritylthio)ethylamine hydrochloride (**222-precursor**), and N-(2-(tritylthio)ethyl)-2-((2-tritylthio)ethyl)amino)acetamide (**222-MAMA**), **Figure 2-3**, were synthesized and characterized according to previous reports.[16]

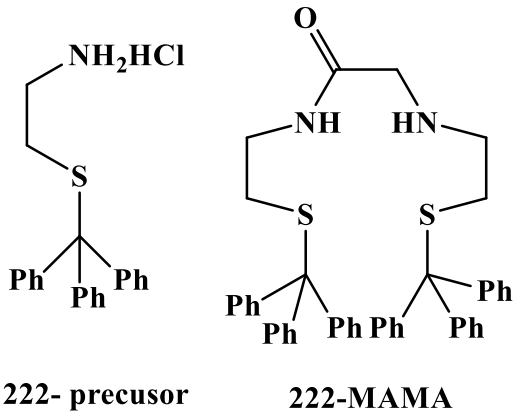

Figure 2-3. Schematic of ligands **222-precurson** and **222-MAMA.**

Synthesis

Ethyl 6-((2-oxo-2-((2-(tritylthio)ethyl)amino)ethyl)(2-(tritylthio)ethyl)amino)hexanoate [222-MAMAhexanoate]. To a scintillation vial equipped with a stir bar, **222-MAMA** (1.01 g, 1.49 mmol) was dissolved in anhydrous MeCN (2 mL; dried over molecular sieves). Diisopropylethylamine (0.25 g, 1.93 mmol) in MeCN (3 mL) was added, followed by slow addition of ethyl-6-bromohexanoate (0.43 g, 4.67 mmol) in 3 mL of MeCN. The reaction mixture was placed in an oil bath and refluxed at 85 °C under N_2 gas, and allowed to react for 24 h. The reaction vessel was brought to room temperature before removal of solvent *in vacuo*. EtOAc (5 mL) was added to the residue, and undissolved particulates were removed by filtration. The volume was reduced by half and 0.5 mL of hexanes was added. The crude product was purified on

a silica gel column (10 g, 1.3 cm diameter) that had been pre-conditioned with 15% EtOAc in hexanes. The column was eluted with 30% EtOAc in hexanes (100 mL) followed by 50% EtOAc in hexanes (200 ml). Fractions (5 mL) were collected and analyzed by TLC analysis (silica gel; 50% EtOAc in hexanes). Fractions showing a single species with Rf = 0.4 were combined, and dried under vacuum overnight to obtain 1.08 g (1.32 mmol, 88% yield) of **222-MAMAhexanoate**. ^{1}H-NMR (500 MHz, CDCl3, δ(ppm)): 1.16-1.36 (m, 7H, C**H**$_3$ & NCH$_2$C**H**$_2$C**H**$_2$), 1.53 (quintet, *J* = 7.6, 2H, C**H**$_2$CH$_2$COO), 2.18-2.28 (m, 6H, C**H**$_2$S, NC**H**$_2$, & C**H**$_2$COO), 2.33-2.41 (m, 4H, SC**H**$_2$ & RNC**H**$_2$), 2.83 (s, 2H, COC**H**$_2$N), 2.96-3.05 (m, 2H, C**H**$_2$NH), 4.07-4.15 (m, 2H, C**H**$_2$CH$_3$), 7.13- 7.32 (m, 18H, Ph), 7.34-7.50 (m, 12H, Ph). ^{13}C-NMR (500 MHz, CDCl3, δ(ppm)): 14.3 (**C**H$_3$), 24.7 (**C**H$_2$CH$_2$COO), 26.8 (NCH$_2$**C**H$_2$**C**H$_2$), 29.9 (**C**H$_2$S), 32.0 (S**C**H$_2$), 34.2 (k), 37.9 (**C**H$_2$NH), 53.8 (N**C**H$_2$), 54.6 (RN**C**H$_2$), 58.2 (CO**C**H$_2$), 60.2 (**C**H$_2$CH$_3$), 66.7 (**C**Ph$_3$), 126.7 (Ph), 127.9 (Ph), 129.5 (Ph), 144.7 (Ph), 171.2 (NH**C**O), 173.5 (**C**OOEt). ESI-MS (m/z): 821.10 (calc. 821.38 [$C_{52}H_{57}N_2O_3S_2^+$]). Anal. calcd for $C_{52}H_{56}N_2O_3S_2 \cdot 2HCl$: C, 69.86; H, 6.54; N, 3.13; S, 7.17. Found: C, 69.88; H, 6.84; N 3.22; S, 7.49.

6-((2-oxo-2-((2-(tritylthio)ethyl)amino)ethyl)(2-(tritylthio)ethyl)amino) hexanoic acid [222-MAMAhexacid]. 222-MAMAhexanoate (0.14 g, 0.17 mmol) was dissolved in 2 mL of tetrahydrofuran (THF) and another 1 mL of THF was used to complete the transfer to a 25 mL round-bottomed flask. Ethanol (3 mL) and 2 mL of a 3M NaOH solution were added to the dissolved **3**. The mixture was refluxed. TLC analysis on plastic-backed silica plates was run in 50:50 ethyl acetate:hexanes until no starting material spot remained visible, approximately 9 h. The solvent was removed by rotary evaporation and the product left under vacuum overnight. **222-MAMAhexacid** was purified on a silica column using pure $CHCl_3$ initially (approximately 200

mL, until TLC analysis showed no further spot under UV light) as the eluent and then eluting with 20% MeOH in $CHCl_3$ (approximately 100 mL, until TLC plate showed no further spot under UV light). The brown-colored fraction contained 0.10 g (0.13 mmol, 76.5% yield) of pure **222-MAMAhexacid**. ^{1}H-NMR (500 MHz, CDCl3, δ(ppm)): 1.18-1.27 (m, 2H, $NCH_2CH_2C\mathbf{H_2}$), 1.32 (tt, *J* = 7.4, 7.4 Hz, 2H, $NC\mathbf{H_2}CH_2$), 1.54 (q, *J* = 7.5 Hz, 2H, $C\mathbf{H_2}CH_2COO$), 2.20-2.29 (m, 6H, $C\mathbf{H_2}S$, $NC\mathbf{H_2}$, & $C\mathbf{H_2}COO$), 2.32-2.42 (m, 4H, $RNC\mathbf{H_2}$ & $SC\mathbf{H_2}$), 2.83 (s, 2H, $COC\mathbf{H_2}$), 3.00 (quartet, *J* = 6.3 Hz, 2H, $C\mathbf{H_2}NH$), 7.14-7.30 (m, 18H,Ph), 7.35-7.42 (m, 12H, Ph), 7.44 (t, *J* = 5.8 Hz, 1H, N**H**). ^{13}CNMR (500 MHz, CDCl3, δ(ppm)): 24.5 ($\mathbf{C}H_2CH_2COO$), 26.7 ($NCH_2CH_2\mathbf{C}H_2$), 26.7($NCH_2\mathbf{C}H_2$), 30.0 ($\mathbf{C}H_2S$), 32.0 ($S\mathbf{C}H_2$), 33.6 ($\mathbf{C}H_2COO$), 37.9 ($\mathbf{C}H_2NH$), 53.8 ($RN\mathbf{C}H_2$), 54.5 ($N\mathbf{C}H_2$), 58.2 ($CO\mathbf{C}H_2$), 66.7 ($\mathbf{C}Ph_3$), 126.7 (Ph), 127.9 (Ph), 129.5 (Ph), 144.7 (Ph), 171.3 (HN**C**O), 177.5 (**C**OOEt). HPLC ESI-MS (m/z, retention time 34.0 min, Betabasic-18 30-65% MeCN with 0.1% TFA over 30 min): 793.8 (calc. 793.35 [$C_{50}H_{53}N_2O_3S_2^+$]); ESI-MS (m/z): 791.38 (calc. 791.33 [$C_{50}H_{51}N_2O_3S_2^{-1}$]). Anal. Calcd for $C_{50}H_{52}N_2O_3S_2\cdot HCl\cdot H_2O$: C, 70.85; H, 6.54; N, 3.31; S, 7.57. Found: C, 70.86; H, 6.30; N 3.34; S, 7.53.

N^1-((5S,8S)-11-((1H-imidazol-4-yl)methyl)-5-carbamoyl-24-(1H-indol-3-yl)-8-isobutyl-20-isopropyl-17-methyl-7,10,13,16,19,22-hexaoxo-2-thia-6,9,12,15,18,21-hexaazatetracosan-23-yl)-2-(6-((2-mercaptoethyl)(2-((2-mercaptoethyl)amino)-2-oxoethyl)amino)hexanamido)pentanediamide [222-MAMA-BBN[7-14]$COONH_2$]. The peptide was synthesized in a model 396 multiple peptide synthesizer (AAPPTEC, Louisville, KY) on Sieber resin using standard, solid-phase, Fmoc protection strategy for linear elongation. Fmoc protected amino acids with protected side-chains (where appropriate) were used to synthesize the amino acid sequence -Gln-Trp-Ala-Val-Gly-His-Leu-Met-NH_2 [BBN(7–14)]. Coupling was

achieved by *in situ* activation with *N,N,N′,N′*-Tetramethyl-*O*-(1*H*-benzotriazol-1-yl)uronium hexafluorophosphate (HBTU) and di-isoproplyethyl amine (DIPEA) at every elongation step. **222-MAMAhexacid** was added as the final amino acid using these same conditions. The product was cleaved and side chains deprotected with 85% trifluoroacetic acid (TFA) and non-reducing scavengers (phenol/water/ triisopropylsilane, 5% each). The synthesis yielded 300 mg of impure **222-MAMA-BBN[7-14]COONH$_2$** (85% pure), which was HPLC purified (20–40% MeCN (0.1% TFA) in H_2O (0.1% TFA) over 40 min) resulting in 80 mg of **222-MAMA-BBN[7-14]COONH$_2$** in >98% purity. LC/ESI-MS (m/z, 10–50% MeCN over 30 min, 1 mL/min, Rt = 15.6 min): 1230.3 (calc. 1230.59 [$C_{55}H_{88}N_{15}O_{11}S_3^+$][M+ H^+]), 615.6 (calc. 615.80 [$C_{55}H_{89}N_{15}O_{11}S_3^{2+}$][M+ $2H^{2+}$]).

^{nat}ReO-222MAMA-6-Ahx-COOCH$_2$CH$_3$ [ReO-222MAMAhex]. Ammonium perrhenate (0.044 g, 0.16 mmol) and sodium citrate dihydrate (0.060 g, 0.20 mmol) were dissolved in 5 mL of DI water. Stannous tartrate (0.10 g, 0.37 mmol) was added and the reaction mixture was stirred at room temperature for 10 min to yield a blue solution. In a separate vial, **222-MAMAhexanoate** (0.050 g, 0.061 mmol) was deprotected in a trifluoroacetic acid (TFA) solution (95% TFA:5% TES(triethylsilane)) with stirring. Solvent residuals were removed with N_2 (g), washed with hexanes (6 × 10 mL), and rotary evaporated to dryness. The rhenium-citrate solution was added to the vial containing the deprotected **222-MAMAhexanoate** and the reaction was refluxed at 85 °C for 4 h. Sodium phosphate (pH 5) was added and the reaction was refluxed for another 4 h. The reaction mixture was cooled to room temperature, extracted with EtOAc (2 × 5 mL), the organic extracts were combined, dried over anhydrous Na_2SO_4 and rotary evaporated to dryness. Approximately 60% yield (0.2 g, 0.37 mmol) of solid **ReO-222MAMAhex** was obtained. HPLC: (Betabasic-18, 10–50% MeCN over 30 min, 1 mL/min) Rt = 30.2 min. LC/ESI-MS (m/z;

Betabasic-18, 10–50% MeCN over 30 min, 1 mL/min; Rt = 29.4 min): 537.3 (calc. 537.09, $[C_{14}H_{26}N_2O_4ReS_2^+][M+ H^+]$).

^{99m}TcO-222MAMA-6-Ahx-COOCH$_2$CH$_3$ [^{99m}TcO-222MAMAhex]. A GAS solution (56.4 mM sodium glucoheptonate, 0.25 M HCl, 3.7 mM $SnCl_2$ solution) was prepared. A mixture of **222-MAMAhexanoate** in ethanol (EtOH) (0.006 M, 0.3 mL), generator eluent (0.3 mL; 370 MBq (10 mCi)), and GAS (0.3 mL) was vortexed and allowed to react at 70°C for 40 min. The EtOH was removed from the reaction mixture under a stream of N_2 and the resultant mixture was extracted with EtOAc (3 × 2.0 mL). The organic layer was analyzed by radio-HPLC (Betabasic-18, 10–50% MeCN over 30 min, 1 mL/min; Rt = 30.4 min). Radiochemical purity: 82 ± 7%.

^{nat}ReO-222MAMA-6-Ahx-BBN(7-14)COONH$_2$ [ReO-222MAMABBN]. Ammounium perrhenate (2.69 mg, 10.04 μmol), sodium citrate dihydrate (5.91 mg, 20.1 μmol) and tin(II) tartrate (8.0 mg, 30.0 μmol) were added to 200 μL of DI water and sonicated for 15 min, or until the light blue color of Re-citrate had formed. **222-MAMA-BBN[7-14]COONH$_2$** (9.27 mg, 0.648 μmol), the $[ReO(citrate)_2]^-$ solution, and 100 μL MeCN were combined in a 1.5 mL snap cap centrifuge tube, and heated at 70°C for 1 h. The reaction mixture was centrifuged and the supernatant collected. The solids were washed with 50:50 MeCN:H_2O (500 μL), centrifuged, and the second supernatant combined with the first. The combined supernatants were filtered through a 0.45 μM filter, purified by HPLC (Betabasic-18, 10–50% MeCN over 30 min at 1 mL/min), and the 25 min product peak was collected. The product was rotary evaporated to dryness to yield **ReO-222MAMABBN** (10 mg; 90%). LC-ESI-MS (m/z; Betabasic-18, 10–50% MeCN over 30

min, 1 mL/min; Rt = 25.4 min): 1430.4 (calc. 1430.52 [$C_{55}H_{85}N_{15}O_{12}ReS_3^+$][M+ H^+]); 1452.5 (calc. 1452.5 [$C_{55}H_{84}N_{15}O_{12}ReS_3Na^+$])

^{99m}TcO-222MAMA-6-Ahx-BBN(7-14)COONH$_2$ [^{99m}TcO-222MAMABBN]. A GAS solution (56.4 mM sodium glucoheptonate, 0.25 M HCl, 3.7 mM $SnCl_2$ solution) was prepared. A mixture of **222-MAMA-BBN[7-14]COONH$_2$** in a 50:50 EtOH:H_2O solution (0.81 mM, 0.1 mL), 0.3 mL of generator $^{99m}TcO_4^{1-}$ eluent (0.925 GBq (25 mCi)), and 0.3 mL of the GAS solution was vortexed and reacted in a 70 °C water bath for 40 min. The product mixture was purified via a Waters Sep-Pak C-18 Plus Light cartridge, which had been pretreated with 10 mL of EtOH followed by 10 mL of H_2O. Three fractions were collected: the load volume, a 1 mL H_2O wash, and a 1 mL EtOH elution. The EtOH fraction contained ~0.21 GBq (5.7 mCi; 65.1% of the activity loaded). An aliquot of the concentrated **^{99m}TcO-222MAMABBN** sample (7–8 μCi) was added to sterile saline and checked for purity (Betabasic-18, 10–50% MeCN over 30 min, 1 mL/min, Rt = 21.6 and 24.3 min in a 1:4 ratio). Radiochemical yield: 53 ± 6%, pre-purification; radiochemical purity: 88 ± 3%, post purification.

***No carrier added (nca)* ^{186}ReO-222MAMA-6-Ahx-BBN(7-14)COONH$_2$ [^{186}ReO-222MAMABBN]. 222-MAMA-BBN[7-14]COONH$_2$** (0.2 mg, 0.1 μmol) in 100 μL of absolute ethanol, 7.4 MBq (0.2 mCi) of *nca* $^{186}ReO_4^{1-}$ and 0.1 mL of GAS solution (56.4 mM sodium glucoheptonate, 0.25 M HCl, 3.7 mM $SnCl_2$ solution) were combined, vortexed and heated in a sand bath at 80°C for 1 h. The reaction mixture was purified on a C-18 column (BondElut, Agilent Technologies, 0.5 in. × 0.5 in.) that had been pretreated with 5 mL of 50:50 MeCN:H_2O. The reaction mixture was loaded, washed with 3 mL of H_2O, and eluted with 5 mL of 50:50

MeCN:H_2O. HPLC (Jupiter C-18 column, at 25 °C with a gradient of 10–70% MeCN with 0.1% TFA in water with 0.1% TFA over 15 min) retention time: 13.1 min, analogous to the macroscopic **ReO-222MAMABBN** standard, indicated formation of **^{186}ReO-222MAMABBN**.

Pharmacokinetic studies in CF-1 mice. All animal experiments were conducted in accordance with protocols approved by the Harry S. Truman Memorial Veteran's Administration Hospital Subcommittee for Animal Studies. Normal mice (CF-1; 8 weeks old; Charles Rivers Laboratories; Wilmington, MA) were injected via the tail vein with approximately 0.37 MBq (10 μCi) of the radiolabeled material in approximately 100 μL of sterile phosphate buffered saline (PBS). The mice were sacrificed at 1 h (eight mice, four with $^{99m}TcO_4^{1-}$ and four with **^{99m}TcO-222MAMABBN**) post injection. The organs and tissues were isolated, weighed, counted using a NaI(Tl) well counter, and the percent injected dose (% ID) and percent injected dose per gram (% ID/g) of each were calculated. The entire blood mass was estimated to be 6.5% of the total body weight. All urinary bladder contents excreted from the time of injection to the time of sacrifice were collected, counted, and reported as urine (% ID).

Results and Discussion

Objectives

The primary objective in this study was determine **222-MAMA-BBN[7-14]COONH$_2$** was suitable for *in vivo* studies when bound to ^{99m}Tc(V), and more importantly Re(V). The focus was to create translational analogs for ^{186}Re, that could later be studied as therapeutic agents. Monoamine-monoamide complexes have previously been studied throughout the literature and have shown promise when conjugated to peptides for receptor targeting, as previously

stated.[13,14,18] With literature precedence for complexation, Re(V), ^{99m}Tc(V), and ^{186}Re(V) 222-MAMA complexes were synthesized and studied for biological application.

Complex Synthesis and Purification

Complex synthesis of **222-precusor** and **222-MAMA** procedures followed closely with those discussed in previous reports.[16] Schematics of complexes synthesized in this chapter can be found in **Figure 2-4**. The ligand synthesis modification of **222-MAMAhexanoate** included substitution of dimethyl formamide as the solvent for acetonitrile (anhydrous). Another condition that was adjusted for **222-MAMAhexanoate** was the removal of reaction containers placed under inert conditions prior to the addition of starting materials. The original procedure called for reaction vessels to be flushed with inert gas; this step was not necessary with the use of acetonitrile. These simple changes to the reaction allowed for easier ligand purification and increased yields from 26.3% to 88% of **222-MAMAhexanoate**.

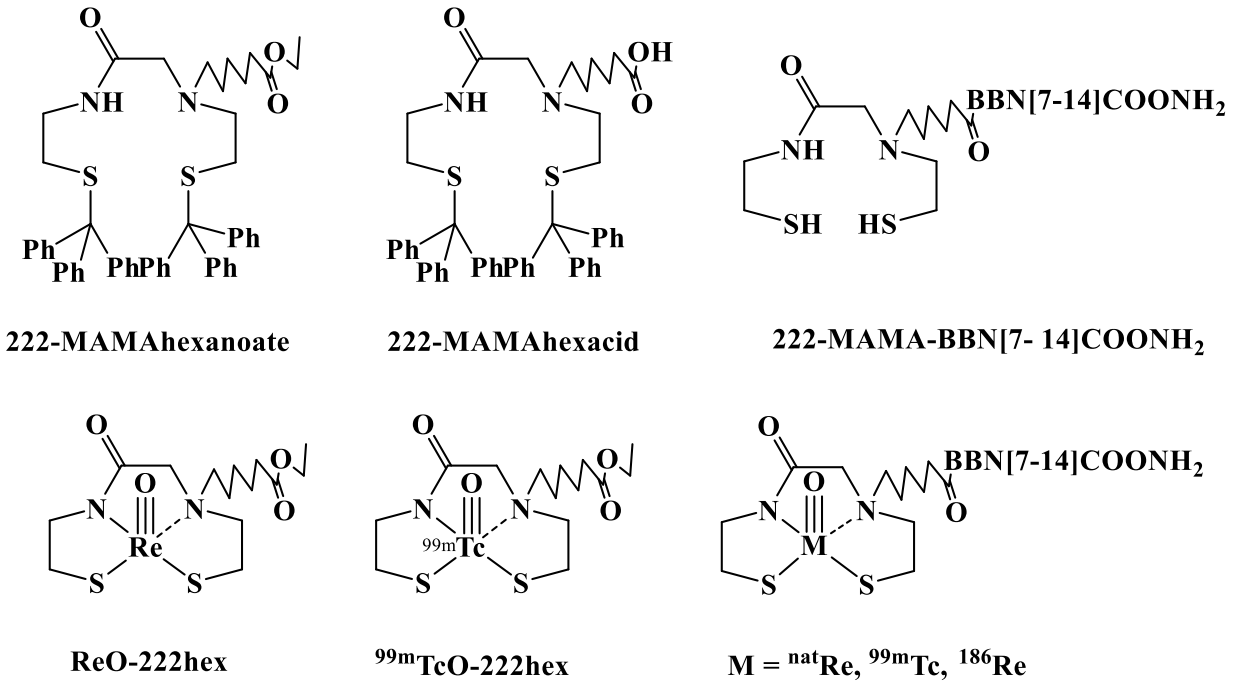

Figure 2-4. Schematic of complexes synthesized in Chapter 2.

Adjustment of conditions set forth by Demoin for Re(V) reactions includes the use of $[ReO(citrate)_2]^-$ in place of $(PPh_3)_2ReOCl_3$ for the synthesis of **ReO-222hex**. In the literature, the majority of Re(V) reactions use the triphenylphosphine rhenium(V) trichloride starting material as it is soluble in most organic solvents. This is a benefit as most Re(V) complexes are hydrophobic, so complexation times may be reduced. The problem is the removal of any unwanted side products to obtain a pure desired complex (ex. PPh_3 or $OPPh_3$). In ^{1}HNMR spectra of Re(V) compounds performed by Demoin, many still contained peaks corresponding to triphenylphosphine, and required further separation by HPLC to isolate **ReO-222MAMAhex**. The change in starting material allowed for a purification that avoided the use of column chromatography, resulting in an increase in yield from 20% to 60%, for **ReO-222MAMAhex**.

Technetium-99m (^{99m}Tc) was reacted with **222-MAMAhexanoate**, **Scheme 2-1**, and was compared to the Re(V) analog via HPLC to confirm complex formation and purity (**Figure 2-5**).

For ^{99m}Tc complexes, the original procedure used phosphate buffer (0.0032 g $NaH_2PO_4 \cdot H_2O$, 0.2620 g $Na_2HPO_4 \cdot 7H_2O$, and 50 mL H_2O, pH 8-9) to adjust the pH of systems to between pH 2-3. This was found to take several mL of phosphate buffer resulting in high volumes of aqueous solution. This caused the MAMA complex to crash from solution, decreasing the overall resulting yields. The amount of organic solution could be increased in order to keep the desired complex in solution, however this diluted the overall concentration of the solution, making analysis difficult. Omission of buffer for tracer scale work showed no change in overall formation of product. The formation of the peak at 21.9 minutes for **^{99m}TcO-222MAMAhex** is suspected to be the result of hydrolysis on **222-MAMAhex**. This likely occurs by the use of acid needed to deprotect the thiol groups prior to coordination, resulting in the conversion of the ester group to the acid; this would result in a shorter retention time as a more hydrophilic species is formed. Demoin originally reported a much shorter retention time for **^{99m}TcO-222MAMAhex**. When compared to his reported Re(V) hexanoate analog, retention times did not match. Upon re-evaluation, retention times align between the two complexes, suggesting that Demoin was possibly synthesizing the ^{99m}TcO-222-MAMAhexacid derivative.

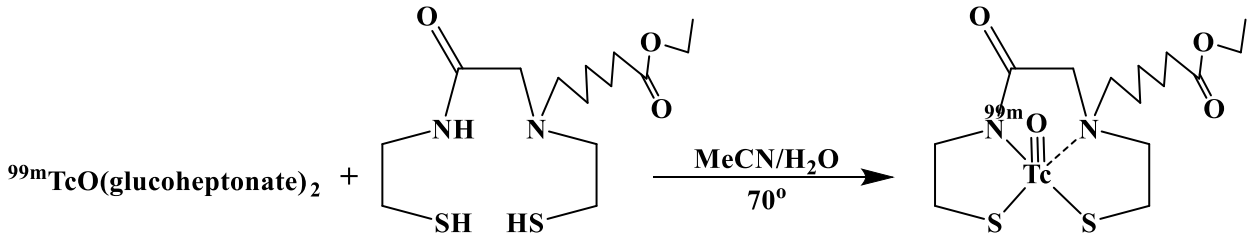

Scheme 2-1. Synthesis procedure for the production of **^{99m}TcO-222MAMAhex**.

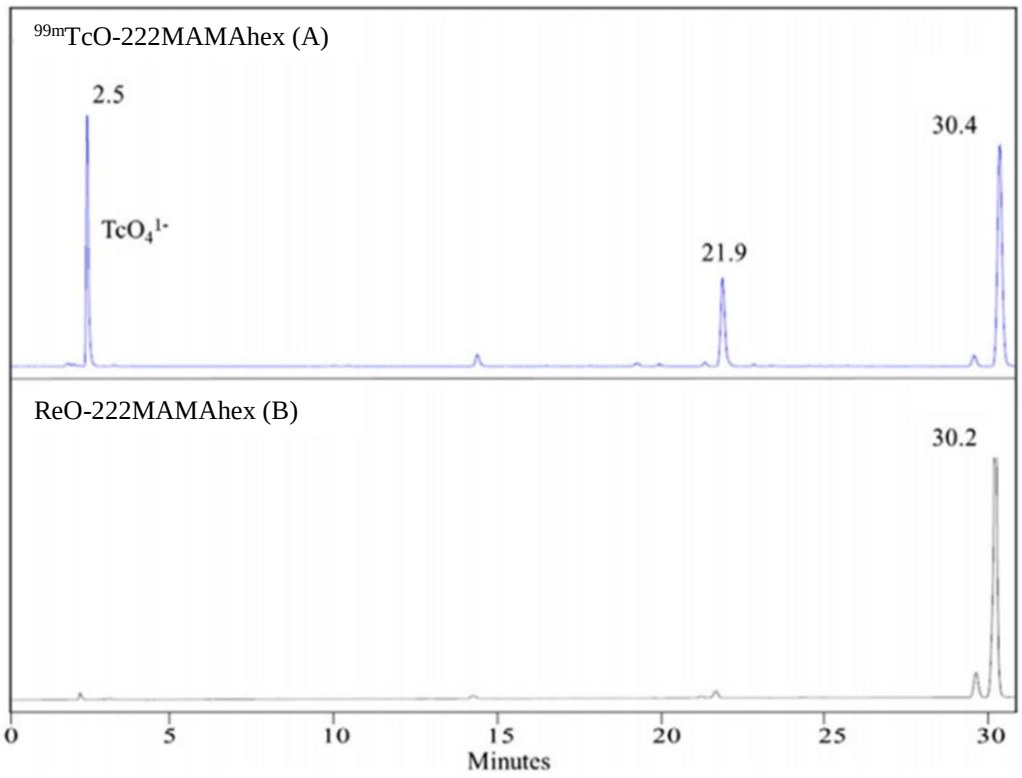

Figure 2-5. HPLC comparison of (A) **^{99m}TcO-222MAMAhex** and (B) **ReO-222MAMAhex** using a Betabasic column with a 10-50% gradient over 30 minutes.

The stability of BBN[7-14]$COONH_2$ chelated complexes was the primary focus of this investigation to determine the reason for the lack of *in vivo* GRP binding in mice observed by Demoin. It was originally found in his studies that *in vitro* results using Re(V) 222-MAMA-BBN[7-14]$COONH_2$ showed IC_{50} values of 2.0 ± 0.7 nM (n = 6) [16], which compared to other bombesin literature values and GRP binding.[26]; however, when testing for *in vivo* binding, results did not match the *in vitro* findings. It is hypothesized that this difference in results is more pronounced on the tracer scale due to impurities in the ligand starting material. Low yields of overall product formation were also shown, which would support this hypothesis. These findings, compared with current studies will be discussed more in the paragraphs that follow.

Changes in synthetic procedure started with the purification of **222-MAMA-BBN[7-14]COONH$_2$**. The crude product, produced by the use of **222-MAMAhexacid** and a model 396 mulitple peptide synthesizer, was purified via HPLC (performed by Gallazzi) to yield a product with greater than 98% purity. This purification was not performed by Demoin, which could have been the primary reasoning for low yields and poor binding. Optimization of chelation included reducing the amount of starting ligand material (**222-MAMA-BBN**) from 0.3 mg to 0.1 mg as large amounts of the ligand are not needed for tracer scale reactions, and the overall stability of the formed complexes were shown not to be affected by this decrease. Changes in Re(V) reactions included the use of $[ReO(citrate)_2]^-$ to produce **ReO-222-MAMABBN, Scheme 2-2**. The use of $[ReO(citrate)_2]^-$ as opposed to $ReOCl_3(PPh_3)_2$ showed an increase from 12% to 90% yield from previous reports. Much like the reaction to produce **ReO-222MAMAhex**, the use of citrate allowed for a much easier to isolate product.

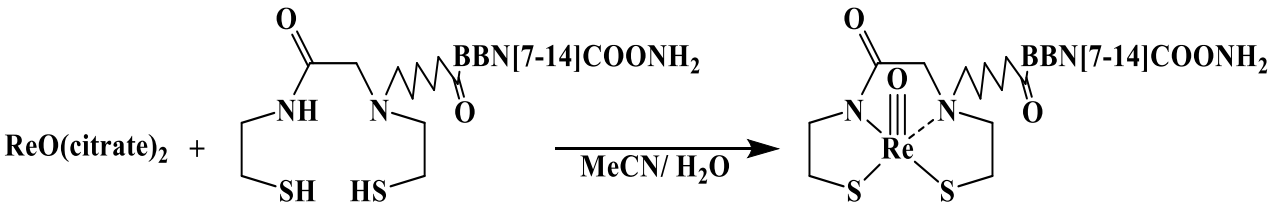

Scheme 2-2. Synthesis procedure for the production of **ReO-222MAMABBN**.

For the synthesis of **^{99m}TcO-222BBN**, modification by exchanging the reaction solvent from MeCN to EtOH removed the step of organic solvent removal. MeCN has to be removed prior to injection in mice and as long as the percentage of EtOH is kept to a minimum (under 10%) it can be a part of the solution for *in vivo* injections. Removal of organic solvent via N_2 showed accelerated degradation of the complex as the organic solvent (MeCN), as the complex is not stable

without the presence of organic solvent. The **^{99m}TcO-222MAMABBN** complex was prepared as described, and purified by Sep-Pak to remove $^{99m}TcO_4^{1-}$, $^{99m}TcO_2$, and **222-MAMA-BBN[7-14]COONH$_2$**. Unreacted ligand (**222-MAMA-BBN**) was still present in the final solution according to the HPLC analysis; however, **^{99m}TcO-222MAMABBN** was not further purified. Approximately 30% of the unchelated **222-MAMA-BBN[7-14]COONH$_2$** (average 0.03 mg) remained in solution following Sep-Pak purification. Radio-HPLC analysis of the purified **^{99m}TcO-222MAMABBN** product mixture showed 88 ± 3% purity in the combined 21.6 and 24.3 min peaks, with the remainder present as pertechnetate. As stated, two peaks correlate to the desired **^{99m}TcO-222MAMABBN** product. It is presumed that each peak corresponds to the *syn*- and *anti*- isomers. This isomerization was confirmed by collecting each individual product (peak) separately, reducing the volume with N_2 (g), and reinjecting a sample (**Figure 2-6**). The species at 21.6 min showed the growth of a peak at 24.3 min, which over time equilibrated to a 1:2 ratio favoring the later eluting species. The 24.3 min species changed very little over time, with <5% in-growth of the 21.6 min species. **^{99m}TcO-222MAMABBN** was also synthesized in early trials and only one peak appeared in HPLC (~25 min). To verify this phenomena of isomer formation in EtOH, an aliquot of **ReO-222MAMABBN**, in MeCN contained only one peak according to HPLC. **ReO-222MAMABBN** was spiked with EtOH (10 µL EtOH in 90 µL MeCN) and analyzed by HPLC over time. Two species were observed at 22.1 and 24.8 min, with the 24.78 min species dominating (89%). The Re(V) complex in acetonitrile only showed the later eluting species as observed. To check initial stability of complexes to be used for *in vivo* studies, **^{99m}TcO-222MAMABBN** was placed in bacteriostatic saline solutions (<10% EtOH) and complexes were monitored over the course of 6 h. **^{99m}TcO-222MAMABBN** stayed relatively stable dropping from

88% to ≥75% remaining intact at 6 h, illustrating how the complex changes over the course of one half-life (**Figure 2-7**).

The no carrier added (*nca*) **^{186}ReO-222MAMABBN** was synthesized similarly to **^{99m}TcO-222MAMABBN** and was analyzed by radio-HPLC (Jupiter C-18 column, at 25ºC with a gradient of 10–70% MeCN in water with 0.1% TFA over 15 min). Initially, only one peak at 13.1 min was observed, which over time separated into two peaks (likely the *syn*- and *anti*- isomers) observed at 12.5 and 13.5 min. Very little chemistry has been performed with *nca* ^{186}Re as the route of production and separation is relatively recent. [24,25] The half-life of ^{186}Re is 3.7 days and the route of production uses an enriched target in a (p,n) reaction ^{186}W. ^{186}Re has a β^- emission, as well as a γ that is suitable for image detection. $^{186}ReO_4^-$ was received from LANL following elution from an anion exchange column using nitric acid. The nitric acid was removed by evaporation and ^{186}Re was reconstituted in hydrochloric acid. Upon arrival it was determined that nitric acid was still present in solution, which inhibited reduction of perrhenate with stannous chloride for synthesis of Re(V) complexes. In order to continue with synthetic procedures, the stock ^{186}Re solution was extracted with DCM/H_2O in the presences of tetrabutylammonium chloride; the $(Bu_4N)^{186}ReO_4$ was extracted into DCM leaving the nitric acid in the aqueous phase. These results are compared with those observed for **ReO-222MAMABBN** and indicate formation of the desired **^{186}ReO-222MAMABBN** product, **Figure 2-8**.

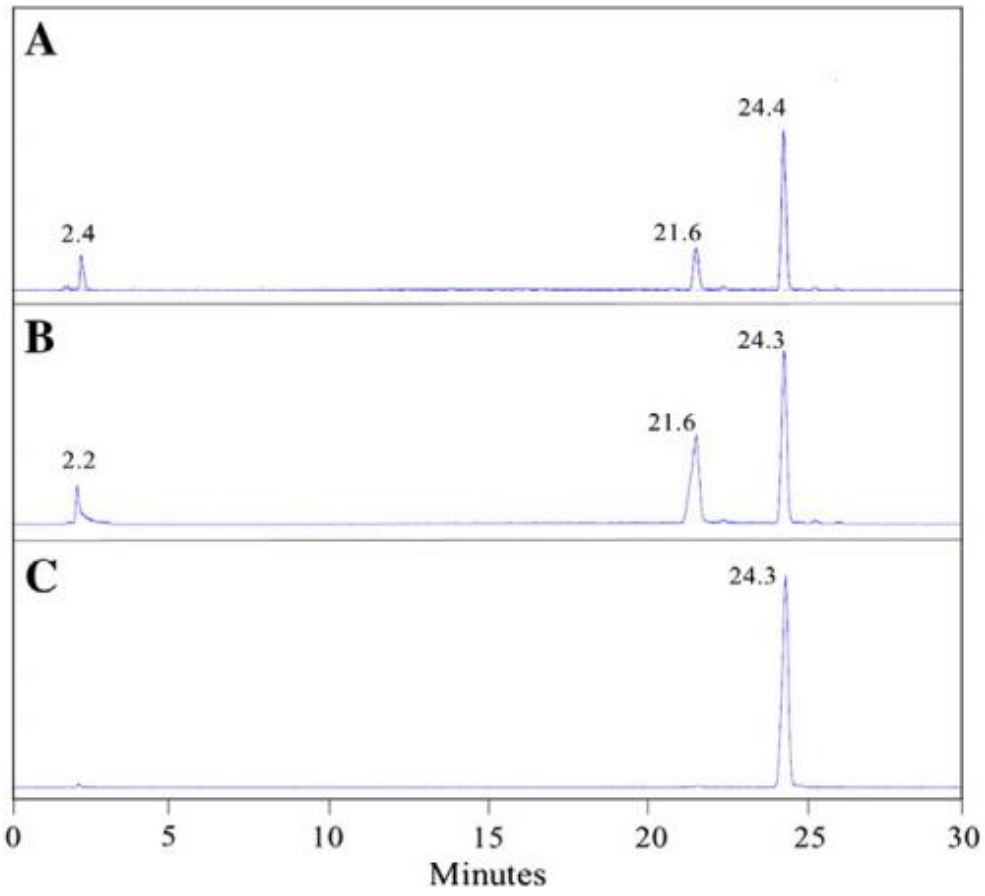

Figure 2-6. Radio-HPLC analysis of (A) isolated **^{99m}TcO-222MAMABBN**, (B) reinjected 21.6 min peak, and (C) reinjected 24.4 min peak (24.3) to illustrate the formation of *syn* and *anti* isomer formation in EtOH.

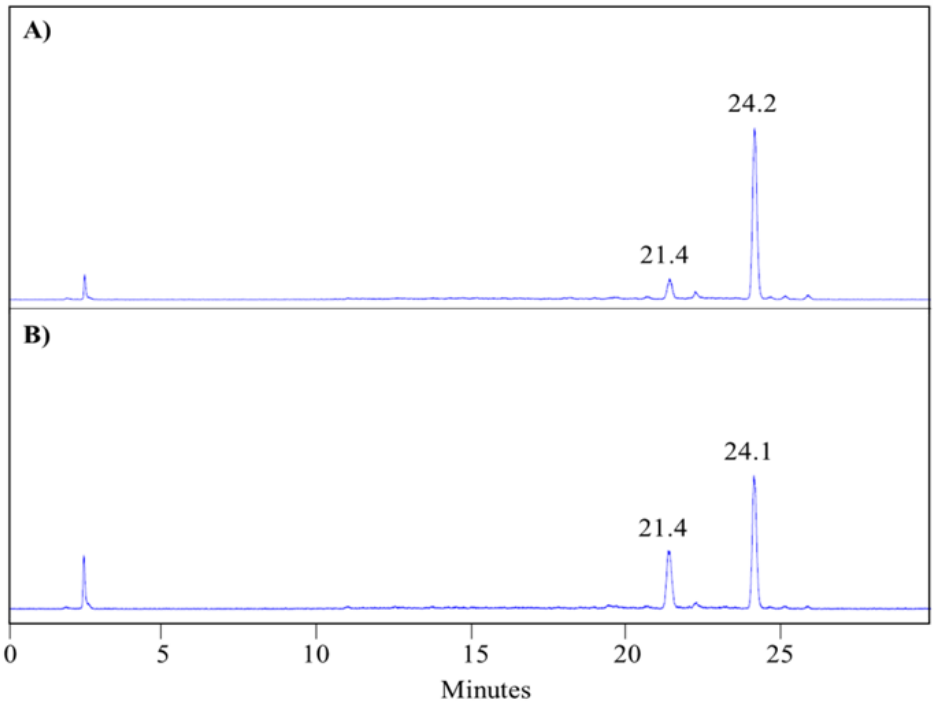

Figure 2-7. Radio-HPLC analysis of ^{99m}**TcO-222MAMABBN** in bacteriostatic solution tested at 0 h (A) and 6 h (B).

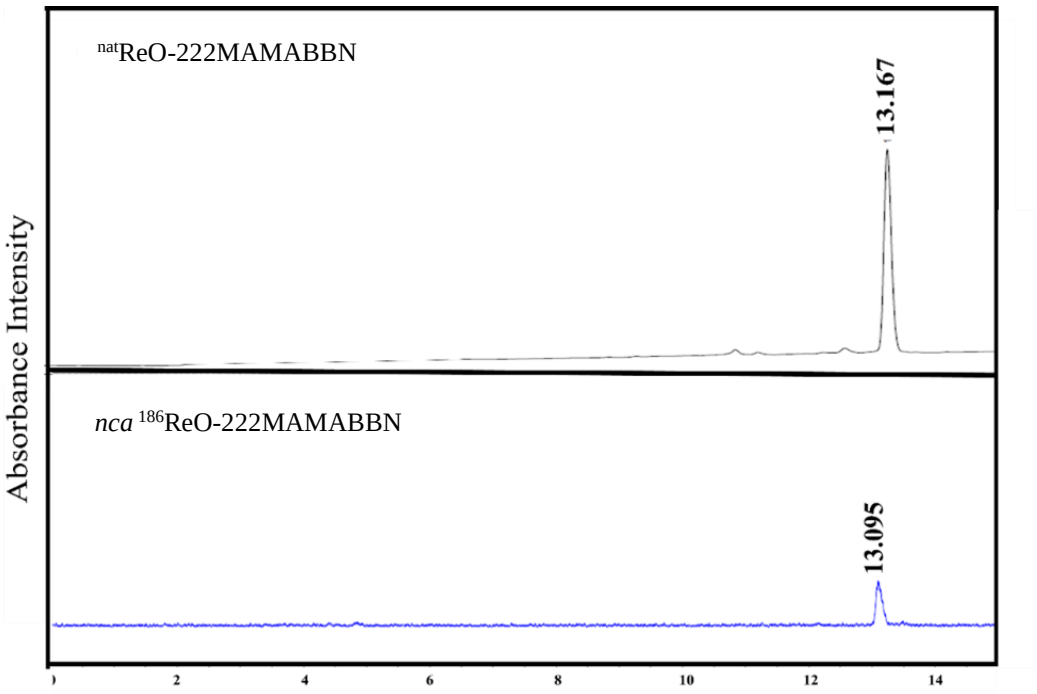

Figure 2-8. Comparison of **^{nat}ReO-222BBN** and the equivalent ***nca*** **^{186}ReO-222BBN**.

In vivo biodistribution studies

Biodistribution studies were carried out because the results of Demoin showed little to no *in vivo* binding taking place.[16] Previous reports indicated *in vitro* studies with **222-MAMABBN** and similar ligand frameworks in the literature showed that our complexes should exhibit *in vivo* binding. In the case of a similar N_2S_2 derivate to 222-MAMABBN, reported by Santos-Cuevas with a TAT/BBN hybrid targeting receptor, studies showed 1.69 ± 0.12 %ID/g, which was lower than the just bombesin derivative at 3.29 ± 0.21.[28] It was observed that upon study of *in vivo* receptor binding of **^{99m}TcO-222MAMABBN**, showed little to no uptake in the pancreas of CF-1 mice (**Table 2-1**), which based on reports like Santos-Cuevas indicated something was incorrect. There was about 0.87 %ID/g of complex in the pancreas (n=4) at 4 h post injection. [16] The pancreas has a large number of GRP receptors (BBN subtype 2 receptors), which should provide a proper environment for **^{99m}TcO-222MAMABBN** binding.[29] Pertechnetate was evaluated in

mice for a direct comparison in order to monitor locations where free pertechnetate distributes, if the complex were to dissociate *in vivo* and oxidize. In reported comparison studies, ^{111}In-DOTA-5-Ava-BBN[7-14]NH_2, which had a similar IC_{50} value to **^{nat}ReO-222MAMABBN** (2.0 ± 0.7 nM [n = 6]), the ^{111}In complex had significant pancreatic uptake (15.78 ±2.54 % ID/g) at 1 h in CF-1 normal mice.[30] Also, ^{99m}TcO-N_3S-5-Ava-BBN(7-14)NH_2 had 13.8 ± 1.62 % ID/g retained in the pancreas at 1 h in CF-1 normal mice.[31] It was hypothesized, based on previous literature reported experiments, that rapid clearance of **^{99m}TcO-222MAMABBN** from the blood to the liver and intestines should have been aided by the high lipophilicity of this complex. These inconsistencies required further evaluation to understand the behavior of **^{99m}TcO-222MAMABBN**.

Table 2-1. Demoin biodistribution (%ID/g) in CF-1 mice for $^{99m}TcO_4^{1-}$ (1 h) and **^{99m}TcO-222MAMABBN** (1 h and 15 min).

	$^{99m}TcO_4^-$ (1 h, n=4)	**^{99m}TcO-BBN (1 h, n=4)**	**^{99m}TcO-BBN (15 min, n=1)**
Bladder	3.59±1.1	1.37±0.47	---
Heart	1.79±0.74	0.25±0.06	---
Lung	3.50±0.93	0.48±0.14	25.91
Liver	3.75±0.67	10.71±1.66	8.86
Kidneys	3.12±0.84	9.02±2.48	0.06
Spleen	1.64±0.45	0.35±0.09	0.04
Stomach	52.68±11.24	1.89±0.84	1.76
S. Intestine	3.26±0.4	21.51±5.47	33.37
L. Intestine	6.16±0.76	9.21±9.80	0.01
Muscle	0.53±0.09	0.09±0.02	0.01
Bone	1.47±0.55	0.14±0.05	---
Brain	0.28±0.10	0.87±0.06	---
Pancreas	2.01±0.33	0.87±0.06	0.14
Blood	14.27±4.69	0.14±0.03	0.39

In the current work, biodistribution studies with **^{99m}TcO-222MAMABBN** were performed in normal CF-1 mice, with four mice injected with **^{99m}TcO-222MAMABBN** (0.26–0.40 MBq; 7–8 μCi) and four mice injected with 0.1 mg BBN[1–14] in 100 μL saline as a blocking agent 5 minutes prior to injection of **^{99m}TcO-222MAMABBN** (0.26–0.40 MBq; 7–8 μCi). The biodistribution data obtained from these studies are tabulated in **Table 2-2** and shown graphically in **Figures 2-9** and **2-10**. Approximately 2% ID/g uptake was observed in the pancreas at 1 h, which was decreased to 0.2% using a blocking agent. This lower pancreatic uptake may be due to the presence of unlabeled **222-MAMA-BBN[7-14]COONH$_2$** competing for receptor sites, as well as the high lipophilicity of the ^{99m}Tc complex. Thus, HPLC purification may be necessary in order increase the specific activity of the tracer, improving pancreas and tumor uptake in future *in vivo* studies. This lipophilicity is consistent with other Re(V) and ^{99m}Tc(V) N_2S_2 complexes reported in the literature and may call for synthetic modifications to better decrease the hydrophobic nature of this system before moving forward with future studies. The pancreatic uptake does suggest BB2r targeting as uptake was blocked by injection of BBN[1–14] prior to injection of **^{99m}TcO-222BBN**. Future studies may be performed with adjustment to the ligand to further improve the lipophilicity of 222-MAMA.

Table 2-2. Biodistribution in CF-1 normal mice for **^{99m}TcO-222MAMABBN** and blocking study at 1 h post injection.

	%ID (n = 4)		%ID/g (n = 4)	
	^{99m}TcO-BBN	Blocked	**^{99m}TcO-BBN**	Blocked
Heart	0.02 ± 0.02	0.05 ± 0.07	0.11 ± 0.16	0.40 ± 0.51
Lung	0.13 ± 0.16	0.15 ± 0.07	0.55 ± 0.69	0.80 ± 0.41
Liver	20.61 ± 4.47	12.47 ± 4.27	10.38 ± 1.88	6.51 ± 1.98
Kidneys	2.00 ± 0.23	1.60 ± 0.39	4.24 ± 0.60	3.57 ± 89
Spleen	0.15 ± 0.20	0.13 ± 0.15	1.07 ± 1.48	0.86 ± 1.10
Stomach	1.64 ± 0.71	1.44 ± 0.33	3.60 ± 2.15	1.87 ± 0.29
S. Intestine	27.40 ± 9.51	59.19 ± 3.14	15.46 ± 6.08	29.72 ± 2.22
L. Intestine	23.20 ± 10.47	0.39 ± 0.05	18.04 ± 8.25	0.37 ± 0.11
Muscle	0.02 ± 0.03	0.10 ± 0.08	0.06 ± 0.12	0.54 ± 0.40
Bone	0.02 ± 0.04	0.11 ± 0.15	0.32 ± 0.64	1.52 ± 2.17
Brain	0.01 ± 0.02	0.03 ± 0.03	0.02 ± 0.04	0.06 ± 0.06
Pancreas	0.72 ± 0.03	0.09 ± 0.06	2.03 ± 0.42	0.24 ± 0.17
Bladder	2.46 ± 1.12	1.40 ± 0.16	0.05 ± 0.02	0.3 ± 0.06
Blood	0.83 ± 0.23	1.09 ± 2.80	0.38 ± 0.09	0.49 ± 0.52
Carcass	5.50 ± 0.53	4.57 ± 0.49	0.24 ± 0.04	0.21 ± 0.03
Urine	-	-	12.95 ± 8.19	18.34 ± 2.22
Cage paper	-	-	4.76 ± 9.25	0.23 ± 0.42

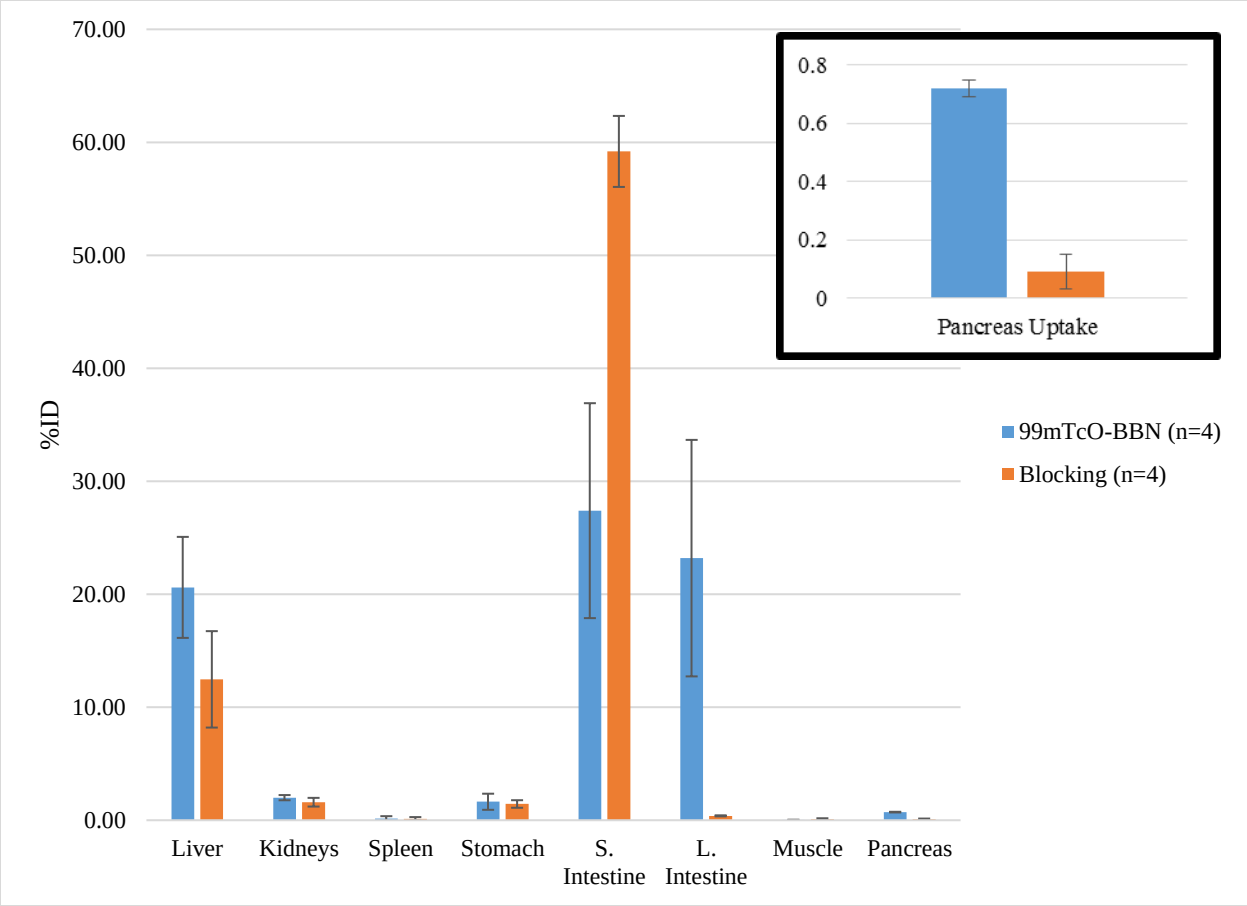

Figure 2-9. %ID of CF-1 mice with blocking and pancreas uptake highlighted.

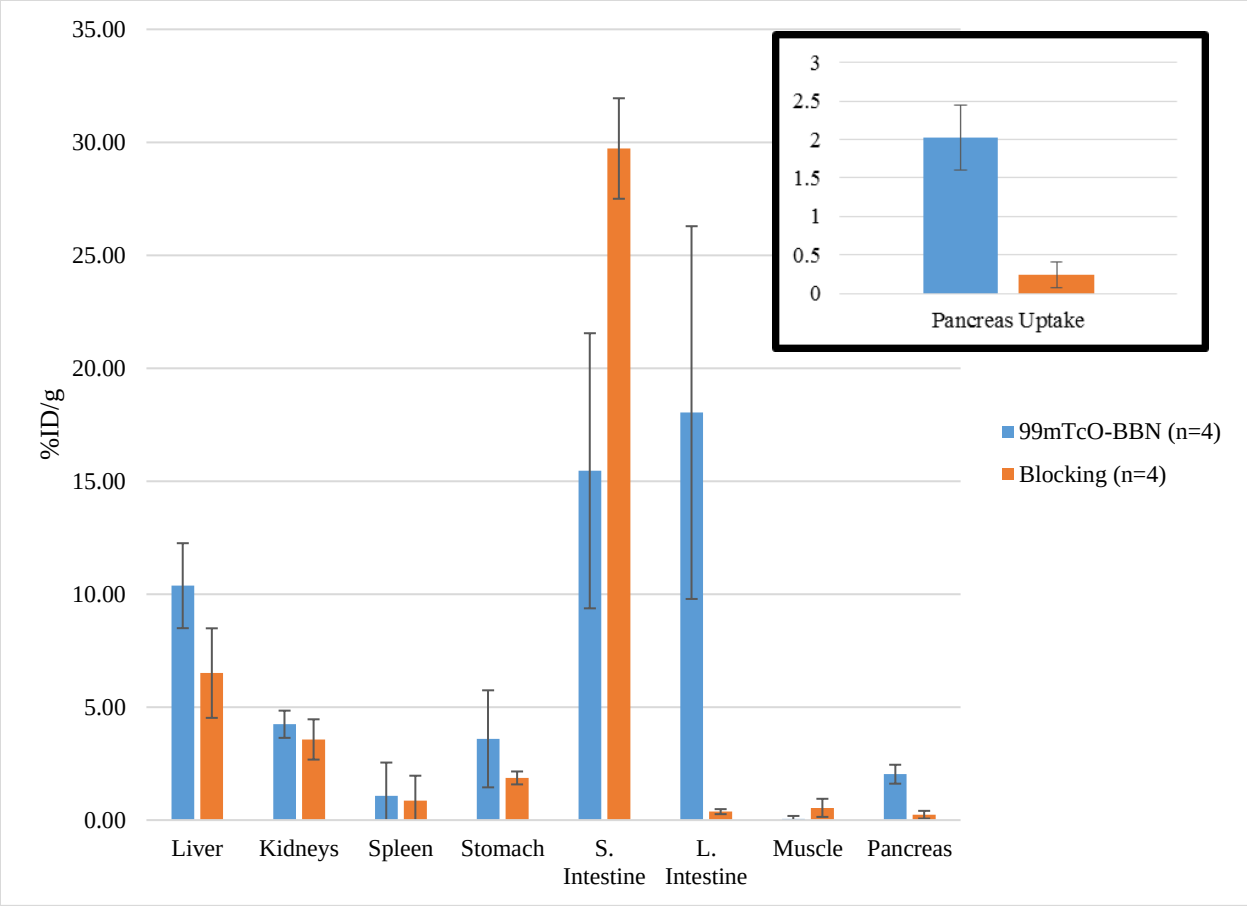

Figure 2-10. %ID/g in CF-1 mice with blocking and pancreas results highlighted.

Conclusion

The 222-MAMA-based chelators were synthesized for potential use in radiopharmaceuticals that incorporate $^{186/188}$Re. The 222-MAMA chelator was conjugated to BBN[7–14]NH_2 and analyzed via ^{99m}Tc, non-radioactive Re, and no carrier added ^{186}Re studies. **^{99m}TcO-222MAMABBN** was shown to be stable in bacteriostatic solution, at greater than 75% over the course of 6h. It was shown that **^{99m}TcO-222MAMABBN** had 2.03 ± 0.42 %ID/g uptake in CF-1 mice pancreas, which was an increase from previously reported studies by Demoin. However, there was also a significant clearance via the liver and intestines, indicating a hydrophobic complex; this is also apparent from HPLC retention times, having eluting times correlating to >40% MeCN with 0.1%

TFA. These studies indicate that **222-MAMA-BBN[7–14]COONH$_2$** chelates to Re(V) and ^{99m}Tc(V) with relatively high yields. The ability show specific targeting for *in vivo* receptor binding to BB2r-positive tissues was also demonstrated with **^{99m}TcO-222MAMABBN**. The future availability of *nca* ^{186}Re, and the formation of **^{186}ReO-222MAMABBN**, gives incentive to develop ^{99m}Tc/^{186}Re "matched pair" agents for imaging and therapy of cancer cells. This study also is one of the first utilizing *nca*^{186}Re, for biological applications; the ability to isolate a single product will help in future studies with *nca*^{186}Re. Most of the research associated with ^{186}Re has been studied with carried added rhenium/^{186}Re, including ^{186}Re-HEDP for bone palliative treatment.[27] The bifunctional chelator, **222-MAMA-BBN[7–14]COONH$_2$**, may be useful for conjugation to other biological targeting vectors and may have utility for delivering therapeutic doses of $^{186/188}$Re to tumor tissues using peptides and antibodies. However, the complex must be redesigned to be more hydrophilic, perhaps through the use of a different linker moiety such as an acetyl or propyl linker in place of the current hexanoate linker. Shorter linkers have been shown to be more hydrophilic, as well as demonstrate more significant uptake in tumor-bearing mice with urinary clearance.[32-34] Luo was able to synthesize room temperature ^{188}Re complexes with a one carbon linker between amide and carboxylic acid end of the peptide for targeting vector conjugation. Tumor uptake was shown to increase over time and the complex was more soluble in aqueous media, according to HPLC retention time, than the **222-MAMA-BBN[7-14]COONH$_2$** complexes studied in this chapter that contain the longer linker chain.[34] Adoption of a shorter chain might make desired complexes more soluble in aqueous reagents and increase stability without the use of high concentrations of organic solvents.

Chapter 3: Rhenium(V) and Technetium(V) complexes with 323-N_2S_2 MAMA ligands for bifunctional chelator agents: Synthesis and comparative evaluation

Introduction

Research in preliminary radiotracer development is the key component to understanding what types of ligands will generate the best framework for *in vivo* stability and targeting. This concept of design covers such a broad area that the scope of this research has been limited to N_2S_2 chelators. In limiting the framework, a variety of 222-N_2S_2 modalities with several coordinated metal centers have been reported, as were discussed in Chapter 2. Several literature agents using the 222-N_2S_2 framework for imaging agents show a high uptake in intestines and liver. Examples by Vanbilloen for the study of ^{99m}Tc(V)-BAT brain imaging agents showed intestinal uptake near 30 %ID/g.[1] Lin et al synthesized a ^{99m}Tc-DADT bombesin analog that has more promising results and clears more readily via the urinary tract. Uptake in the pancreas is 8.95 ±0.98 %ID/g at 15 minutes and 16.4 ±2.80 in the kidneys. Lin was able to demonstrate blocking and varied targeting vector results. [2]

This chapter involves investigating the effect of cavity size on Re(V)O-N_2S_2 stability. In searching for larger ring size ligands, most of the early work focused on macrocyclic ligand frameworks with di-oxo metal bonds. [3] Blake et al studied the coordination of cyclam with Re(V) di-oxo complexes for the purpose of delving deeper into future catalysis studies. The focus of the current study is on open chain, tetradentate ligands, with N_2S_2 chelates. There are fewer of these reported apart from the 222-N_2S_2 framework bound with Re(V) and Tc(V). [4a-c] Luyt synthesized a 232-N_2S_2 ligand bound to both Re(V) and ^{99m}Tc(V) for the application of future work with

biological applications. Luyt was studying the *syn*- and *anti*- isomeric characteristics of these complexes. The yields of Re(V) complexes were over 85% and for ^{99m}Tc(V) were greater than 70%. [5] Research by Kieffer studied ^{99m}Tc-TropaBAT derivatives (^{99m}Tc-norchloro-TropaBAT and ^{99m}Tc-TropaBAT) and ^{99m}Tc-PipBAT were synthesized as brain imaging agents, **Figure 3-1**. No synthetic information was reported relating to yields of complexation; however, biodistribution data indicated a negative effect on the DAT binding affinity, but not on the overall brain uptake, as compared to ^{99m}TcTRODAT-1. Replacement of the tropane skeleton by a piperidine ring produced no DAT binding affinity nor brain uptake.[6] Pillai studied the complexation of ^{99m}Tc when bound to amine and imine phenols. The complexes he studied varied in the number of carbon atom linkers in the backbone and the amine ligands are of particular interest to current studies. As the number of carbons was increased, there was only small differences in extracted yields. This indicated that expansion of the backbone does not inhibit overall yield of products. [7] Jurisson looked into the tetradentate N_4 ligand frameworks as analogous studies of ^{99m}TcO-HMPAO. **[**8] Her research indicated that both ethyl and propyl carbon backbones have very similar production yields, but once the number of carbon atoms increases to five, yields reduce. In the future reference of this work, the "222" and "323" in ligand naming, refers to the number of bridging carbons between metal coordinated atoms, ethylene (2) or propylene (3) in this study.

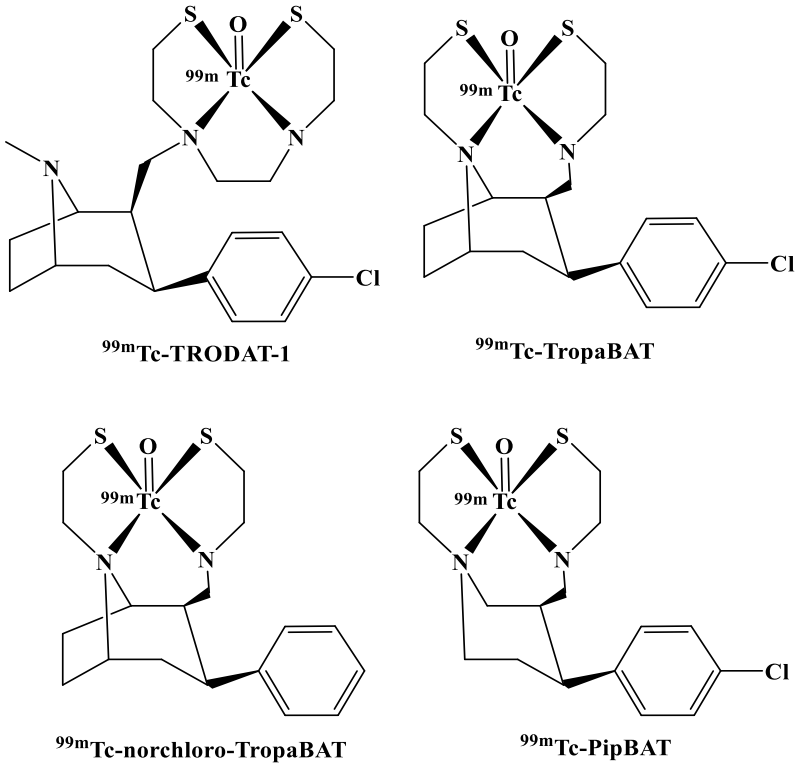

Figure 3-1. Proposed schematics of ^{99m}Tc-TRODAT-1, ^{99m}Tc-TropaBAT derivatives (^{99m}Tc-norchloro-TropaBAT and ^{99m}Tc-TropaBAT) and ^{99m}Tc-PipBAT.

As an extension of the research discussed in Chapter 2, which focused on 222-MAMA coordinating ligands, we wanted to study the effect of changing the ring size of monoamine-monoamide on chelation to Re and ^{99m}Tc. As already stated, the predominate ligand framework for Re/^{99m}Tc has been the 222-MAMA and its analogs. A 323-MAMA chelate was synthesized that may allow for the metal to coordinate closer to the pocket of the tetradentate ligand. This could provide more stability in Re(V) complexes, once chelated. In this chapter, the findings for the reactivity of 323-MAMA ligands with Re(V) and ^{99m}Tc(V) are presented, as well as competition studies to compare binding with 323-MAMA and 222-MAMA (Chapter 2) for metal chelation.

Methods

General methods

All chemicals, unless otherwise indicated, were commercially available and used without further purification. Technetium-99m, as pertechnetate, was available from saline elution of a $^{99}Mo/^{99m}Tc$ generator (Mallinckrodt Medical, St. Louis, MO). Microwave reactions were performed using a CEM Discover SP Activent, Model 909150 instrument. NMR studies were performed with a Bruker DRX 300 or 500 MHz Spectrometer (as noted). ESI-MS was performed using a Finnigan TSQ7000 triple-quadrupole mass spectrometer. HPLC analyses were performed with a Shimadzu HPLC system outfitted with both UV-vis and radioisotope detectors. The HPLC column used was a Jupiter C-18 column (Phenomenex, Torrance, CA, 250 mm × 4.60 mm, 5 μm, 300 Å pore size). All HPLC mobile phases used acetonitrile (MeCN) in water with 0.1% trifluoroacetic acid (TFA); the specific conditions (i.e., column, gradient, flow rate) are indicated for purifications and analyses. Radio-TLC strips (Saturation pads, Analtech, Newark, DE) were counted by cutting the TLC strips and counting them in a NaI(Tl) well detector (Harshaw Chemical Company, Serial Number EX-53, with Ortec electronics and a Canberra high-voltage supply). A Beckman Coulter HPLC system in series with an ion trap mass analyzer (a LCQ FLEET instrument, Thermo Fisher Scientific, with positive ion ionization) was used to obtain LC/ESI-MS results (Betabasic-18, 10-50% MeCN over 30 min, 1 mL/min). A Thermo Nicolet AEM FT-IR instrument was used for IR analysis (KBr pellets).

Synthesis

3-(tritylthio)propan-1-amine hydrochloride **[323-precursor].** 3.0 g (23.1 mmol) of 3-chloropropylamine hydrochloride were dissolved in 40 mL of 2M NaOH and 40 mL of DI-H_2O, and placed in a 300 mL round bottom (RB) flask. 6.377 g (23.1 mmol) of triphenylmethane thiol

were dissolved in 50 mL of acetone, with gentle heating to ensure the starting material was fully dissolved, and added to the round bottom flask. The reaction mixture immediately turned pink in color and was stirred at RT for 6 hours. The organic solvents were removed by rotary evaporation; 20 mL of ethyl acetate (EtOAc) and 10 mL of DI H_2O were added to the flask and used for extraction of the desired product. The organic layer was retained and the aqueous layer was extracted twice more with EtOAc. Anhydrous sodium sulfate was used to remove any residual water from the organic layer. The organic solution was reacted with HCl (g), while stirring, to produce the desired, white powdered product. The product was washed with EtOAc, and dried *in vacuo*. The filtrate was left to reduce in volume overnight, as further amounts of the desired product precipitated from the solution. After two further crop separations of product, 5.207 g total(14.1 mmol, 61.1% yield) were collected. ^{1}H-NMR (300 MHz, d_6-DMSO, δ(ppm)): 1.58 (quintet, J = 7.5 Hz, 2H, $CH_2C\mathbf{H_2}CH_2$), 2.15 (t, J = 7.5 Hz, 2H, $C\mathbf{H_2}S$), 2.60 (t, J = 7.5 Hz, 2H, $C\mathbf{H_2}N$), 7.20–7.38 (m, 15H, Ph), 7.75 (s, 3H, Ph). ^{13}C-NMR (300 MHz, *d*6-DMSO, δ(ppm)): 26.8 ($CH_2\mathbf{C}H_2CH_2$), 28.4 ($\mathbf{C}H_2S$), 38.2 ($\mathbf{C}H_2N$), 66.1 ($\mathbf{C}Ph_3$), 126.7 (Ph), 128.0 (Ph), 129.0 (Ph), 144.4 (Ph).

N-*(3*-(tritylthio)propyl)-2-((3-(tritylthio)propyl)amino)acetamide [323-MAMA]. 323-precursor (4.0624 g, 10.98 mmol) was dissolved in 20 mL of CH_2Cl_2 and 5.5 mL of triethylamine (NEt_3). The solution was cooled to 0°C while stirring. Bromoacetylbromide (0.479 mL, 5.50 mmol) was added slowly, and the resulting solution was stirred at 0°C for 1 h, followed by stirring at RT for 24 h. The product mixture was sequentially washed with 50 mL of dilute H_2SO_4 (pH ~ 3), 30 mL of saturated $NaHCO_3$, and 30 mL of saturated NaCl. The organic layer was dried with anhydrous Na_2SO_4 and solvent reduced by rotary evaporation. The product was purified on a silica

gel column (10 g, 1.3 cm diameter) and eluted with $CHCl_3$, collecting fractions with R_f= 0.5 (single species), with TLC elution solvent of 3% MeOH in $CHCl_3$. The $CHCl_3$ was removed *in vacuo* to yield 1.69g (2.4 mmol, 50.5% yield) of **323-MAMA**. ^{1}H-NMR (500 MHz, $CDCl_3$, δ(ppm)): 1.43–1.57 (m, 4H, $CH_2C\mathbf{H_2}CH_2$), 2.12 (t, *J* = 7.3 Hz, 2H, $SC\mathbf{H_2}$), 2.18 (t, *J* = 7.3 Hz, 2H, $SC\mathbf{H_2}$), 2.46 (t, *J* = 6.8 Hz, 2H, $HNC\mathbf{H_2}$), 3.07 (s, 2H, $COC\mathbf{H_2}N$), 3.14 (dt, J = 6.5, 6.5 Hz, 2H, $C\mathbf{H_2}NH$), 7.15–7.34 (m, 18H, Ph), 7.34–7.54 (m, 12H, Ph). ^{13}C-NMR (500 MHz, $CDCl_3$, δ(ppm)): 28.5 ($CH_2\mathbf{C}H_2CH_2$), 28.7($CH_2\mathbf{C}H_2CH_2$), 29.3 ($S\mathbf{C}H_2$), 29.5 ($\mathbf{C}H_2S$), 38.0 ($\mathbf{C}H_2NH$), 48.8 ($NH\mathbf{C}H_2$), 52.2 ($CO\mathbf{C}H_2NH$), 66.6 ($\mathbf{C}Ph_3$), 126.6 (Ph), 127.9 (Ph), 129.5 (Ph), 144.8 (Ph), 171.3 (**C**O).

ethyl 6-((2-oxo-2-((3-(tritylthio)propyl)amino)ethyl)(3-(tritylthio)propyl)amino)hexanoate [323-MAMAhexanoate]. To a scintillation vial equipped with a stir bar, **323-MAMA** (1.041 g, 1.49 mmol) was dissolved in anhydrous MeCN (2 mL; dried over molecular sieves). Diisopropylethylamine (0.564 ml, 3.24 mmol) in MeCN (3 mL) was added, followed by slow addition of ethyl-6-bromohexanoate (0.524 g, 2.35 mmol) in 3 mL of MeCN. The reaction mixture was placed in an oil bath and refluxed at 85ºC under N_2 gas, and allowed to react for 24 h. The reaction vessel was brought to room temperature before removal of solvent *in vacuo*. Ethyl acetate (EtOAc) (5 mL) was added to the residue, and undissolved particulates were removed by filtration. The volume was reduced by half and 0.5 mL of hexanes was added. The crude product was purified on a silica gel column (10 g, 1.3 cm diameter) that had been pre-conditioned with 15% EtOAc in hexanes. Following loading, the column was eluted with 30% EtOAc in hexanes (100 mL) followed by 50% EtOAc in hexanes (200 ml). Fractions were collected (5 mL) and analyzed by TLC (silica gel: 50% ethylacetate in hexanes). Fractions showing a single species with R_f = 0.4 were combined, and dried under vacuum overnight to obtain 1.19 g (1.40 mmol, 95.2% yield) of **323-MAMAhexanoate**. ^{1}H-NMR(500 MHz, $CDCl_3$, δ(ppm)): 1.16-1.26 (m, 2H, $NCH_2CH_2C\mathbf{H_2}$),

1.24 (t, *J* = 7.0 Hz, 3H, C**H₃**), 1.26-1.35 (m, 2H, NCH₂C**H₂**), 1.42 (tt, *J* = 7.1, 7.3 Hz, 2H, CH₂C**H₂**CH₂), 1.48 (tt, *J* = 7.1, 7.3 Hz, 2H, CH₂C**H₂**CH₂), 1.57 (tt, *J* = 7.5, 7.5 Hz, NCH₂CH₂CH₂C**H₂**), 2.10 (t, *J* = 7.3 Hz, 2H, SC**H₂**), 2.11 (t, *J* = 7.0 Hz, 2H, C**H₂**S), 2.25 (t, *J* = 7.3 Hz, 2H, C**H₂**COO), 2.25-2.35 (m, 4H, N(C**H₂**)₂), 2.86 (s, 2H, COC**H₂**N), 3.10 (dt, *J* = 6.8, 6.8 Hz, 2H, C**H₂**N), 4.11 (q, *J* = 7.2 Hz, 2H, C**H₂**CH₃), 7.09 (t, *J* = 6.0 Hz, 1H, Ph), 7.15-7.22 (m, 6H, Ph), 7.22-7.30 (m, 12H, Ph), 7.35-7.43 (m, 12H, Ph). ^{13}C-NMR (500 MHz, $CDCl_3$, δ(ppm)): 14.2 (CH₂**C**H₃), 24.7 (**C**H₂CH₂COO), 26.2 (CH₂**C**H₂CH₂), 26.6 (NCH₂**C**H₂), 26.8 (NCH₂CH₂**C**H₂), 28.6 (CH₂**C**H₂CH₂), 29.4 (S**C**H₂), 29.8 (**C**H₂S), 34.2 (**C**H₂COO), 38.1 (**C**H₂NH), 54.3 (RN**C**H₂), 54.9 (N**C**H₂R), 58.4 (CO**C**H₂N), 60.2 (**C**H₂CH₃), 66.5-66.6 (**C**Ph₃), 126.6 (Ph), 127.8 (PH), 129.5 (Ph), 144.8 (Ph), 171.3 (**C**O), 173.5 (**C**OCH₂CH₃).

ReO-323-MAMA. *Method 1:* **323-MAMA** (0.1524 g, 0.22 mmol) was combined in a scintillation vial with trifluoroacetic acid (0.5 mL) and triethylsilane (0.2 mL) and placed on a shaker plate to shake for 2 h. The solution was then evaporated under a nitrogen stream and the remaining oil was washed with hexanes (25 mL). The oil was then dried in vacuo and placed in 20 mL of dry acetonitrile. The ligand solution was transferred to a round bottom flask and 0.02 mM solution of $[ReO(citrate)_2]^-$ (11.28 mL) was added. The reaction was refluxed at 95ºC for 20 h. At the 18 h mark the pH was adjusted to 6 with

ammonium acetate and the reaction was continued. Solvent was removed by rotary evaporation and the residue was extracted with dichloromethane and water, 10 mL each. The organic phase was dried and filtered over anhydrous sodium sulfate. The product was dried *in vacuo* and washed with 10 mL each of hexanes, cold toluene, and hexanes twice more consecutively. The product was dried overnight and re-crystallized from acetone. HPLC (Jupiter C-18, 10–50% MeCN over

15 min, 1 mL/min) Rt = 12.06 min. Dark purple/brown crystals were obtained at X-ray defraction quality. 0.0266 g, %Yield: 15.53. ^{1}H-NMR (500 MHz, $CDCl_3$, δ(ppm)): 4.49 (dd, 1H), 4.38 (d, 1H), 3.78 (d, 1H), 3.71 (m, 1H), 3.31 (m, 2H), 2.98 (m, 2H), 2.77 (dd, 1H), 2.62 (m, 2H), 2.55 (t, 1H), 1.92 (m, 2H), 1.25 (m, 1H)

Method 2: Making of $[ReO(citrate)_2]^-$: NH_4ReO_4 (24.26 mg, 0.09 mmol), sodium citrate dihydrate (145.81 mg, 0.50 mmol) and tin(II) tartrate (110 mg, 0.41 mmol) were combined in a scintillation vial with 5 mL of DI H_2O and stirred at RT for 20 min. **323-MAMA** (46.81 mg, 0.07 mmol) was deprotected using trifluoroacetic acid (750 µL) and triethyl silane (80 µL) with shaking for 4h. The solution was dried using N_2 (g) and washed with hexanes (10 mL, 3 times). The deprotected **323-MAMA** was placed in 5 mL of MeCN and put into a 35 mL snap-cap microwave tube. The $[ReO(citrate)_2]^-$ solution was pipetted into the snap-cap tube containing the deprotected ligand. Reaction microwave settings: 10 min, high stirring, 100ºC. After the reaction mixture cooled to 40ºC (roughly 15 min), the vessel was removed and the solution was deep purple. Solvent was removed *in vacuo* and the desired product was extracted using EtOAc:H_2O, (10 mL of each). The organic layer was dried over anhydrous Na_2SO_4, and solvent removed by rotovap. Solids were washed with hexanes and cold (-30ºC) toluene to remove residual unreacted ligand. Yield: 10.1 mg (0.03 mmol), 36.15%. Analysis same as Method 1.

ReO-323-MAMAhexanoate. Synthesis of $[ReO(citrate)_2]^-$: NH_4ReO_4 (100 mg, 0.37 mmol), sodium citrate dihydrate (7.35 g, 24.99 mmol) and tin(II) tartrate (300 mg, 1.12 mmol) were combined in a round bottom (RB) flask with 30 mL of DI H_2O and stirred at RT for 4 h, until light blue in color, and purged with N_2 (g). **323-MAMAhexanoate** (88.13 mg, 0.10 mmol) was deprotected using trifluoroacetic acid (750 µL) and triethyl silane (80 µL) with shaking for 4 h.

The solution was evaporated using N_2 (g) and the residue was washed with hexanes (10 mL, 3 times). The ligand was placed in a RB flask in 10 mL of MeCN (yellow in color), and 10.86 mL (78.26 mg, 0.13 mmol) of the $[ReO(citrate)_2]^-$ solution was added. The solution was stirred and refluxed 18 h at 90ºC. After cooling to RT, the reaction mixture separated into two layers, with the more organic layer being a deep purple in color. The organic layer was collected and dried *in vacuo*. The residue was extracted with dichloromethane and water (10 mL each) and the organic layer was dried over anhydrous Na_2SO_4 and rotary evaporated to dryness. The remaining residue was washed with 10 mL of hexanes, and 10 mL of cold toluene. The toluene became yellow/green in color (due to removal of excess ligand and a very minor amount of desired product, according to ^{1}H-NMR of extracted undesired products). Remaining residue was washed with $CHCl_3$ to produce a green solution containing **ReO-323-MAMAhexanoate**. Yield: 5.76 mg, 9.82% (total mixture); MS suggests: 4.61 mg (**ReO-323-MAMAhexanoate)**. LC-MS(10-50% MeCN with 0.1% TFA, 30 min, R_t=30.51): 565.25 (calc: 565.12 [$C_{16}H_{29}N_2O_4ReS_2^+$][M+$H^+$])

^{99m}TcO-323-MAMA. A GAS solution (56.4 mM sodium glucoheptonate, 0.25 M HCl, 3.7 mM $SnCl_2$ solution) was prepared. A mixture of **323-MAMA** in MeCN (0.006 M, 0.2 mL), generator eluent (0.3 mL; 370 MBq (10 mCi)), and GAS (0.3 mL) was vortexed and allowed to react at 70 °C for 40 min. An aliquot was removed for radio-TLC yield determination. To the remaining reaction mixture, 0.3 mL of MeCN was added and the entire reaction mixture was filtered with a 0.2 µM filter. The solution of **^{99m}TcO-323-MAMA** was analyzed by radio-HPLC (Jupiter C-18, 10–50% MeCN over 15 min, 1 mL/min; Rt = 12.9 min). %Yield: 13.1. Radiochemical purity: 32.6 ± 4.7%.

^{99m}TcO-323-MAMAhexanoate. A GAS solution (56.4 mM sodium glucoheptonate, 0.25 M HCl, 3.7 mM $SnCl_2$ solution) was prepared. A mixture of **323-MAMAhexanoate** in MeCN (0.006 M, 0.2 mL), generator eluent (0.3 mL; 300 MBq (10 mCi)), and GAS (0.3 mL) was vortexed and allowed to react at 70 °C for 40 min. An aliquot was removed for radio-TLC yield determination. To the remaining solution, 0.3 mL of MeCN was added and the entire solution was filtered with a 0.2 μM filter. The solution of **^{99m}TcO-323-MAMAhexanoate** was analyzed by radio-HPLC (Jupiter C-18, 10–50% MeCN over 15 min, 1 mL/min; Rt = 15.6 min). Radiochemical purity: 4.62 ± 1.3 %.

Results and Discussion

Prior work had been performed by Demoin with the 323-MAMA ligand framework.[7] The purpose of this research is for a comparison between 222-MAMA and 323-MAMA complexes of Re(V) and Tc(V). **Figure 3-2** includes ligand frameworks for 222-MAMA and 323-MAMA derivatives.[7] The majority of the ligand synthesis procedures were followed as reported; slight modifications were made to increase yields of ligands or to afford easier separations. Prior reports of Re(V) and ^{99m}Tc(V) complexed with 323-MAMAhexanoate indicated poor yields or no product, with little characterization performed. [7] Demoin dissertation optimization of studies described in Chapter 2, warranted further investigation of 323-MAMA chelates for Re(V) and ^{99m}Tc. The comparison of 222-MAMA and 323-MAMA would aid in determination of the more stable chelate for potential future studies, as well as verify the computational results of stability found by Demoin. [7]

For the synthesis of the **323-precursor**, acetone was used in place of ethanol, as the triphenylmethane thiol was much more soluble in acetone with gentle heating. The visual color

change of the reaction, from yellow to a light, bubblegum pink, indicated formation of product over time. The adjustment of solvent for this reaction also gave an increased yield of roughly 20% (44.5% to 62%) for the **323-precursor** over previous methods.[7] The **323-precursor** was used as previously described by Demoin, for the synthesis and isolation of **323-MAMA**. For the synthesis of **323-MAMAhexanoate**, the prior report used air-free exclusion techniques and polar solvents with very high boiling points. This procedure was modified to avoid air exclusion and dimethylformamide, which was replaced with dry acetonitrile. This allowed for **323-MAMAhexanoate** to be more easily isolated. The only other conditions that were modified from the previous report were that the overall reaction time was increased, and an adjustment to solvents for product purification. These adjustments resulted in an increase from 26% to 95.2% yield of **323-MAMAhexanoate**.

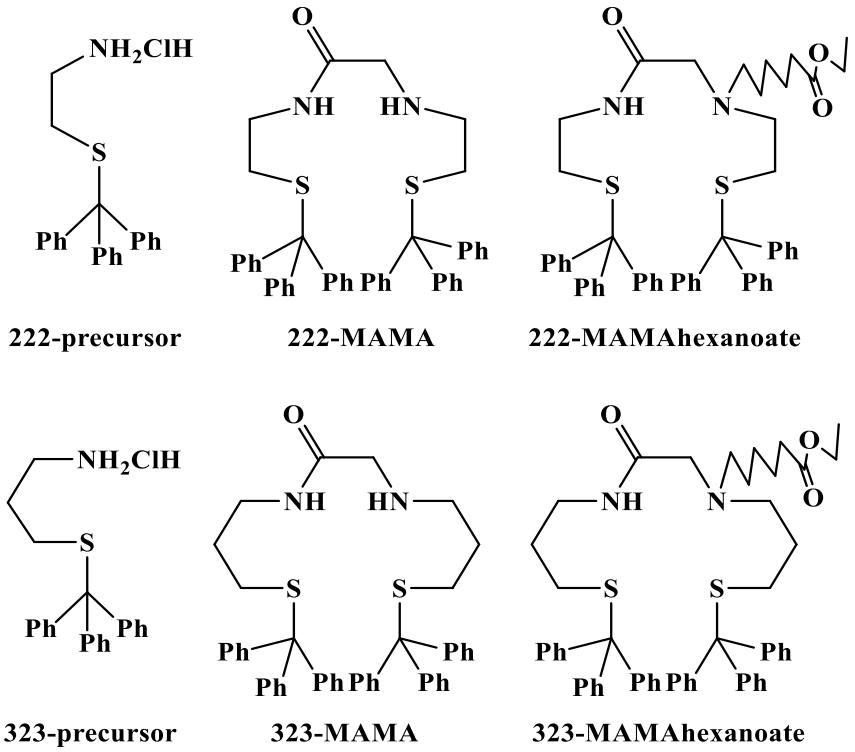

Figure 3-2. Schematic of 222-MAMA and 323-MAMA derivatives.

The original proposed reasoning for the synthesis of 323-MAMA was to determine the preferential ligand framework for complexation to Re(V) and ^{99m}Tc(V). Computational research performed by Demoin indicated a preference in metal chelation for 222-MAMA analogs versus 323-MAMA frameworks. [9] The order of preferred chelation was determined to be: 222-MAMA, 232-MAMA, 323-MAMA, and 333-MAMA. The 232-MAMA would have been the logical next choice in the study of preferred binding. As stated in the introduction, Luyt synthesized 232-N_2S_2 metal complexes [5], with great success. Pillai was also successful in his study of expanded backbone frame works of O_2N_2 ^{99m}Tc complexes [7]; however, starting materials to synthesize 232-MAMA were currently unavailable with only one oxo group in the ligand (i.e., Br, CO, CH_2CH_2Br). This resulted in the choosing 323-MAMA and derivatives for comparison. Prior to complexation, the protecting groups were removed via trifluroracetic acid and triethylsilane to produce the thiols for further reactivity **of 323-MAMA**. For the synthesis of **ReO-323MAMA**, $[ReO(citrate)_2]^-$ was reacted with deprotected **323-MAMA** by two methods. $[ReO(citrate)_2]^-$ is not used as commonly in the literature as other Re(V) starting materials, such as $ReOCl_3(PPh_3)_2$ or $[NBu_4]ReOCl_4$. The advantage of using $[ReO(citrate)_2]^-$ over that of $(PPh_3)_2ReOCl_3$ in the reactions is the avoidance of column separations to remove residual triphenylphosphine and its oxide, a step that reduces yield to product loss on silica gel columns. As previously stated, ReO-MAMA complexes are hydrophobic, thus, separation may be performed by simple extractions to purify complexes when using $[ReO(citrate)_2]^-$. Method one for the formation of **ReO-323MAMA** uses a long reflux, bench top reaction, **Scheme 3-1**, that takes 20 h for completion to produce a yield of 15.53% **ReO-323MAMA**. This reaction procedure afforded crystalline material that was analyzed by X-ray diffraction, **Figure 3-3**, in order to view the binding of Re(V) to **323-MAMA**.

The Re-S and Re-N bond lengths are listed in **Table 3-1**. These values have been compared to the 3,10-diethyl-5,8-diazadodecane-3,10- dithiolato(3-)-N,N',S,S']oxorhenium(IV), a 222-N_2S_2 analog structure reported by Trevor Hambley, **Figure 3-4**.[10] Formation **of ReO-323MAMA** illustrates the ability for Re(V) to coordinate to expanded frameworks. The crystalline product remained stable for over a year; this was confirmed by dissolving the crystalline solid in an acetonitrile solution and motoring HPLC analysis, **Figure 3-5**.

The second method of synthesis for **ReO-323MAMA** utilized microwave synthesis conditions. Microwave synthesis allows for reactions to react a higher temperature, much more quickly than benchtop reactions. This shorter time of reaction can also be useful in the minimization of unwanted side products forming, compared to longer reaction times. Using microwave synthesis methods not only for a decrease in reaction time, from 20 h to 15 min, but also increased the overall yield of the reaction from 15.53% to 42%.

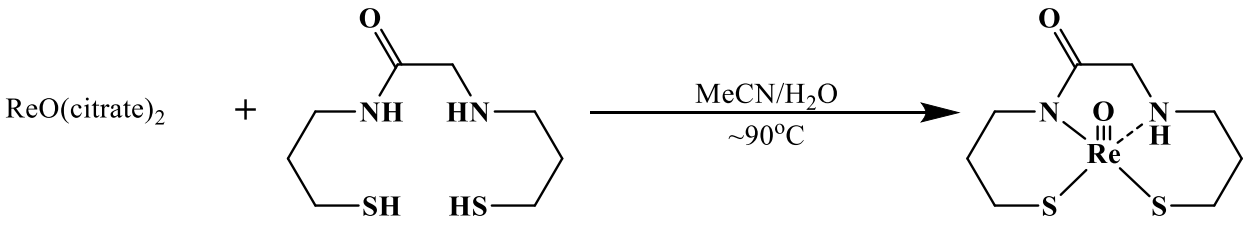

Scheme 3.1. Reaction of $[ReO(citrate)_2]^-$ and deprotected **323-MAMA** to produce **ReO-323MAMA**.

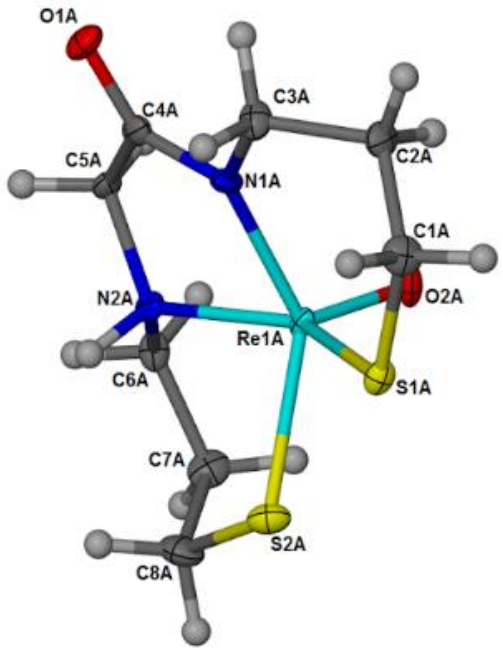

Figure 3-3. Molecular structure of the **ReO-323MAMA** at 50% thermal ellipsoids, solvent removed for clarity.

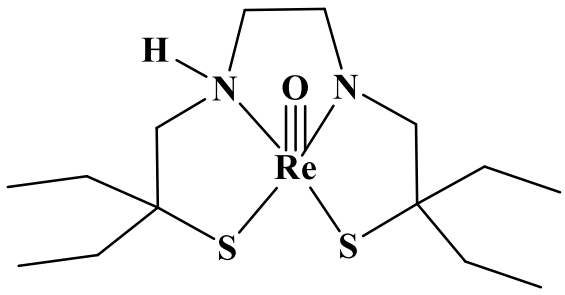

Figure 3-4. Schematic of Hambley crystal structure: 3,10-diethyl-5,8-diazadodecane-3,10-dithiolato(3-)-N,N',S,S']oxorhenium(V). [10]

Table 3-1. Comparison of select bond lengths (Å) and angles between **ReO-323MAMA** and [Re($C_{14}H_{29}N_2S_2$)O]•$CHC1_3$ (**Figure 3-4**). [10] This illustrates the ability of Re(V) to stretch to accommodate binding to a larger framework.

	ReO-323MAMA	[Re($C_{14}H_{29}N_2S_2$)O]•$CHC1_3$
Re(1)-O(1)	1.671(5)	1.737(8)
Re(1)-N(1)	2.015(6)	1.93(1)
Re(1)-N(2)	2.132(6)	2.17(1)
Re(1)-S(1)	2.2813(17)	2.278(4)
Re(1)-S(2)	2.3005(18)	2.260(4)
S(1)-Re-N(1)	92.64(17)˚	82.8(3)˚

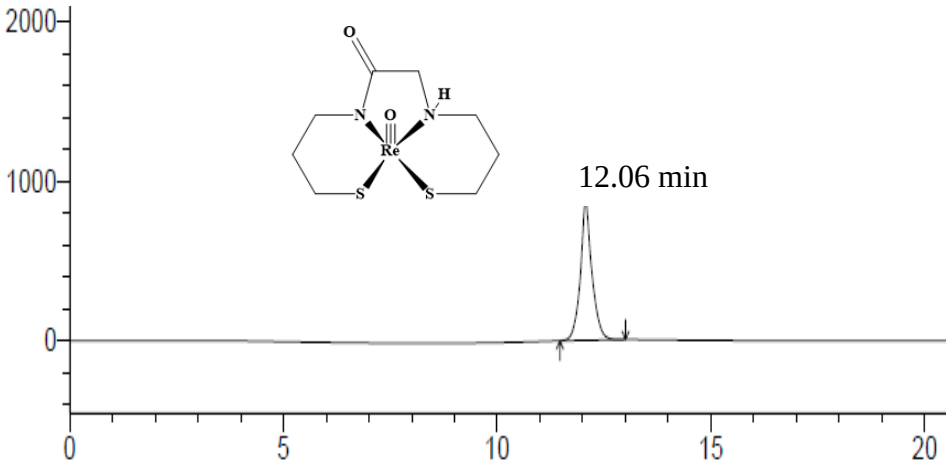

Figure 3-5. HPLC chromatogram of **ReO-323-MAMA**, one year post synthesis (Jupiter C-18,10-50% MeCN with 0.1% TFA over 15 min, 380 nm).

HPLC analysis of reactions on the tracer level mimic Re(V) retention times indicating formation of tracer analogs; ^{99m}Tc(V) reactions were monitored by both radio-HPLC and radio-

TLC. Radio-tracer reactions were performed with acetonitrile present, which affords a higher pH (pH= 3.5), eliminating the need to pH adjust for complexation. It was determined for **^{99m}TcO-323MAMA**, **Figure 3-6**, there is a single peak, by HPLC, at 12.9 minutes that corresponded to the Re(V) analog at 12.1 minutes. The overall reaction yield of **^{99m}TcO-323MAMA** was determined to be 13% according to radio-TLC analysis.

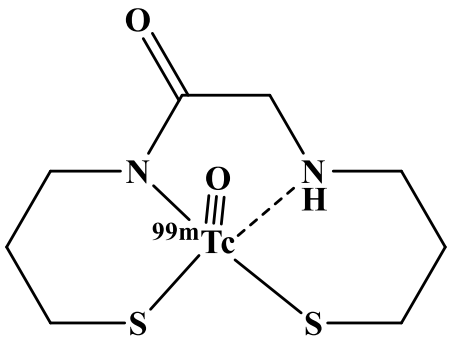

Figure 3-6. Schematic of **^{99m}TcO-323MAMA.**

Moving forward with studies post success of **323-MAMA** complexes, **323-MAMAhexanoate** was attempted for metal chelation. Prior to reaction with rhenium, deprotection of **323-MAMAhexanoate** using trifluoroacetic acid and triethylsilane was done by shaking for 4 hours. This solution was then washed 3-4 times with hexanes and solvent evaporated with N_2 (g). ^{1}H-NMR was performed to confirm deprotection prior to chelation. With this analysis, it was determined that hydrolysis of **323-MAMAhexanoate** had occurred, as a mixture of the hexanoate and the hexanoic acid derivatives was observed by the addition of OH protons in the ^{1}H-NMR spectra. This peak in ^{1}H-NMR was only be observed in polar organic solvents, excluding alcohols, which may have caused the hydrolysis to be unnoticed in previous reports. Hydrolysis was less

prevalent with the 222- derivative of the MAMA-hexanoate ligand and did not affect the reactivity of 222-MAMAhexanoate with metal centers.

Chelation of **323-MAMAhexanoate** to both Re(V) and ^{99m}Tc, **Scheme 3-2**, proved difficult, and yields were greatly reduced. $[ReO(citrate)_2]^-$ was reacted with **323-MAMAhexanoate** for 20 h at 90ºC. This reaction produced a similar color to its analog ReO-222-MAMAhexanoate, a very deep purple/brown. Upon drying the separated organic layer, as described above, the dark residue became insoluble in organic solvents, and instead a green solution formed. When analyzed via ^{1}H-NMR, this green solution was determined to be a mixture of the desired **ReO-323-MAMAhex**, and a small amount of unreacted ligand. LC-MS characterization revealed a mixture of ligand starting material and desired product, **Figure 3-7**. The product overlap made the mixture difficult to purify. The decreased yield between ReO-222-MAMAhex and **ReO-323-MAMAhex** follows the trend observed by Demoin's calculations with 222-MAMA being the thermodynamically preferred chelate. [9] Attempts to synthesize **ReO-323-MAMAhex** in the microwave to increase yields proved unsuccessful.

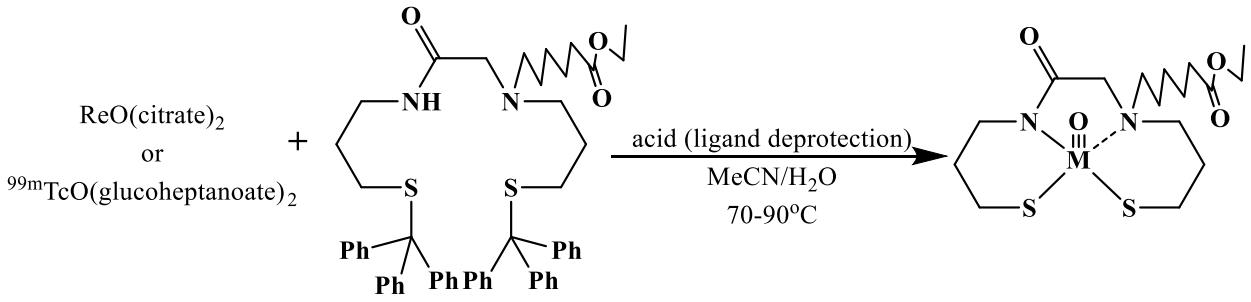

Scheme 3-2. General reaction scheme for **ReO-323-MAMAhex** and **^{99m}TcO-323MAMAhex**.

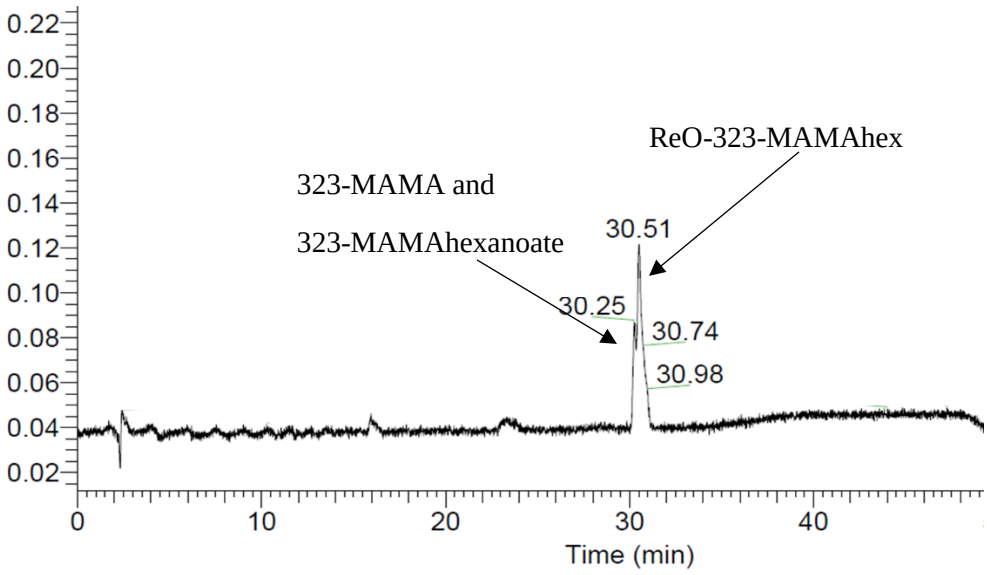

Figure 3-7. LC-MS chromatogram of **ReO-323-MAMAhex**. The First peak at 30.25 min corresponds to **323-MAMAhexanoate** ligand and the 30.51 minute to **ReO-323-MAMAhex**.

323-MAMAhexanoate reacted with ^{99m}Tc produced 3 species in the radio-HPLC. These peaks were small in area, but determined to correlate to **^{99m}TcO-323MAMA**, **^{99m}TcO-323hexanoic acid**, and **^{99m}TcO-323MAMAhex**. This indicated some **323-MAMA** impurity remained from the reaction to produce **323-MAMAhexanote**. Minor impurities observed by ^{1}H-NMR indicate a mixture of products in the ligand starting material. The formation of **^{99m}TcO-323MAMA** is much more readily observed over that of **^{99m}TcO-323MAMAhex**. The amount of ^{99m}Tc-MAMA product formation correlated to 19.2% total according to radio-TLC. The results for the 323-MAMA chelated complexes concur with the difficulty of product formation found by Demoin. Some advances were made in increasing yields for characterization purposes.

Much like the study performed by Kung et al to show ligand preference [11], we wanted to determine the relative propensity for metal-ligand chelation between 222-MAMA and 323-

MAMA. According to calculations performed by Demoin, the order of ligand preference for Re(V) and ^{99m}Tc(V) should go as follows: 222-BAT≈ 222-MAMA> 323-MAMA. [9] In order to do this study, we combined 10 mCi of $^{99m}TcO_4^{1-}$, 0.5 mg of ligand in 0.1 mL MeCN (each ligand, listed in combinations below), and 0.3 mL GAS solution in a snap cap vial. The reaction mixture was heated to 70ºC, with gentle stirring. At 40 minute intervals, 0.1 mL of the reaction solution was removed and 0.3 mL of MeCN was added to ensure that the desired complexes did not stick to the filter. The ligand combinations were **323-MAMA** with 222-MAMAhexanoate, and **323-MAMAhexanoate** with 222-MAMA, **Scheme 3-3**. The purpose for this was to avoid overlap of HPLC peaks, as ring size alone does not alter the retention time enough for separation, but the addition of linker on the amine does. Injections (10 µCi in 150 µL solution) were monitored by radio-HPLC. For the reaction between 323-MAMA and 222-hexanoate, the amount of **^{99m}TcO-323MAMA** produced went from 13.8% to 3.54% over the course of 3 h monitoring. The amount of ^{99m}TcO-222hexanoate, increased from 86.2% to 96.46% according to radio-HPLC. For the reaction between 323-hexanoate and 222-MAMA, almost no **^{99m}TcO-323MAMAhex** product could be detected (<1%). These results point to a preference for chelation of 222-MAMA ligands over that of the 323-MAMA ligands. This preference can be explained by the difference in size of the two coordination ligand cavities.

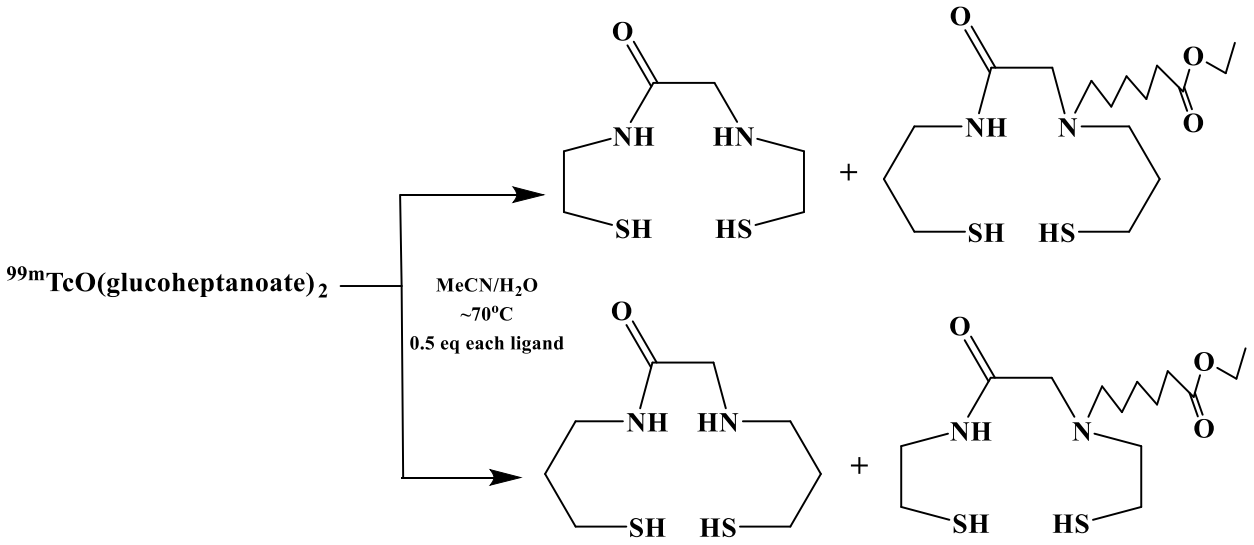

Scheme 3-3. Reaction conditions for competition study of 222-MAMA and 323-MAMA ligand frameworks.

To attempt another approach to determine the favored chelate, we evaluated if once coordinated to a metal center, the 222-MAMA chelate would be able to displace the 323-MAMA in **^{99m}TcO-323MAMA**. This experiment was performed by reacting 323-MAMA with ^{99m}Tc to produce **^{99m}TcO-323MAMA**. The product was isolated by collecting radio-HPLC fractions, and 0.25 mg 222-MAMAhexanoate in 50 µL acetonitrile was added to the solution, along with 3 µL of concentrated HCl for deprotection of the 222-MAMAhexanoate. The combination was heated at 70ºC and aliquots were removed at 40 minutes and 160 minutes. Fractions on the order of 3 µCi and 5 µCi, respective to time point, were analyzed for changes in radio-HPLC, as an indication of product conversion. Surprisingly, it was observed that little change in product distribution occurred; only **^{99m}TcO-323MAMA**, with a minor amount of $^{99m}TcO_4^{1-}$ from degradation of the overall product was observed with time. There was a very small peak at 15 minutes indicating formation of a ^{99m}TcO-222MAMA product; however, this could result from the reaction of 222-

MAMAhexanoate with pertechnetate that had formed in solution. This was still less than 2% of the overall products in the reaction mixture. These competition reactions, and the overall yields associated with Re and ^{99m}Tc MAMA complexation, illustrate that 222-MAMA analogs do have a preference for binding over the 323-MAMA chelates to these metals. However, unlike the experiments performed by Kung, where it was shown that various MAMA ligands were able to compete with bisaminoethanethiol (BAT) chelated technetium complexes with a preference for MAMA chelation, these complexes did not show a conversion of coordinated products.[11]

Conclusion

Monoamine-monoamide ligands, **323-MAMA** and **323-MAMAhexanoate**, have been shown to chelate to Re(V) and ^{99m}Tc(V). The crystallographic structure of **ReO-323MAMA** allowed its comparison to that of the previously reported 222-MAMA analogs in the literature. Preference between 222-MAMA and 323-MAMA derivatives for ^{99m}Tc chelation has been determined and shows a preference of binding for the 222-MAMA analogs. Preliminary studies suggest that once complexes are formed, they remain stable with time and against binding of 222-MAMA ligand framework analogs. Further research needs to be developed to increase the hydrophilic nature of these ligand frameworks in order to continue this research towards potential radiopharmaceutical use. The 323-MAMA will not be pursued in future studies with Re(V) and ^{99m}Tc(V), though it may find better applications in other areas of radiological studies.

Chapter 4: Synthetic Evaluation of Tetrathioether Rhodium(III) Complexes: Precursor Exploration for Radiopharmaceutical Targeting Vectors

Introduction

Radiotherapy involves the use of radionuclides to image or annihilate cancer cells. There are several approaches that include selection of the nuclide to specifically target or selection of a conjugated chelate to targets receptors on tumors. Focus has been with no particular type of emission (α, $\beta^{+/-}$, γ), but more on the cost to benefit ratio of treatment and availability. Metals with alpha emissions are gaining ground in research as more and more studies are being done; however, most of the current treatment agents use some combination of beta and gamma emitting radionuclide. Beta particles have the ability to "kill" cancer cells and are more preferred for larger tumors as they have a larger range of emission (0.2–12 mm range in tissue).[1] For biological ingestion or injection, consideration of the half-life of a radionuclide is very important for patients. If the half-life is too short, the complex does not have enough time to accumulate at the desired target site and the risk of degradation and unnecessary radiation or toxicity builds up. If the half-life is too long, patients much be kept under monitor, until sufficient decay and excretion can occur. This would mean more time under hospital care, which can be costly. Another important consideration with nuclear medicine, from a bifunctional chelate stand point, is to determine the right kind of chelate to keep the metal bound until the complex has sufficient time to target and to clear the body. For example, when ^{99m}Tc is oxidized, pertechnetate will accumulate in areas such as the stomach and salivary glands. This gives areas of unwanted radiation in a patient and depending on the area that needs to be imaged, can prevent valuable information from being obtained. Bifunctional chelates for radionuclides cover a wide variety of research. Most of the area of research focuses on two main components, diagnostics and radiotherapy of cancer. The chelate

plays a largest role in how the complex is handled in the body. If working with a complex that is extremely lipophilic, clearance through the hepatobiliary system leads to uptake in the liver and intestines inhibits imaging of tumors and gives an unnecessary radiation dose to normal (healthy) tissues located in the same area.

In previous work, ^{105}Rh has been studied as a potential radiotherapuetic nuclide due to its promising nuclear properties. ^{105}Rh has a dual use, both a 566 keV β^-_{max} emission useful for therapy of solid tumors, as well as accompanying γ emmissons (319 keV [19%], 306 keV [5%]) that are useful for diagnostics and monitoring.[2] With a moderate half-life of 35.36 h, and the ability to be produced in high specific activity from neutron irradiation of ^{104}Ru, ^{105}Rh has the potential to be shipped over long distances as needed. When considering the chemistry of rhodium, it is a borderline soft Lewis acid, preferring soft donor atoms such as sulfur. The most common oxidation states are 3+ and 1+, with the 3+ being more important for nuclear medicinde application and the 1+ for catalytic applications.[3] Rhodium(III) forms kinetically inert, low spin metal complexes, which have octahedral geometries. In order for complexes to form with Rh(III), catalytic reduction from 3+ to 1+ needs to occur. The use of refluxing alcohol in order to synthesize Rh(III) complexes has long been used in the literature. Milutinović used ethanol in a recent paper to synthesize Rh(III) pincer complexes for biomolecule study. [4] Exchange from Rh(III) to Rh(I) was first observed by M. Delphine, reporting a mechanism that involves a 2 electron reduction of Rh(III) to an intermediate Rh(I) generating acetaldehyde from ethanol, **Figure 4-1**. The mechanism, described below, was confirmed by detection of trace amounts of acetaldehyde.[5] Rhodium reactions are generally performed in acidic media due to Rh(III) being highly sensitive to changes in pH and form insoluble $Rh(OH)_3$ in basic solutions. Due to the kinetic inertness of Rh(III), once such species are formed they cannot be easily converted back to a soluble products.[6]

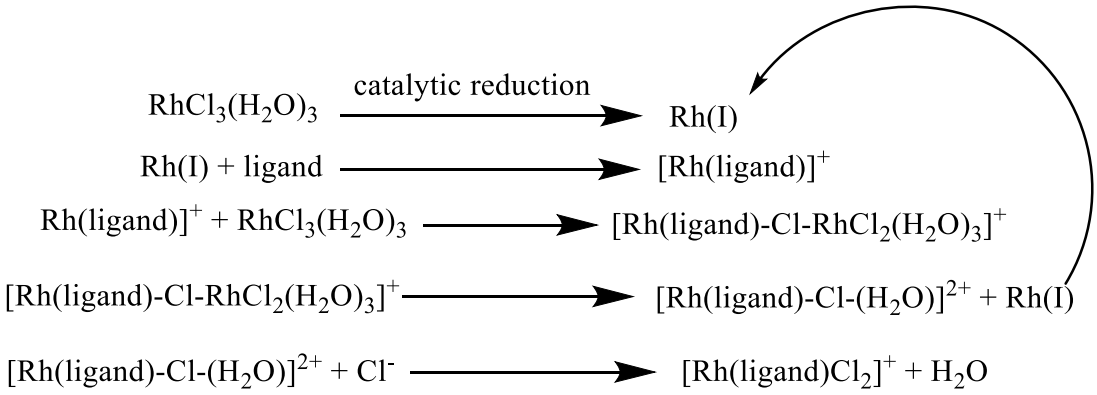

Figure 4-1. Ligand exchange process catalyzed by reduction of Rh(III). In the first step Rh(III) is catalyzed with hot EtOH to produce Rh(I). The reduced metal reacts with ligand in solution, forming an intermediate product. The cycle continues until the rhodium in solution has been converted and reacted in solution. [5]

Early examples of ^{105}Rh complexes include research with frameworks such as cyclam and cyclen derivatives (**Figure 4-2**). Cyclam has the ability to provide a substrate for octahedral substitution, which is the preferred binding configuration for Rh(III) systems.[7] The cyclic framework coordinates the four equatorial sites of the octahedron, with the remaining two sites occupied by monodentate ligands such as chloride. Kruper et al. reported the synthesis of three cyclam ^{105}Rh derivatives and radiochemical yields of >85% were achieved.[8] Other researchers continued the progression by using a combination of N and O donor groups, including work by Troutner et al. Using oxime ligands, non-radioactive rhodium(III) complexes were synthesized in order to understand the octahedral binding, using X-ray crystallographic data to fully characterize.[9] The ^{105}Rh bidentate oximes were found to have high radiochemical yields for desired complexes, with conjugation yields of greater than 90% with human γ-globulin. These

Rh(III) oxime complexes also proved suitable when ^{105}Rh radiolabeled complexes were studied for antibody receptor targeting.[10]

At this time there was a shift in Rh(III) chemistry that change the focus from harder donor atoms, N or O, to more soft S donor atoms; which rhodium(III) is much better suited for as previously stated.[12] Venkatesh et al. reported the carrier free synthesis of a ^{105}Rh-[16]ane-S4-diol with >90% radiochemical yield, **Figure 4-3**.[11] Li built off of these ligand frameworks and synthesized a carboxylic acid functionalized S_4 macrocycle (**Figure 4-4**), which was coupled to a bombesin derivative, giving a radiochemical yield of 95 ± 5% of the ^{105}Rh-S4-5-Ava-BBN. A GRP receptor specific uptake of 2.25 ± 1.02 %ID/tumor was found in the normal pancreas at 2 h. [13] However, large uptake was also noted in the liver, kidney, and intestines, noting that changes to the overall bifunctional chelate would need to be made to enhance urinary clearance for treating prostate tumors. Another deterrent to ^{105}Rh-S4-5-Ava-BBN was that sufficient yields of complexation, greater than 90%, required harsh conditions (3 h heating at 80ºC), which are problematic for consideration of translation to more temperature sensitive antibody ligand couplings that are temperature sensitive.[13]

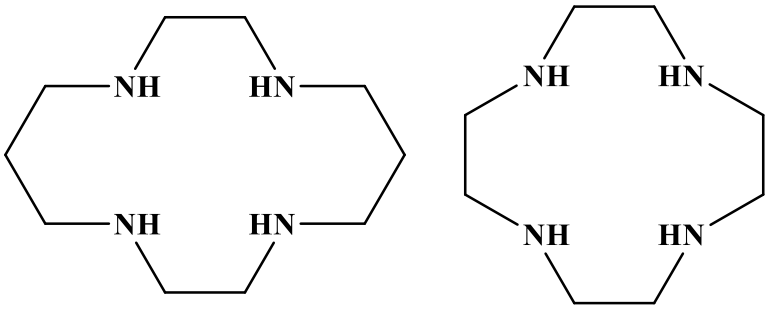

Figure 4-2. Schematic of un-derivatized cyclam (left) and cyclen (right), used in early Rh(III) chemistry. [8]

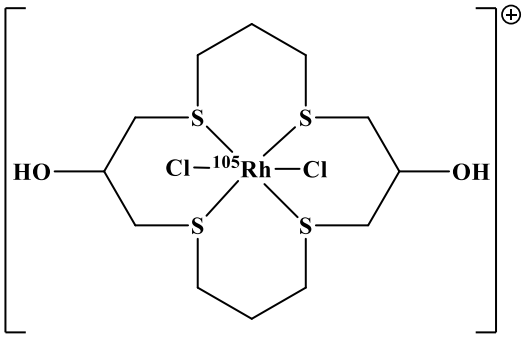

Figure 4-3. Schematic of ^{105}Rh-[16]ane-S4-diol by Venkatesh [11]

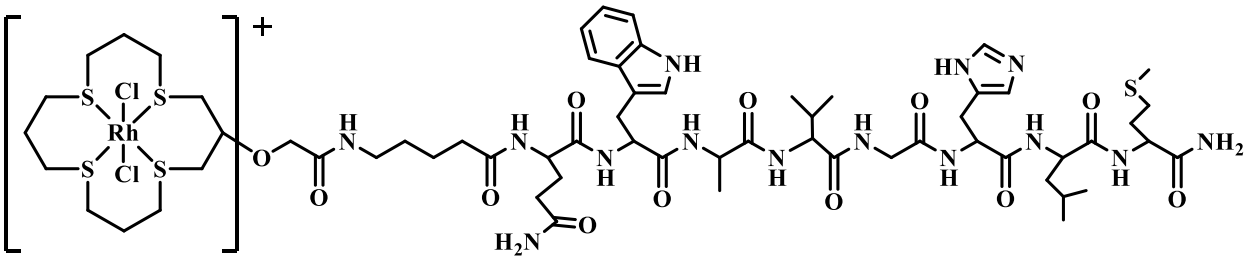

Figure 4-4. Rh-S_4-5-Ava-BBN(7-14)NH_2. [13]

Acyclic tetrathioether Rh(III)-S_4 complexes were reported by Goswami in order to determine if utilizing an acyclic ligand system, as opposed to a macrocyclic framework, would result in higher radiolabelling yields with shorter reaction times. [15] Four ligand frameworks were originally studied: 222-S_4, 232-S_4, 333-S_4, and 323-S_4, **Figure 4-5**. The number denotation before the S_4 in the list of ligands refers to the number carbon linkers between coordinating atoms, as in previous chapters. These ligands were synthesized with either dicarboxylic acid pendant groups or dibenzyl pendant groups. Complexes with dibenzyl pendant arms were analyzed by single diffraction X-ray crystallography. These structures afforded information about the coordination to Rh(III), as well as the coordinating chlorides. In the larger cavity frames of the S_4 ligands, chlorides

were bound *trans* to each other; the *cis* formation was adopted for coordinating chlorides with smaller cavity ligands. There were also some mixed species, both *cis* and *trans*, formed based on the structure's cavity arrangement. Out of the four complexes studied, only the 222-S_4 and the 333-S_4 ligands resulted in a reported single isomer upon complexation with Rh(III) on the macroscopic scale, resulting in *cis* and *trans*-chloro Rh(IIII) complexes, respectively. [14,15] To further assess the reactivity of Rh(III), the 222-S_4 and 333-S_4 ligands were radiolabeled by refluxing a solution of the ligand in 40% ethanol with a weakly acidic pH 4 -5 solution of $^{105}RhCl_3$, producing radiochemical yields of >95%.

Carroll extended the project started by Goswami to further analyze the complexes in preparation for *in vivo* studies.[16] Rh(333-S_4) complexes were synthesized on both the macroscopic and tracer scales. Upon reaction, issues arose with the repeating synthesis of the tetrathioether ^{105}Rh(III) complexes. Using refluxing ethanol as the reductant for the metal center, in conjunction with ligands containing carboxylic acid pendent arms and the presence of HCl resulted in multiple isomers, **Figure 4-6**. This was much more prevalent on the tracer scale, as at least four different isomers were formed according to HPLC. The discovery of multiple products being formed in solution was also coupled with low radiotracer yields, calling for routes of synthesis to be re-evaluated.

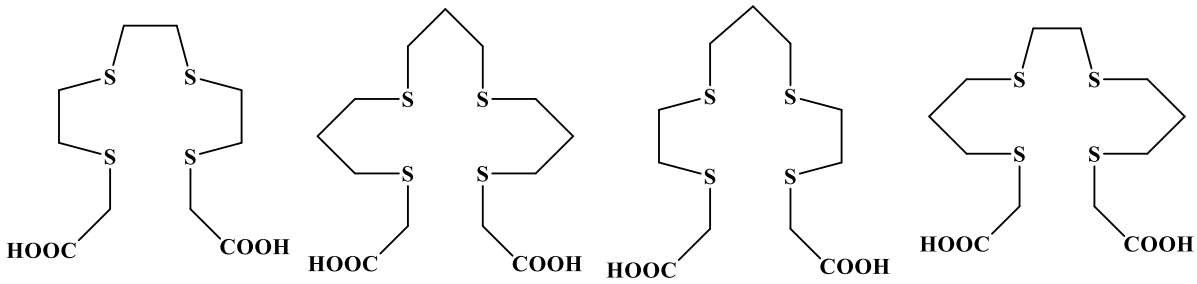

Figure 4-5. Ligand frameworks studied by Goswami:

222-, 333-, 232-, 323-S_4-diAcOH, respectively [15]

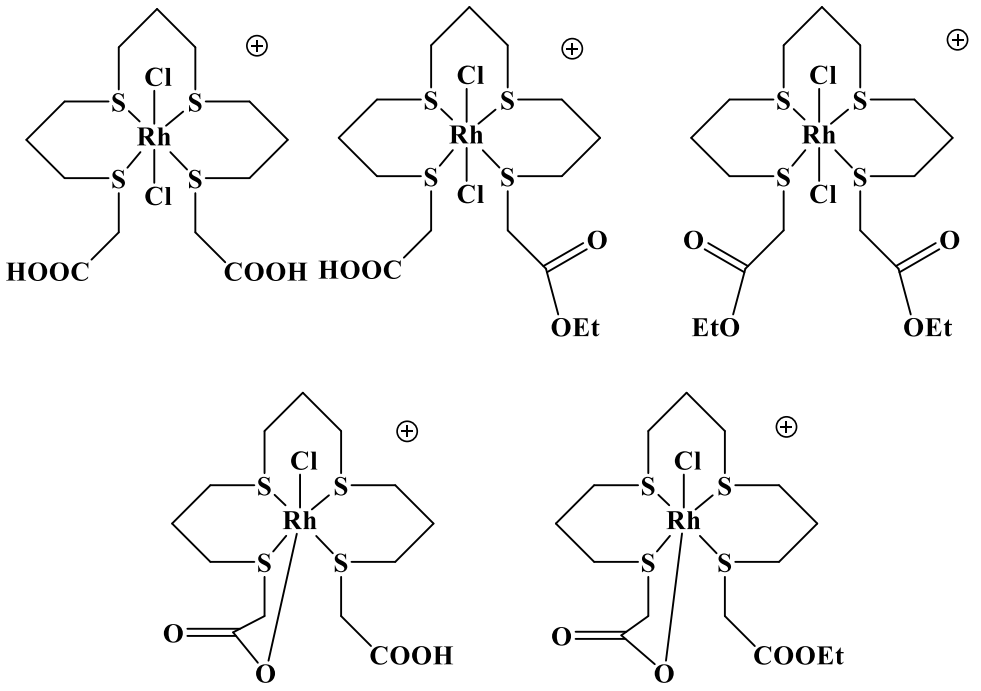

Figure 4-6. Rh-333-S_4-diAcOH complexes formed by Carroll using ethanol. [16]

It was proposed that the exchange of ethanol by tin(II) chloride as a catalytic reductant could reduce the affinity for the formation of multiple isomeric species caused by alcohol reacting with the carboxylic acid pendant arms. The investigation of tin(II) chloride was initially carried out by Creshaw using the same 333-S_4-diAcOH framework as Carroll. [17] It was reported that with the change in reductant, 3 main species were present upon reaction of Rh(III) with 333-S_4-diAcOH. This proved to be a better route of production, reducing the number of unwanted species, however there was still more flexibility to the 333-S_4 ligand, showing as minor impurities in HPLC analysis.

Goswami found in his research that 222-S_4-diAcOH ligand showed the greatest stability in PBS solutions, over the course of 5 days, from 97% to 95%; whereas ^{105}Rh-333-S_4-diAcOH showed a lower stability, from 90% to 80%. [14] Both have what would be considered sufficient

stablility for *in vivo* studies. With the results shown by Carroll, noting a variety of complexes being formed in solution using ethanol as the reductant, these low complexation yields could be attributed to multiple species forming.[16,17] To determine if reaction conditions are affecting overall *in vivo* results, the chemistry of macroscopic and tracer reactions needed to be further investigated. Building off the promising results of tin(II) being used as a reductant limiting possible side products, herein we report the synthesis of Rh(222-S_4)X_2 complexes using $SnCl_2$ as a reductant.

Methods

General methods

All chemicals, unless otherwise indicated, were commercially available and used without further purification. Microwave reactions were performed using a CEM Discover SP Activent, model 909150 instrument. NMR studies were performed with a Bruker DRX 300 or 500 MHz Spectrometer (as noted). HPLC analyses were performed with a Shimadzu HPLC system outfitted with UV-vis detector set to monitor at 220 and 280 nm. The HPLC column was a Jupiter C-18 column (Phenomenex, Torrance, CA, 250 mm × 4.60 mm, 5 μm, 300 Å pore size). All HPLC mobile phases used acetonitrile (MeCN) in water with 0.1% trifluoroacetic acid (TFA); the specific conditions (i.e., column, gradient, flow rate) are indicated for purifications and analyses. A Beckman Coulter HPLC system in series with an ion trap mass analyzer (a LCQ FLEET instrument, Thermo Fisher Scientific, with positive ion ionization) was used to obtain LC/ESI-MS results (Betabasic-18, percentage of MeCN with 0.1%TFA, varied by reaction). **Intermediate 1**, **222-S_4-diAcOMe**, and **222-S_4-diAcOH** were synthesized using a modified procedure.[18]

Synthesis

Methyl 2-((2-chloroethyl)thio)acetate (Intermediate 1). While stirring at RT the following were added to a 500 mL RB flask: 1,2-dichloroethane (1119 mmol, 88.6 mL) and triethylamine (123.01 mmol, 17.15 mL). The reaction was then heated to reflux (90ºC) and methyl mercaptoacetate was added dropwise (111.83 mmol, 10 mL). A condenser was added and N_2 (gas, dry) was added to the reaction, to keep the reaction under inert conditions. The reaction was checked for completion via TLC for the absence of methyl mercaptoacetate (50/50 hexanes, ethyl ether). After 18h, the reaction was cooled to RT and ethyl ether (200 mL) was added to precipitate trimethylammonium salts. The reaction was filtered and solids were washed with ethyl ether. The filtrate volume was reduced to 1 mL *in vacuo* (60-70ºC). A silica gel column (50:1 ratio silica) with hexanes: ethyl ether, and the reaction mixture was loaded. Fractions were collected (R_f=0.5) and combined. Upon solvent removal, **Intermediate 1** as an oily product was isolated. Yield: 14.75 g, 78.2%. ^{1}HNMR (500MHz, $CDCl_3$): 3.72 (s, C**H**$_3$, 3H), 3.66 (t, C**H**$_2$Cl, 2H), 3.26 (s, C**H**$_2$COO, 2H), 2.97 (t, CH_2C**H**$_2$S, 2H). ^{13}CNMR (500MHz, $CDCl_3$): 170.67 (1C, COOMe), 52.63 (1C, OCH_3), 42.68 (1C, CH_2), 34.77 (1C, CH_2), 33.59 (1C, CH_2S).

Dimethyl 3,6,9,12-tetrathiotetradecanedioate (222-S$_4$-diAcOMe). **Intermediate 1** (9.01 g, 53.36 mmol), trimethylamine (7.44 mL, 53.36 mmol), and 1,2-dithioethane (1.79 mL, 21.34 mmol) were combined in a 500 mL RB flask, along with 10 mL of benzene. The reaction mixture was heated to reflux under N_2 (gas, dry) at 100ºC. Completion was determined by TLC analysis for disappearance of 1,2-dithioethane (R_f= 0.5) using 80:20 hexanes:ethyl ether. After 28 h, the reaction was cooled to RT and ethyl ether (20 mL) was added to precipitate trimethylammonium salts. The salts were removed via filtration and washed with several portions of ethyl ether. Solvent

was removed by rotary evaporation to produce a crude oily product. This was recrystallized from hot ether, by quickly cooling (-10ºC). Further workup included separation via silica gel column (200 g, 4 x 35 cm) and eluting with the following: 80:20 hexanes:ethyl ether, 50:50 hexanes/ethyl ether. Like products were combined (R_f=0.05, in 80:20 hexanes:ethyl ether) and dried to yield **222-S_4-diAcOMe**. Yield: 3.4 g, 44.4%. ^{1}H-NMR (500MHz, acetone-d_6): 3.68 (s, 6H, OC**H**$_3$), 3.34 (s, 4H, C**H**$_2$COO), 2.85- 2.89 (m 4H, C**H**$_2$), 2.81- 2.83 (m, 4H, C**H**$_2$), 2.80 (s, 4H, SC**H**$_2$C**H**$_2$S). ^{13}C-NMR (500MHz, acetone-d_6): 166.6 (2C, **C**OOMe), 52.32 (2C, **C**H$_3$), 39.17 (2C, S**C**H$_2$), 33.28 (2C, **C**H$_2$), 33.06 (2C, **C**H$_2$), 32.57 (2C, **C**H$_2$).

3,6,9,12-tetrathiatetrodecanedioic acid (222-S_4-diAcOH). **222-S_4-diAcOMe** (0.538 g, 1.50 mmol), was dissolved in 10 mL 0.7 M KOH in methanol. The reaction mixture was added to a 35 mL snap cap tube and microwaved for 15 min at 90ºC. Solid particulates were removed via filtration and washed with dry methanol. Crude solids were dissolved in 20 mL of DI H_2O and 6 M HCl was added dropwise (pH=1, 5 mL) to produce **222-S_4-diAcOH**. The solid was collected over a glass frit, washed with 2M HCl, pH=1 and dried *in vacuo*. 0.342 g **222-S_4-diAcOH** was produced. Yield: 66%. ^{1}H-NMR: previously characterized [18]

[$RhCl_2$-222-S_4-diAcOMe]Cl. $RhCl_3$• $3H_2O$ (50.1 mg, 0.19 mmol) and **222-S_4-diAcOMe** (92.7 mg, 0.26 mmol) were placed in a 100 mL RB flask with 25 mL of MeCN. This mixture was heated to 80ºC for 15 min while stirring. $SnCl_2$ (22.2 mg, 0.098 mmol) was added to the stirring solution. The reaction was refluxed at 90ºC for 1h. The solution turned from orange to yellow in color. The reaction mixture was cooled to RT, and allowed to precipitate overnight. The yellow precipitate

was filtered using a frit and washed with Et_2O. The supernatant was allowed to evaporate slowly to produce further crops of solid product, which were collected and washed with Et_2O to yield **[RhCl$_2$-222-S$_4$-diAcOMe]Cl**. All solids were combined and dried *in vacuo* to yield 65.1 mg (60.4%). ^{1}H-NMR (500MHz, DMSO-d_6): 4.409 (m, 2H, SC**H**$_2$C), 4.115 (m, 2H, SC**H**$_2$C), 3.72 (s, 6H, OC**H**$_3$), 3.65 (m, 4H, C**H**$_2$), 3.57 (m, 4H, C**H**$_2$), 3.19 (m, 4H, C**H**$_2$). HPLC (Betabasic C-18, 10-30% MeCN with 0.1%TFA over 20 min): 14.91 min. LC-MS (Betabasic 10-50% MeCN with 0.1%TFA over 30 min= 14.6 min) 532.6 (calc. 531.88 $[C_{12}H_{22}Cl_2O_4RhS_4]^+$ [M+ H^+]).

[RhCl$_2$-222-S$_4$-diAcOMe)]PF$_6$. *Method 1*: $RhCl_3$• $3H_2O$ (50.55 mg, 0.19 mmol), and **222-S$_4$-diAcOMe** (93.61 mg, 0.26 mmol) were placed in a 100 mL RB flask with 30 mL MeCN and 15 mL of DI H_2O. This mixture was heated to 60ºC while stirring, for 15 min. $SnCl_2$ (35 mg, 0.16 mmol) was added to the stirring solution, and the reaction was refluxed at 90ºC for 1h. The reaction mixture became orange in color. The orange solution was brought to RT and was centrifuged. The supernatant was removed and cooled in an ice bath (0ºC, 5-10 min). NH_4PF_6 (34.6 mg, 0.21 mmol) was added and stirring on ice proceeded for 10 min, followed by 5 min at RT. The solvent was removed by rotory evaporation and the solids were extracted using dichloromethane and DI H_2O(15 mL of each). The organic layer contained residual unreacted ligand. Solid formation of the desired product occurred at the interface of the two phases. The product was filtered to remove and dried *in vacuo* to yield: 75.4 mg (58%). XRD crystals of **[RhCl$_2$-222-S$_4$-diAcOMe]PF$_6$** were obtained from acetone. ^{1}H-NMR: same as **[RhCl$_2$-222-S$_4$-diAcOMe]Cl**. ^{31}P-NMR: -154 to -131 (septet). HPLC (Jupiter column, 10-50% MeCN with 0.1%TFA, in 30 min)= 30.58 min. LC-MS (Betabasic C-18, 10-50% MeCN with 0.1%TFA, in 30 min= 30.1 min): 531.07 (calc. 531.88 $[C_{12}H_{22}Cl_2O_4RhS_4]^+$ [M+ H^+])

Method 2: $RhCl_3$• $3H_2O$ (26.1 mg, 0.1 mmol), **222-S_4-diAcOMe** (59.86 mg, 0.17 mmol), and $SnCl_2$ (17.9mg, 0.08 mmol) were place in a 35 mL snap cap tube with 10 mL of MeCN and 2 mL of DI H_2O. This mixture, yellow in color, was microwaved at 90ºC for 15 min while stirring. The reaction mixture was brought to RT and NH_4PF_6 (20.1 mg, 0.12 mmol) was added; stirring on ice proceeded for 15 min. Solid precipitate from the reaction mixture was determined to be **[$RhCl_2$-222-S_4-diAcOMe]Cl**. The mixture was centrifuged, separated, and the solvent was removed from the supernatant by rotary evaporation. The crude product was extracted using chloroform and DI H_2O (10 mL of each). Solid formation at the interface of solvent layer phases occurred and the reaction mixture was filtered to obtain the desired **[$RhCl_2$-222-S_4-diAcOMe]PF_6**. Solids were dried to yield 62.45 mg (93%). Characterization matched Method 1.

[Rh Cl_2 -222S_4-diAcOH]Cl. *Method 1*: $RhCl_3$• $3H_2O$ (51.9 mg, 0.2 mmol), **222S_4-diAcOH** (50.9 mg, 0.15 mmol), and $SnCl_2$ (48 mg, 0.21 mmol) were placed in a 35 mL (covered) snap cap tube with 6 mL of MeCN and 4 mL of DI H_2O. This mixture, yellow in color, was microwaved at 90ºC for 15 min, while stirring. The reaction was brought to RT, centrifuged and solvent removed by rotary evaporation. The crude product was extracted with chloroform and DI H_2O (10 mL of each). The desired product was in the aqueous layer. The solution was dried to yield (total) 71.4 mg (92.3%). HPLC (Jupiter column, 2% MeCN with 0.1% TFA for 5 min, and 5-35% over 45 min, 280 nm): 8.79 min. LC-MS (Betabasic C-18, same as HPLC= 2.33-4.45 min (3 peaks)): 432.5, 468.2, 503.1 (calc: 430.9 ($[C_{10}H_{16}O_4RhS_4]^+$), 466.87 ($[C_{10}H_{17}ClO_4RhS_4]^+$), 502.85 ($[C_{10}H_{18}Cl_2O_4RhS_4]^+$)).

Method 2: $RhCl_3$• $3H_2O$ (25.88 mg, 0.1 mmol), **222-S_4-diAcOH** (24.8 mg, 0.08 mmol), and $SnCl_2$ (10 mg, 0.04 mmol) were placed in a 35 mL snap cap tube, covered in aluminum foil, with 4 mL

of DI H_2O. This mixture (removed of foil), yellow in color, was microwaved at 100ºC for 10 min, while stirring. The reaction was brought to RT (pH=1) and 11 mL of DI H_2O was added. This was centrifuged and the solvent removed. The solids were washed once more with 15 mL of water, centrifuged, and the supernatant collected. The solutions were combined and dried via rotary evaporation. Yield (total): 33.98 mg, 90.2%. HPLC (Jupiter column, 2% MeCN with 0.1% TFA for 5 min, and 5-35% over 45 min):13.10 min. LC-MS (Betabasic C18, same as HPLC= 2.5-13.9 min): 430.97, 467.76, 502.96 (calc: 430.9 ($[C_{10}H_{16}O_4RhS_4]^+$), 466.87 ($[C_{10}H_{17}ClO_4RhS_4]^+$), 502.85 ($[C_{10}H_{18}Cl_2O_4RhS_4]^+$))

Results and Discussion

As stated in the introduction, Goswami reported preliminary results showing that 222-S4-diAcOH ligand possessed a greater stability in solution [15], over the 333-S_4 analog, studied by Carroll and Crenshaw. Crenshaw was able to observe three main isomers with the synthesis of [Rh-333-S_4diAcOHCl_2]Cl using Sn(II) as the reductant, however there were some minor products observed in the HPLC analysis.[17] This is hypothesized to be due to the flexibility of the larger cavity size of the 333-S_4 ligand framework. Each sulfur in the ligand has the ability to coordinate in two ways, even once the first sulfur has bound to the metal center. The transition to the 222-S_4 ligand creates a more rigid framework for chelation and fewer isomers; thus the reasoning for exploration of this ligand for complexing Rh(III).

Prior synthesis conditions and methods from research by Crenshaw were used in the synthesis of these tetrathioether complexes and an outline for the synthesis of ligands: **Intermediate 1, 222-S_4-diAcOMe, 222-S_4-diAcOH (Figure 4-9)**.[17,18] Some reaction times were adjusted, to ensure completion, as monitored via TLC methods. For the synthesis of **222-S_4-**

diAcOMe, the overall yield dropped from 60% with the 333-S4 analog to 44% with the **222-S_4-diAcOMe**. This could be in part due to tripling the reaction size scale. Other adjustments in the synthesis included increasing the temperature from 50˚ to 100˚, which allowed the reaction to proceed at a faster rate, given the increase in scale. For the reaction of **222-S_4-diAcOH**, **222-S_4-diAcOMe** was combined with base and reacted at 90˚. This reaction differs from previous reports in that microwave technology was used for the synthesis. This decreased the reaction time from reported by Carroll of roughly 1 h, to 15 min. [16] Yield of **222-S_4-diAcOH** was not drastically affected, however shortening the reaction time is an improvement.

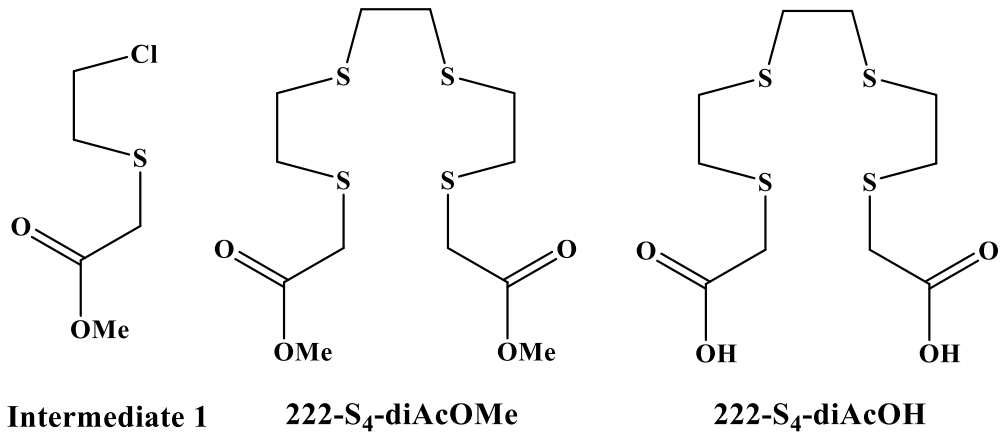

Intermediate 1 **222-S_4-diAcOMe** **222-S_4-diAcOH**

Figure 4-9. Schematic of ligand frameworks.

Moving forward with Rh(III) chelation, **222-S_4-diAcOMe** was reacted with $RhCl_3(H_2O)_3$ to synthesize **[$RhCl_2$-222-S_4-diAcOMe]Cl**. This was analogous to the reaction performed by Crenshaw to produce [Rh(333-S_4-diAcOMe)Cl_2]PF_6.[17] The reasoning for starting with the synthesis of the methylated pendant arms was to test conditions to give insight for future reactions; **Scheme 4-1** illustrates the reaction for *cis*-**[$RhCl_2$-222-S_4-diAcOMe]Cl** . This reaction was further modified to produce *cis*-[**$RhCl_2$-222-S_4-diAcOMe]PF_6, Scheme 4-2** . This change in anion allows

for an increase in the overall product solubility, as *cis*-[**$RhCl_2$-222-S_4-diAcOMe]Cl** is only soluble in polar solvents such as DMSO. *cis*-[**$RhCl_2$-222-S_4-diAcOMe]PF_6** was soluble in solvents such as acetonitrile and acetone, assisting in crystallization. The product was crystallized from acetone to afford crystal suitable for X-ray structure determination as shown in **Figure 4-10**. **Table 4-1** compares the bond lengths and angles of *cis*-[Rh(222-S_4-diBz)Cl_2]PF_6 (produced by Goswami) [14], *trans*-[Rh(333-S_4-diAcOMe)Cl_2]PF_6 (produced by Crenshaw) [17], and *cis*-[**Rh-222-S_4-diAcOMeCl_2]PF_6**, to illustrate the difference in bond lengths between the smaller and larger ring cavities. This confirmed the assumption of decreased ring size facilitated the *cis* coordination of chlorides to the Rh(III) center. Goswami postulated both *cis* and *trans* chloro species bound to the Rh(III) metal center with the 232-S_4 and 323-S_4 ligand systems. [15] *cis*-[**Rh-222-S_4-diAcOMeCl_2]PF_6** was analyzed via NMR, HPLC, and LC-MS with only one isomer present in solution according to these methods.

Moving forward with the synthesis of *cis*-[**$RhCl_2$-222-S_4-diAcOH]Cl**, it was important to understand the findings from previous reports. Macroscopic reactions performed by Carroll indicated at least 5 isomers, according to HPLC, were observed for the 333-S_4-diAcOH analog of *cis*-[**Rh Cl_2-222-S_4-diAcOH]Cl**, **Figure 4-11**, although it is difficult to determine.[16] The reported data indicated broad peaks in the HPLC analysis. This could contain multiple species located under the curves, hidden due to a fast gradient being utilized. This reaction was performed in ethanol, with and without saline (NaCl) present. The saline provided an excess of chloride ions in order to force the reaction to produce the dichloro- rhodium(III) product. The quick gradient (1-90% MeCN with 0.1% TFA, over 8 min), however, eluted the various isomers very close together, and difficult to separate. It was determined that the use of ethanol in reactions was causing these multiple species. At elevated temperatures, ethanol can cause esterification in the presence of acid

and carboxylic acid pendent groups.[4] It was at this point, a different reducing agent was introduced. Crenshaw used tin(II) chloride in place of refluxing ethanol to facilitate reaction between Rh(III) and the S_4 ligands.[17] This reduced the primary number of species formed in the reaction to three, which were easily separated by HPLC and a slower gradient (10-30% MeCN with 0.1% TFA, over 60 min).

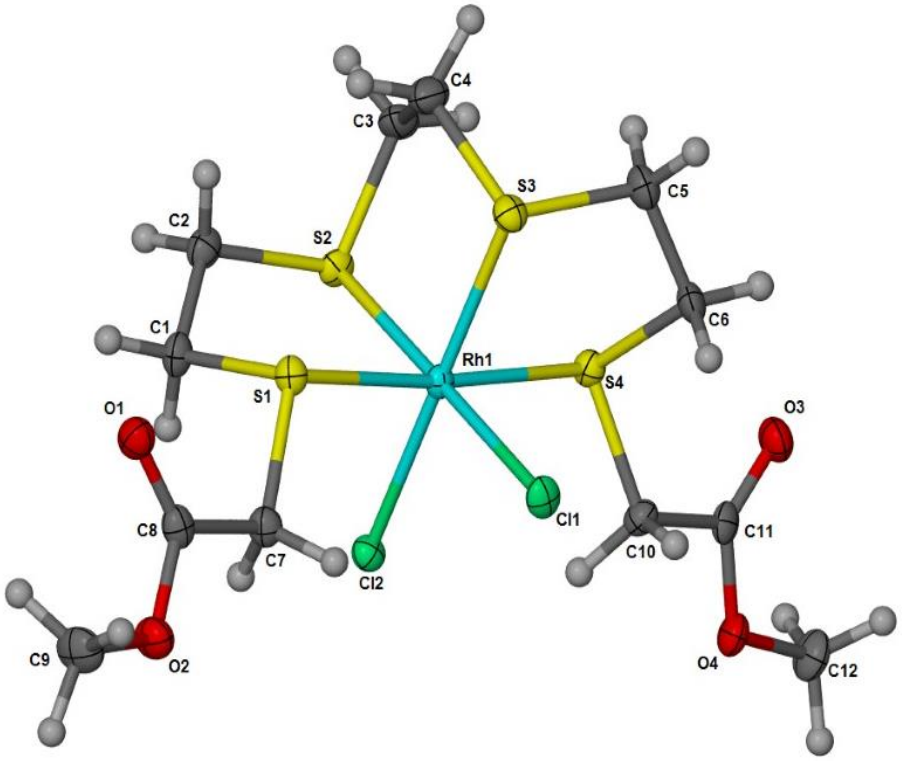

Figure 4-10. Crystal structure of [**$RhCl_2$-222-S_4-diAcOMe]PF_6**, shown with 50% ellipsoids. Counter ion and hydrogens removed for clarity.

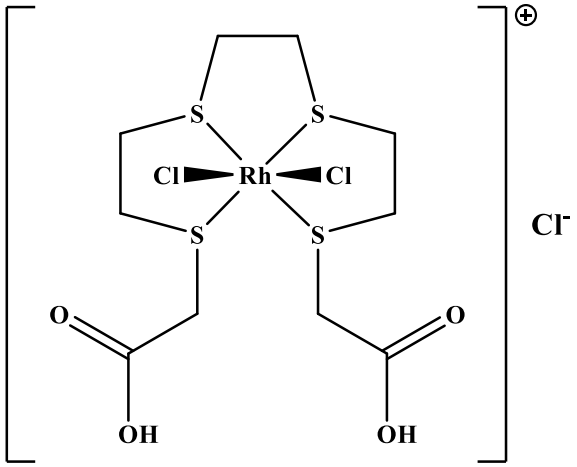

Figure 4-11. Schematic of **[RhCl$_2$-222S$_4$-diAcOH]Cl**.

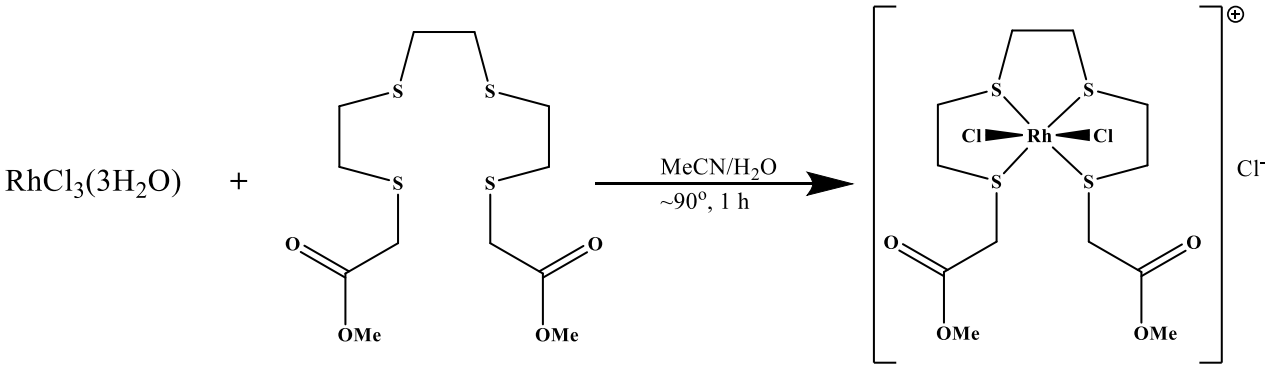

Scheme 4-1. General reaction for the production of [**RhCl$_2$-222-S$_4$-diAcOMe]Cl**.

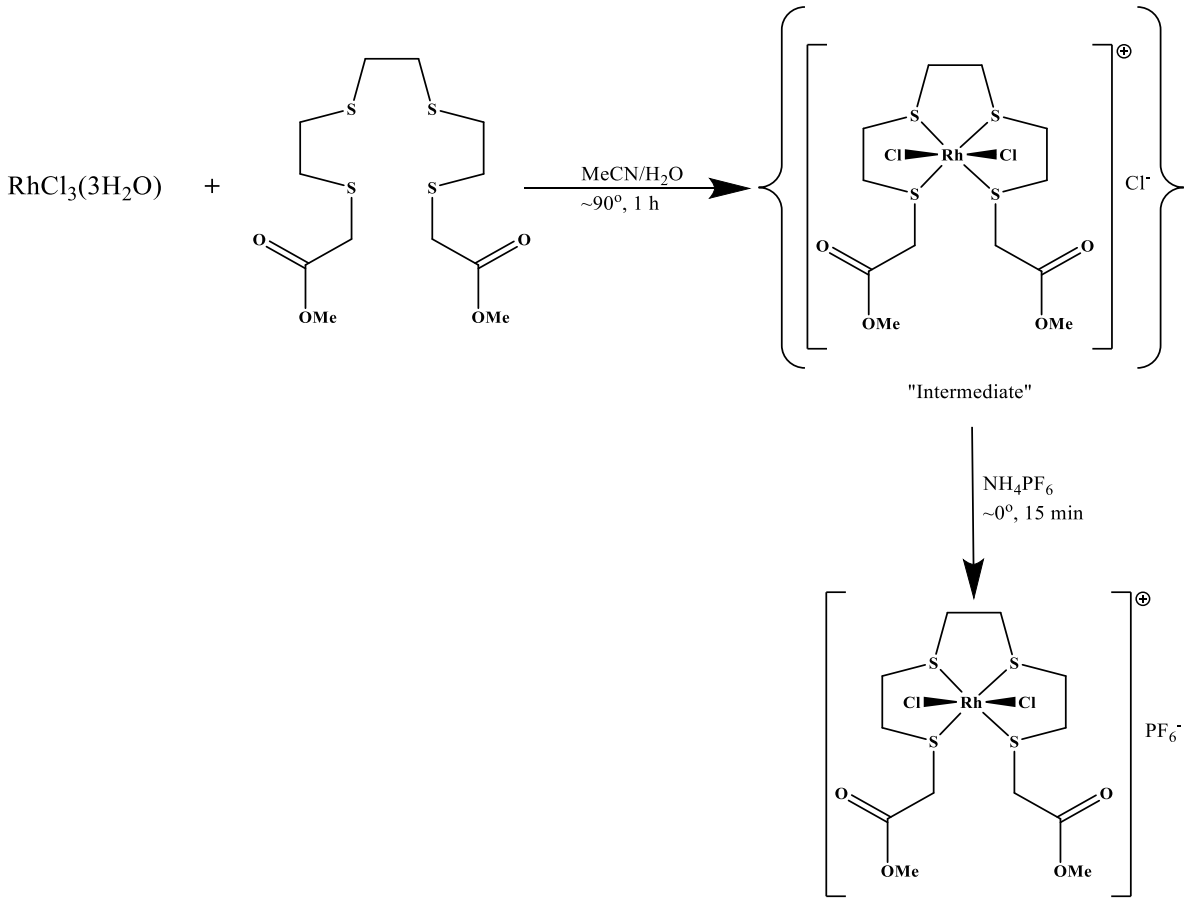

Scheme 4-2. General reaction for the production of [**$RhCl_2$-222-S_4-diAcOMe]PF_6.**

Table 4-1. Select bond distances (Å) and angles for *cis*-[Rh(222-S_4-diBz)Cl_2]PF_6, *trans*-[$RhCl_2$-333-S_4-diAcOMe]PF_6,and [**$RhCl_2$-222-S_4-diAcOMe]PF_6.**

	***cis*-$RhCl_2$-222-S_4-diBz**	***trans*-$RhCl_2$-333-S_4-diAcOMe**	***cis*-$RhCl_2$-222-S_4-diAcOMe**
Rh(1)-S(1)	2.347(2)	2.3713(7)	2.3275(10)
Rh(1)-S(2)	2.293(3)	2.3453(7)	2.2955(10)
Rh(1)-Cl(1)	2.349(2)	2.3459(7)	2.3575(10)
Rh(1)-Cl(2)	2.366(2)	2.3467(7)	2.3651(10)
Cl(1)-Rh-Cl(2)	93.33(8)˚	178.36(2)˚	92.38(4)˚

This was the starting point for the synthesis of *cis*-[**$RhCl_2$-222-S_4-diAcOH)]Cl**. The synthesis was first attempted in a similar fashion to that of *cis*-[**$RhCl_2$-222-S_4-diAcOH)]Cl**, however the change in dangling pendant arms from methoxy to carboxylic acids caused the overall product to be much more soluble in water. This meant that purification needed to be modified from the reaction of *cis*-[**$RhCl_2$-222-S_4-diAcOH)]Cl** in order to isolate *cis*-[**$RhCl_2$-222-S_4-diAcOH)]Cl**. Solubility also had to be taken into consideration, when performing HPLC and LC-MS characterization, using a much more hydrophilic gradient compared to the analogous methoxy complex (2% MeCN over 5 min, increased to 35% over 45 min, with 0.1% TFA present). In early attempts of purification, faster gradients (10-30% MeCN over 30 min) were used, and all species washed off the column near the void volume in one broad peak; thus the reason for slowing the gradient. Two reaction conditions were attempted for the synthesis, one containing acetonitrile and one with just water present. None of the starting materials are particularly soluble in only water, however the final product is. Use of the CEM microwave was utilized in these reactions not only to shorten the time of reaction from hours to minutes, but use of the microwave also resulted in an increase in overall yields. It was found that when attempting these reactions, in the absence of covering the reaction (with foil or cloth) black particulates were observed in solution. It is likely that these dark solids are from the tin reducing agent, reduced by light exposure. To ensure that the tin was able to react, aluminum foil was place over the reaction until placed in the microwave. The microwave itself has a light function to allow for reaction monitoring, this was disabled. When analyzed by LC-MS, three peaks were observed corresponding to the coordination of both, one, or neither of the carboxyl arms to the metal center, **Figure 4-12**.

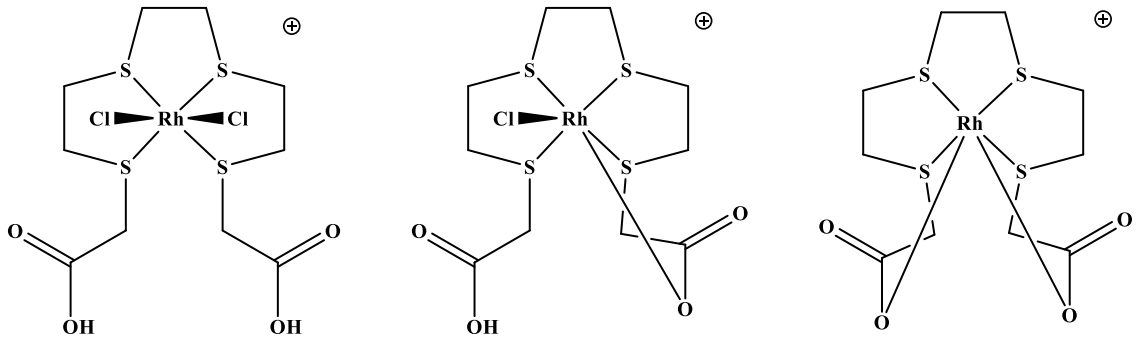

Figure 4-12. Schematic of three products formed in the reaction of *cis*-[**RhCl$_2$-222-S$_4$-diAcOH)]Cl**, shown without chloride counter ion for clarity. According to LC-MS and HPLC data, products can be separated via hydrophilic gradient (2% MeCN with 0.1% TFA for 5 minutes, and increasing to 35% over 45 minutes), showing peaks at: 13.8, 9.4, 2.5 minutes, matching in order to the above schematic.

Further investigation of the three species was performed in order to further characterize what was happening in solution. Utilizing a slow gradient, separation of the three products was easily performed. As previously stated, the reaction for *cis*-[**RhCl$_2$-222-S$_4$-diAcOH)]Cl** was done via two routes (changes in solvent conditions) and it was determined that adjustment of solvent conditions could cause a change in the overall products yielded. If acetonitrile was present, higher amounts of the products with carboxylate arms coordinated are formed. The reasoning for this is thought to be due partly in account for the higher pH of reactions when acetonitrile is present, as the pH is a bit more difficult to control. However, when acetonitrile is removed, higher amounts of the dichloro-product are produced. This could be due to the fact that the pH of the later reaction is inherently lower than that of the reaction containing acetonitrile, causing the carboxyl groups to remain protonated. Originally, the Rh(III) di-chloro species was the product in pursuit. The

product formation moves from 90% of complex without coordinated chlorides (one or both) to 27% by changing reaction solvents, **Figure 4-12**.

When considering translation to biologics, the possibility of three isomers in solution would be reduced to two, due to one arm being replaced by bombesin for *in vivo* targeting. It was illustrated that some conversion may occur in solution between isomers, over time. This was witnessed by taking back to back HPLC chromatograms of *cis*-[**$RhCl_2$-222-S_4-diAcOH)]Cl** , that was spiked with acetonitrile to ensure solubility of all 3 isomers. An increase of the di-chloro product from 66.7 to 73%, and of the no chloro product from 23.9% to 25.5% There was a subsequent decrease of the mono-chlroide product from 9.4% to 1.5%. The ratios of products with chlorides removed versus both intact is nearly a 1:3 ratio in favor of two coordinated chlorides. Future studies would need to be investigated in order to determine, on the tracer level, if these conversions occur once the three isomers have been isolated; this will need to be investigated with both the **222-S_4-diAcOH**, as well as for the bombesin analog. If so, there may be no need to purify radiolabeled complexes prior to *in vitro* and *in vivo* studies. It is known that the final solution for studies will be closer to philological pH, and could affect the final product yielded. If it is determined that interconversion cannot be controlled, no purification steps will have to be taken into account, and the first step will be to study the *in vitro* stability.

Conclusion

The synthesis, isolation, and characterization of **222-S_4-diAcOMe** and **222-S_4-diAcOH** has been described in details above. These ligands were collected in sufficient yield and used for the macroscopic scale chelation to Rh(III). *cis*-[**$RhCl_2$-222-S_4-diAcOMe)]PF_6** resulted in X-ray quality crystals and the crystallographic data further supports the *cis* orientation of the coordinated chlorides to the metal center. This was compared to previously reported models by Gosawami and

Crenshaw for the 222-S_4 and 333-S_4 with Rh(III) analogs, respectively. In regards to *cis*-[**$RhCl_2$-222-S_4-diAcOH)]Cl** , previous findings by Carroll, using the Rh-333-S_4 analog. suggested up to five species formed in reaction mixtures when using ethanol as a reductant.[16] When shifting to tin(II) as the reducing agent, multiple species were still found to form; however they were easily identifiable and isolated. All of three species formed in solution are very hydrophilic, aiding in future biological application. The formation of the three product species was found as the di-chloro, mono-chloro, no chloro. Reaction conditions can be manipulated to favor product formation (between the three species) by changing the solution acidity; done mostly by adjusting reaction solvent conditions, as previously stated. The di-chloro species was found to be the most hydrophobic of the three species according to HPLC retention times, eluting at around 15% MeCN. The mono- and no chloro species both elute with under 5% MeCN according to HPLC retention times. These findings, while helpful, will be less relevant with regards to the tetrathioether bombesin analog, which should have a different solubility because of the bombesin linker. The number of products will be reduced to two or less with the replacement of 222-S_4-diAcOH in reactions to the bombesin analog. This will eliminate one pendant arm from binding to rhodium, thus limiting the number of overall reaction products.

The next stages in synthesis and analysis would be to investigate these reactions on the tracer scale, with ^{105}Rh. The tracer normally comes in acidic, aqueous media, which has been shown to not be an issue with S_4 chelation on the macroscopic scale. The number of species formed will need to be determined via radio-HPLC and separated. At this point, it would be interesting to determine if interconversion occurs in solution between the various chloro species on the tracer level. The hypothesis, supported with macroscopic HPLC analyses, that conversion does in fact take place between the three species in solution, could eliminate the need for HPLC purification

of the ^{105}Rh products. If once complexes are isolated, conversion may allow for reformation of the other two species. The deciding factor will be based on how quickly this conversion occurs, and if one species exhibits poor *in vitro*/ *in vivo* targeting and clearance and non-target tissues. If this conversion is slow, the multiple species will need to be studied separately, for *in vitro* stability. In closing 222-S_4 chelates for Rh(III) have produced a new macroscopic scale product, *cis*-[**$RhCl_2$-222-S_4-diAcOH)]Cl**, which warrants further research and evaluation in biological systems.

Chapter 5: Conclusion and Application of Bifunctional Chelate Approaches to Radiopharmaceuticals

In each of the previous chapters, bifunctional chelate approaches were discussed for select radioisotopes for diagnostic and therapy purposes. While this approach is not novel, in terms of development, characterization of the complexes synthesized does expand on knowledge of previously reported data for targeting vectors to provide a better understanding of potential bifunctional chelates for Re and Rh radioisotopes.

Monoamine-monoamide Re(V) and ^{99m}Tc(V) Complexes

The MAMA ligand frameworks were synthesized with Re(V), ^{99m}Tc(V), and ^{186}Re(V) in order to study the stability of 222-MAMA and 323-MAMA chelates, as discussed in Chapters 2 and 3. In a report by Santos-Cuevas, ^{99m}Tc-N_2S_2 complexes conjugated to both TAT and bombesin for dual targeting, were analyzed *in vivo* and similar values were reported to the findings indicated in this report. Santos-Cuevas complex showed 2.89±1.01 %ID/g pancreas receptor binding at 0.25 h in normal mice; this was shown as an increased receptor uptake, compared to the standard kit of ^{99m}TcEEDA/HYNIC-Lys^3-BN, in mice with PC-3 tumors at almost fifty percent. Santos-Cuevas stated that their complex a decrease in the uptake and clearance through the intestines, and cleared through the urinary tract more readily.[1] **^{99m}TcO(222-MAMA)BBN[7-14]COONH$_2$** was re-analyzed for *in vitro* and *in vivo* stability and targeting of PC-3 human cells and CF-1 mice, respectively. In earlier reports, this bombesin complex was found to have 0.45 %ID/g pancreas uptake.[2] The lack of pancreas receptor binding could be due to a few different issues, namely with purification of the **222-MAMA-BBN[7-14]COONH$_2$**. The original study reported a poor ligand purity of only 75% for **222-MAMA-BBN[7-14]COONH$_2$**.In repeating this work, further

purification steps were performed to produce **222-MAMA-BBN[7-14]COONH$_2$** with greater than 98% purity for the re-evaluation of ^{99m}Tc and ^{186}Re MAMA-BBN complexes. Very few examples of *nca* ^{186}Re have been performed, and *nca* **^{186}ReO-222MAMA-BBN[7-14]COONH$_2$** (**Figure 5-1**)was synthesized with ~70% purity. *In vivo* studies performed with **^{99m}TcO-222MAMA-BBN[7-14]COONH$_2$** (**Figure 5-2**) showed 2.03 ± 0.42 %ID/g targeting to pancreas, which is comparable to that of similar ^{99m}Tc-N_2S_2 complexes in the literature. [1,3,4] HPLC retention times and location of clearance of this complex in mice through the intestines indicates it very lipophilic.

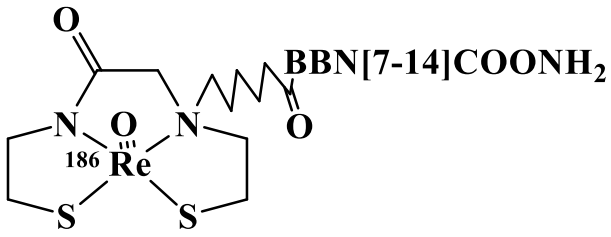

Figure 5-1. Structural representation of **^{186}ReO-222MAMA-BBN[7-14]COONH$_2$**.

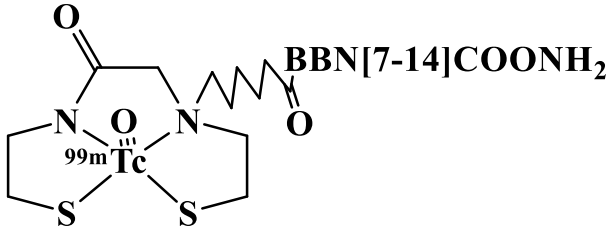

Figure 5-2. Structural representation of **^{99m}TcO-222MAMA-BBN[7-14]COONH$_2$**.

There are currently superior agents for pancreas tumor receptor imaging, for example ^{99m}Tc-N_3S chelating systems, have been shown to clear predominately via the kidneys and have an average of 7 %ID/g binding in mouse pancreas.[5] This is a benefit over the 222-MAMA-BBN complex that has hepatobiliary clearance. These findings of the 222-MAMA-BBN studies

reveal that more work needs to be performed on the bifunctional chelate design as the 222-MAMA derivatives investigated are too hydrophobic for biological systems. With the intent of using these complexes as a pancreas tumor imaging agent (^{99m}Tc) or as a theranostic tool (^{186}Re), rapid clearance via the kidneys is preferred. Currently, these MAMA complexes are too lipophilic.

While the monoamine-monoamide complexes we have studied are not ideal for the intended biological purpose, a comparison of the 222-MAMA and 323-MAMA ligand systems were performed to provide insight into designing a better chelate for Re(V) and ^{99m}Tc(V). Based on previous computational experiments, the preferred order of Re(V) and Tc(V) chelation based on thermodynamics is: 222-MAMA>232-MAMA>323-MAMA>333-MAMA.[2] Synthetic experiments were designed in order to determine if experimental results supported the computational findings. Prior to competition studies, 323-MAMA ligands were synthesized and chelated with Re(V). **ReO-323MAMA** and **ReO-323MAMAhex**, **Figure 5-3**, both were characterized via HPLC. The 323-MAMA complex was much easier to isolate and afforded crystallographic data allowing comparison to previously reported complexes. 323-MAMAhexanoate complexes were very difficult to isolate and prone to hydrolysis and oxidation to perrhenate or pertechnetate. This was also true at the radiotracer scale.

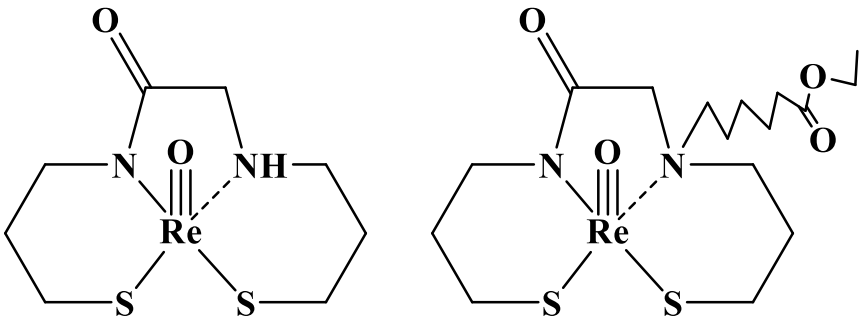

Figure 5-3. Structural representation of **ReO-323MAMA** and **ReO-323MAMAhex**.

Experimental set ups for competition studies combined each of the ligands: **222-MAMA** and **323-MAMAhex**, **323-MAMA** and **222-MAMAhex** to understand which ligand framework formed the most stable Re(V)/Tc(V) complexes. It was determined that 222-MAMA derivatives have a preferential binding over the 323-MAMA derivatives. We believe that the size of the ring formed by each of the ligands seems to be the largest contributing factor to overall product formation. The smaller sing size of the 222-MAMA is preferred in chelation with Re(V) and Tc(V) over that of 323-MAMA; product yields also support this hypothesis as 222-MAMA complexes formed in higher yields than their analogous 323-MAMA complexes. However, once metal complexes formed, based on radio-HPLC experiments, there is no conversion from one ligand to the other. This was a somewhat surprising result based on the preference for 222-MAMA chelation. With its unfavorable retention times and difficultly in isolation, the 323-MAMA ligand system and its Re(V)/Tc(V) complexes were not further pursued as potential biological agents.

Rhodium (III) Tetrathioether Frameworks

The rhodium chemistry with tetrathioether frameworks was revisited to develop new synthetic methods for se at the radiotracer level. In particular, a change in reducing agent was needed at the no carrier added ^{105}Rh level because the combination of HCl and carboxcylic acid pendant groups led to a mixture of isomers (ester formation) when refluxing ethanol was used as the reductant. The original work by Goswami indicated that the **222-S_4-diAcOH** would be more stable and suited for Rh(III) than the 333-S_4-diAcOH analog, and current findings seem to support this early research.[6] Carroll reported multiple isomers were formed by using ethanol as a solvent and reducing agent.[7] Crenshaw went on to pursue other methods of reduction, such as $SnCl_2$,

and reported that the number of isomers could be reduced. Both studies were performed with the 333-S_4-diAcOH ligand, which has some flexibility from a larger ring size (propane bridges between the sulfur atoms).[8] Crenshaw reported three primary products (isomers by LC-MS) from reactions of Rh(III) with 333-S_4-diAcOH, with the addition of minor products observed as well. The **222-S_4-diAcOH, Figure 5-4,** is a much more rigid ligand with only ethylene bridges between sulfur atoms. The use of $SnCl_2$ as a reductant resulted in three species formed in solution: **$RhCl_2$(222-S_4-diAcOH)** $^+$, **RhCl(222-S_4-diAcOH)** $^+$**, Rh(222-S_4-diAcOH)**$^+$ (**Figure 5-5)**. All three were isolated by HPLC methods and were identified via LC-MS analysis. LC-MS analysis showed the presence of all three species, even if one was isolated; however, it was not determined fully if interconversion between the three happens in solution following seperation, thus eliminating the need for HPLC purification. It was determined that the particular isomer formation can be manipulated and the percentage of the three species can vary with time, based on reaction conditions. Reactions performed in acetonitrile and at a higher pH produced more of the no-chloro and mono-chloro species, while reactions in aqueous solutions at lower pH produced more of the di-cholor species. Further investigations need to be performed to determine what will happen at physiological pH and whether a particular isomer can selectively be synthesized.

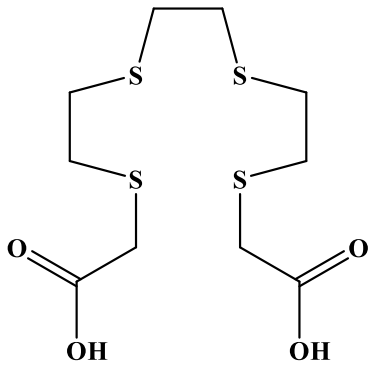

222-S_4-diAcOH

Figure 5-4. Structural representation of **222-S_4-diAcOH**.

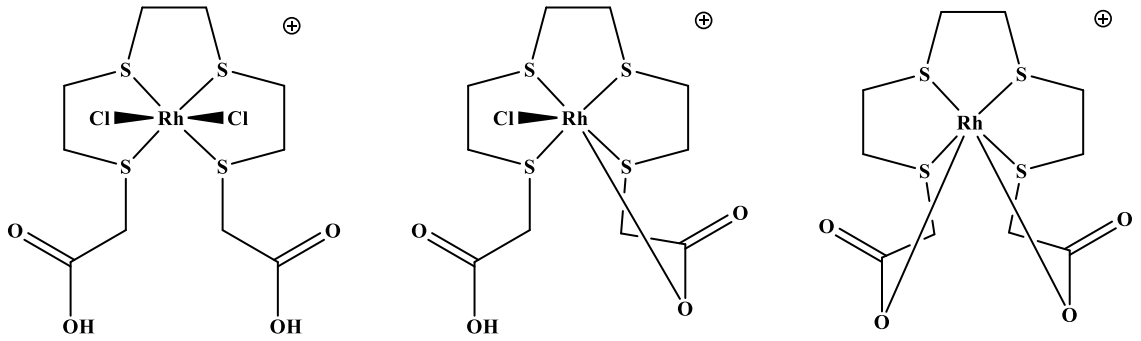

Figure 5-5. Three species formed in the reaction of Rh(III) and 222-S_4-diAcOH: di-, mono-, no chloro complexes, respectively.

. The overall utility this new reduction method for these complexes will be determined when investigations of tracer scale ^{105}Rh takes place. In my work, isomeric species were found to be easily isolated on the macroscopic level, using much slower gradients than previously reported. The tracer scale chemistry, with the 222-S_4-BBN[7-14] analog should show a decrease in the number of isomers formed as one of the pendant arms will have been conjugated to a peptide limiting its coordination to the metal center.

The findings reported in this dissertation have several areas that warrant future research, as mentioned above. Studies have already been continued toward ^{105}Rh production and translation to the ^{105}Rh radiotracer scale with 222-S_4-diAcOH will follow.

References

Chapter 1

[1] http://www.cnbc.com/2016/06/02/the-worlds-2015-cancer-drug-bill-107-billion-dollars.html

[2] Radiopharmaceuticals, American Chemical Society, https://www.cancer.org/treatment/treatments-and-side-effects/treatment-types/radiation/science-behind-radiation-therapy/how-is-radiation-given-radiopharmaceuticals.html, March 2017.

[3] https://www.oncolink.org/cancers/thyroid/treatments/radioactive-iodine-i-131-therapy-for-thyroid-cancer

[4] Pattillo, R.A., et al., *J Nucl Med*., **1995**, 36 (1), 29-36.

[5] Bauman, G., *Radiotherapy and Oncology*, **2005**, 75, 258.e1–258.e13.

[6] Som, P., et al., *J Nucl Med*, **1980**, 21 (7) 670-675.

[7] https://www.radiochemistry.org/nuclearmedicine/radioisotopes/ex_iso_medicine.htm

[8] Brechbiel, M. W., Bifunctional Chelates for Metal Nuclides. *The Quarterly Journal of Nuclear Medicine and Molecular Imaging : Official Publication of the Italian Association of Nuclear Medicine (AIMN) [and] the International Association of Radiopharmacology (IAR)*, **2008**, *52*(2), 166–173.

[9] Mark Stradiotto, Rylan J. Lundgren, Ligand Design in Metal Chemistry: Reactivity and Catalysis, John Wiley & Sons, Oct 17, 2016, page 8

[10] Boniface, G. R.; Izard, M. E.; Walker, K. Z.; McKay, D. R.; Sorby, P. J.; Turner, H.; Morris, J. G. Labeling of Monoclonal Antibodies with Samarium-153 for Combined Radioimmunoscintigraphy and Radioimmunotherapy. *J. Nucl. Med.*, **1989**, 30, 683-691.

[11] Kozak, R. W.; Raubitschek, A.; Mirzadeh, S.; Brechbiel, M. W.; Junghaus, R.; Gansow, O. A.; Waldmann, T. A., Nature of the Bifunctional Chelating Agent Used for Radioimmunotherapy with Yttrium-90 Monoclonal Antibodies: Critical Factors in Determining in vivo Survival and Organ Toxicity., *Cancer Res.*, **1989**, 49, 2639-2644.

[12] Deshpande, S. V.; DeNardo, S. J.; Kukis, D. L.; Moi, M. K.; McCall, M. J.; DeNardo, G. L.; Meares, C. F. Yttrium-90-Labeled Monoclonal Antibody for Therapy: Labeling by a New Macrocyclic Bifunctional Chelating Agent, *J. Nucl. Med*., **1990**, 31, 473- 479.

[13] A. Blake, G.R., M. Schroder, , Platinum Metal Thioether Macrocyclic Complexes: Synthesis, Electrochemistry and Single-crystal X-Ray Structures of cis-[RhCl2L2]PF6 and trans-[RhCl2L3]PF6 (L2 = 1,4,8,11-tetrathiacyclotetradecane, L3 = 1,5,9,13-tetrathiacyclohexadecane). *Journal of the Chemical Society, Dalton Transactions*, **1989**, 1675-1680.

[14] Bockisch, A., *Eur J Nucl Med Mol Imaging*, **2011**, 38, S1-3

[15] Kim, W.H., et al., *Ann Nucl Med*, **2016**, 30, 369–379

[16] Journal of Cardiovascular Pharmacology and Therapeutics 16(3-4) 321-331

[17] [a]Jurisson, S. S.; Lydon, J. D., Potential Technetium Small Molecule Radiopharmaceuticals., *Chem. Rev.* **1999,** *99* (9), 2205-2218.[b] Mahmood, A.; Jones, A. G., Technetium Radiopharmaceuticals. *In Handbook of radiopharmaceuticals: radiochemistry and applications,* Welch, M. J.;Redvanly, C. S., Eds. John Wiley & Sons Ltd: West Sussex, England, **2003**; 323-362.[c] Liu, S., Bifunctional coupling agents for radiolabeling of biomolecules and targetspecific delivery of metallic radionuclides, *Adv. Drug Deliver. Rev.* **2008,** *60*, 1347-1370.

[18] Carroll, V.; Demoin, D. W.; Hoffman, T. J.; Jurisson, S. S., Inorganic chemistry in nuclear imaging and radiotherapy: current and future directions. *Radiochim.Acta* **2012,** *100* (8-9), 653-667.

[19] Zalutsky, M. R.; Lewis, J. S., Radiolabeled antibodies for tumor imaging and therapy. *In Handbook of radiopharmaceuticals: radiochemistry and applications*, Welch, M. J.; Redvanly, C. S., Eds. John Wiley & Sons Ltd: West Sussex, England, **2003**, 714-685.

[20] Pillai, M.R., Dash, A., Knapp, F.F. Jr., *Curr Radiopharm*., **2012**, 5(3):228-43

[21] [a]Fassbender, M., et al., *Radiochim Acta*, **2013**, 101(5), 339–346. [b]Gott, M, et al., *Radiochim Acta*, **2014**, 102(4), 325-332.

[22] Jurisson, S. S.; Cutler, C. S.; Smith, S. V., Radiometal complexes: characterization and relevant in vitro studies. *Q. J. Nucl. Med. Mol. Im.* **2008,** *52*, 222-234.

[23] Anna Leonidova, Vanessa Pierroz, Riccardo Rubbiani, et al., Photo-induced uncaging of a specific Re(I) organometallic complex in living cells, *Chem. Sci.*, **2014**, 5, 4044-4056

[24] Brent Grazman, D.E.T., ^{105}Rh as a potential radiotherapeutic agent. *Applied Radiation and Isotopes*, **1988**, 39(3), 257-260.

[25] M. J. Heeg and S. S. Jurisson, *Acc. Chem. Res*, **1999**, 32, 1053-1060.

[26] [a]Li, N., *Department of Chemistry*. **1996**, University of Missouri., 141. [b]Lothar Helm, *A.E.M., J. Chem. Soc., Dalton Trans*., **2002**(5), 633-641. [c]Efe, G.E., et al., *Polyhedron*, **1991**, **10**(14), 1617-1624. [d]Jurisson, S., A. Ketring, and W. Volkert, *Transition Metal Chemistry*, **1997**, 22(3), 315-317. [e]Li, N., et al., *Nuclear Medicine and Biology*, **1997**, 24(1), 85-92.

Chapter 2

[1] Bockisch, *Eur J Nucl Med Mol Imaging* ,**2011**, 38.

[2] Müeller et al., *THE JOURNAL OF NUCLEAR MEDICINE,* **2012**, 53(12)

[3] https://home.cern/cern-people/updates/2013/01/therapeutic-use-radioactive-isotopes.

[4] International Atomic Energy Agency, Technetium-99m Radiopharmaceuticals: Manufacture of Kits, *Vienna*, **2008**, ISBN 9789201004086.

[5] Maria Argyrou, Alexia Valassi, Maria Andreou, and Maria Lyra, Dosimetry and Therapeutic Ratios for Rhenium-186 HEDP, *ISRN Molecular Imaging*, **2013**, Article ID 124603, 6 pages, doi:10.1155/2013/124603.

[6] Powell Richards, Walter D. Tucker, Suresh C. Srivastava, Technetium-99m: An historical perspective, The International Journal of Applied Radiation and Isotopes, Volume 33, Issue 10, 1982, Pages 793-799

[7] R.M. BALL, CHARACTERISTICS OF NUCLEAR REACTORS USED FOR THE PRODUCTION OF MOLYBDENUM-99, IAEA, VIENNA, 1999, p 26

[8] J. L. Snelgrove, G. L. Hofman, T. C. Wiencek, C. T. Wu, G. F. Vandegrift, S. Aase, B. A. Buchholz, D. J. Dong, R. A. Leonard, and B. Srinivasan, DEVELOPMENT AND PROCESSING OF LEU TARGETS FOR MO-99 PRODUCTION--OVERVIEW OF THE ANL PROGRAM, *1995 International Meeting on Reduced Enrichment for Research and Test Reactors*, September 18-21, 1994 Paris, France, http://www.rertr.anl.gov/MO99/JLS.pdf

[9] Raymond M. Reilly, Monoclonal Antibody and Peptide-Targeted Radiotherapy of Cancer, *Oncology Book of 2011*, British Medical Association's Medical Book Awards, 62-63.

[10] Jurisson SS and Lydon JD., Potential Technetium Small Molecule Radiopharmaceuticals, *Chem. Rev.*, **1999**, 99: 2205-18.

[11] Carroll V, Demoin DW, Hoffman TJ, and Jurisson SS. Inorganic chemistry in nuclear imaging and radiotherapy: current and future directions, *Radiochim. Acta,* **2012**, 100: 653-67.

[12] Liu S., Bifunctional coupling agents for radiolabeling of biomolecules and target-specific delivery of metallic radionuclides, *Adv. Drug Deliver. Rev*., 2008, 60: 1347-70.

[13] O'Neil JP, Wilson SR, and Katzenellenbogen JA. Preparation and Structural Characterization of Monoamine-Monoamide Bis(thiol) Oxo Complexes of Technetium(V) and Rhenium(V), *Inorg. Chem.*, **1994**, 33: 319-23.

[14] Friebe, M. et al, *Journal of Medicinal Chemistry*, **2001**, 44(19), 3132-3140.

[15] Oya, Shunichi et al., *Nuclear Medicine and Biology* , 25(2) , 135 – 140.

[16] D. Demoin, Utilizing an Experimental and Computational Approach to Ligand Design for Chelating Oxorhenium(V) and Oxotechnetim(V), University of Missouri-Columbia, May 2014.

[17] [a]Ono M, Ikeoka R, Watanabe H, Kimura H, Fuchigami T, Haratake M, et al., Synthesis and Evaluation of Novel Chalcone Derivatives with ^{99m}Tc/Re Complexes as Potential Probes for Detection of Amyloid Plaques. *ACS Chem. Neurosci.* **2010**, 1, 598-607. [b]Francesconi LC, Graczyk G, Wehrli S, Shaikh SN, McClinton D, Liu S, et al., Synthesis and characterization of neutral $M^{V}O$ (M = technetium, rhenium) amine-thiol complexes containing a pendant phenylpiperidine group. *Inorg. Chem*. **1993**, 32, 3114-24.

[18] Luo T-Y, Tang I-C, Wu Y-L, Hsu K-L, Liu S-W, Kung H-C, et al., Evaluating the potential of ^{188}Re-SOCTA-trastuzumab as a new radioimmunoagent for breast cancer treatment, *Nuc. Med. Biol.*, **2009**, 36, 81-8.

[19] Coy, D.H., *J. Biol. Chem*., **1989**, 264, 14691-7.

[20] https://www.ncbi.nlm.nih.gov/gene/2925

[21] [a]Smith CJ, Gali H, Sieckman GL, Higginbotham C, Volkert WA, and Hoffman TJ, Radiochemical investigations of ^{99m}Tc−N_3S-X-BBN[7−14]NH_2: An *in vitro*/*in vivo* structure−activity relationship study where X = 0-, 3-, 5-, 8-, and 11-carbon tethering moieties, *Bioconjugate Chem*., **2002**, 14: 93-102. [b]Smith CJ, Gali H, Sieckman GL, Hayes DL, Owen NK, Mazuru DG, et al., Radiochemical investigations of ^{177}Lu-DOTA-8-Aoc-BBN[7-14]NH_2: an in vitro/in vivo assessment of the targeting ability of this new radiopharmaceutical for PC-3 human prostate cancer cells, *Nuc. Med. Biol*., **2009**, 30: 101-9. [c]Hoffman TJ, Gali H, Smith CJ, Sieckman GL, Hayes DL, Owen NK, et al., Novel series of ^{111}In-labeled bombesin analogs as potential radiopharmaceuticals for specific targeting of gastrin-releasing peptide receptors expressed on human prostate cancer cells., *J. Nuc. Med.*, **2003**, 44, 823-31. [d]Jackson AB, Nanda PK, Rold TL, Sieckman GL, Szczodroski AF, Hoffman TJ, et al., ^{64}Cu-NO2A-RGD-Glu-6-Ahx-BBN(7-14)NH_2: A heterodimeric targeting vector for positron emission tomography imaging of prostate cancer. *Nuc. Med. Biol*., **2012**, 39, 377-87.

[22] Oya, S.; Plössl, K.; Kung, M.-P.; Stevenson, D. A.; Kung, H. F., Small and Neutral TcVO BAT, Bisaminoethanethiol (N_2S_2) Complexes for Developing New Brain Imaging Agents. *Nuc. Med. Biol.* **1998,** *25*, 135-140.

[23] Yamamura, N.; Magata, Y.; Arano, Y.; Kawaguchi, T.; Ogawa, K.; Konishi, J.; Saji, H., Technetium-99m-Labeled Medium-Chain Fatty Acid Analogues Metabolized by β-Oxidation: Radiopharmaceutical for Assessing Liver Function. *Bioconjugate Chem.* **1999,** *10* (3), 489-495.

[24] Fassbender, M., et al., *Radiochim Acta*, **2013**, 101(5), 339–346.

[25] Gott, M, et al., *Radiochim Acta*, **2014**, 102(4), 325-332.

[26] Smith, C. J.; Gali, H.; Sieckman, G. L.; Hayes, D. L.; Owen, N. K.; Mazuru, D. G.; Volkert, W. A.; Hoffman, T. J., Radiochemical investigations of 177Lu-DOTA-8-Aoc-BBN[7-14]NH2: an in vitro/in vivo assessment of the targeting ability of this new radiopharmaceutical for PC-3 human prostate cancer cells. *Nuc. Med. Biol.* **2003,** *30* (2), 101-109.

[27] Maria Argyrou, Alexia Valassi, Maria Andreou, Maria Lyra, *ISRN Molecular Imaging*, **2013**, Article ID 124603, 6 pages

[28] Clara L. Santos-Cuevas, Guillermina Ferro-Flores, et al., Design, preparation, in vitro and in vivo evaluation of 99mTc-N2S2-Tat(49–57)-bombesin: A target-specific hybrid radiopharmaceutical, *International Journal of Pharmaceutics*, **2009**, Volume 375, Issues 1–2, 22, 75-83.

[29] http://www.guidetopharmacology.org/GRAC/FamilyIntroductionForward?familyId=9

[30] Hoffman, T. J.; Gali, H.; Smith, C. J.; Sieckman, G. L.; Hayes, D. L.; Owen, N. K.; Volkert, W. A., *J. Nuc. Med.* **2003,** *44* (5), 823-831.

[31] Smith, C. J.; Gali, H.; Sieckman, G. L.; Higginbotham, C.; Volkert, W. A.; Hoffman, T. J., *Bioconjugate Chem.* **2002,** *14* (1), 93-102.

[32] K. E. Baidoo and S. Z. Lever, *Bioconjugate Chem*. **1990**, 1, 132-137.

[33] T.-Y. Luo et al. Evaluating the potential of ^{188}Re-SOCTA–trastuzumab as a new radioimmunoagent for breast cancer treatment, *Nuclear Medicine and Biology*, **2009**, 36, 81–88.

[34] S. Celen et al., Synthesis and evaluation of a ^{99m}Tc-MAMA-propyl-thymidine complex as a potential probe for in vivo visualization of tumor cell proliferation with SPECT, *Nuclear Medicine and Biology*, **2007**, 34, 283–291.

Chapter 3

[1] H.P. Vanbilloen et al., *Nuclear Medicine and Biology*, **2005**, 32, 607 – 612.

[2] Kuo-Shyan Lin, Andrew Luu, Kwamena E. Baidoo, et al, A New High Affinity Technetium-99m-Bombesin Analogue with Low Abdominal Accumulation, *Bioconjugate Chem*., **2005**, 16, 43−50.

[3] Alexander J. Blake, John A. Greig, and Martin Schrode, *J. Chem. Soc. Dalton Trans.*, **1988**, 2645-2647.

[4] [a]Terrence Nicholson and Jon Zubieta, *Inorg. Chem*. **1987**, 26, 2094-2101. [b]Andrea Marchi, Lorenza Marvelli,a Roberto RossLa Lucian Magoma Valerio Bertolasi, Valeria Ferretti and Paola Gilli, J. *CHEM. SOC. DALTON TRANS*. **1992**, 1485-1490. [c]Luigi G. Manilli,J Mariusz G. BanaszczykJ, Lory Hansen, Zsuzsanna Kuklenyik, Renzo Chis and Andrew Taylor, Jr., *Inorg. Chem*. 1994,33, 4850-4860.

[5] Leonard G. Luyt, Hilary A. Jenkins, and Duncan H. Hunter, *Bioconjugate Chem*., **1999**, 10, 470−479.

[6] Davy M. Kieffer, Hubert P. Vanbilloen, Bernard J. Cleynhens, Christelle Y. Terwinghe, Luc Mortelmans, Guy M. Bormans, Alfons M. Verbruggen, Biological evaluation of a technetium-99m-labeled integrated tropane-BAT and its piperidine congener as potential dopamine transporter imaging agents, *Nuclear Medicine and Biology*, **2006**, 33, 125 – 133.

[7] Pillai et al, *Appl Radiat. Isot*., **1990**, 41(6), 557-561

[8] Jurisson et al, *Inorganic Chemistry*, **1987**, 26, 3576

[9] D. Demoin, Utilizing an Experimental and Computational Approach to Ligand Design for Chelating Oxorhenium(V) and Oxotechnetim(V), University of Missouri-Columbia, May 2014.

[10] Treavor W. Hambley, *Acta Cryst.*, **1995**. C51, 203-205.

[11] Shunichi Oya, Karl Plo¨ssl, Mei-Ping Kung, D. Andrew Stevenson, Hank F. Kung, *Nuclear Medicine & Biology*, **1998**, 25, 135–140.

Chapter 4

[1] Sofou, S., *Int J Nanomedicine*, **2008**, 3(2), 181–199.

[2] https://www-nds.iaea.org/relnsd/vcharthtml/VChartHTML.html

[3] https://www.britannica.com/science/rhodium

[4] Milan M. Milutinović, *Dalton Trans.*, **2016**, 45, 15481

[5] John V. Rund, F.B., Ralph G. Pearson, Catalysis of Substitution Reactions of Rhodium(III) Complexes. The Reaction of Aquopentachlorodate(III) Ion with Pyridine. *Inorganic Chemistry*, **1964**, 3(5), 658-661.

[6] Drljaca, A., et al., Kinetics of Water Exchange on the Dihydroxo-Bridged Rhodium(III) Hydrolytic Dimer. Inorganic Chemistry, **1996**, 35(4), 985-990.

[7] E. J. BOUNSALL, S. R. KOPRICH, *CANADIAN JOURNAL OF CHEMISTRY*., **1970**, 48.

[8] Kruper Jr., W.J., et al., Functionalized polyamine chelants and rhodium complexes thereof and process for their preparation, *http://www.patentlens.net/patentlens/patent/EP_0296522_B1/?language=,en*., **1988**, Dow Chemical Company.

[9] Lo, J.M., et al., Radiochemical purity evaluation of rhodium-105 complexes by magnesium oxide. *International Journal of Radiation Applications and Instrumentation. Part A. Applied Radiation and Isotopes*, **1990**, 41(1), 103-105.

[10] Efe, G.E., et al., Rhodium complexes of two bidentate secondary amine oxime ligands and application to the labelling of proteins. *Polyhedron*, **1991**, 10(14), 1617-1624.

[11] Venkatesh, M., et al., An Rh-105 complex of tetrathiacyclohexadecane diol with potential for formulating bifunctional chelates. *Nuclear Medicine and Biology*, **1996**, 23(1), 33-40.

[12] Jurisson, S., A. Ketring, and W. Volkert, Rhodium-105 complexes as potential radiotherapeutic agents. *Transition Metal Chemistry*, **1997**, 22(3), 315-317.

[13] Li, N., et al., Biodistribution of model 105Rh-labeled tetradentate thiamacrocycles in rats, *Nuclear Medicine and Biology*, **1997**, 24(1), 85-92.

[14] Goswami, N., *^{105}Rh(III) Complexes With Acyclid Tetrathioether Ligands: Potential Radiotherapeutic Agents*, University of Missouri-Columbia, **1996**, 160.

[15] Goswami, N., et al., Rhodium(III) Complexes with Acyclic Tetrathioether Ligands. Effects of Backbone Chain Length on the Conformation of the Rh(III) Complex. *Inorganic Chemistry*, **1996**, 35(26), 7546-7555.

[16] Valerie Carroll, Development of a Rhodium Tetrathioether Bombesin Analogue and Investigation of Cyclic and Acyclic Ligand Systems for ^{105}Rh(III), University of Missouri-Columbia, May 2013.

[17] Crenshaw, Nicole, Characterization of Acyclic Rhodium Tetrathioether Ligand Systems for ^{105}Rh(III), University of Missouri-Columbia, **May 2015**

[18] Nef, W., Ph.D. Thesis, University of Basel, 1996.

Chapter 5

[1] Clara L. Santos-Cuevas, Guillermina Ferro-Flores, Consuelo Arteaga de Murphy, Flor de M. Ramírez, Myrna A. Luna-Gutiérrez, Martha Pedraza-López, Rocío García-Becerra, David Ordaz-Rosado, *International Journal of Pharmaceutics***, 2009**, 375(1-2), 75–83.

[2] D. Demoin, Utilizing an Experimental and Computational Approach to Ligand Design for Chelating Oxorhenium(V) and Oxotechnetim(V), University of Missouri-Columbia, May 2014.

[3] Alves S, Paulo A, Correia JDG, Gano L, Smith CJ, Santos I, et al., *Bioconjug Chem*., **2005**,16, 438– 49.

[4] Charles J. Smith , Wynn A. Volkert , Timothy J. Hoffmana, *Nuclear Medicine and Biology*, **2005**, 32, 733 – 740.

[5] C.C. Liolios et al., *International Journal of Pharmaceutics*, **2012**, 430, 1–17.

[6] Goswami, N., et al., Rhodium(III) Complexes with Acyclic Tetrathioether Ligands. Effects of Backbone Chain Length on the Conformation of the Rh(III) Complex. *Inorganic Chemistry*, **1996**, 35(26), 7546-7555.

[7] Carroll, Valerie, Development of a Rhodium Tetrathioether Bombesin Analogue and Investigation of Cyclic and Acyclic Ligand Systems for ^{105}Rh(III), University of Missouri-Columbia, **May 2013**.

[8] Crenshaw, Nicole, Characterization of Acyclic Rhodium Tetrathioether Ligand Systems for ^{105}Rh(III), University of Missouri-Columbia, **May 2015**

Appendix and Supplementary Data

Listed by Chapter and Complex Order

Chapter 2

222-MAMA-hexanoate

^{1}HNMR:

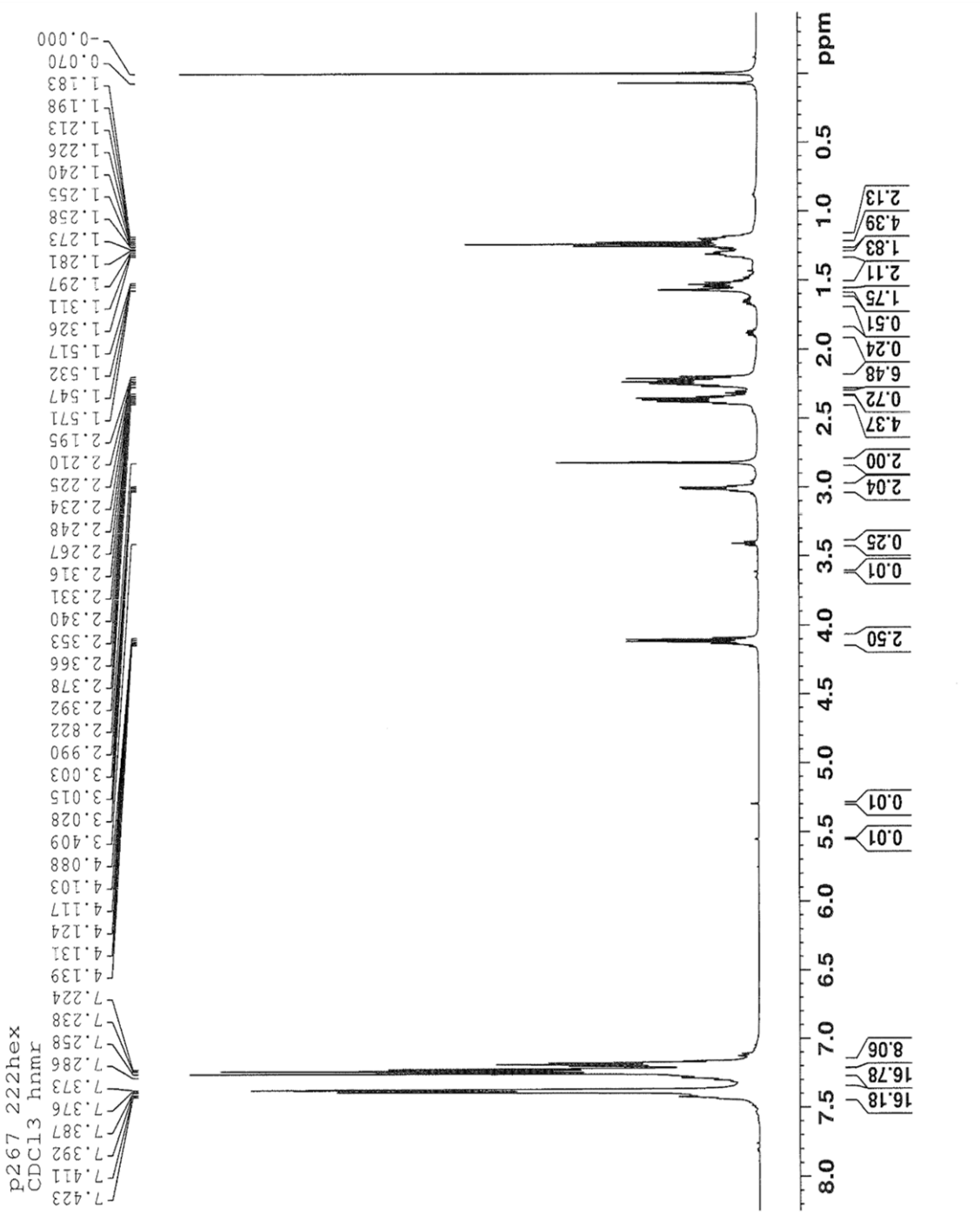

p267 222hex
CDC13 hnmr
4.139
4.131
4.124
4.117
4.103
4.088
3.613
3.422
3.409
3.395
3.028
3.015
3.003
2.990
2.822
2.392
2.378
2.366
2.353
2.340
2.331
2.316
2.301
2.267
2.248
2.234
2.225
2.210
2.195
1.895
1.880
1.865
1.689
1.674
1.658
1.643
1.571
1.547
1.532
1.517
1.326
1.311
1.297
1.281
1.273
1.258
1.255
1.240
1.226
1.213
1.198
1.183
1.168
ppm
4.0
3.5
3.0
2.5
2.0
1.5
2.50
0.01
0.25
2.04
2.00
4.37
0.72
6.48
0.24
0.51
1.75
2.11
1.83
4.39
2.13

^{13}CNMR:

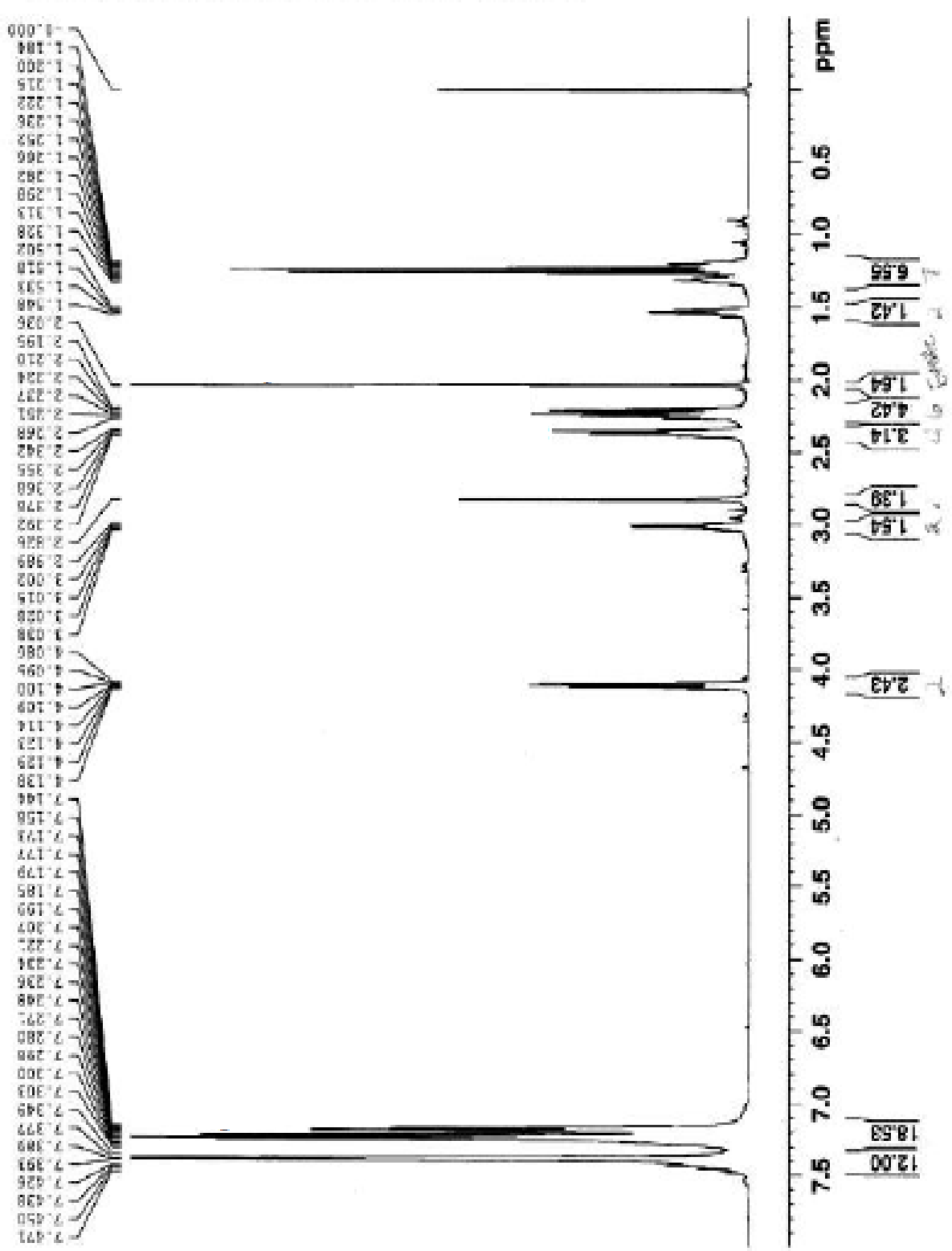
ppm
0.5
1.0
1.5
2.0
2.5
3.0
3.5
4.0
4.5
5.0
5.5
6.0
6.5
7.0
7.5
6.55
1.42
1.64
4.42
3.14
1.38
1.54
2.43
18.58
12.00

222-MAMA-hexanoic acid

^{1}HNMR:

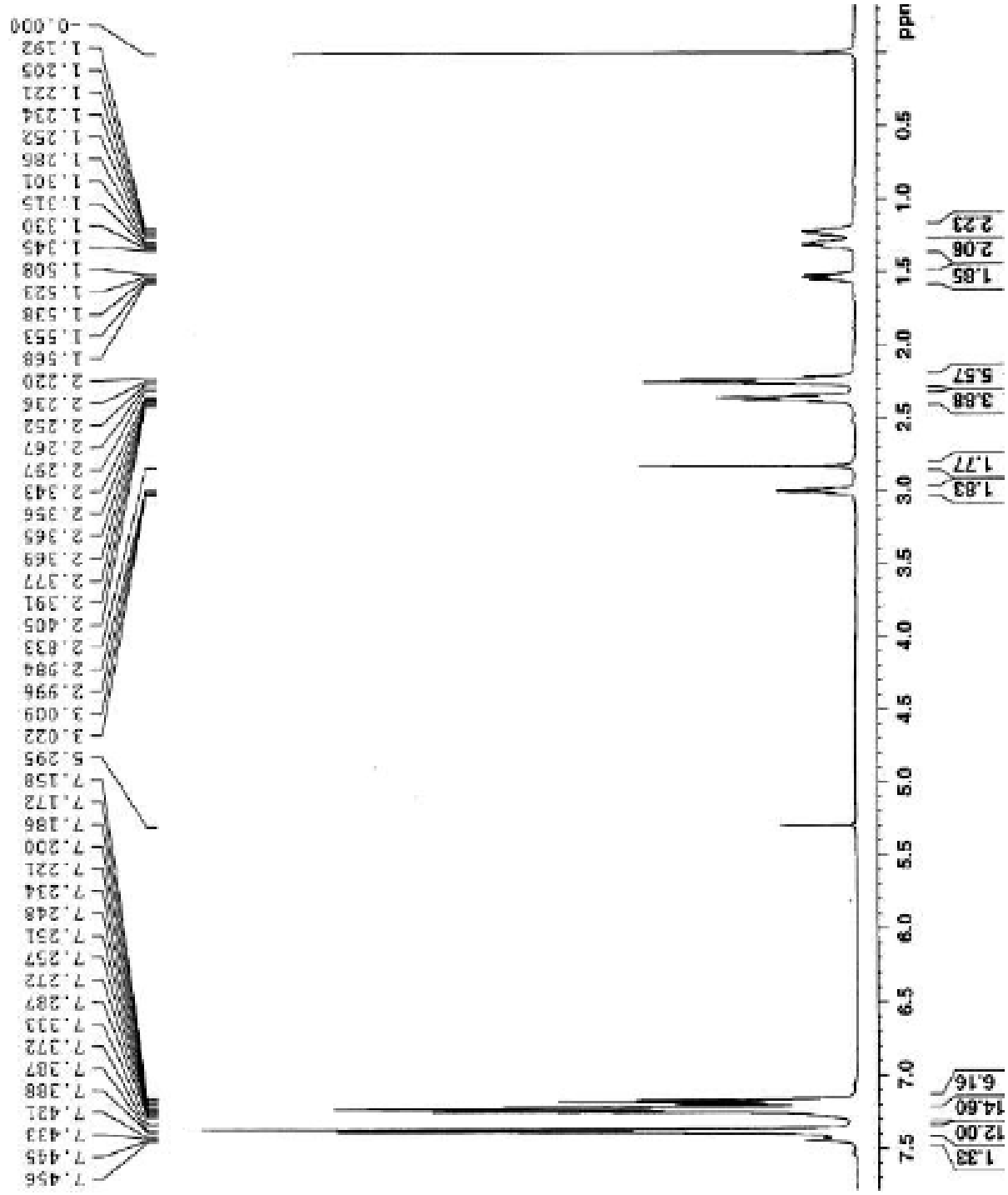

^{13}CNMR:

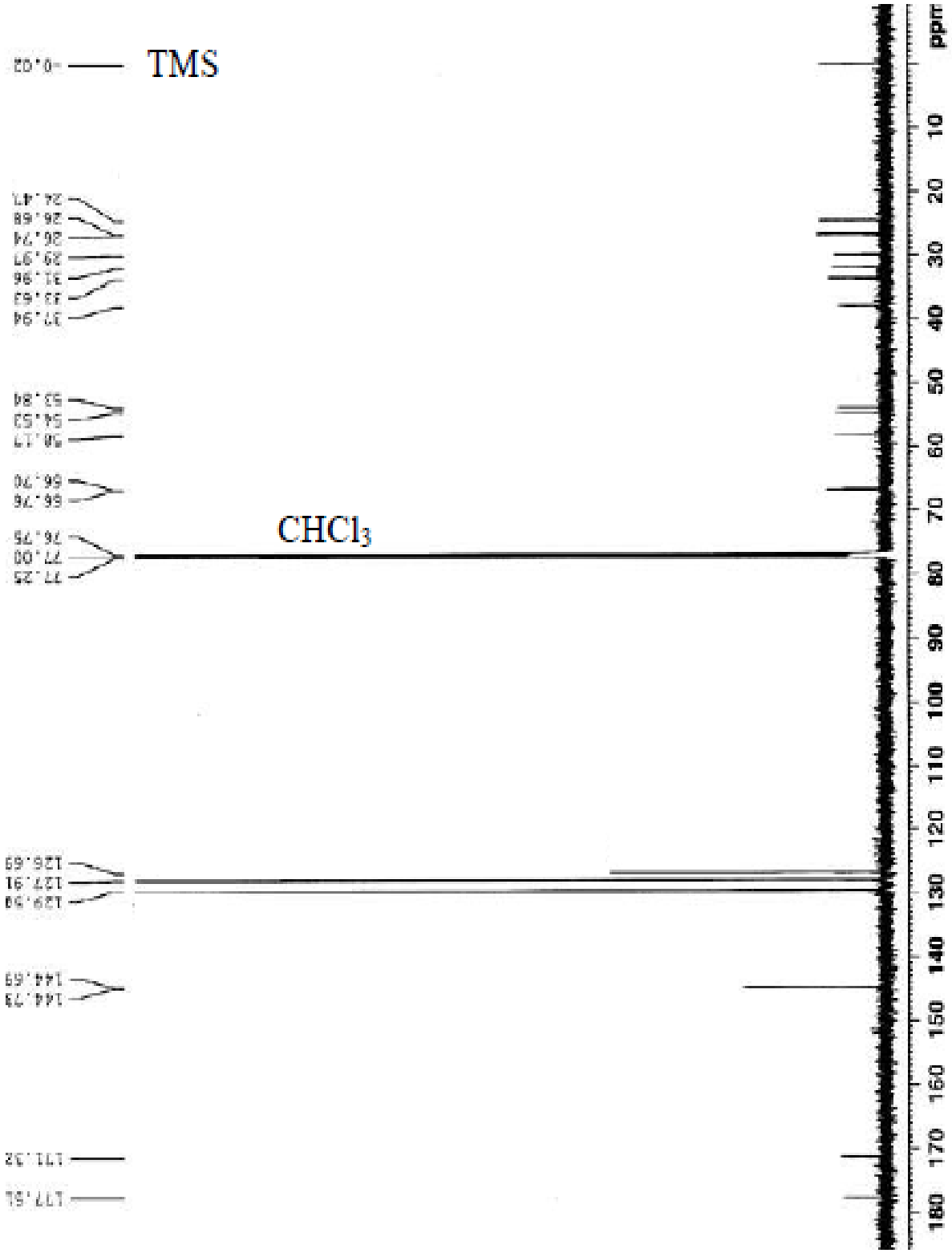

ReO222-MAMA-hexanoate

^{1}HNMR:

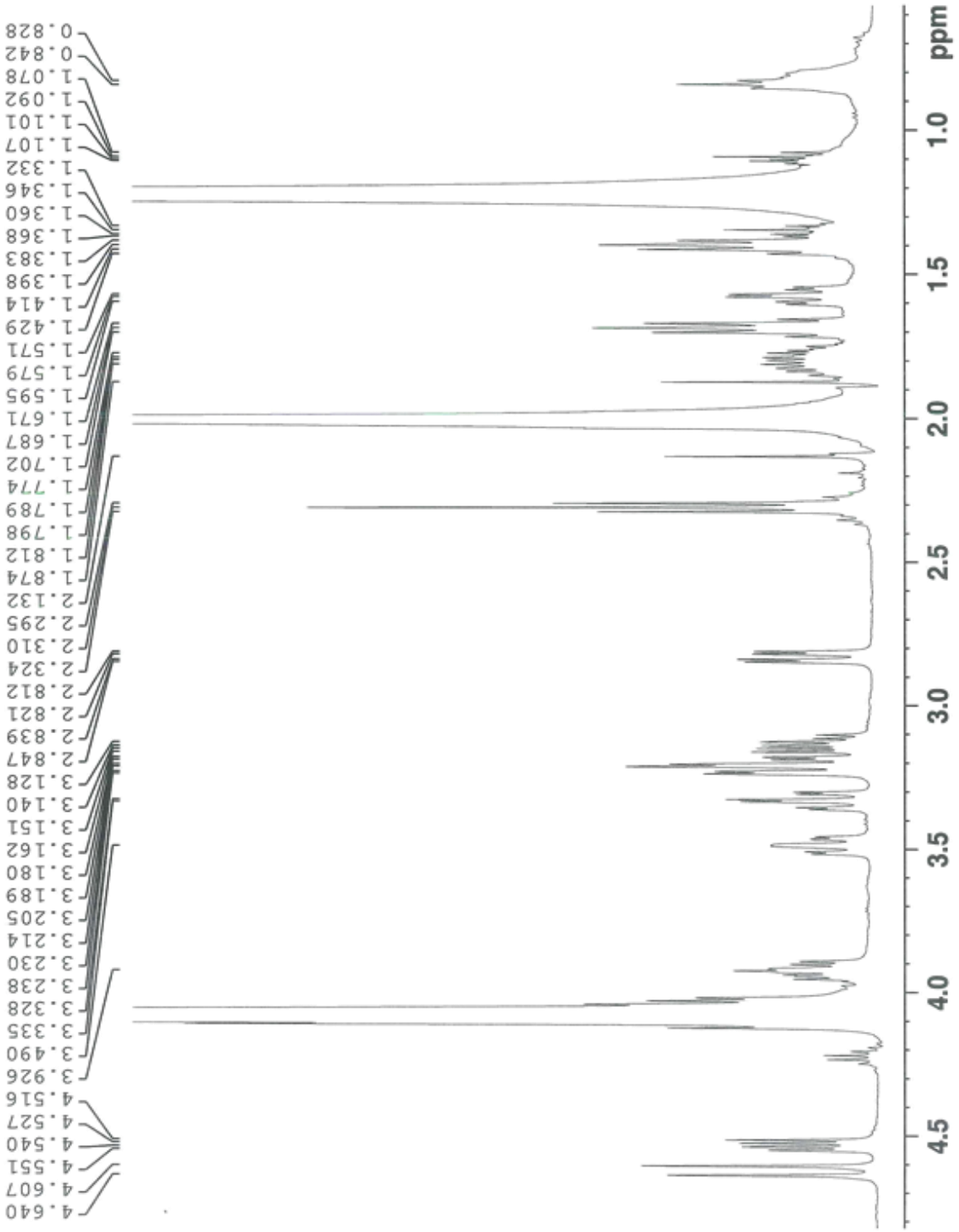

HPLC:

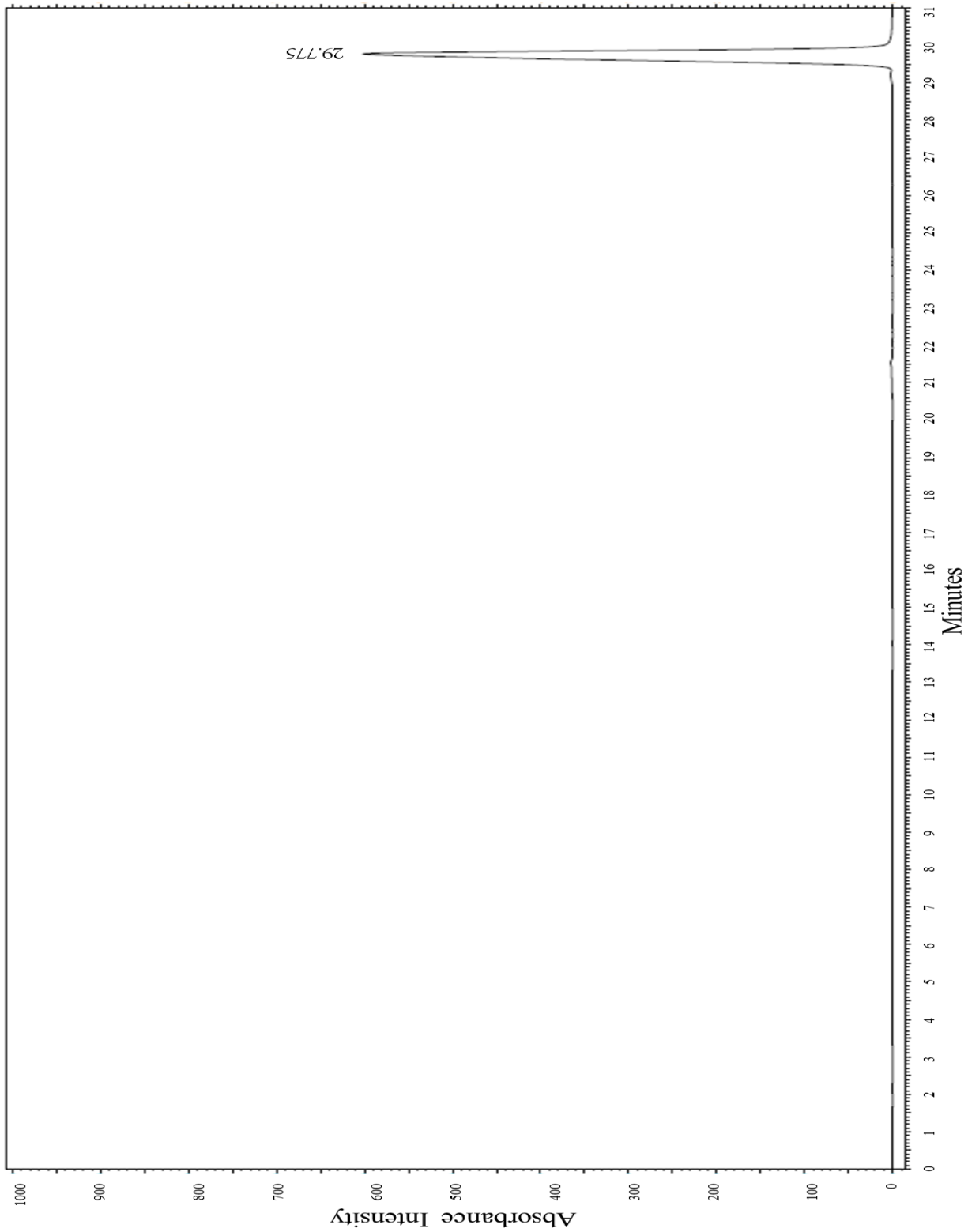
29.775
Absorbance Intensity
1000
900
800
700
600
500
400
300
200
100
0
Minutes
0 1 2 3 4 5 6 7 8 9 10 11 12 13 14 15 16 17 18 19 20 21 22 23 24 25 26 27 28 29 30 31

LC-MS:

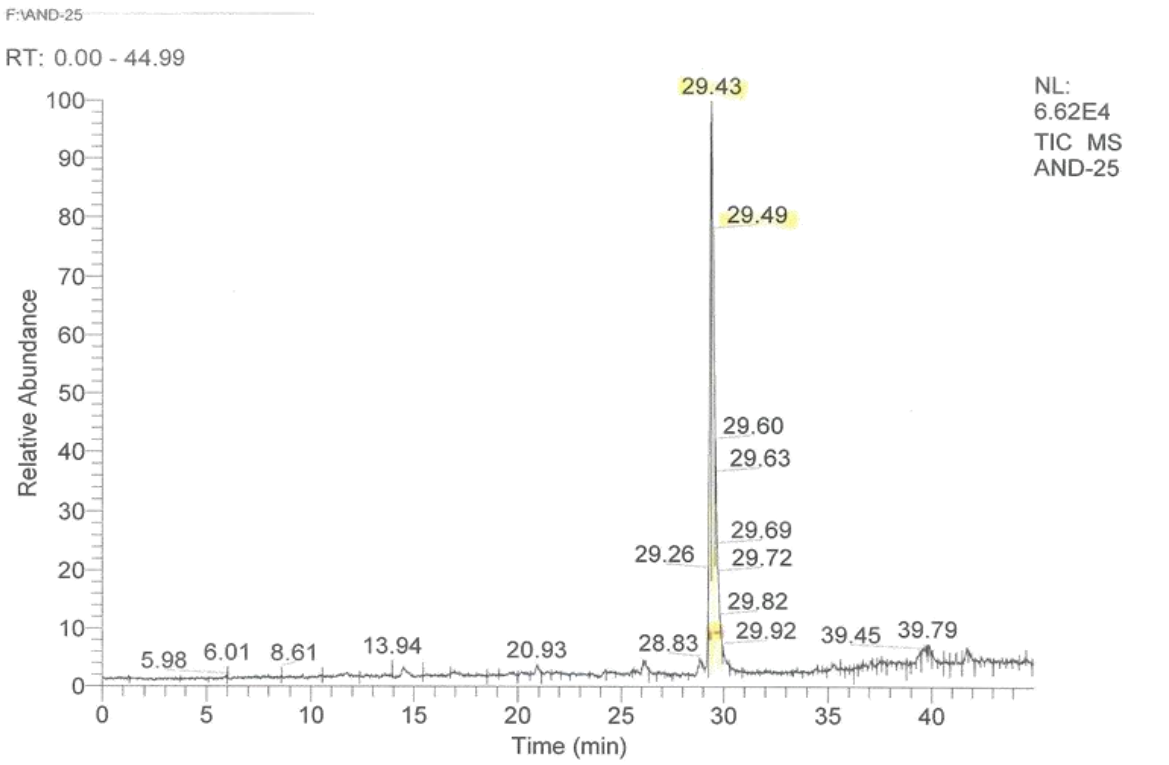
F:\AND-25
RT: 0.00 - 44.99
NL:
6.62E4
TIC MS
AND-25
Relative Abundance
Time (min)
29.43
29.49
29.60
29.63
29.69
29.26
29.72
29.82
29.92
28.83
39.45
39.79
5.98
6.01
8.61
13.94
20.93

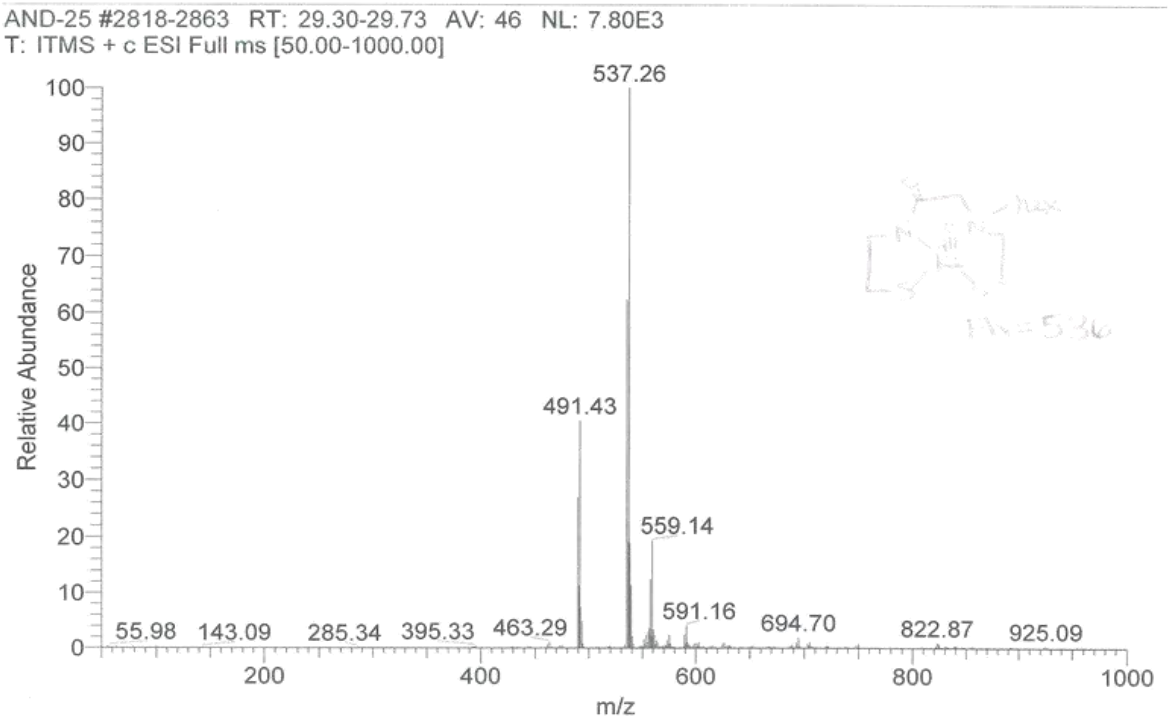
AND-25 #2818-2863 RT: 29.30-29.73 AV: 46 NL: 7.80E3
T: ITMS + c ESI Full ms [50.00-1000.00]
Relative Abundance
m/z
537.26
491.43
559.14
591.16
694.70
822.87
925.09
55.98
143.09
285.34
395.33
463.29

^{99m}TcO-222-MAMA-hexanoate

Radio-HPLC:

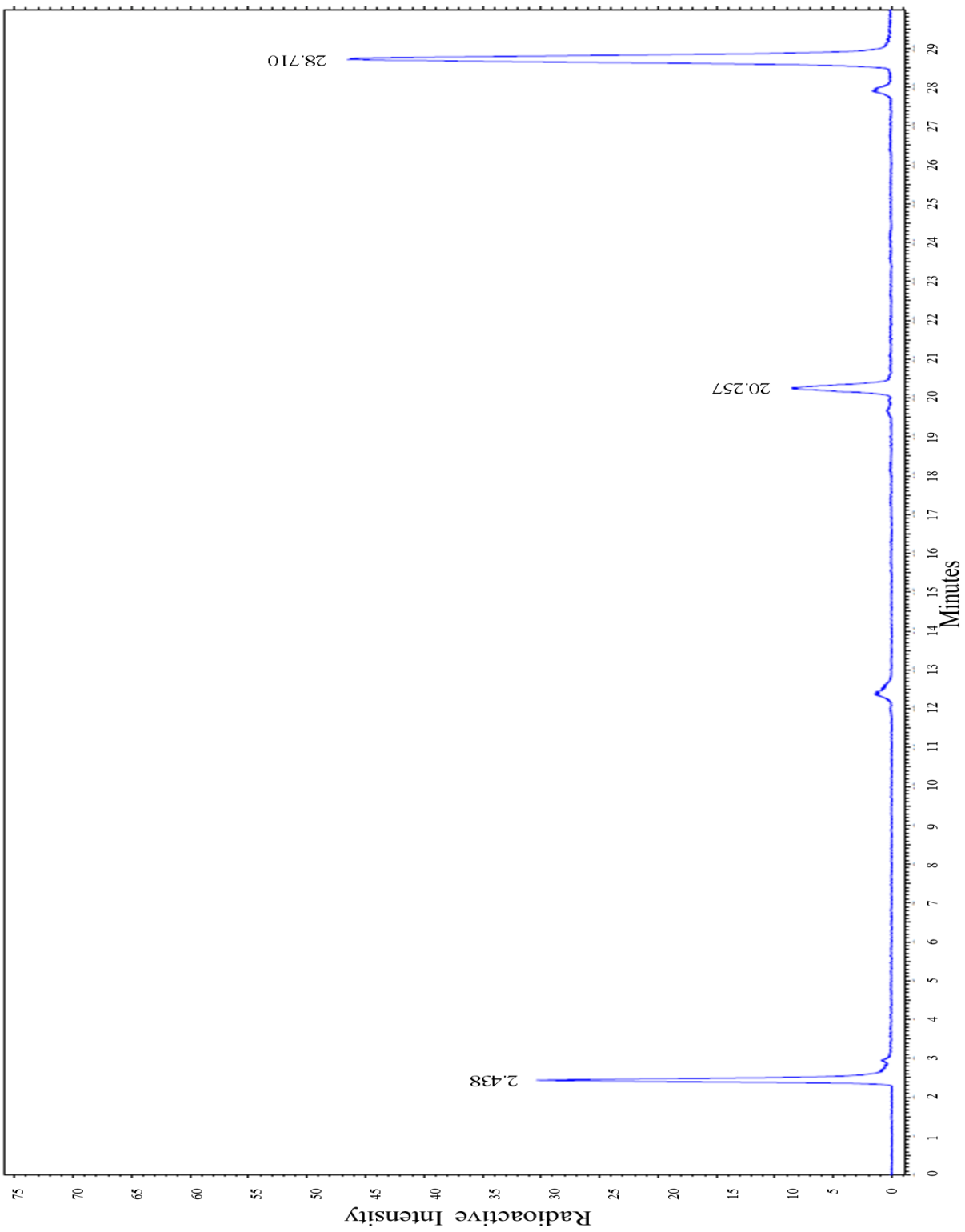

^{nat}ReO-222-MAMA-BBN[7-14]NH_2

HPLC:

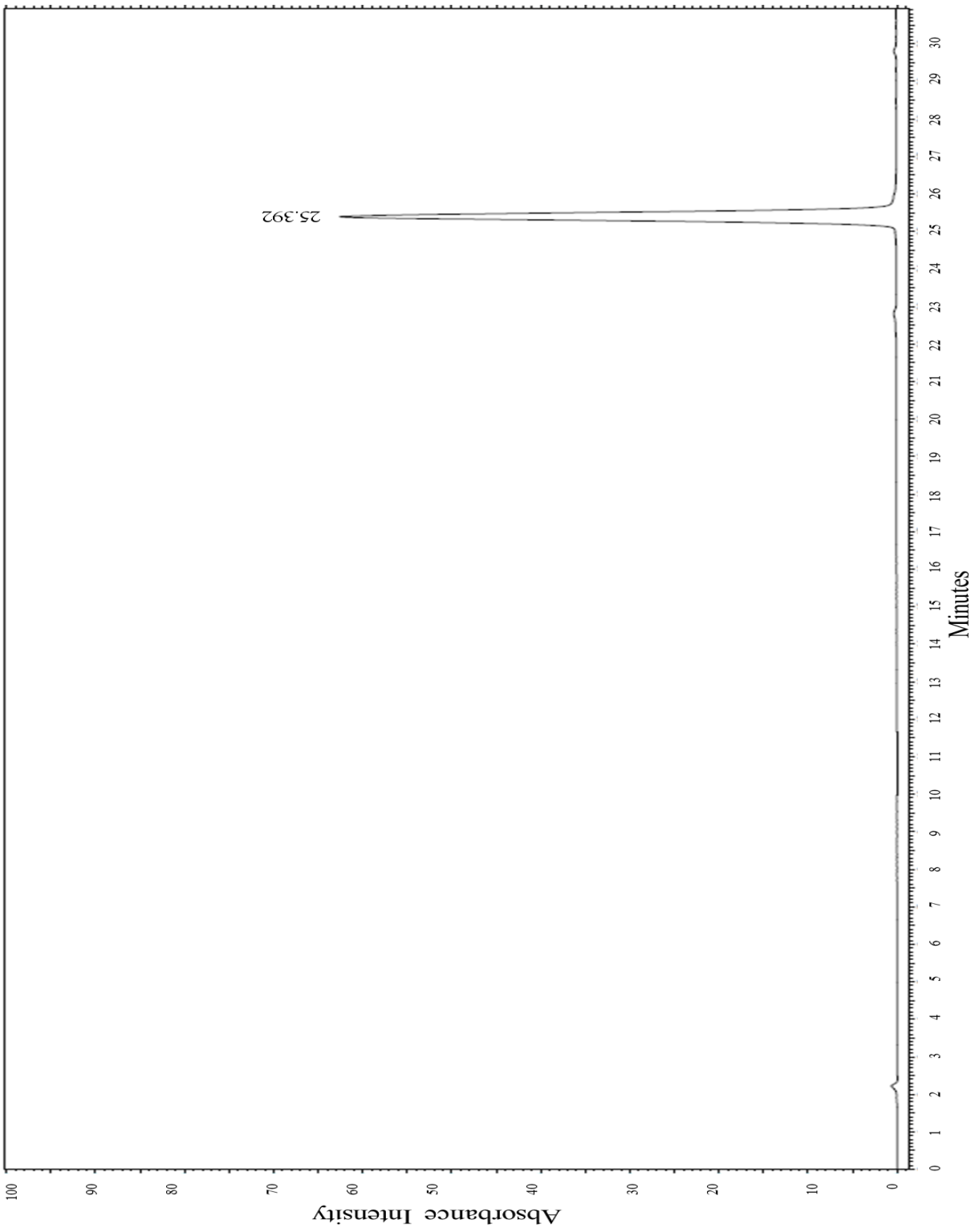

HPLC of ^{nat}ReO-222-MAMA-BBN[7-14]NH_2, spiked with EtOH:

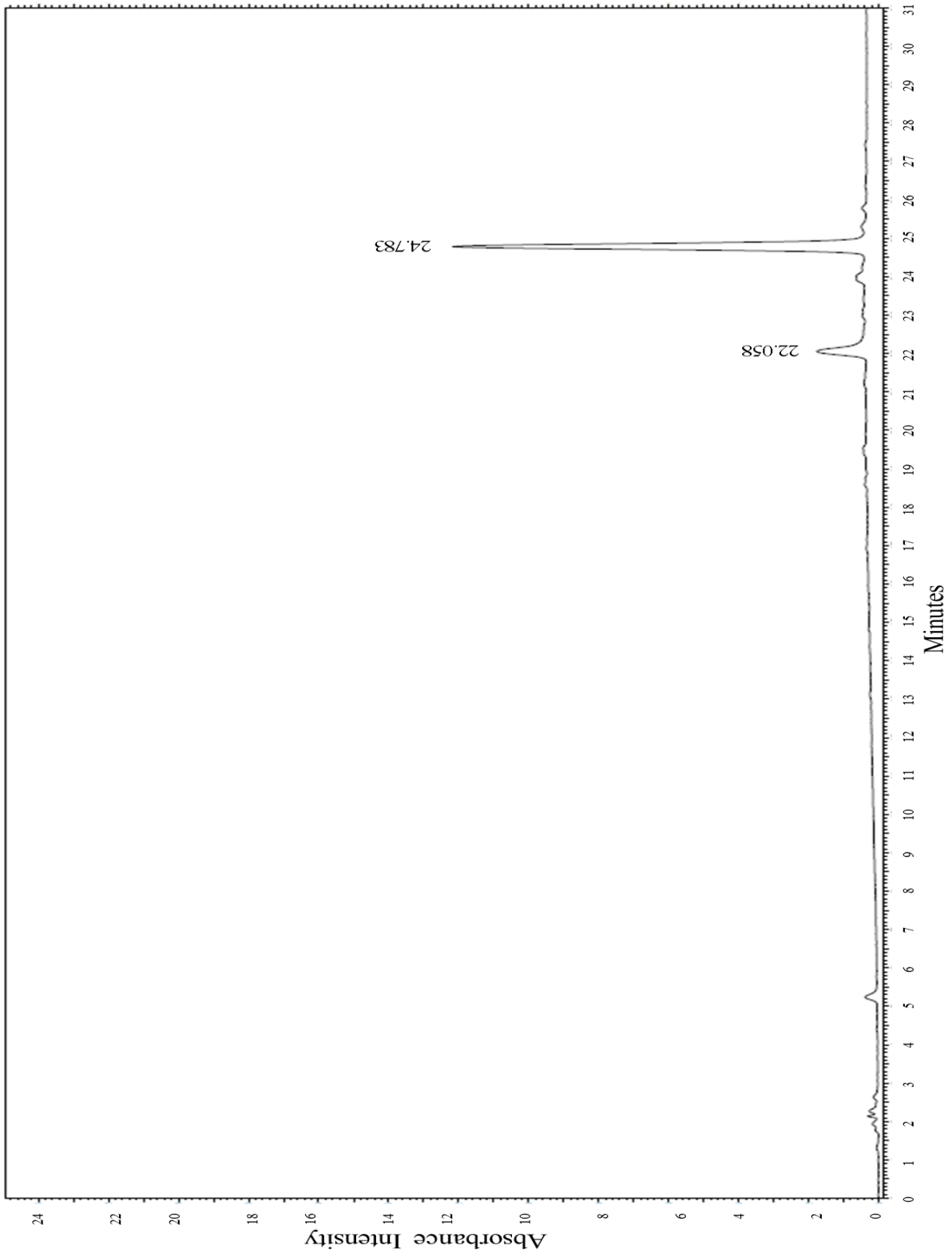

LC-MS:

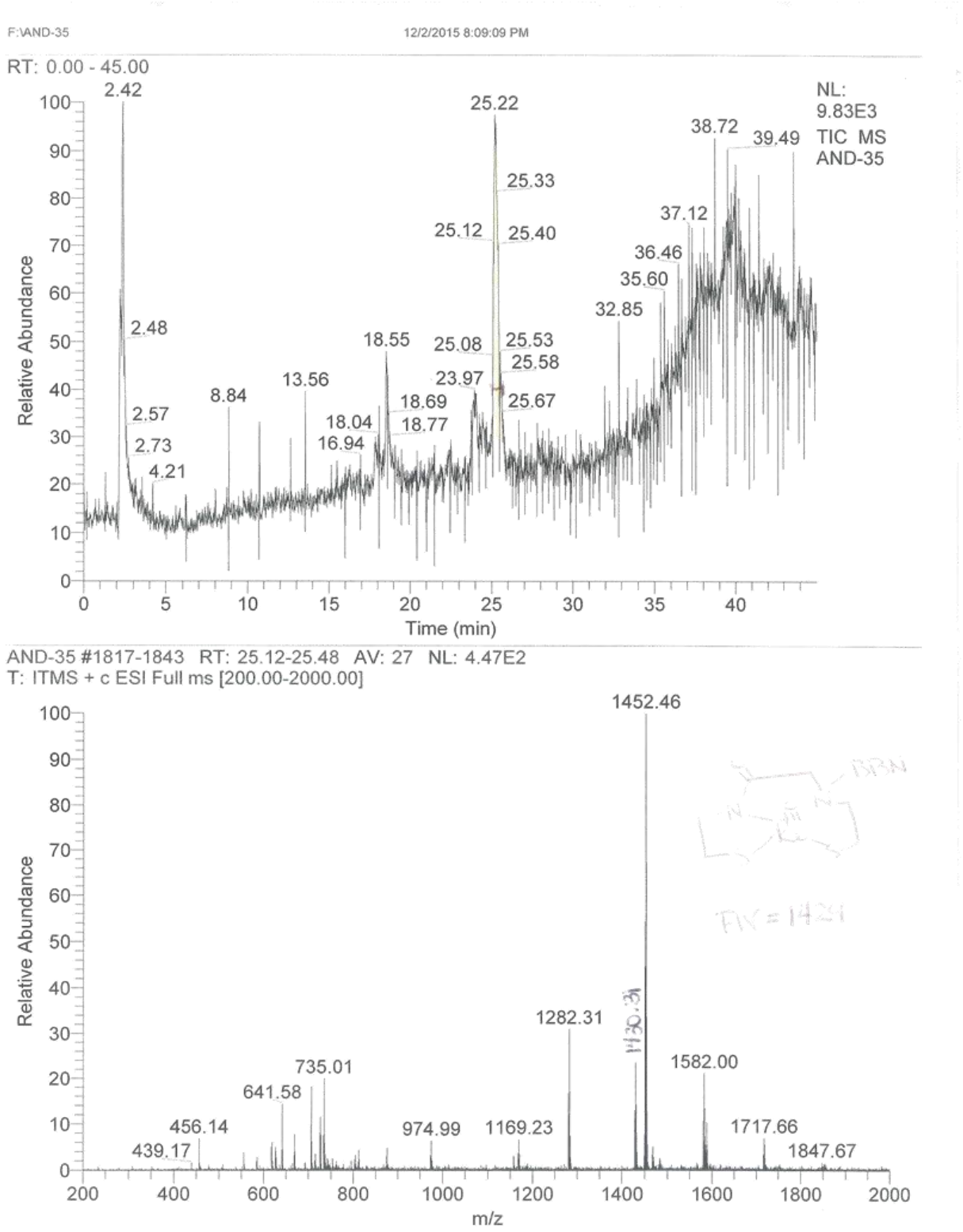
F:\AND-35
12/2/2015 8:09:09 PM
RT: 0.00 - 45.00
NL:
9.83E3
TIC MS
AND-35
Relative Abundance
Time (min)
2.42
25.22
38.72
39.49
25.33
37.12
25.12
25.40
36.46
35.60
32.85
2.48
18.55
25.08
25.53
25.58
13.56
23.97
8.84
18.69
25.67
2.57
18.04
18.77
16.94
2.73
4.21
AND-35 #1817-1843 RT: 25.12-25.48 AV: 27 NL: 4.47E2
T: ITMS + c ESI Full ms [200.00-2000.00]
Relative Abundance
m/z
1452.46
1282.31
1582.00
735.01
641.58
456.14
974.99
1169.23
1717.66
439.17
1847.67

^{99m}TcO-222-MAMA-BBN[7-14]NH_2

Radio-HPLC:

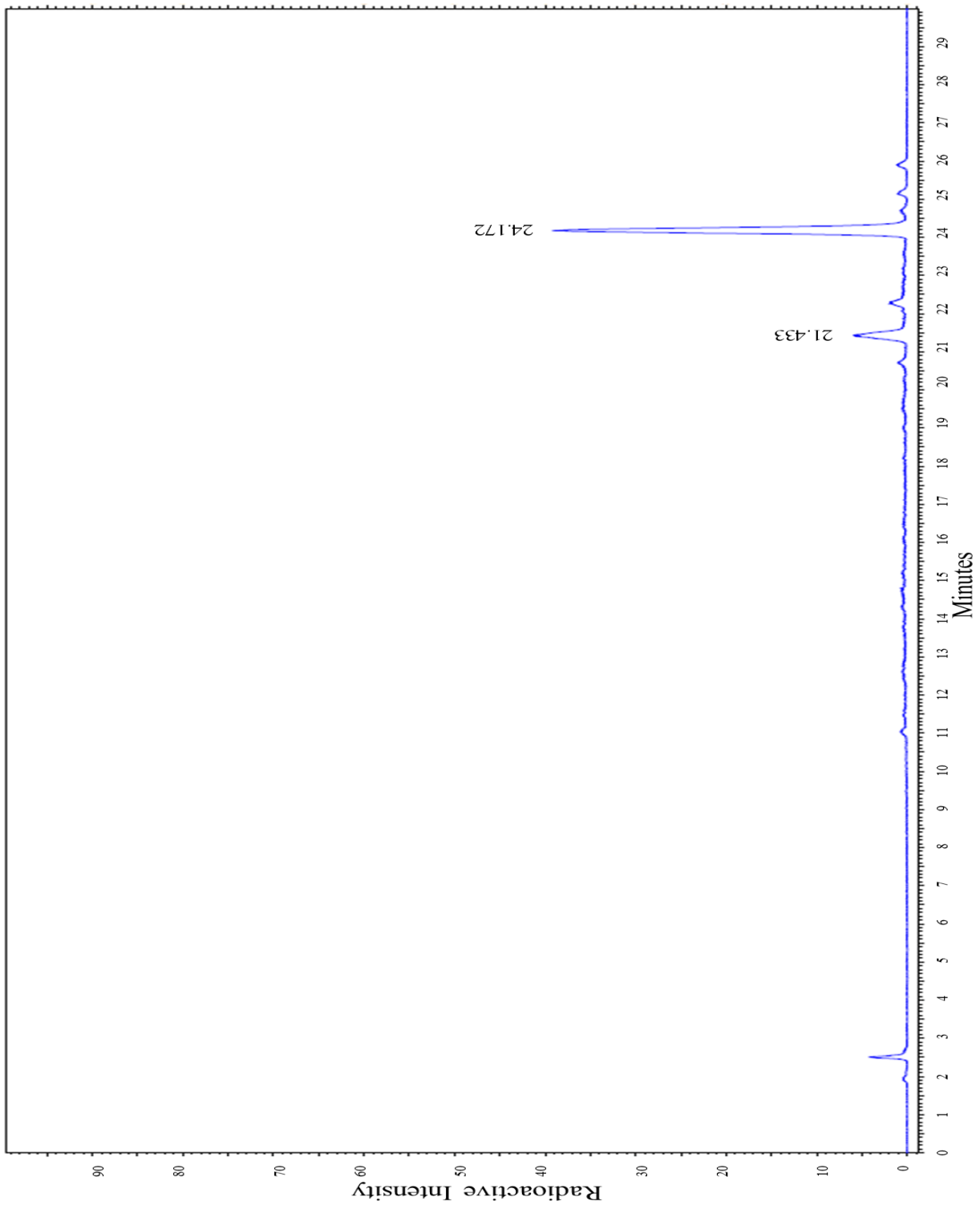

Reinjected ~22 minute peak, radio-HPLC:

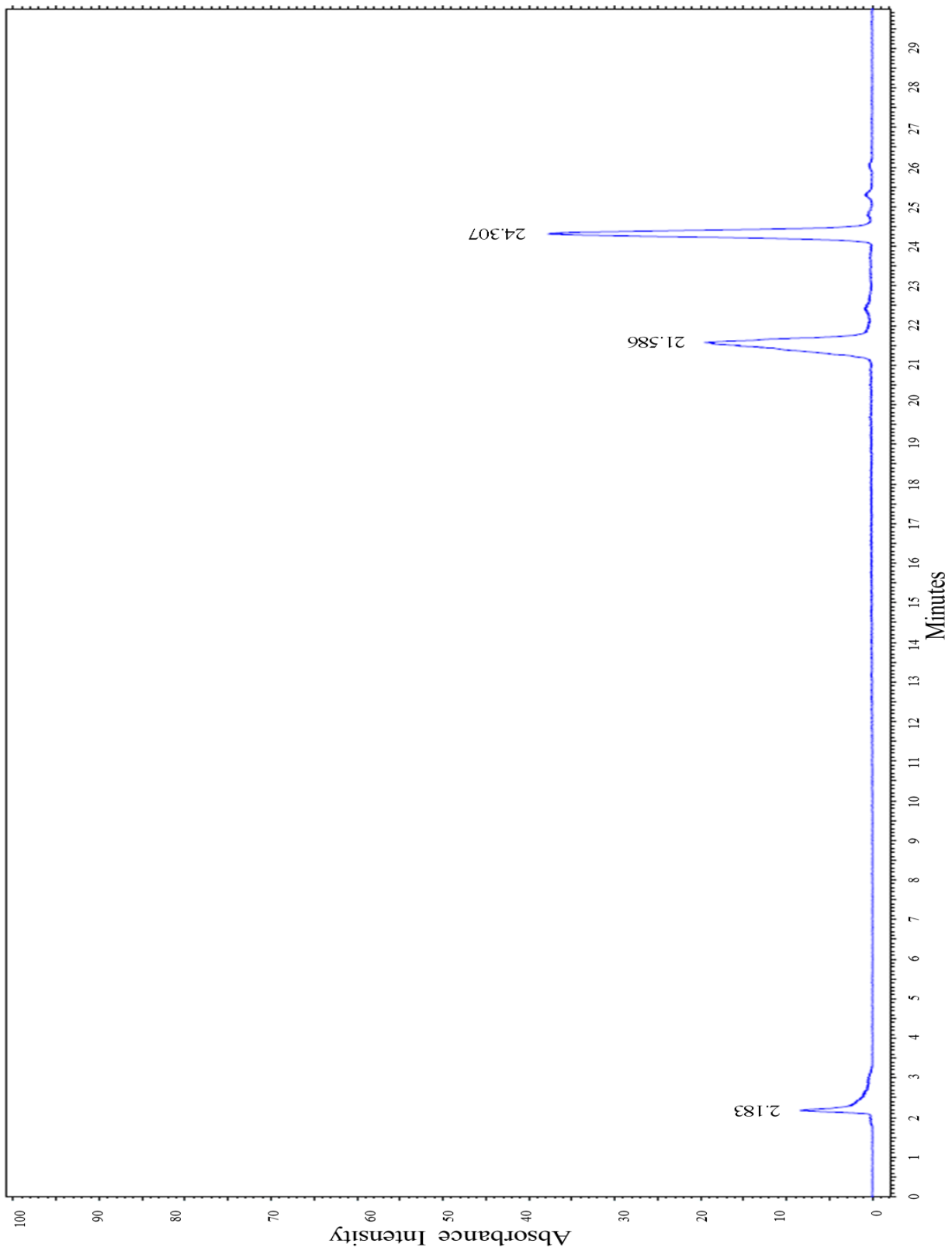

Reinjected ~24 minute peak, radio-HPLC:

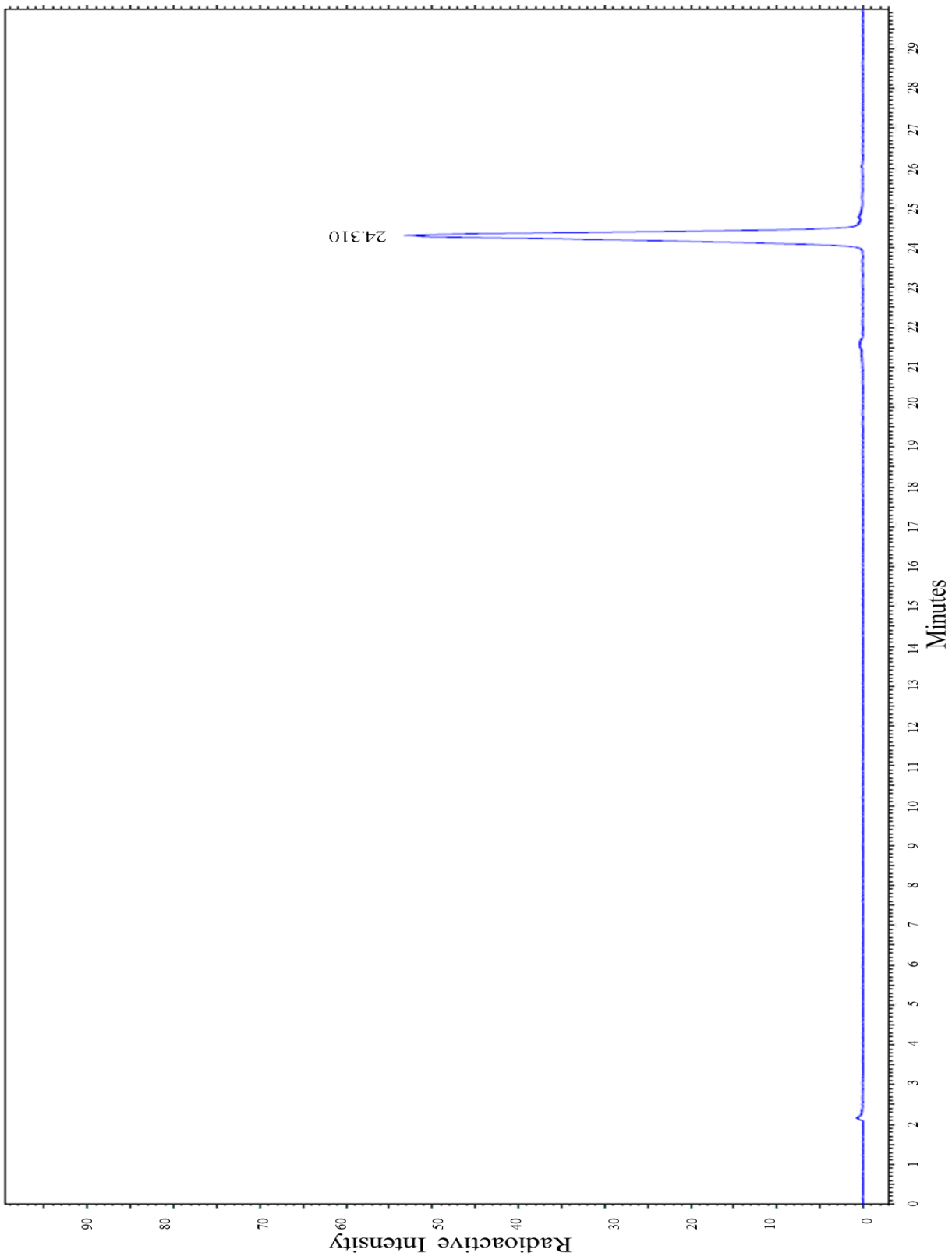

Mice injected dose 0h, radio-HPLC:

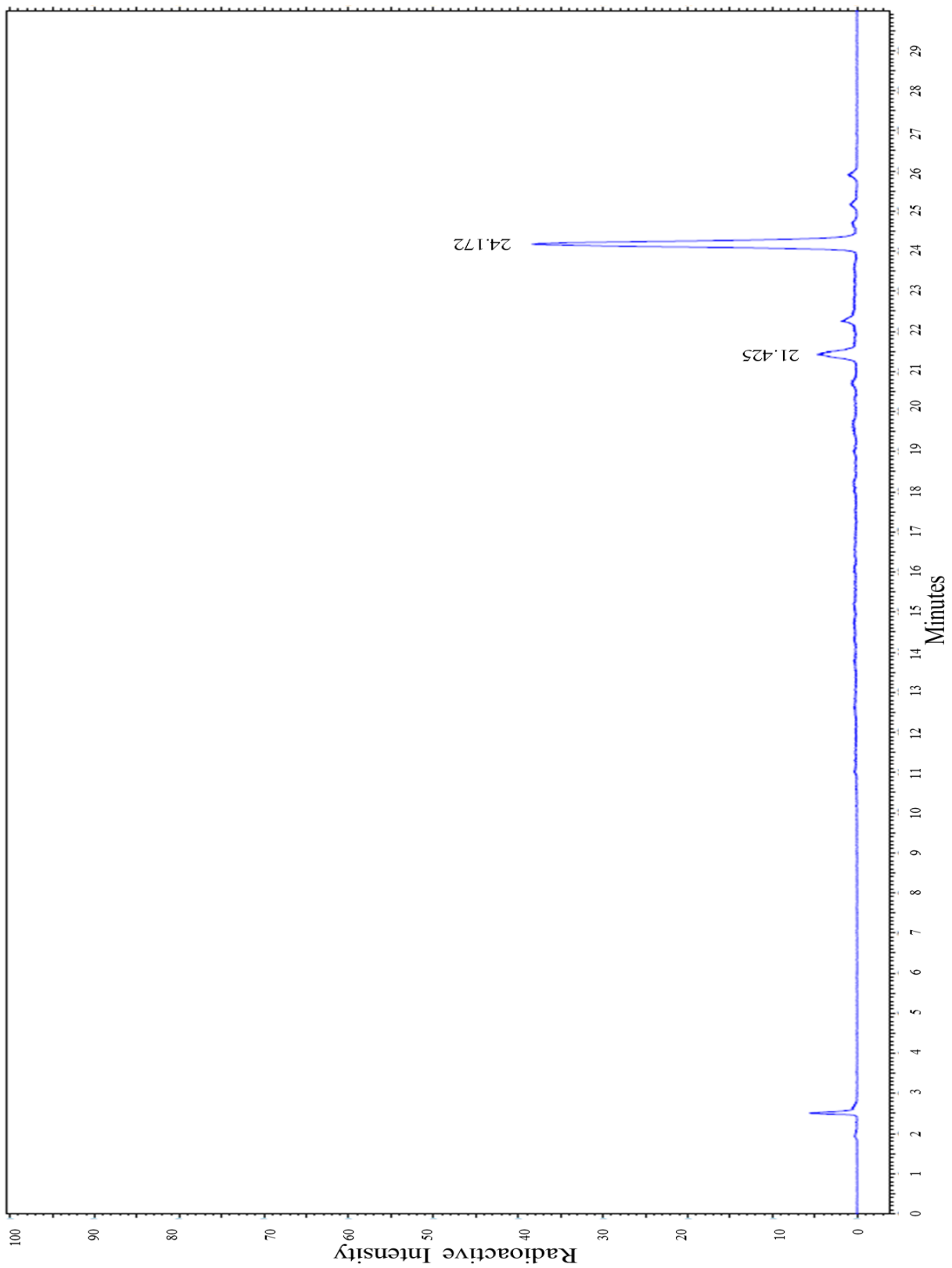

Injected dose 6h, radio-HPLC:

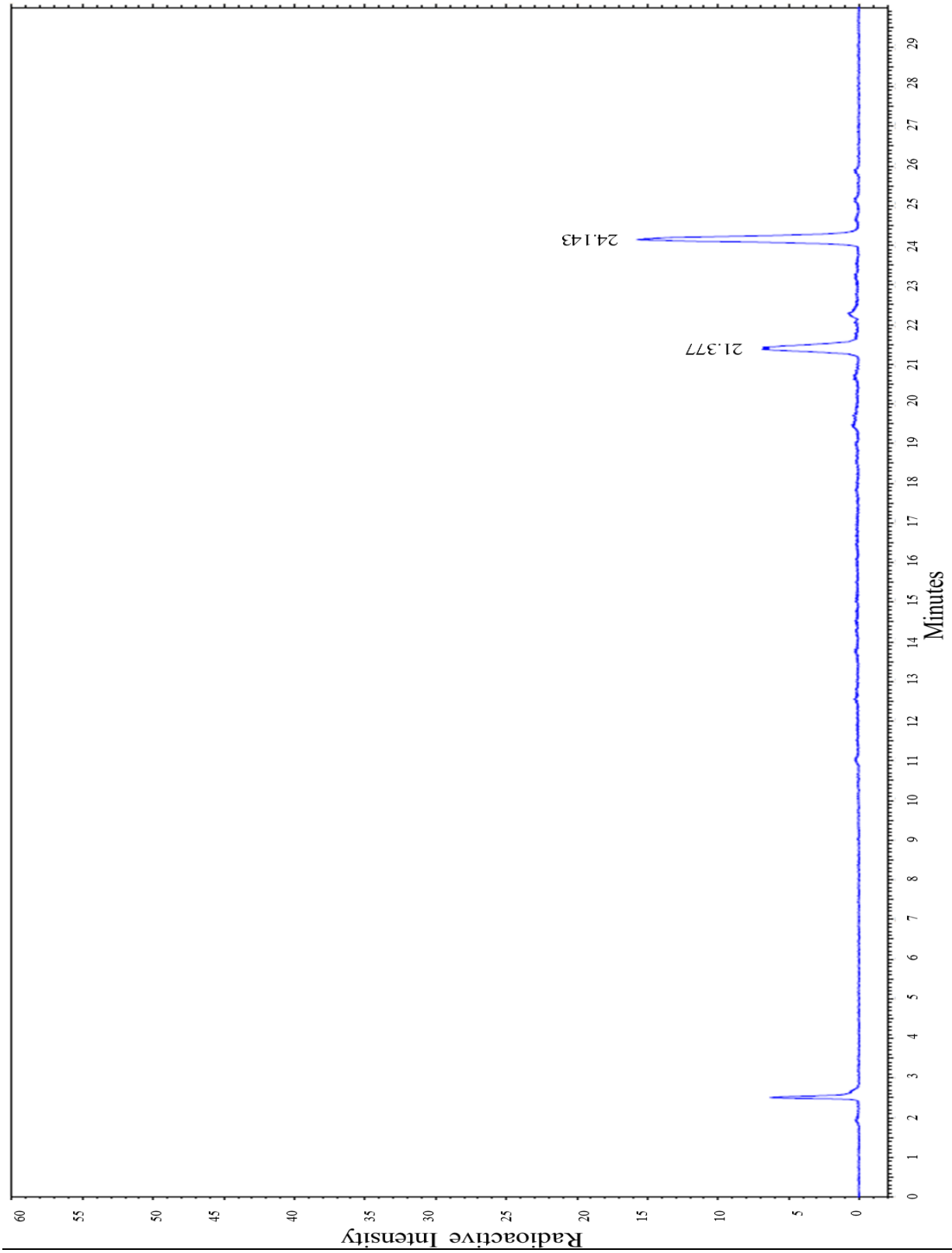

Chapter 3

3-(tritylthio)propan-1-amine hydrochloride

^{1}HNMR:

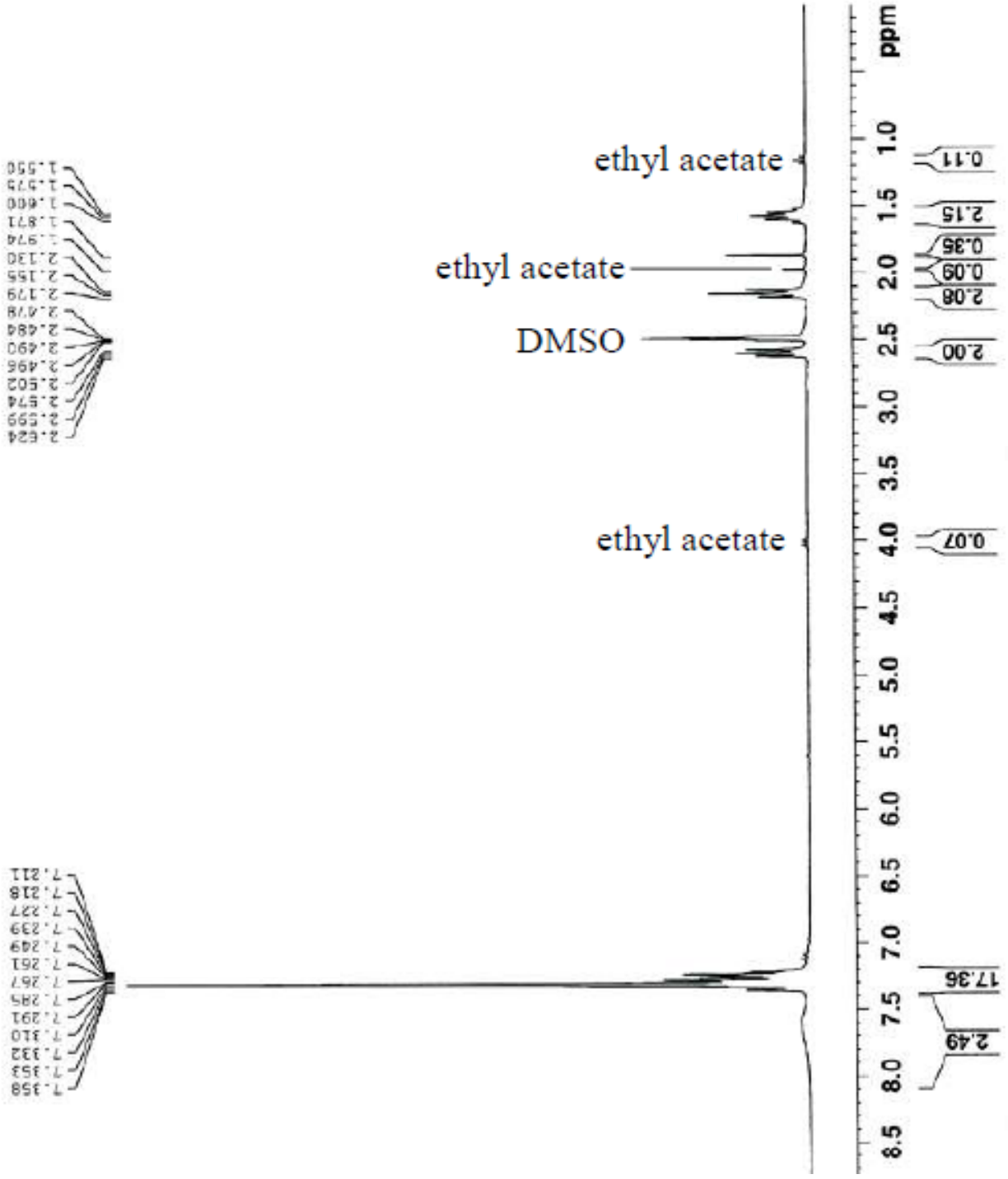

^{13}CNMR:

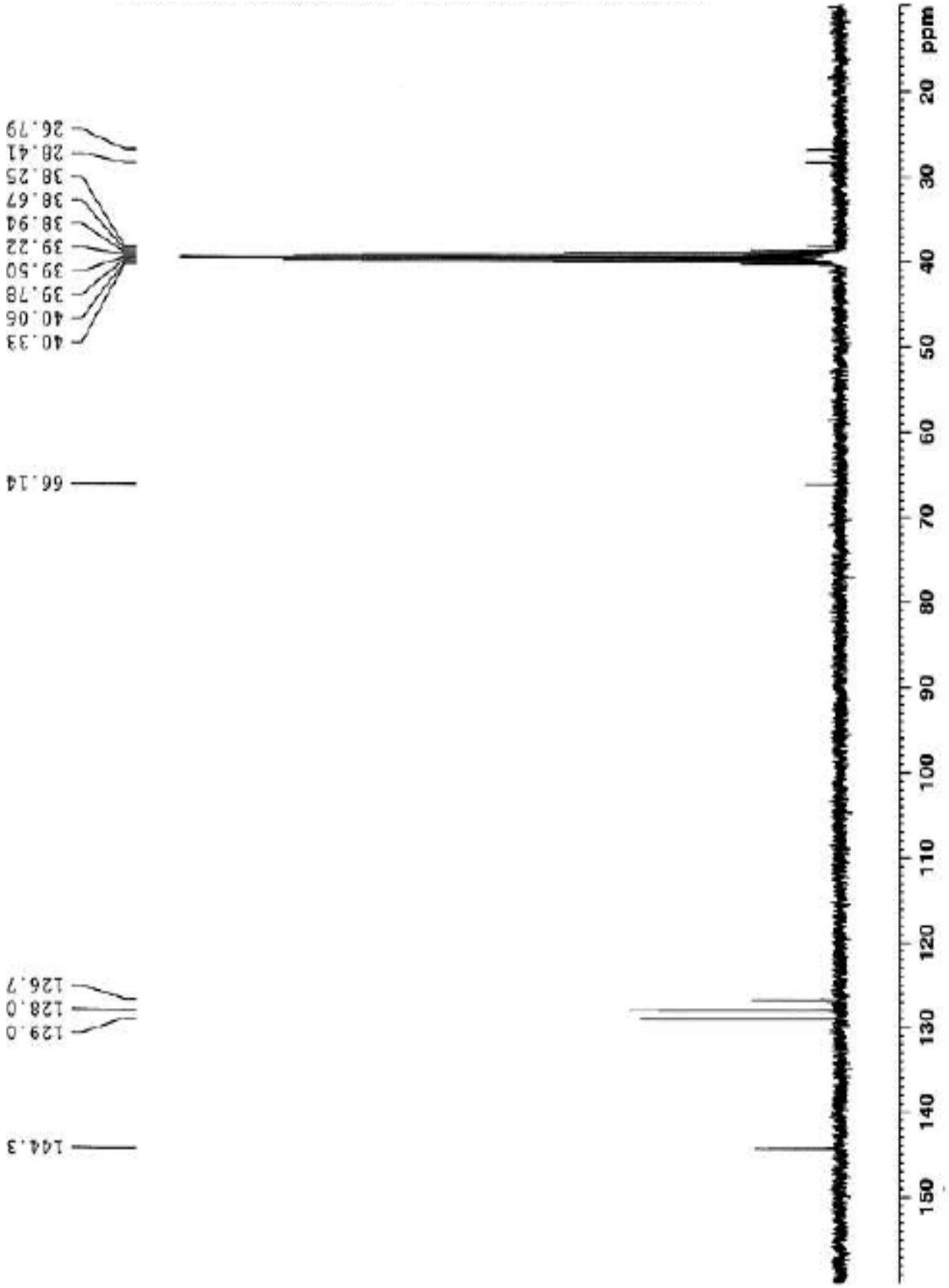
26.79
28.41
38.25
38.67
38.94
39.22
39.50
39.78
40.06
40.33
66.14
126.7
128.0
129.0
144.3
ppm
20
30
40
50
60
70
80
90
100
110
120
130
140
150

323-MAMA

^{1}HNMR:

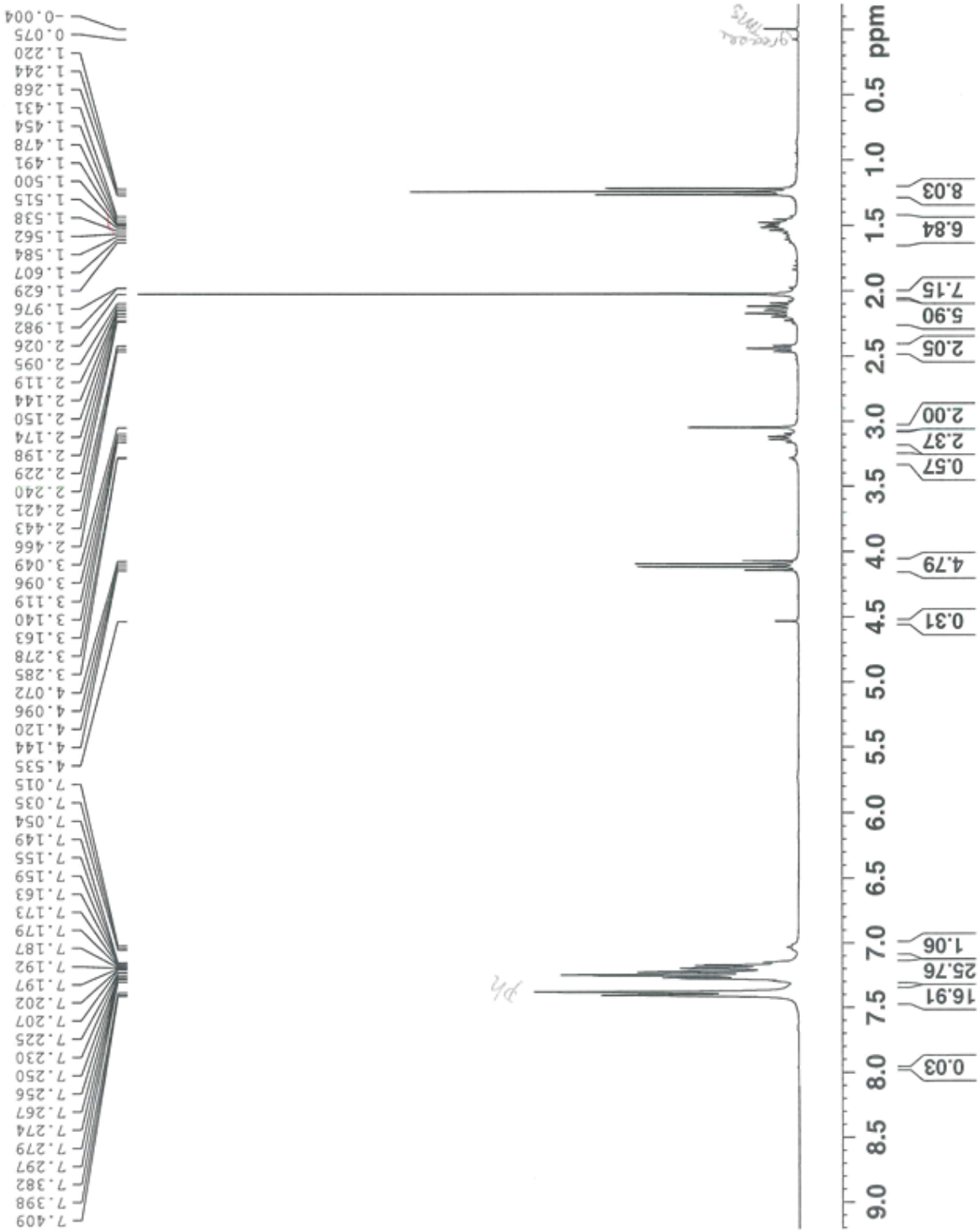

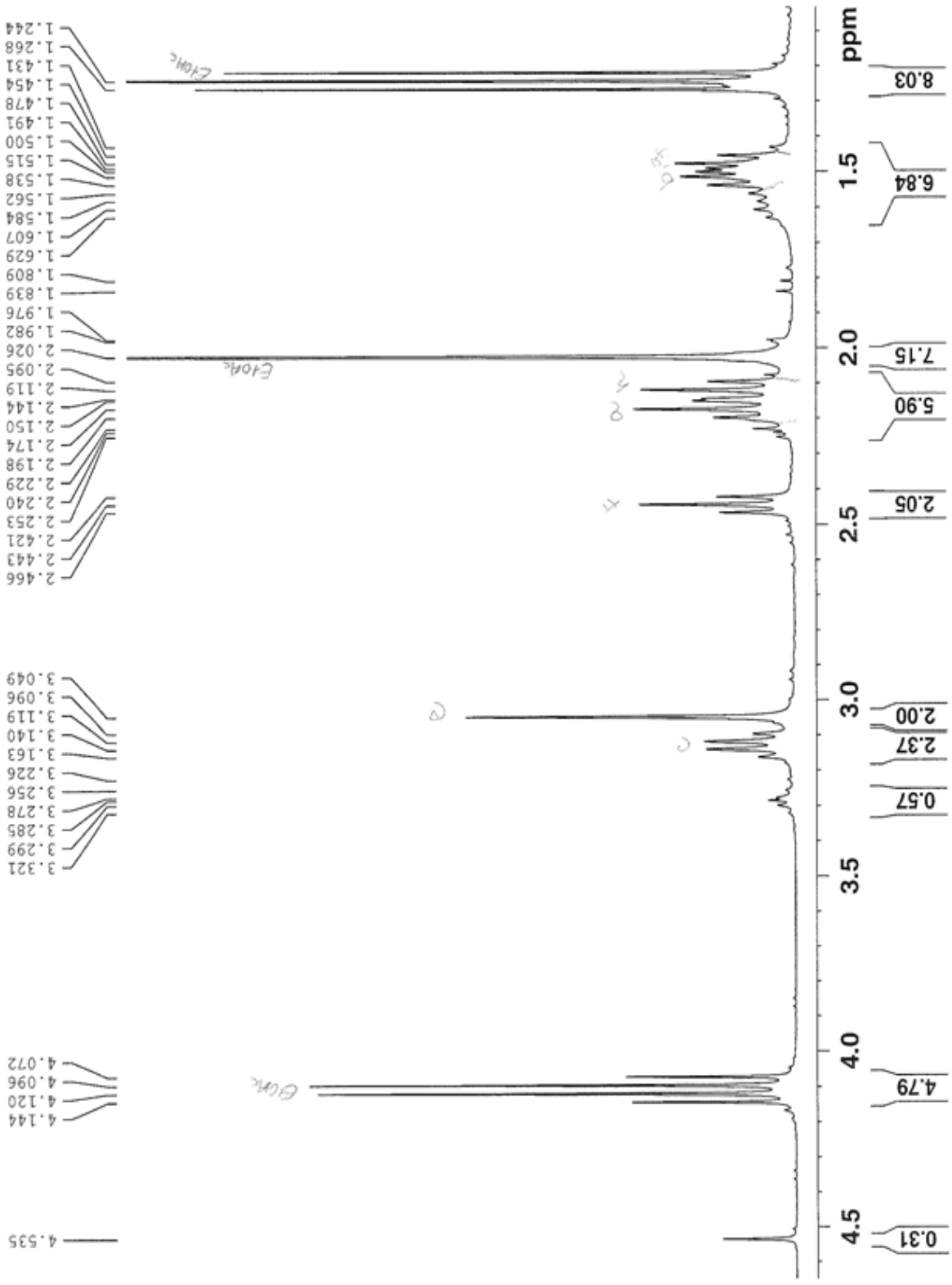
ppm
8.03
6.84
7.15
5.90
2.05
2.00
2.37
0.57
4.79
0.31
EtOAc
EtOAc
EtOH
4.535
4.144
4.120
4.096
4.072
3.321
3.299
3.285
3.278
3.256
3.226
3.163
3.140
3.119
3.096
3.049
2.466
2.443
2.421
2.253
2.240
2.229
2.198
2.174
2.150
2.144
2.119
2.095
2.026
1.982
1.976
1.839
1.809
1.629
1.607
1.584
1.562
1.538
1.515
1.500
1.491
1.478
1.454
1.431
1.268
1.244

^{13}CNMR:

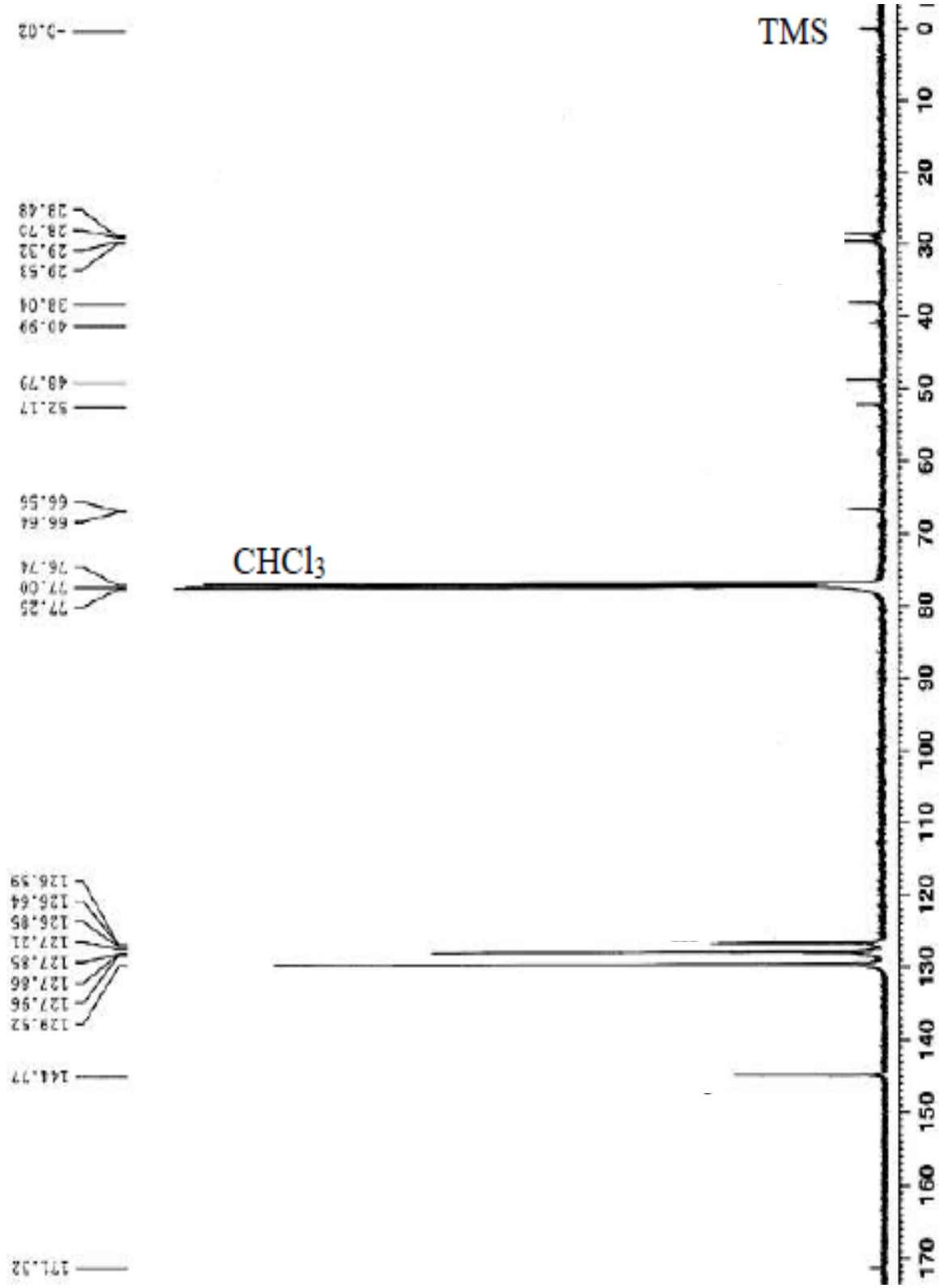
TMS
CHCl3
-0.02
28.48
28.70
29.32
29.53
38.04
40.99
48.79
52.17
66.56
66.64
76.74
77.00
77.25
126.39
126.64
126.85
127.21
127.85
127.86
127.96
128.52
144.77
171.32
0
10
20
30
40
50
60
70
80
90
100
110
120
130
140
150
160
170

323-MAMA-hexanoate

^{1}HNMR:

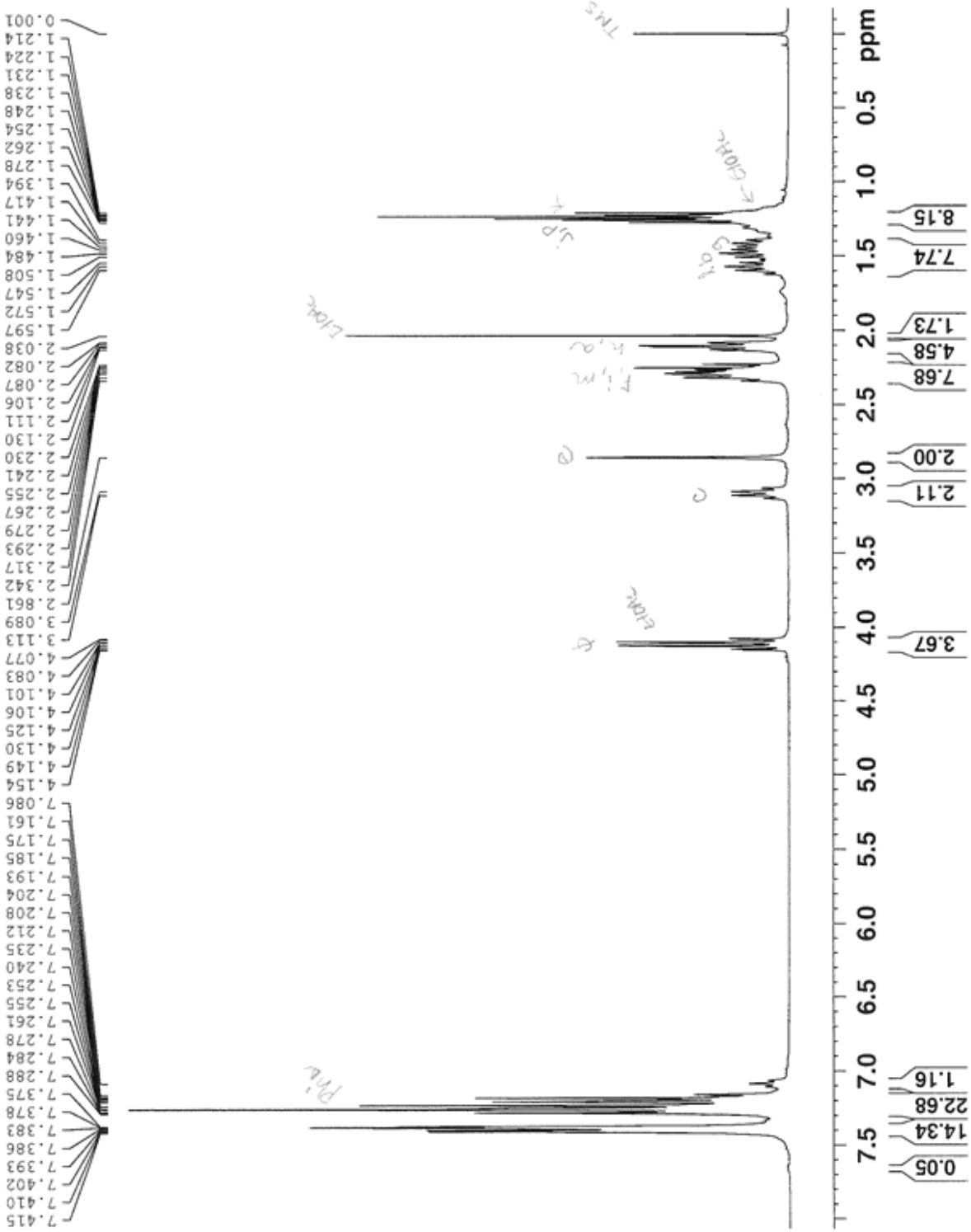

^{13}CNMR:

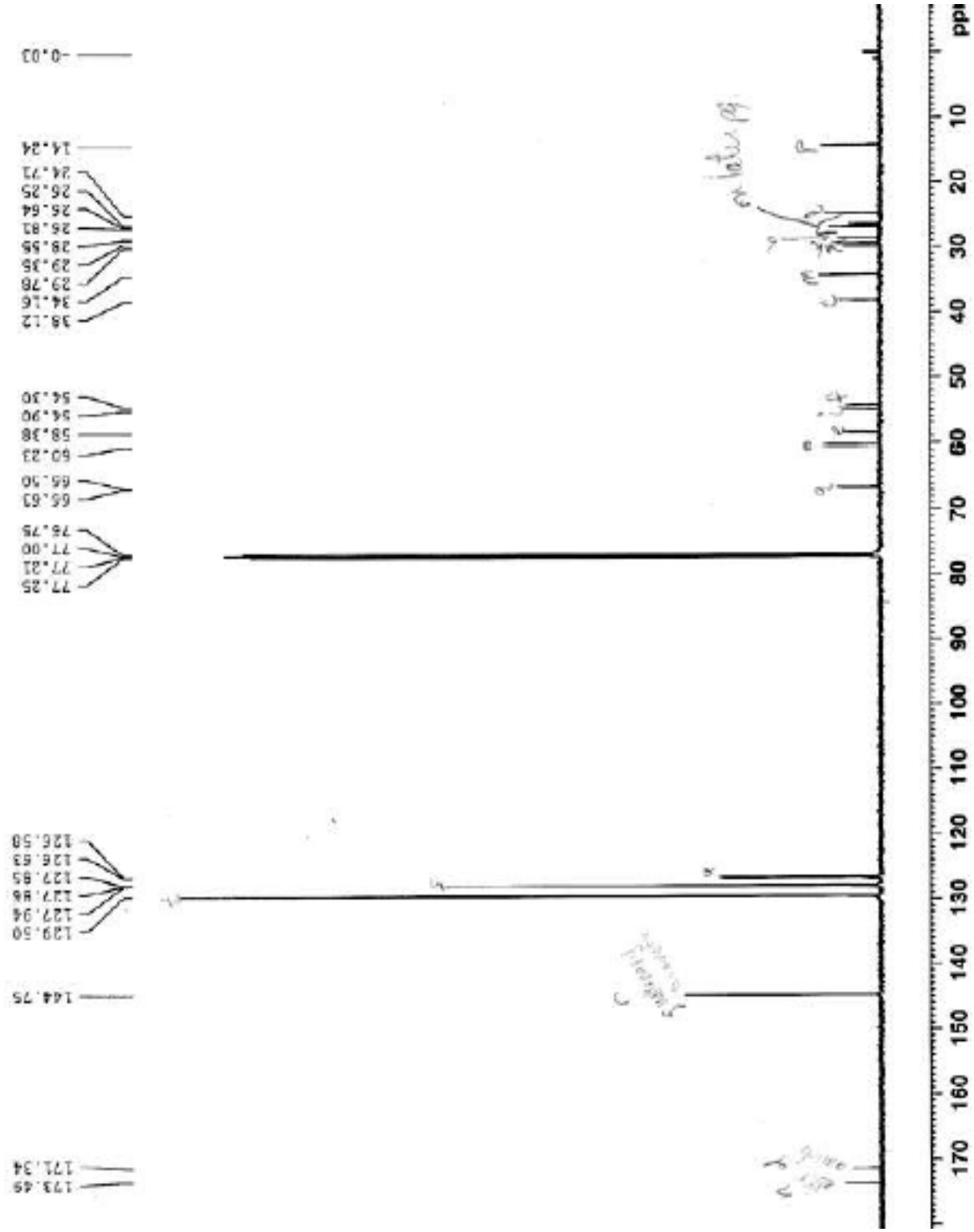
-0.03
14.24
24.71
25.25
25.64
25.83
28.59
29.35
29.78
34.16
38.12
54.30
54.90
58.38
60.23
65.50
65.63
76.75
77.00
77.21
77.25
126.58
126.63
127.85
127.86
127.94
129.50
144.75
171.34
173.49
ppm
10
20
30
40
50
60
70
80
90
100
110
120
130
140
150
160
170

ReO323-MAMA

^{1}HNMR:

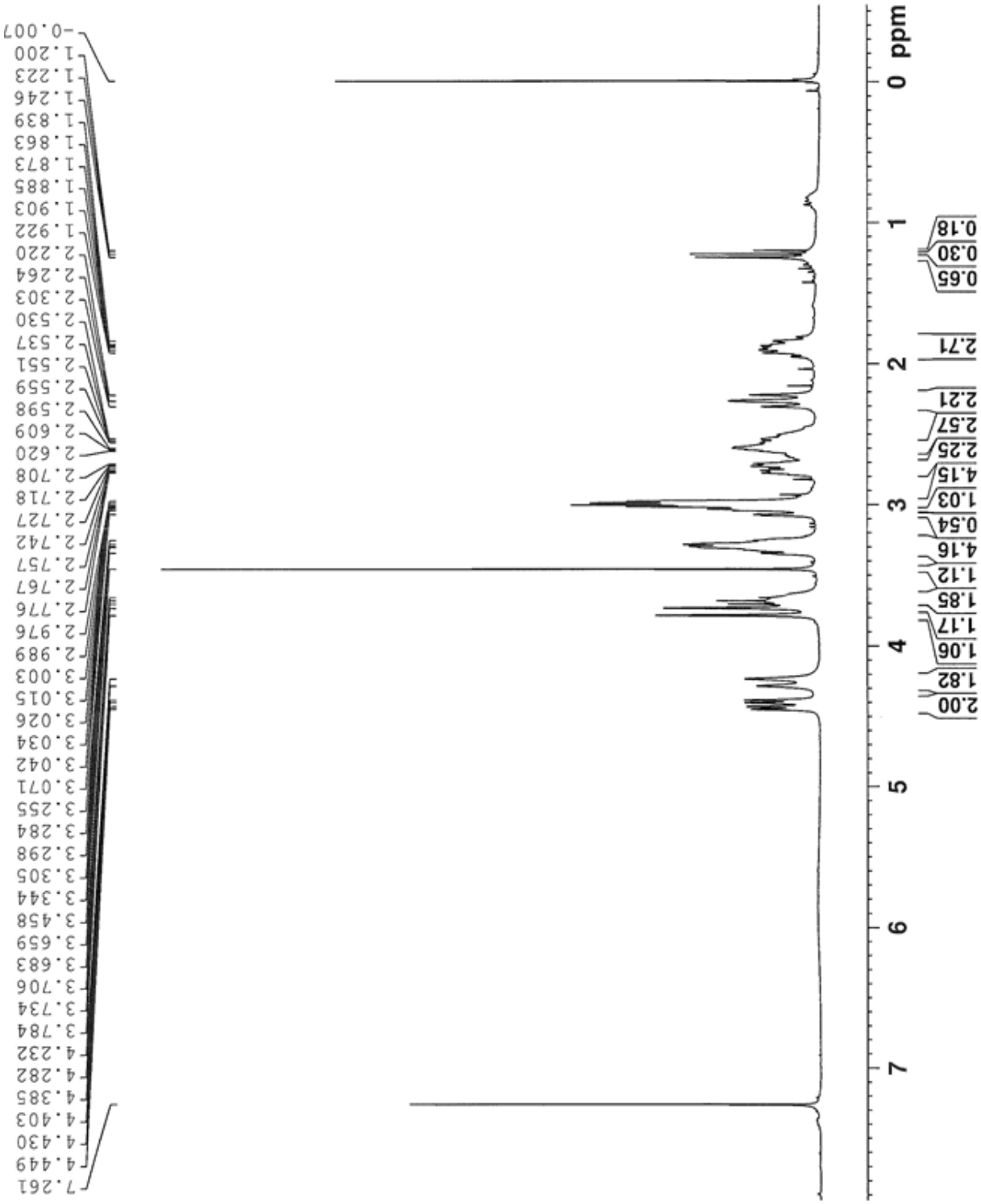

^{13}CNMR (dept):

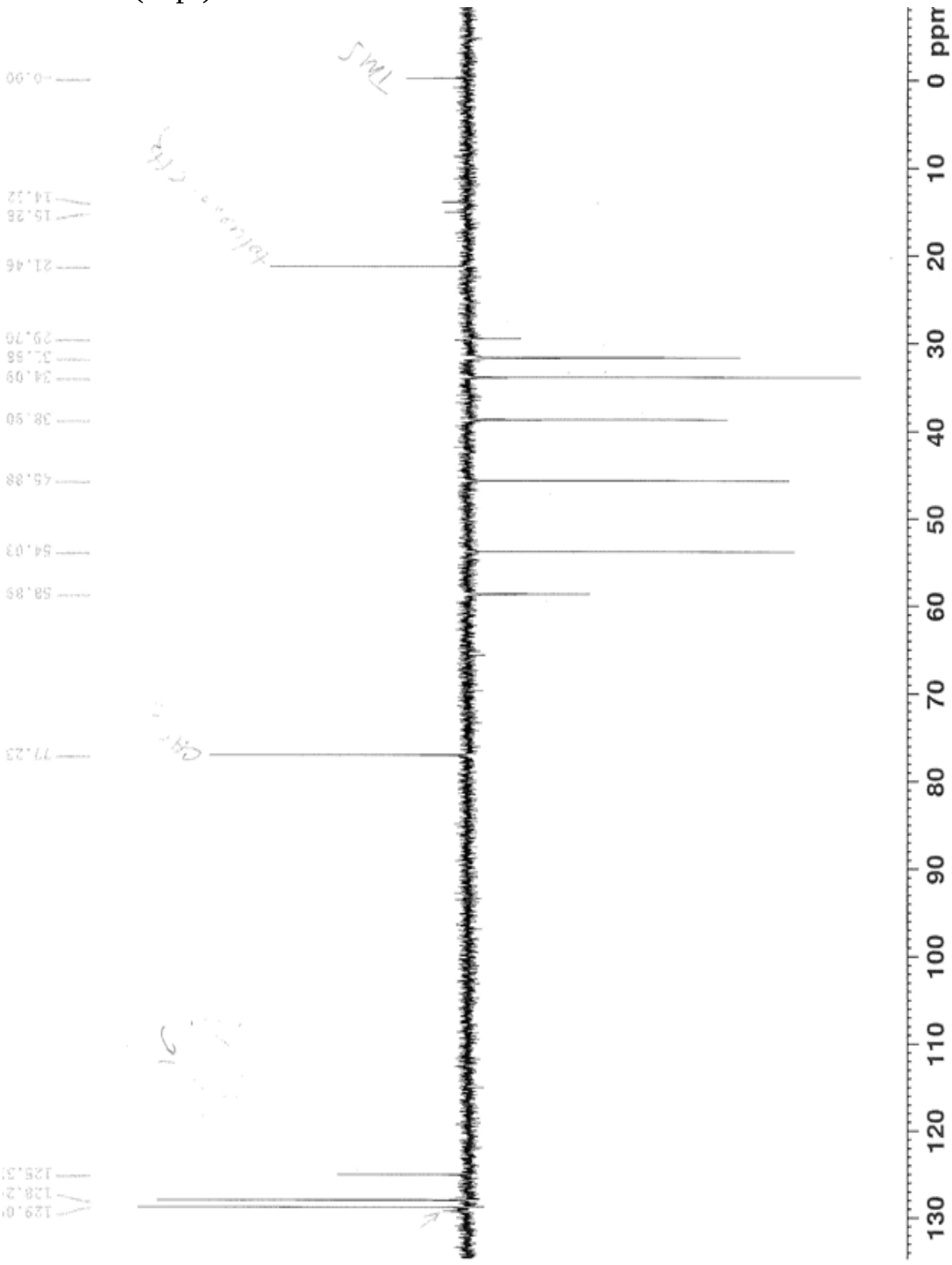
0 ppm
10
20
30
40
50
60
70
80
90
100
110
120
130
-0.00
14.32
15.26
21.46
29.76
32.68
34.09
38.50
45.88
54.03
58.85
77.23
125.31
128.21
129.01

HPLC:

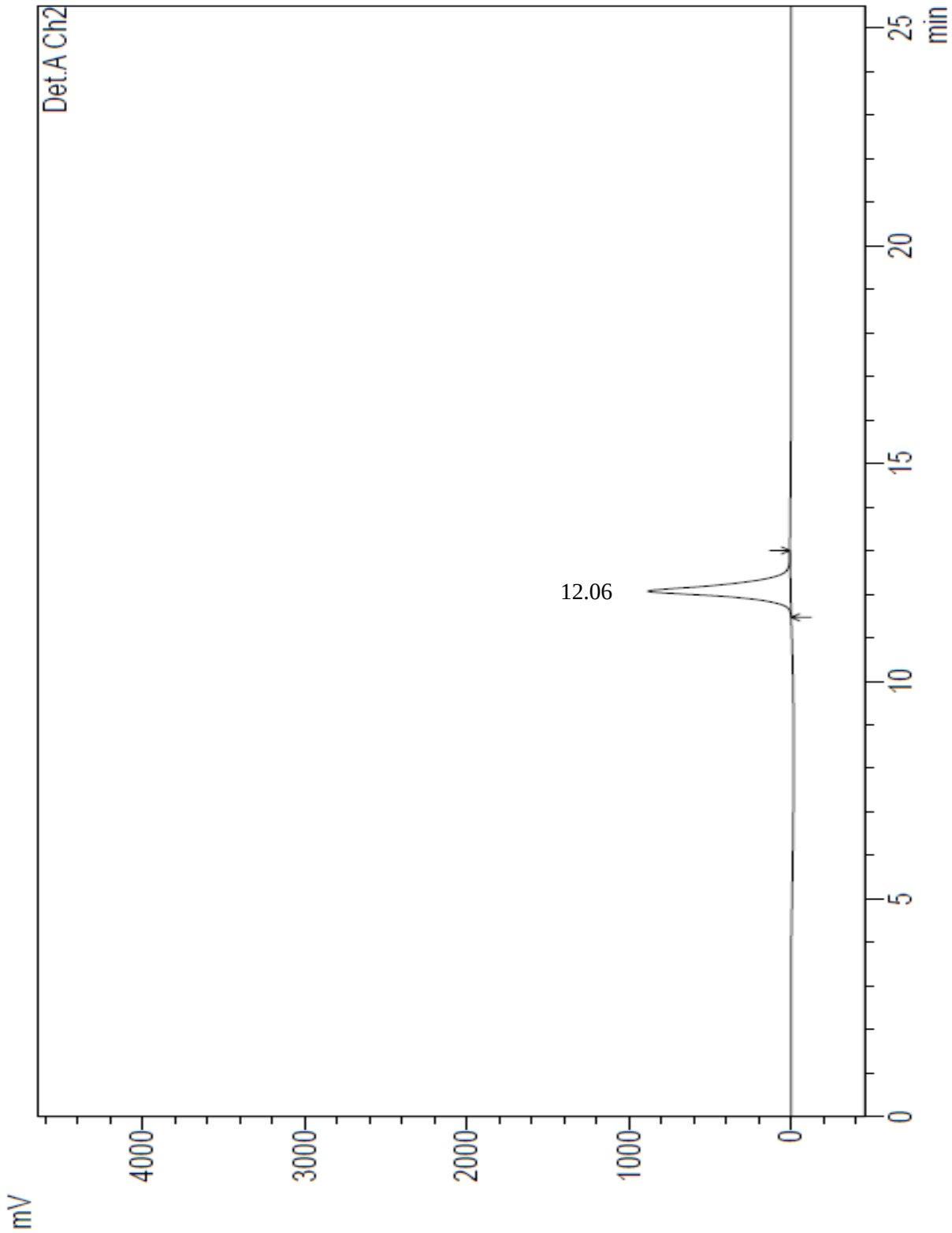

Crystal Data Information, ReO-323MAMA:

Data_ANDJ3

audit_creation_method SHELXL-2014/7

shelx_SHELXL_version_number 2014/7

chemical_formula_moiety 'C8 H15 N2 O2 Re S2'

chemical_formula_sum 'C8 H15 N2 O2 Re S2'

exptl_crystal_description Prism

exptl_crystal_colour Brown/Purple

diffrn_ambient_temperature 100(2)

chemical_formula_weight 421.54

space_group_crystal_system monoclinic

space_group_IT_number 14

space_group_name_H-M_alt 'P 21/c'

space_group_name_Hall '-P 2ybc'

cell_length_a 7.5153(15)

cell_length_b 14.649(3)

cell_length_c 21.739(4)

cell_angle_alpha 90

cell_angle_beta 98.613(2)

cell_angle_gamma 90

cell_volume 2366.3(8)

cell_formula_units_Z 8

cell_measurement_temperature 100(2)

cell_measurement_reflns_used 9976

cell_measurement_theta_min 2.7

cell_measurement_theta_max 27.5

exptl_crystal_density_diffrn 2.367

exptl_crystal_F_000 1600

exptl_crystal_size_max 0.500

exptl_crystal_size_mid 0.400

exptl_crystal_size_min 0.200

exptl_absorpt_coefficient_mu 10.606

shelx_estimated_absorpt_T_min 0.076

shelx_estimated_absorpt_T_max 0.226

exptl_absorpt_correction_type multi-scan

exptl_absorpt_correction_T_min 0.11

exptl_absorpt_correction_T_max 0.23

Select Bond Lengths and Angles:

Re1A O2A 1.671(5)

Re1A N1A 2.015(6)

Re1A N2A 2.132(6)

Re1A S1A 2.2813(17) .

Re1A S2A 2.3005(18)

O2A Re1A N1A 111.2(2)

O2A Re1A N2A 104.9(2)

N1A Re1A N2A 78.1(2)

O2A Re1A S1A 108.29(18)

N1A Re1A S1A 92.64(17)

N2A Re1A S1A 146.63(16)

O2A Re1A S2A 110.86(19)

N1A Re1A S2A 137.57(18)

N2A Re1A S2A 85.82(16)

S1A Re1A S2A 79.67(7)

ReO323-MAMAhexanoate

^{1}HNMR:

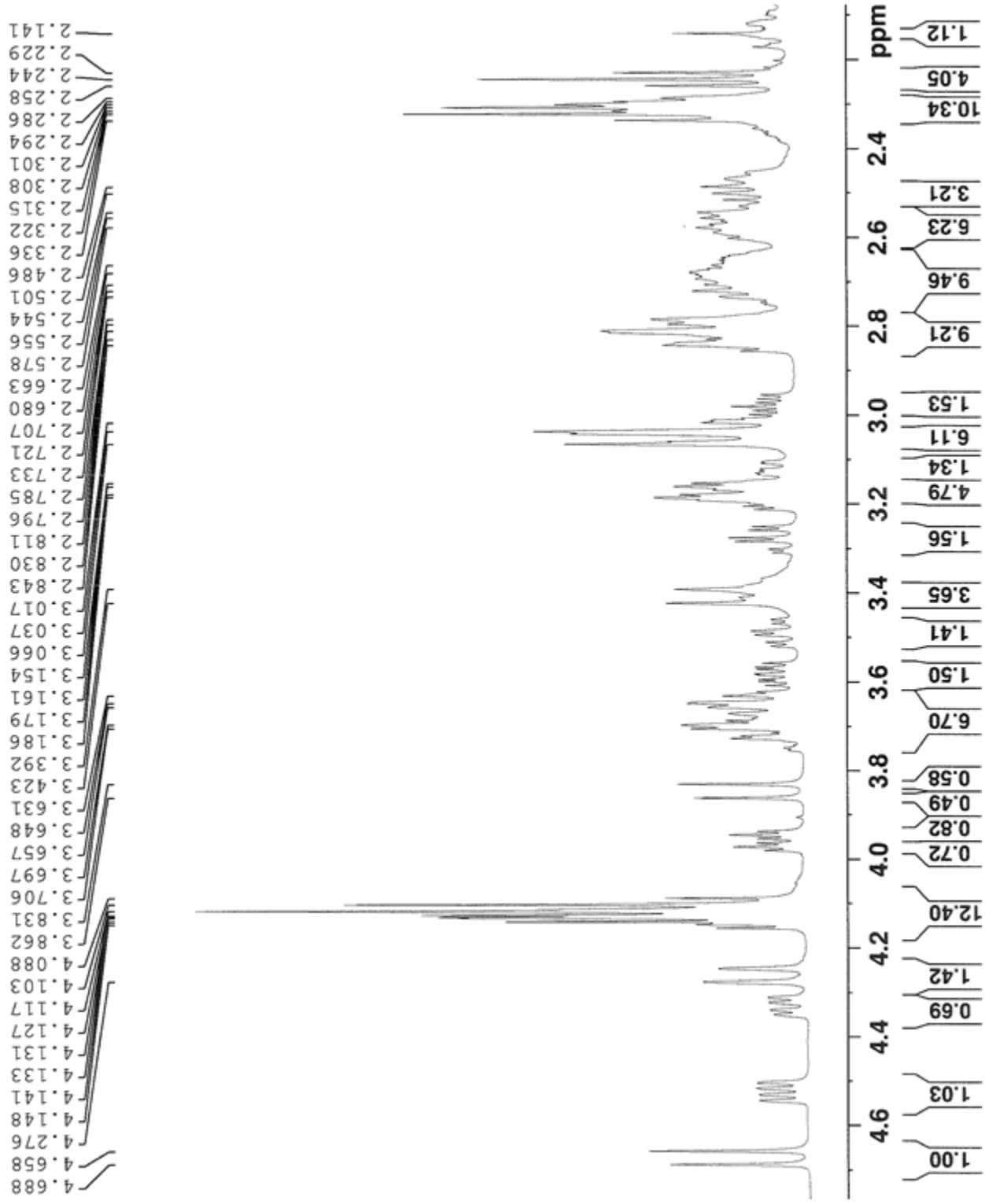

^{13}CNMR:

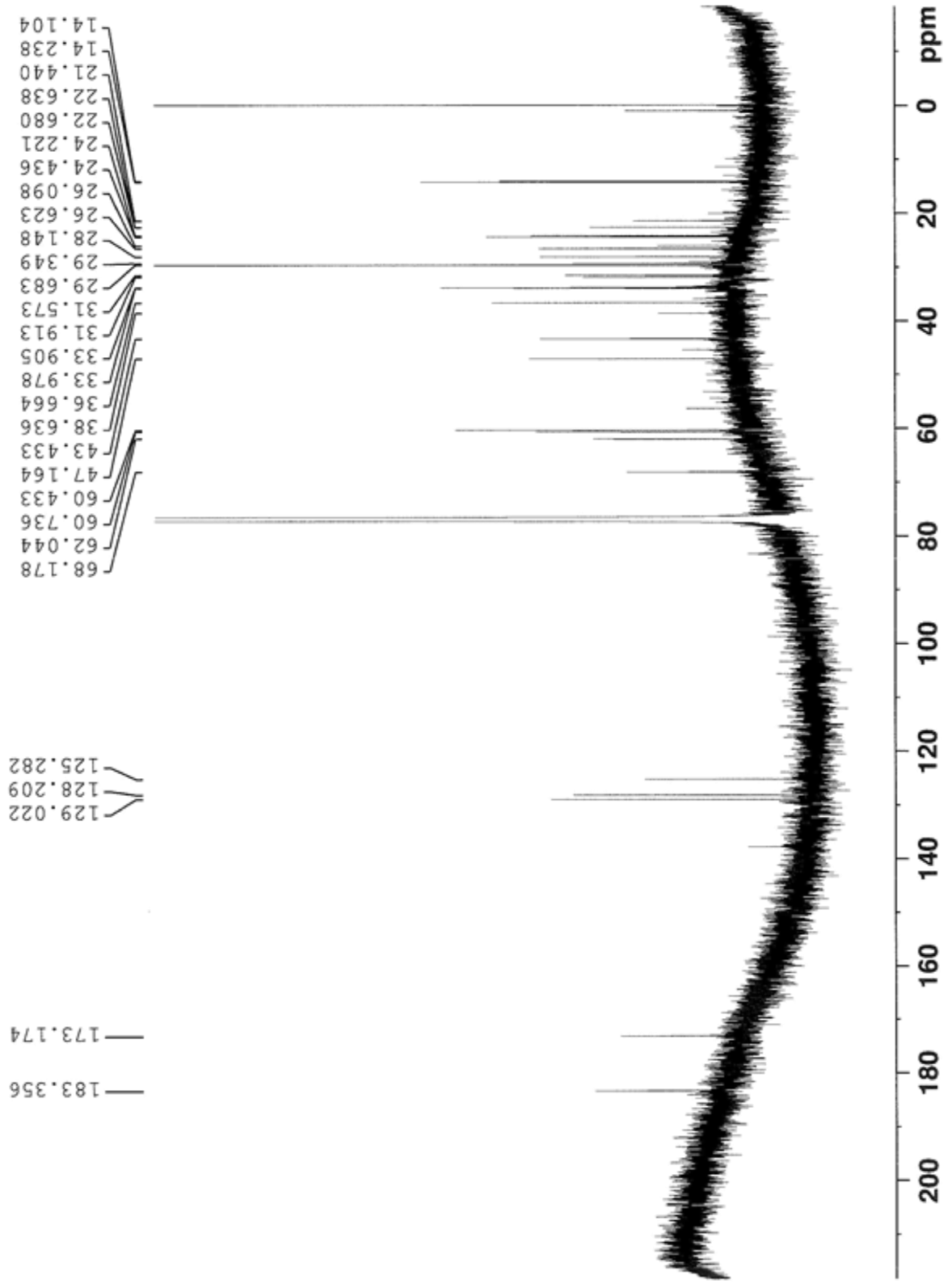
14.104
14.238
21.440
22.638
22.680
24.221
24.436
26.098
26.623
28.148
29.349
29.683
31.573
31.913
33.905
33.978
36.664
38.636
43.433
47.164
60.433
60.736
62.044
68.178
125.282
128.209
129.022
173.174
183.356
0
20
40
60
80
100
120
140
160
180
200
ppm

LC-MS:

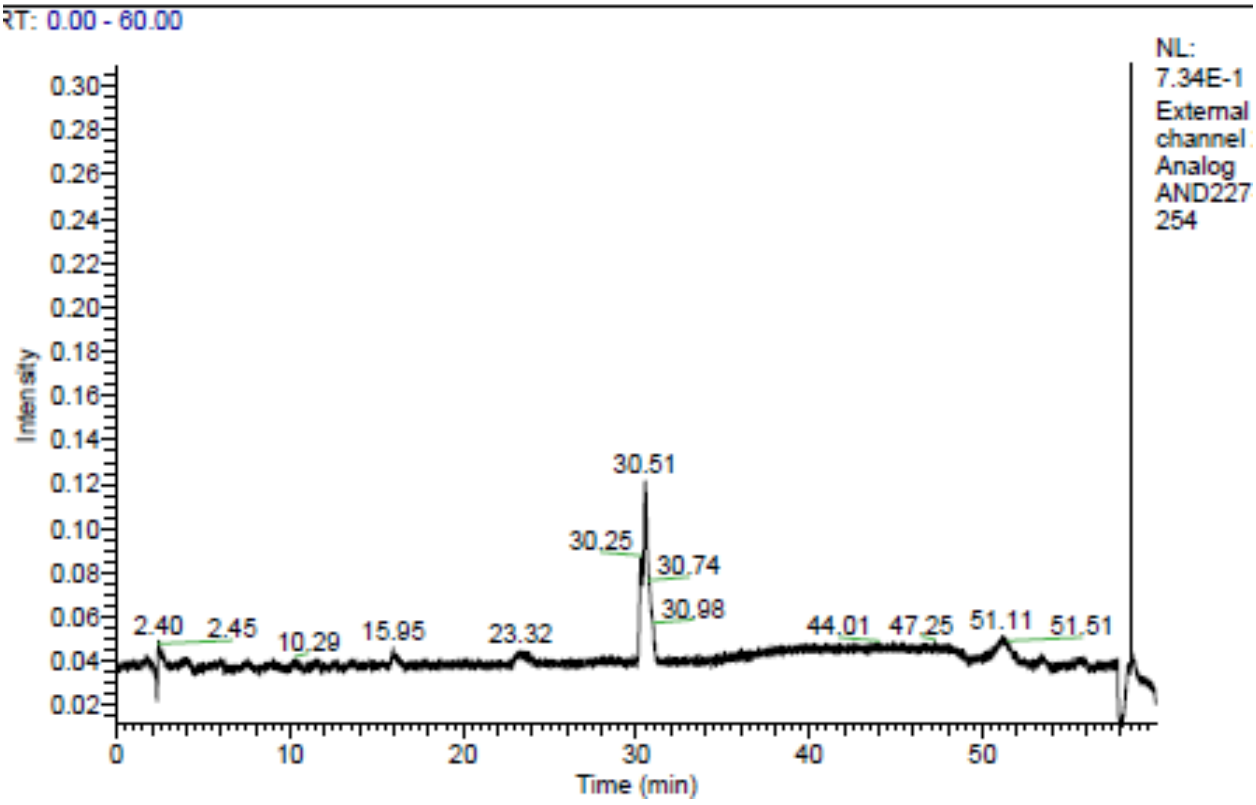
RT: 0.00 - 60.00
NL:
7.34E-1
External
channel
Analog
AND227
254
Intensity
Time (min)
30.51
30.25
30.74
30.98
2.40
2.45
10.29
15.95
23.32
44.01
47.25
51.11
51.51

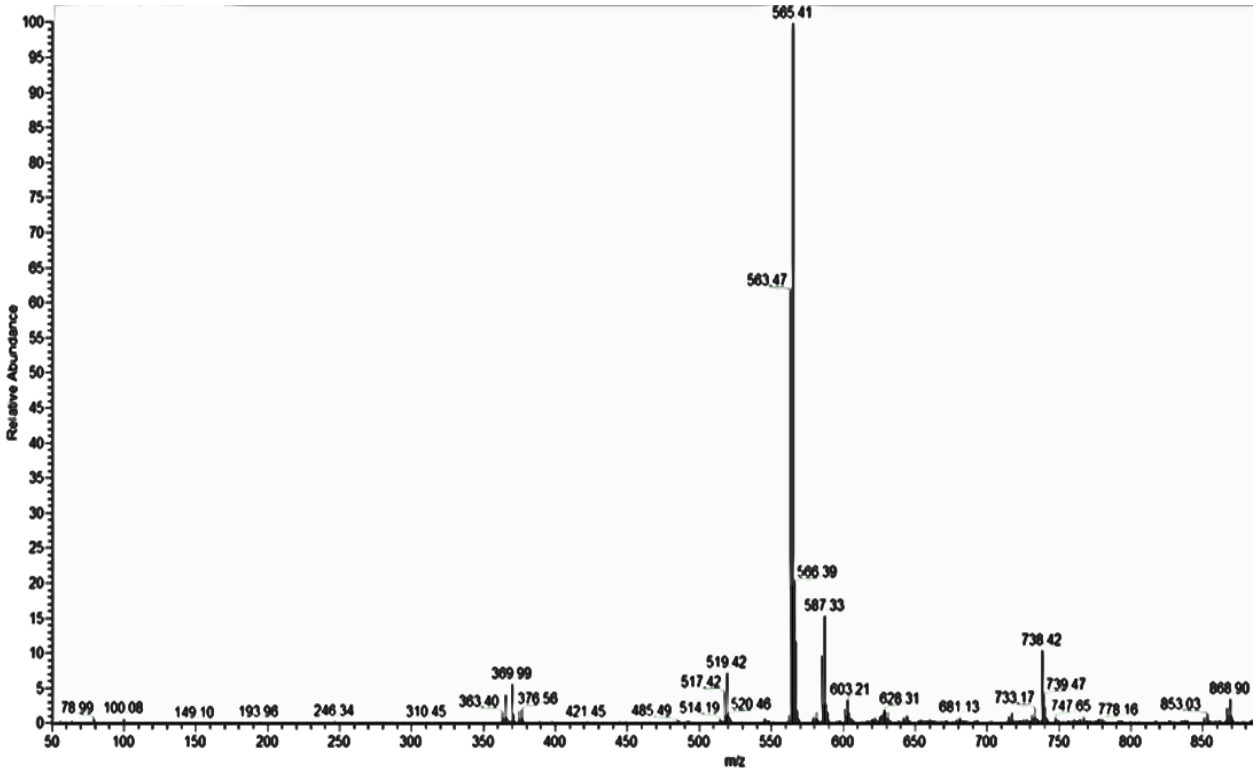
Relative Abundance
m/z
565.41
563.47
566.39
587.33
519.42
517.42
738.42
739.47
603.21
628.31
681.13
733.17
747.65
778.16
853.03
868.90
389.99
376.56
363.40
421.45
485.49
514.19
520.46
310.45
246.34
193.96
149.10
100.08
78.99

^{99m}TcO323-MAMA

Radio-HPLC:

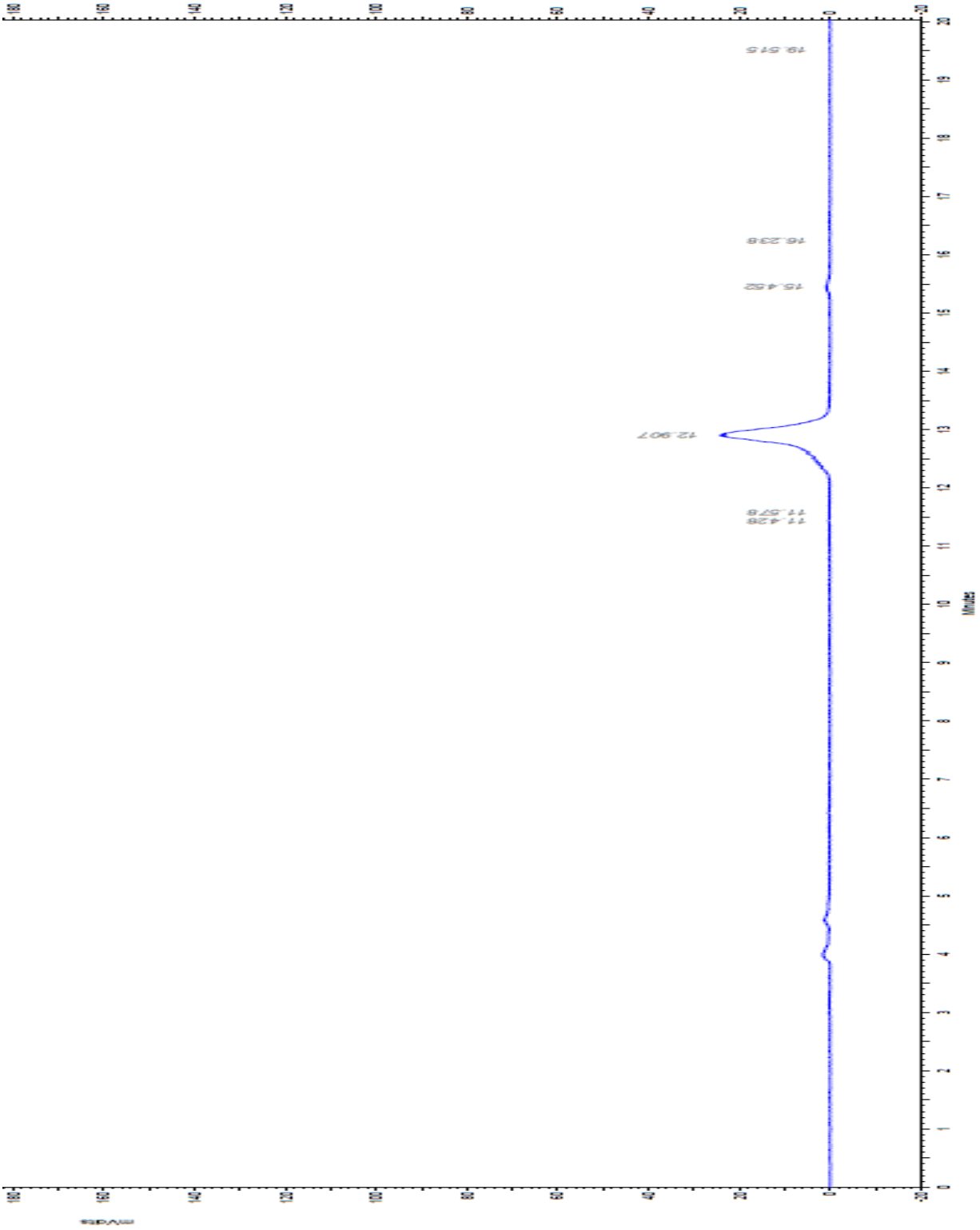

Comparison of ^{99m}TcO-323MAMA and 222-hexanoate, radio-HPLC

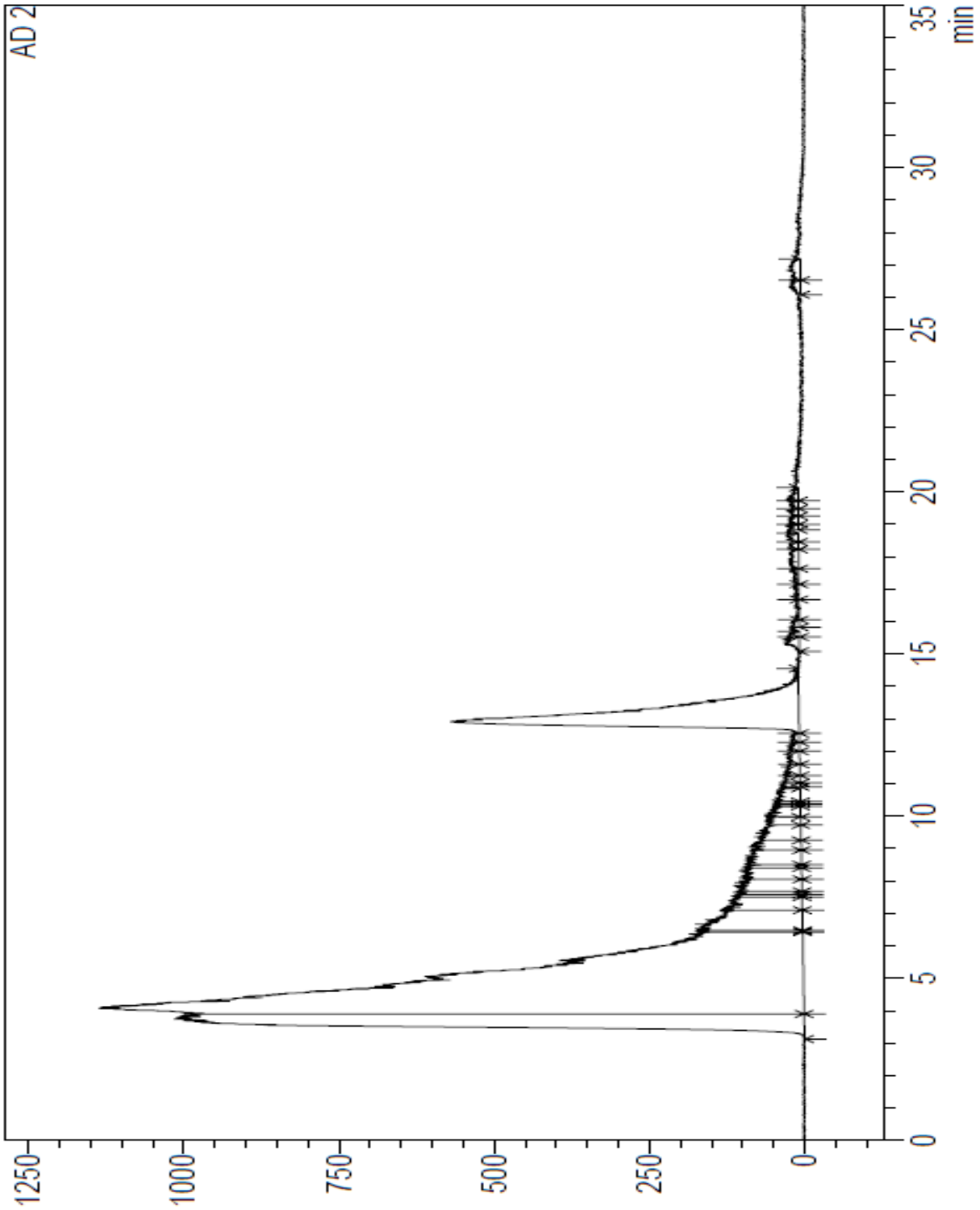

Chapter 4

methyl 2-((2-chloroethyl)thio)acetate (Intermediate 1)

^{1}HNMR:

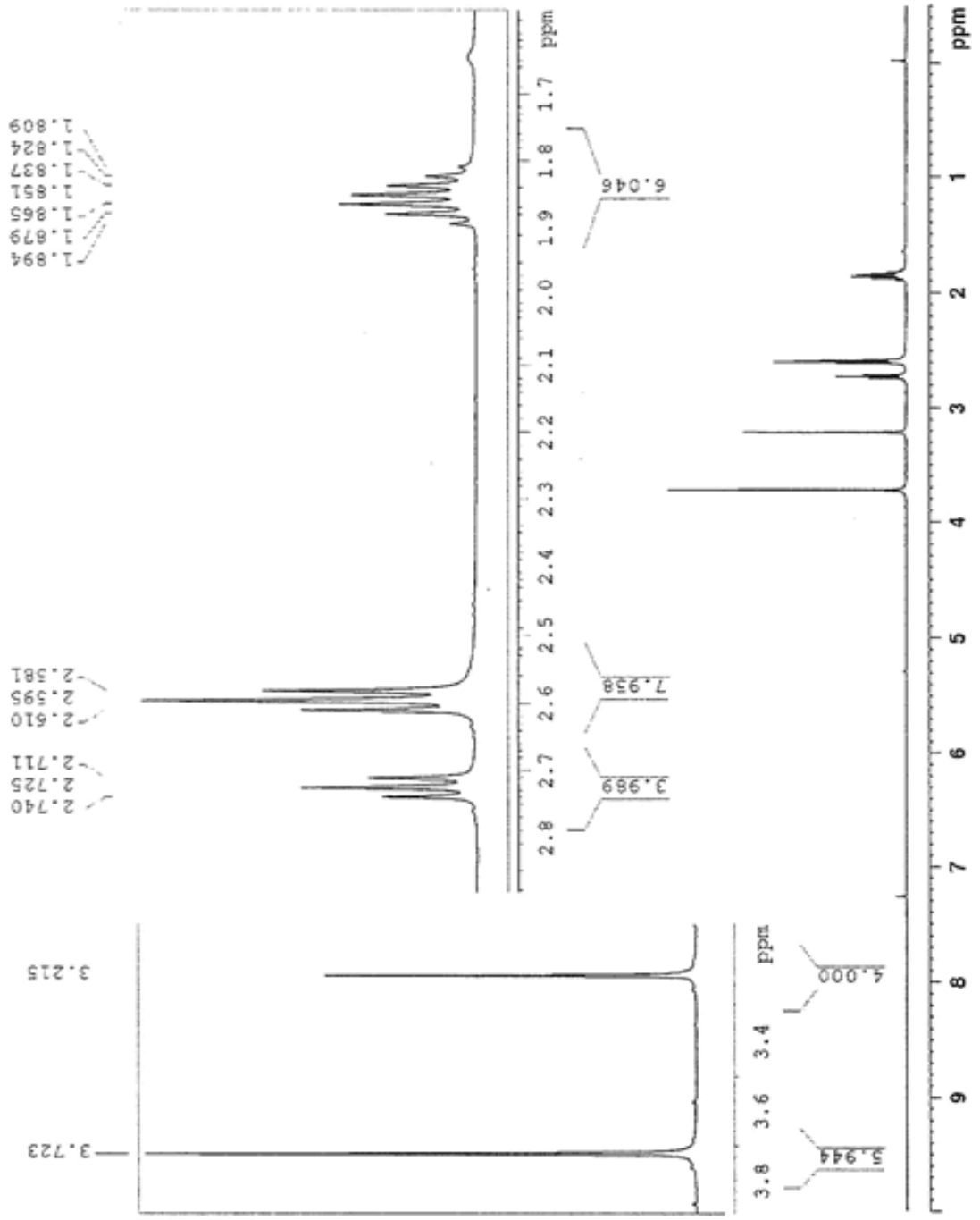

^{13}CNMR:

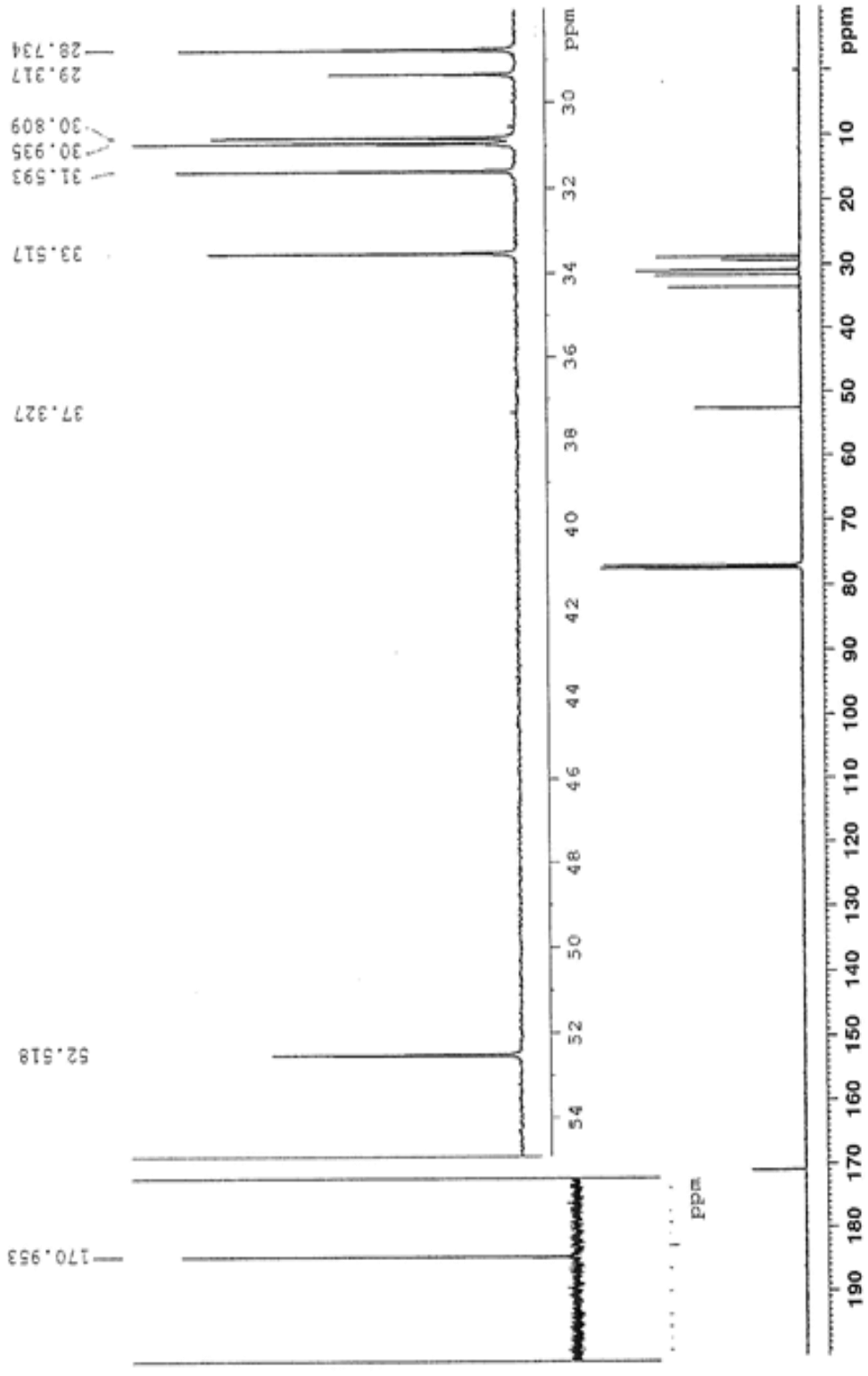
28.734
29.317
30.809
30.935
31.593
33.517
37.327
52.518
170.953
ppm
ppm

222-S_4-diAcOMe

^{1}HNMR:

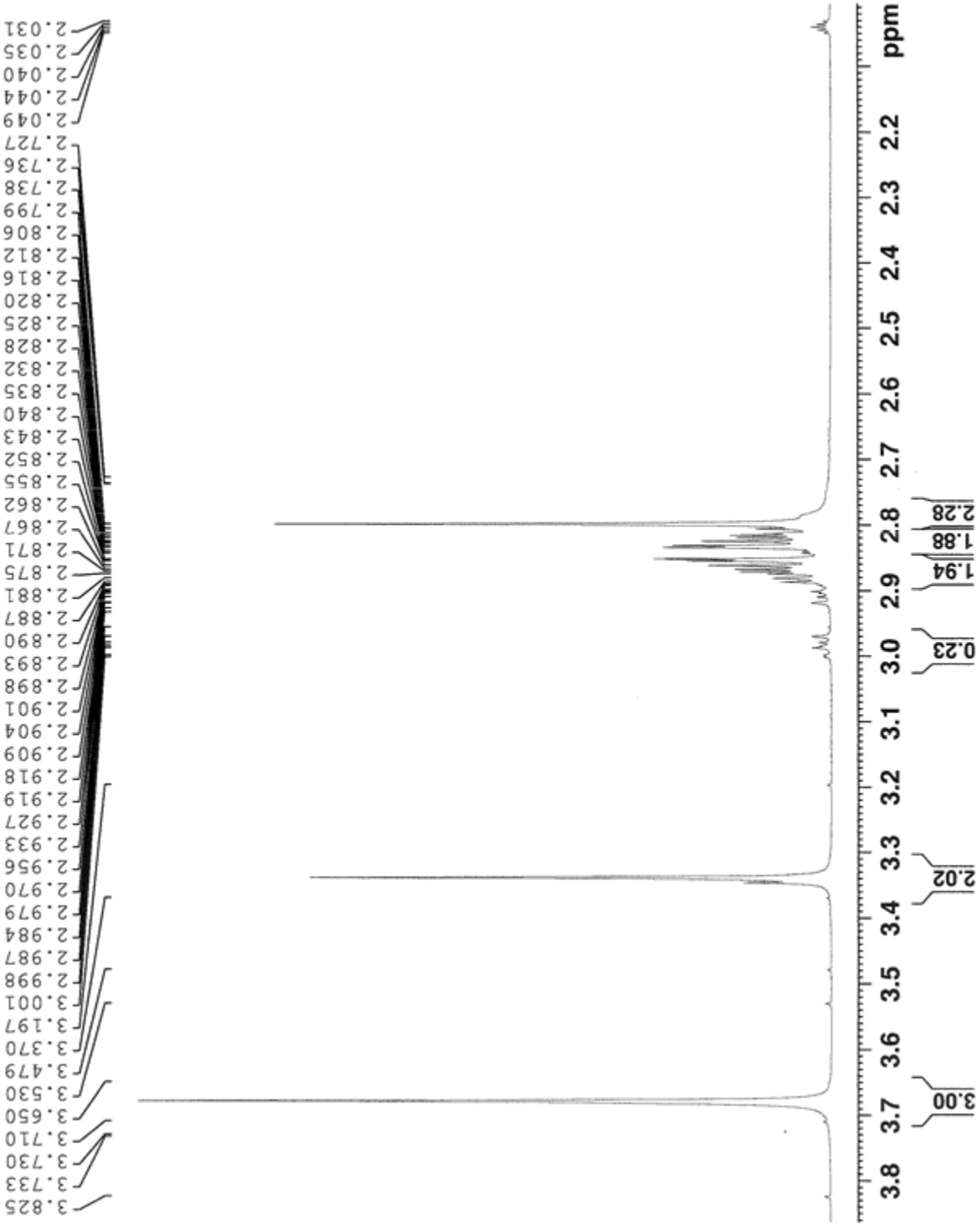

^{13}CNMR:

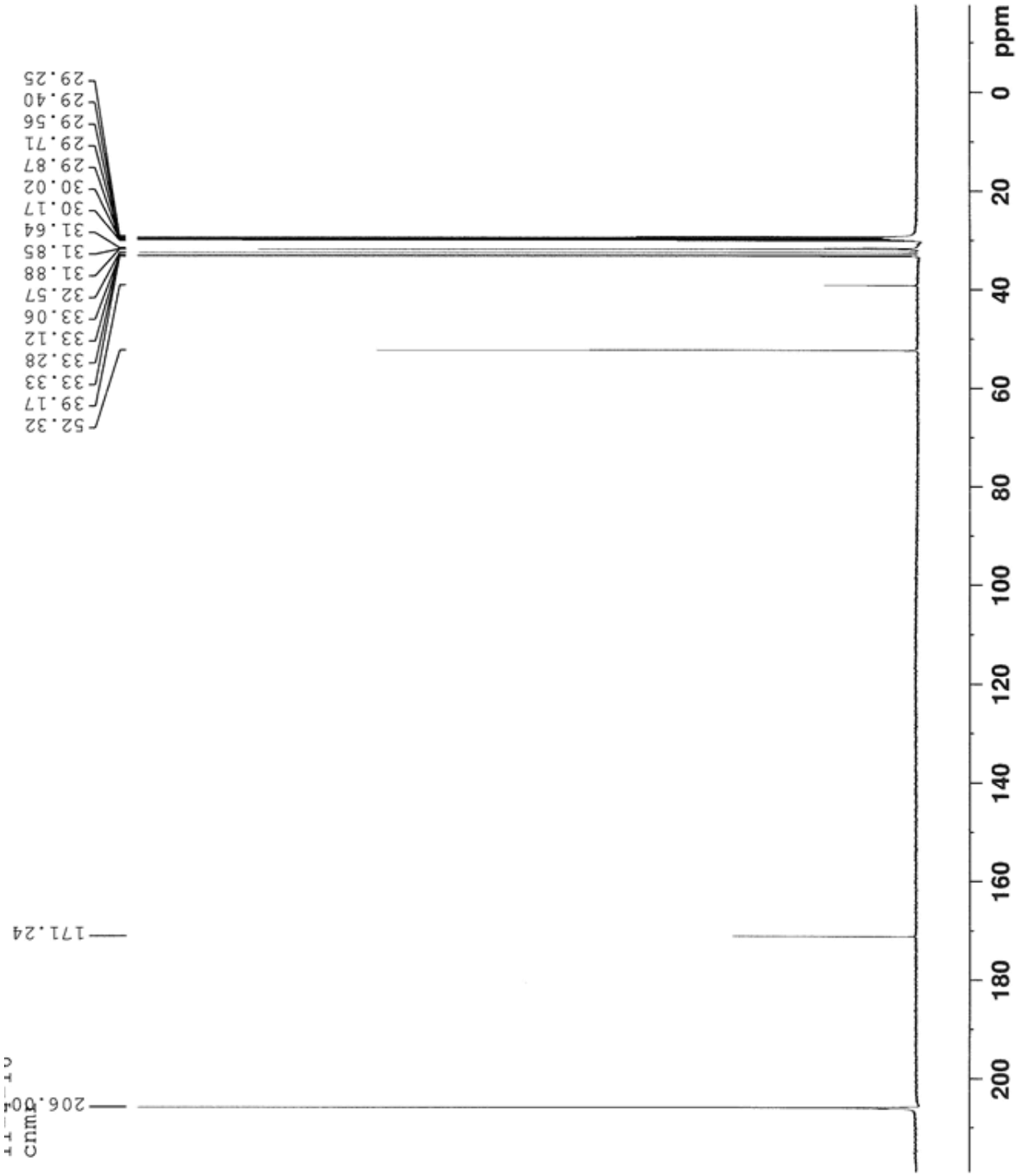
29.25
29.40
29.56
29.71
29.87
30.02
30.17
31.64
31.85
31.88
32.57
33.06
33.12
33.28
33.33
39.17
52.32
171.24
206.70
ppm
0
20
40
60
80
100
120
140
160
180
200

Rh(222-S_4-diAcOMe)Cl_2[Cl]

^{1}HNMR:

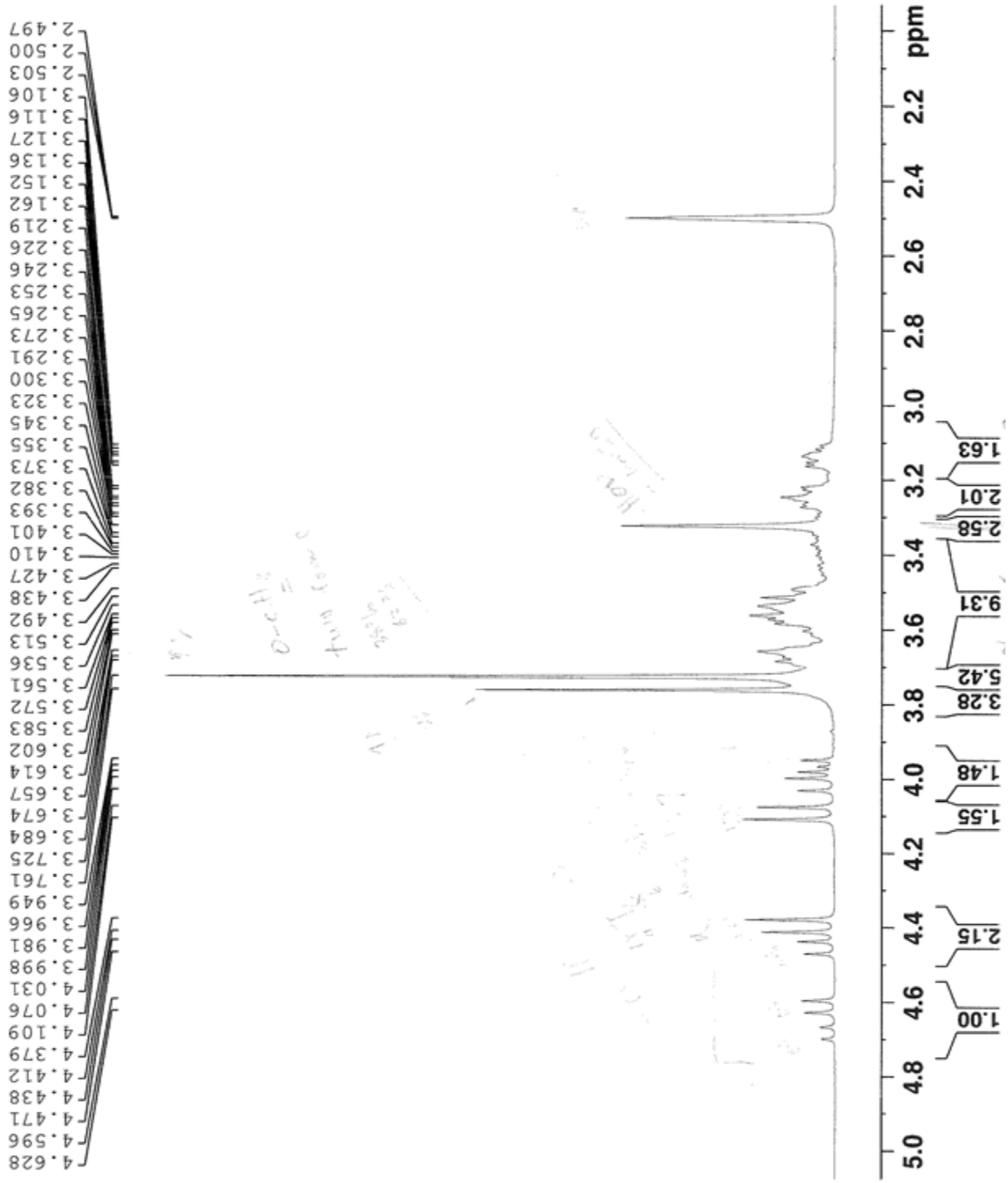

^{13}CNMR:

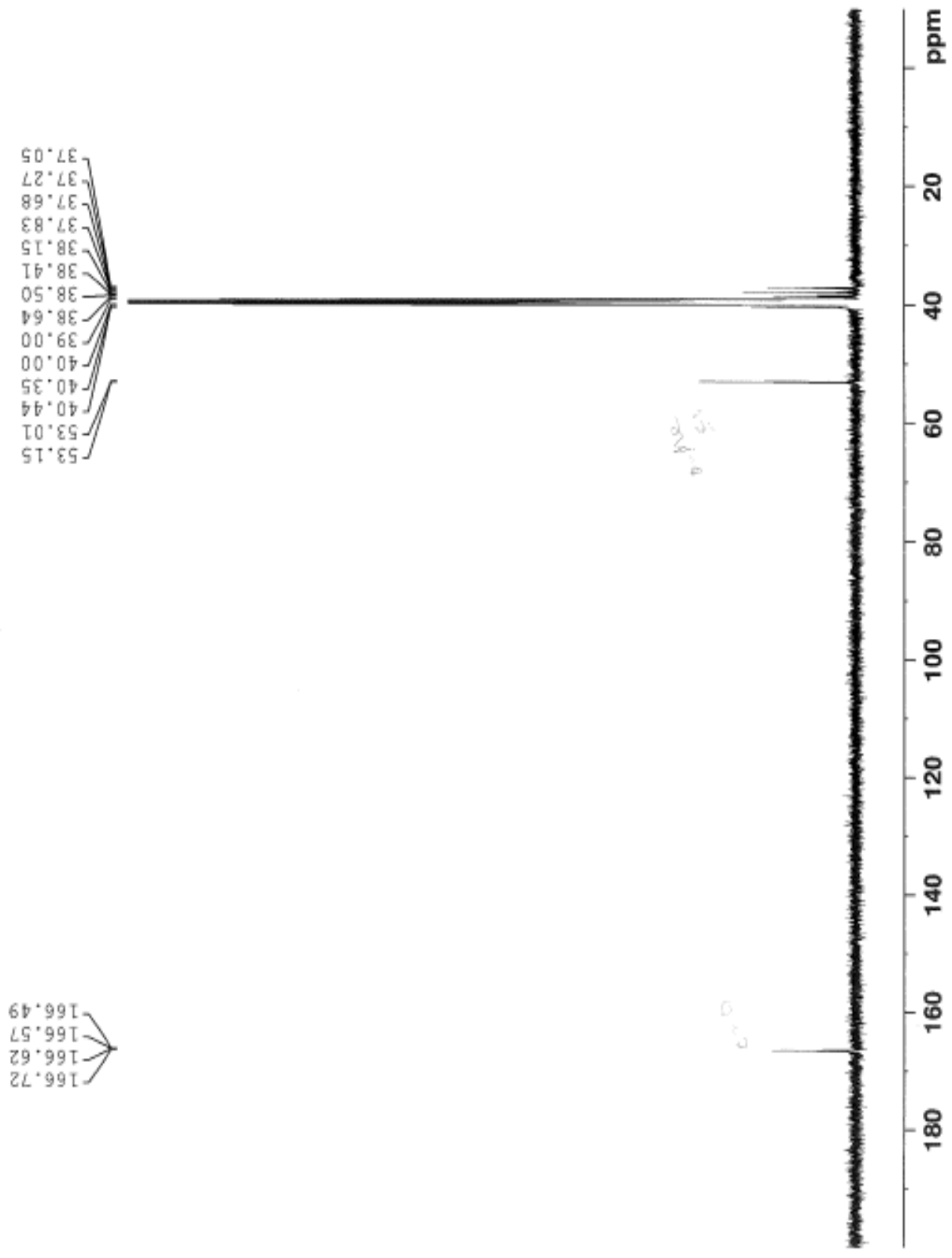
37.05
37.27
37.68
37.83
38.15
38.41
38.50
38.64
39.00
40.00
40.35
40.44
53.01
53.15
166.49
166.57
166.62
166.72
ppm
20
40
60
80
100
120
140
160
180

HPLC:

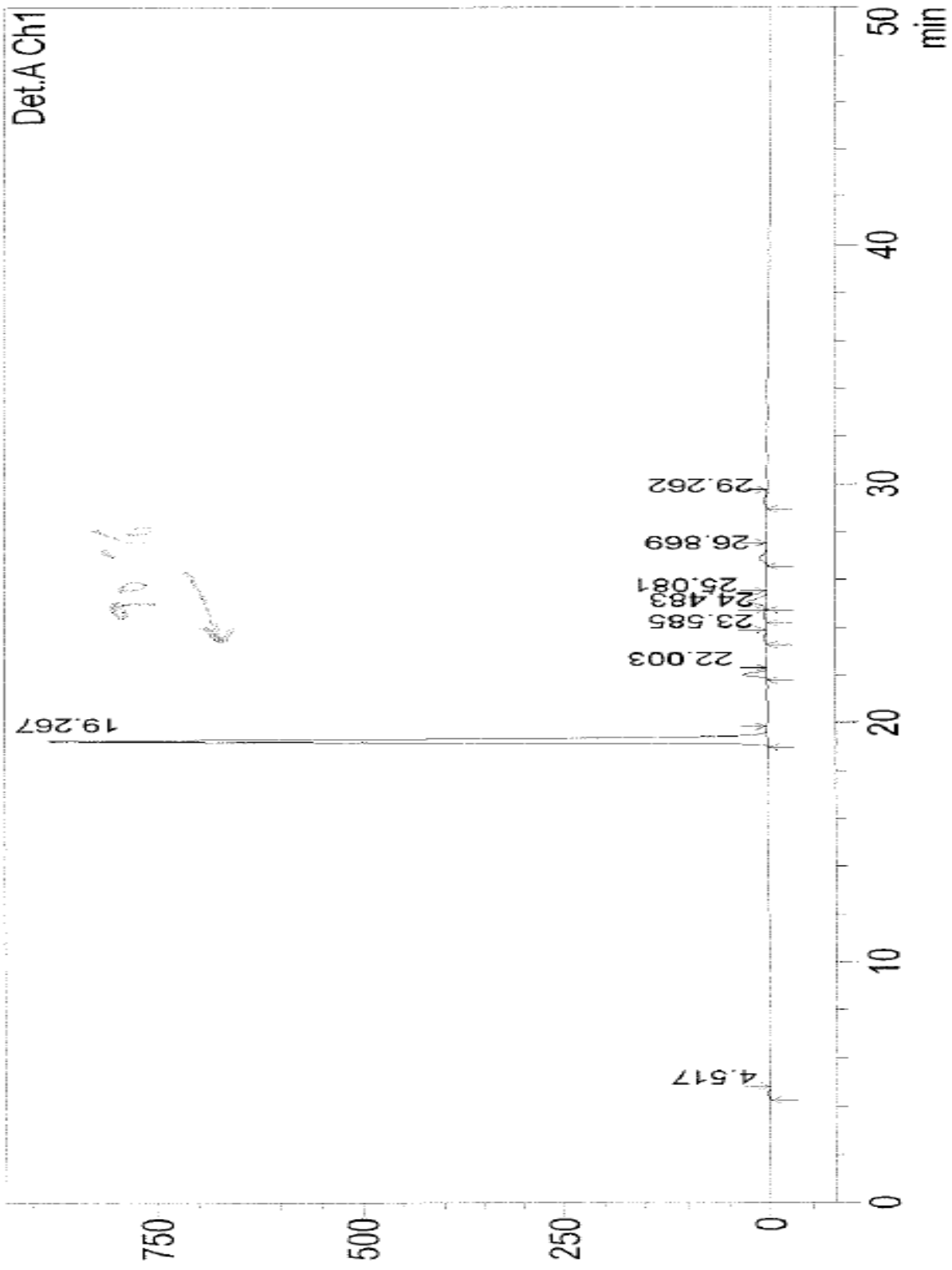
Det.A Ch1
750
500
250
0
0
10
20
30
40
50
min
4.517
19.267
22.003
23.585
24.483
25.081
26.869
29.262

Rh(222-S_4-diAcOMe)Cl_2[PF_6]

^{1}HNMR:

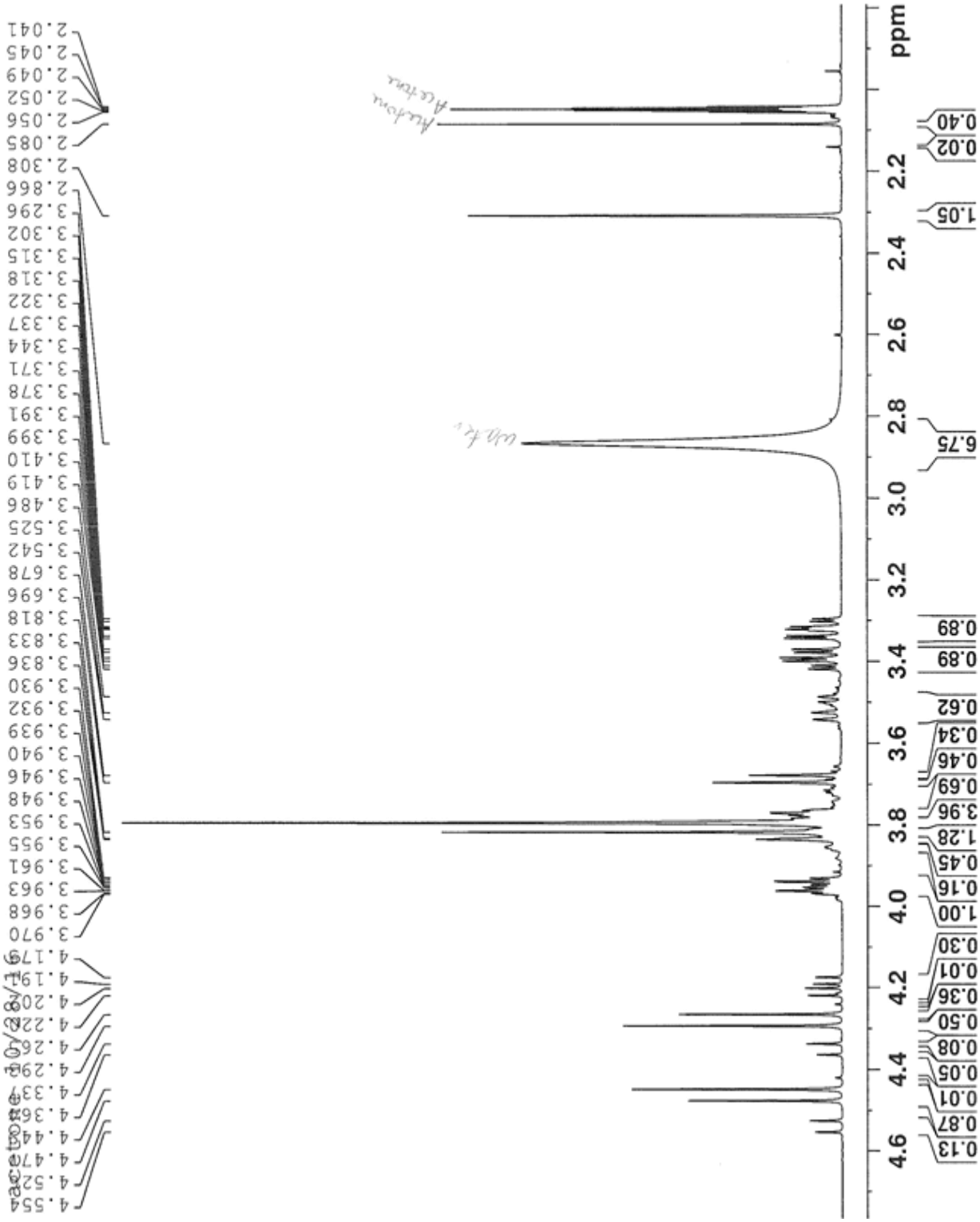

^{13}CNMR:

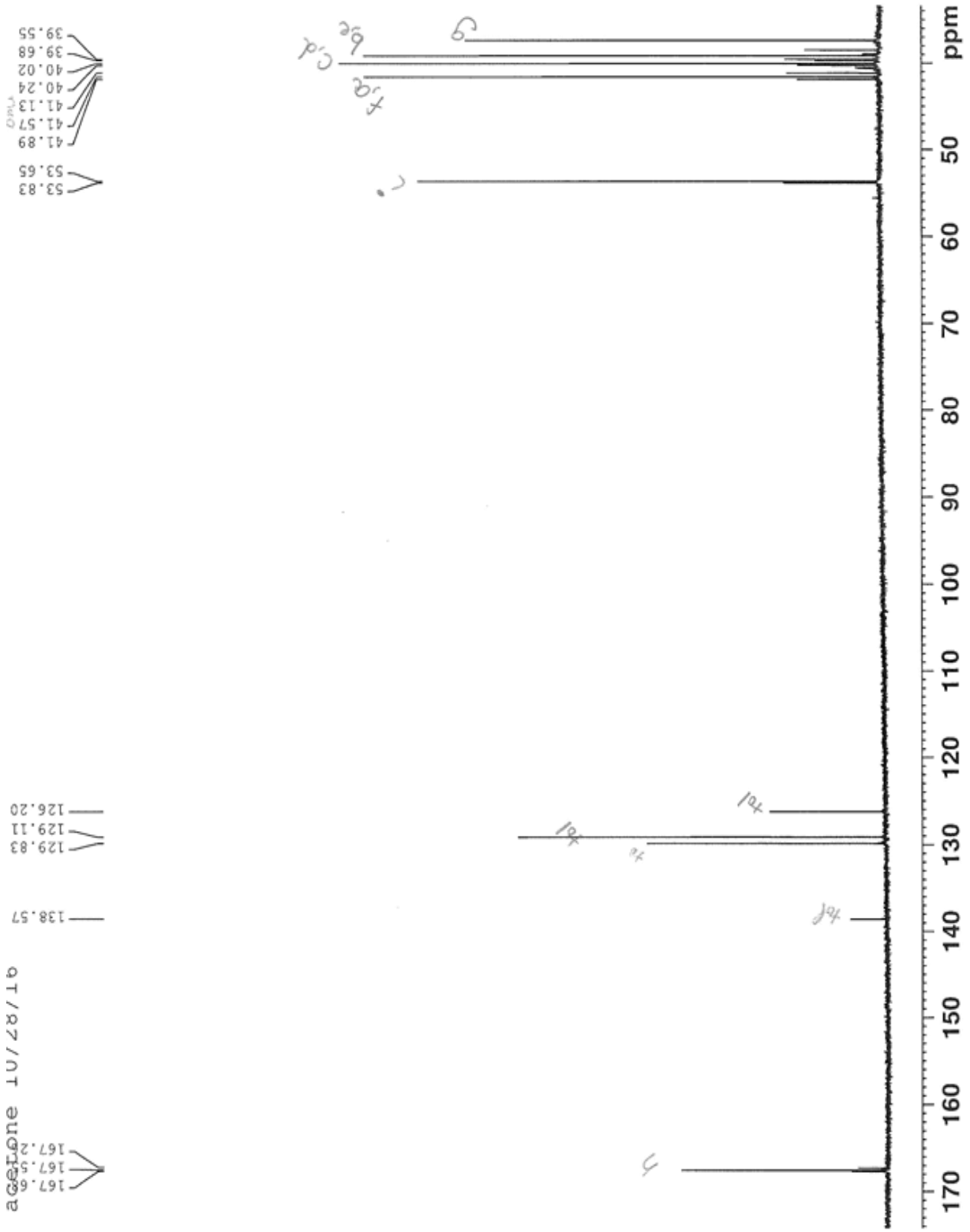
ppm
50
60
70
80
90
100
110
120
130
140
150
160
170
39.55
39.68
40.02
40.24
41.13
41.57
41.89
53.65
53.83
126.20
129.11
129.83
138.57
167.22
167.57
167.68
acetone

^{31}PNMR:

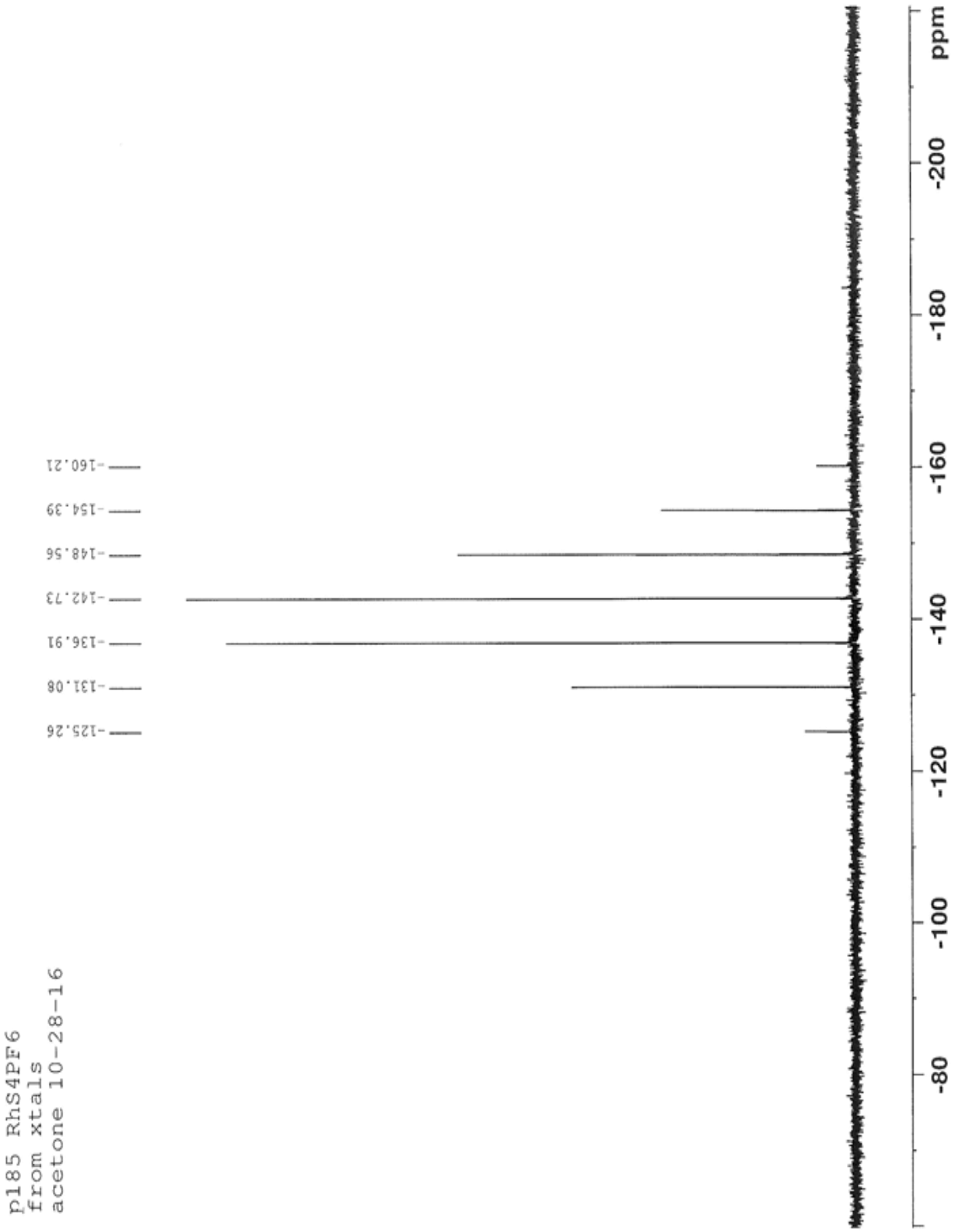
p185 RhS4PF6
from xtals
acetone 10-28-16
-125.26
-131.08
-136.91
-142.73
-148.56
-154.39
-160.21
-80
-100
-120
-140
-160
-180
-200
ppm

HPLC:

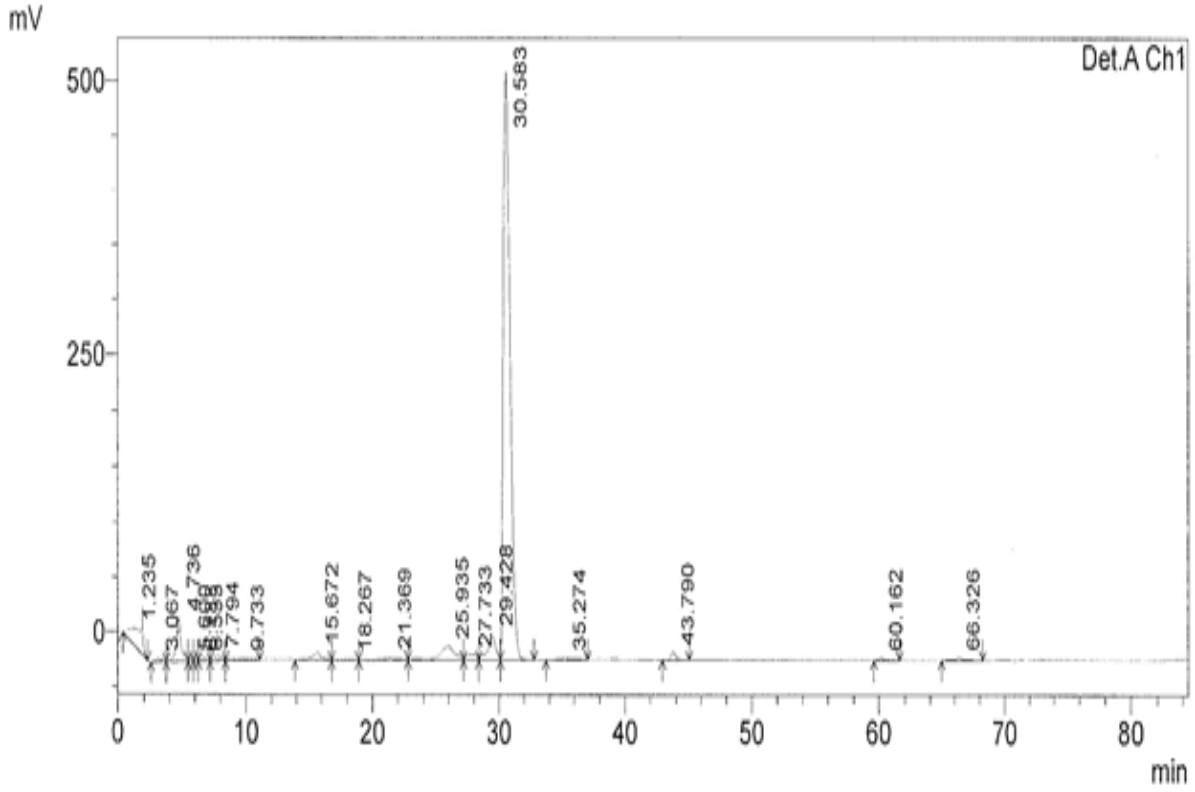
mV
Det.A Ch1
500
250
0
30.583
1.235
3.067
4.736
7.794
9.733
15.672
18.267
21.369
25.935
27.733
29.428
35.274
43.790
60.162
66.326
0
10
20
30
40
50
60
70
80
min

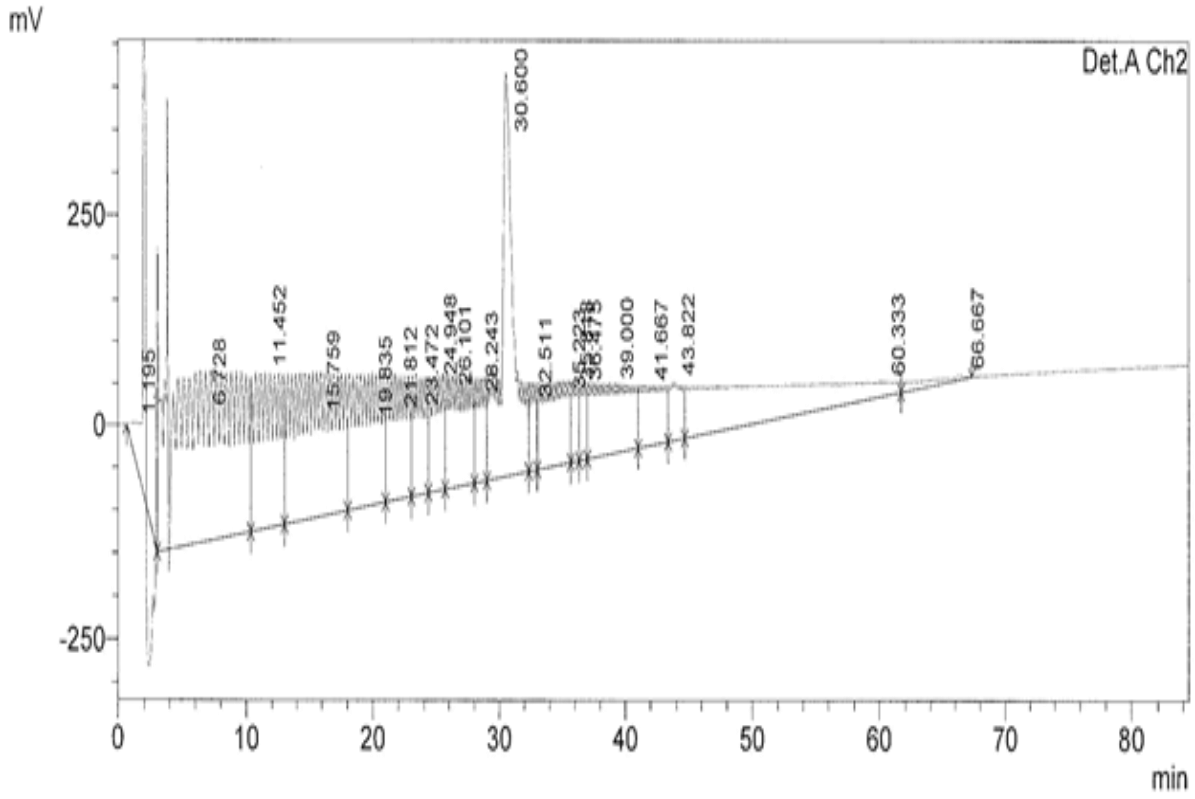
mV
Det.A Ch2
250
0
-250
30.600
1.195
6.728
11.452
15.759
19.835
21.812
23.472
24.948
26.101
28.243
32.511
39.000
41.667
43.822
60.333
66.667
0
10
20
30
40
50
60
70
80
min

LC-MS:

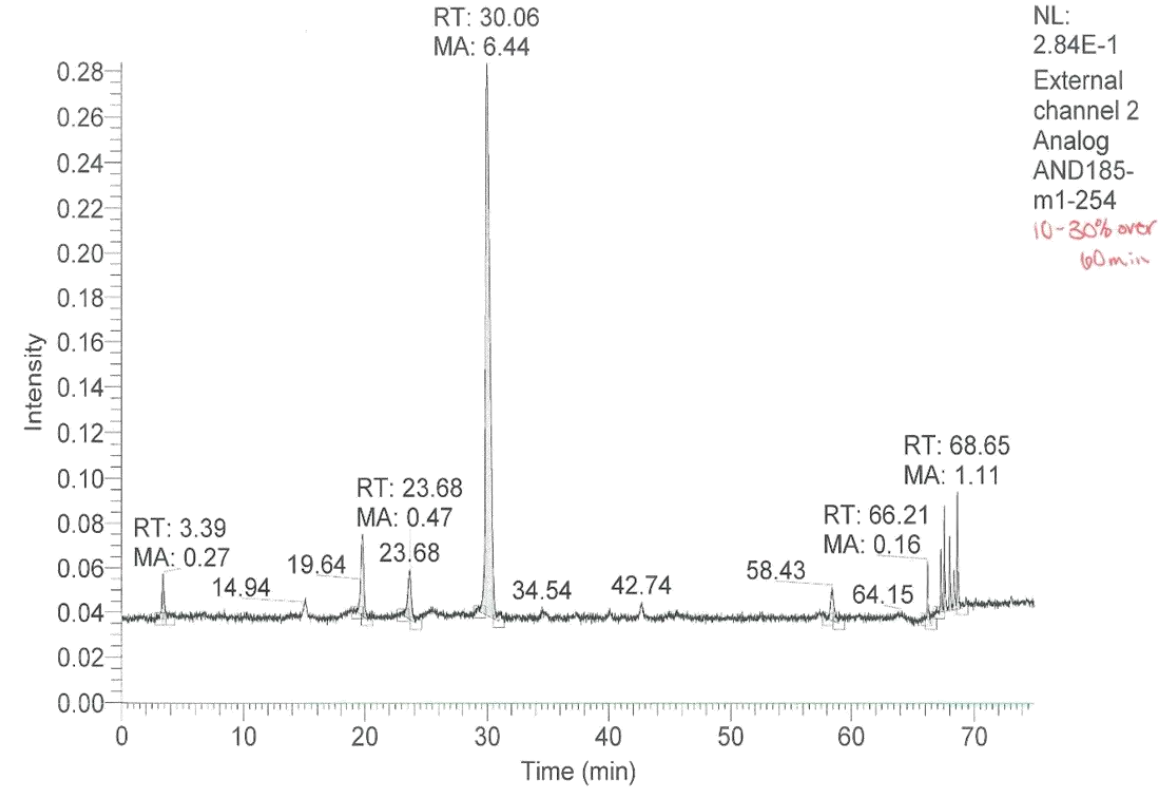
RT: 30.06
MA: 6.44
NL:
2.84E-1
External
channel 2
Analog
AND185-
m1-254
10-30% over
60 min
RT: 68.65
MA: 1.11
RT: 23.68
MA: 0.47
RT: 66.21
MA: 0.16
RT: 3.39
MA: 0.27
19.64
23.68
14.94
34.54
42.74
58.43
64.15
Intensity
Time (min)

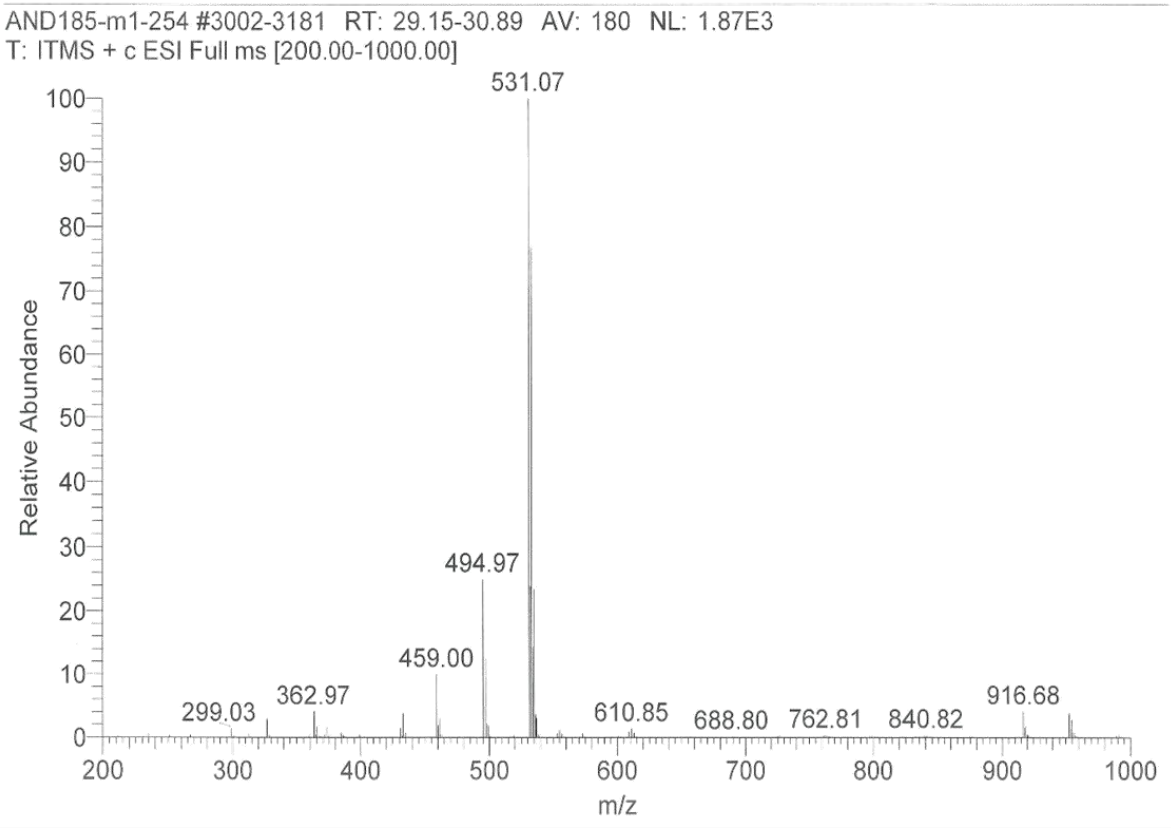
AND185-m1-254 #3002-3181 RT: 29.15-30.89 AV: 180 NL: 1.87E3
T: ITMS + c ESI Full ms [200.00-1000.00]
531.07
494.97
459.00
362.97
299.03
610.85
688.80
762.81
840.82
916.68
Relative Abundance
m/z

Crystal Data Information, Rh(222-S_4-diAcOMe)$Cl_2[PF_6]$:

data_AND185

audit_creation_method SHELXL-2014/7

shelx_SHELXL_version_number 2014/7

chemical_formula_moiety 'C12 H22 Cl2 45 P Rh S4, P F6, C3 H6 O'

chemical_formula_sum 'C15 H28 Cl2 F6 O5 P Rh S4'

exptl_crystal_description Needle

exptl_crystal_colour Yellow

diffrn_ambient_temperature 100(2)

chemical_formula_weight 735.39

space_group_crystal_system triclinic

space_group_IT_number 2

space_group_name_H-M_alt 'P -1'

space_group_name_Hall '-P 1'

cell_length_a 6.3098(3)

cell_length_b 13.1952(5)

cell_length_c 17.5540(7)

cell_angle_alpha 106.025(2)

cell_angle_beta 99.445(2)

cell_angle_gamma 102.093(2)

cell_volume 1334.71(10)

cell_formula_units_Z 2

cell_measurement_temperature 100(2)

cell_measurement_reflns_used 9886

cell_measurement_theta_min 2.7

cell_measurement_theta_max 72.0

exptl_crystal_density_diffrn 1.830

exptl_crystal_size_max 0.400

exptl_crystal_size_mid 0.050

exptl_crystal_size_min 0.020

exptl_absorpt_coefficient_mu 11.151

shelx_estimated_absorpt_T_min 0.095

shelx_estimated_absorpt_T_max 0.808

exptl_absorpt_correction_T_min 0.43

exptl_absorpt_correction_T_max 0.81

Select Bond Lengths and Angles:

Rh1 S2 2.2955(10)

Rh1 S3 2.3021(10)

Rh1 S1 2.3275(10)

Rh1 S4 2.3458(10)

Rh1 Cl1 2.3575(10)

Rh1 Cl2 2.3651(10)

S2 Rh1 S3 91.19(4)

S2 Rh1 S1 87.39(4)

S3 Rh1 S1 89.20(4)

S2 Rh1 S4 89.87(4)

S3 Rh1 S4 86.28(4)

S1 Rh1 S4 174.67(4)

S2 Rh1 Cl1 178.37(4)

S3 Rh1 Cl1 88.16(4)

S1 Rh1 Cl1 91.11(4)

S4 Rh1 Cl1 91.58(4)

S2 Rh1 Cl2 88.29(4)

S3 Rh1 Cl2 179.12(4)

S1 Rh1 Cl2 91.48(4)

S4 Rh1 Cl2 93.01(4)

Rh(222-S_4-diAcOH)Cl_2[Cl]

HPLC, Method 1:

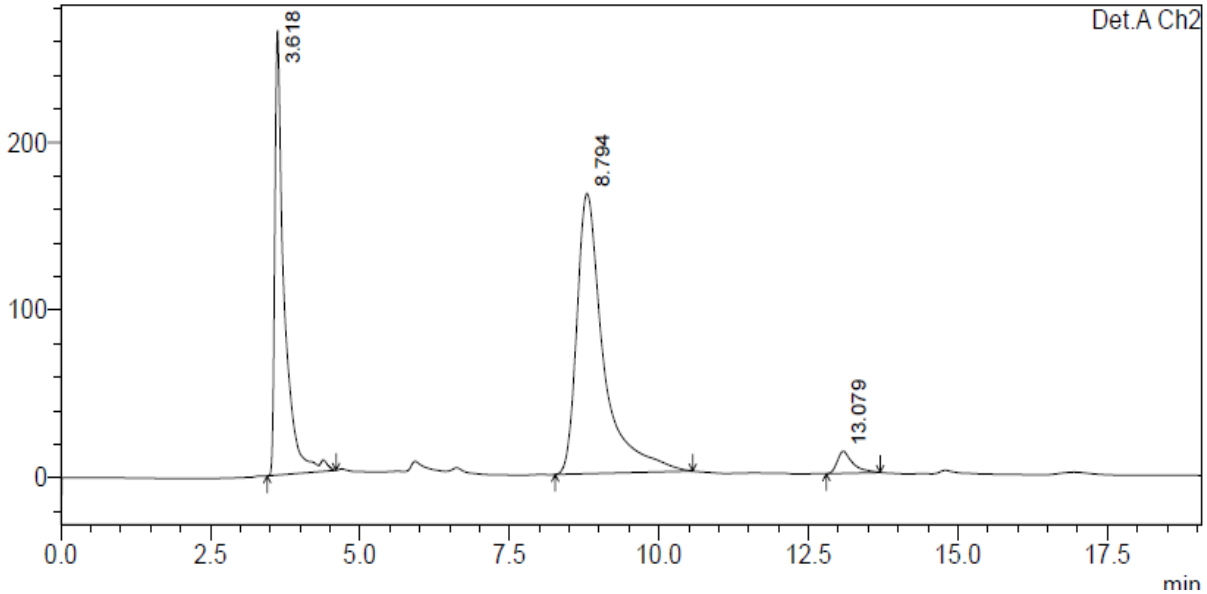

HPLC, Method 2:

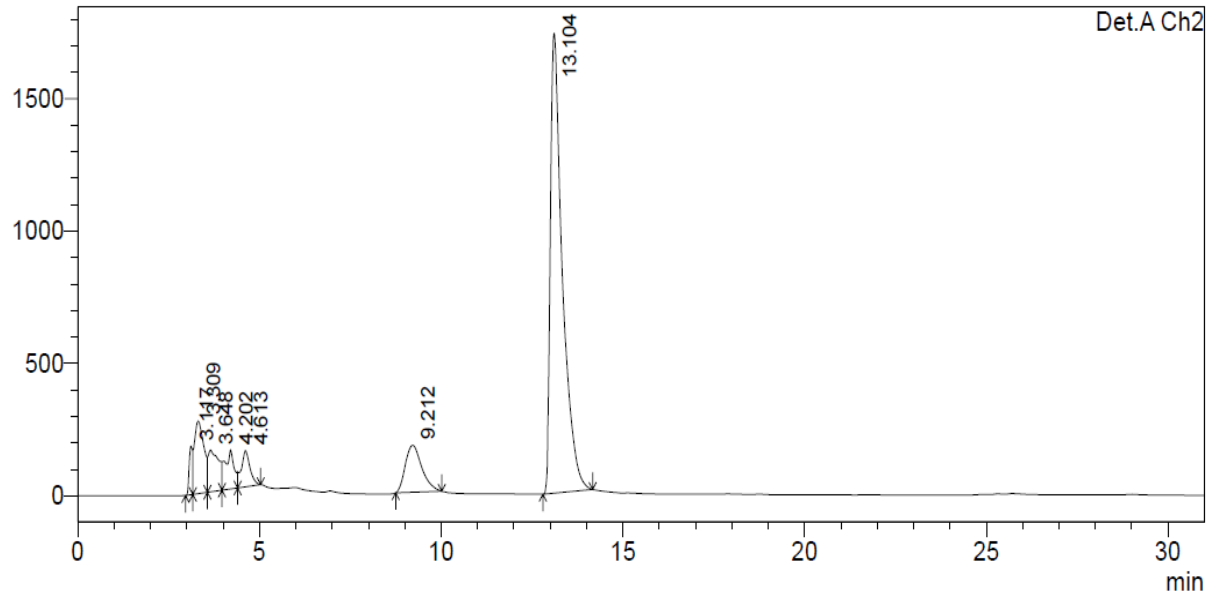

LC-MS, Method 1:

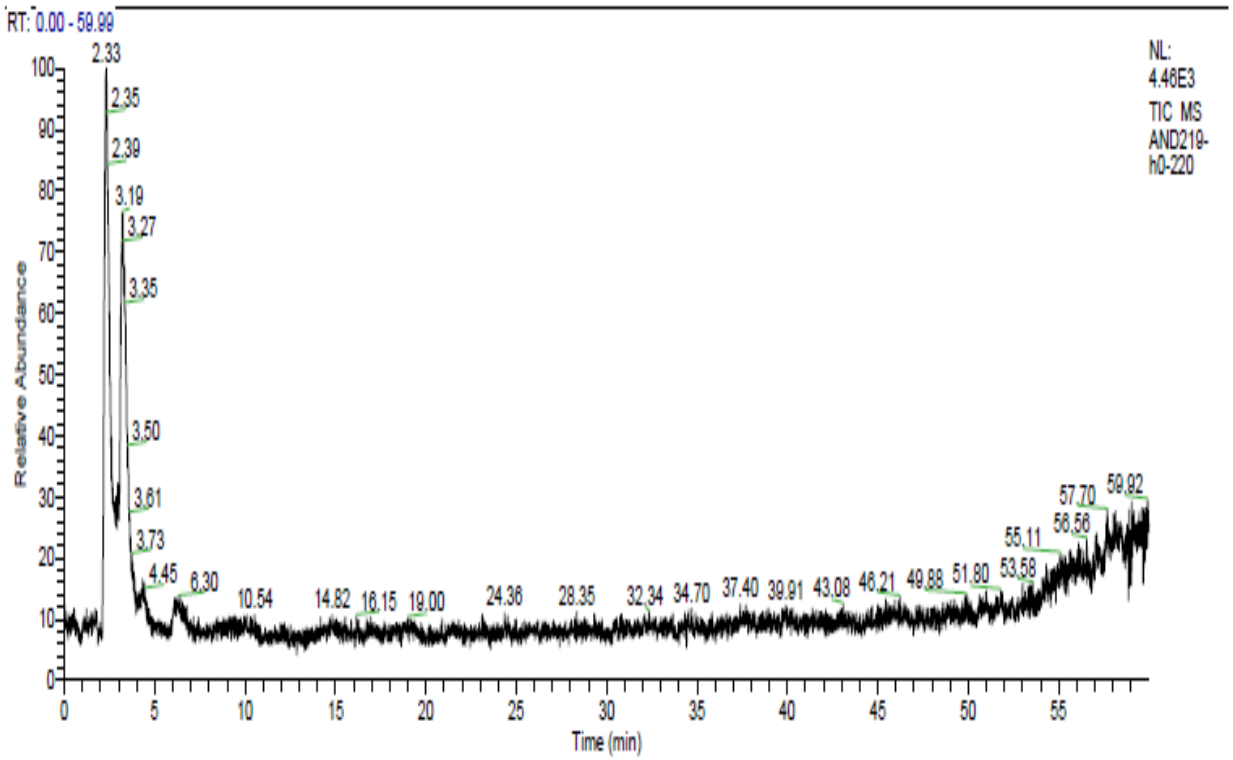

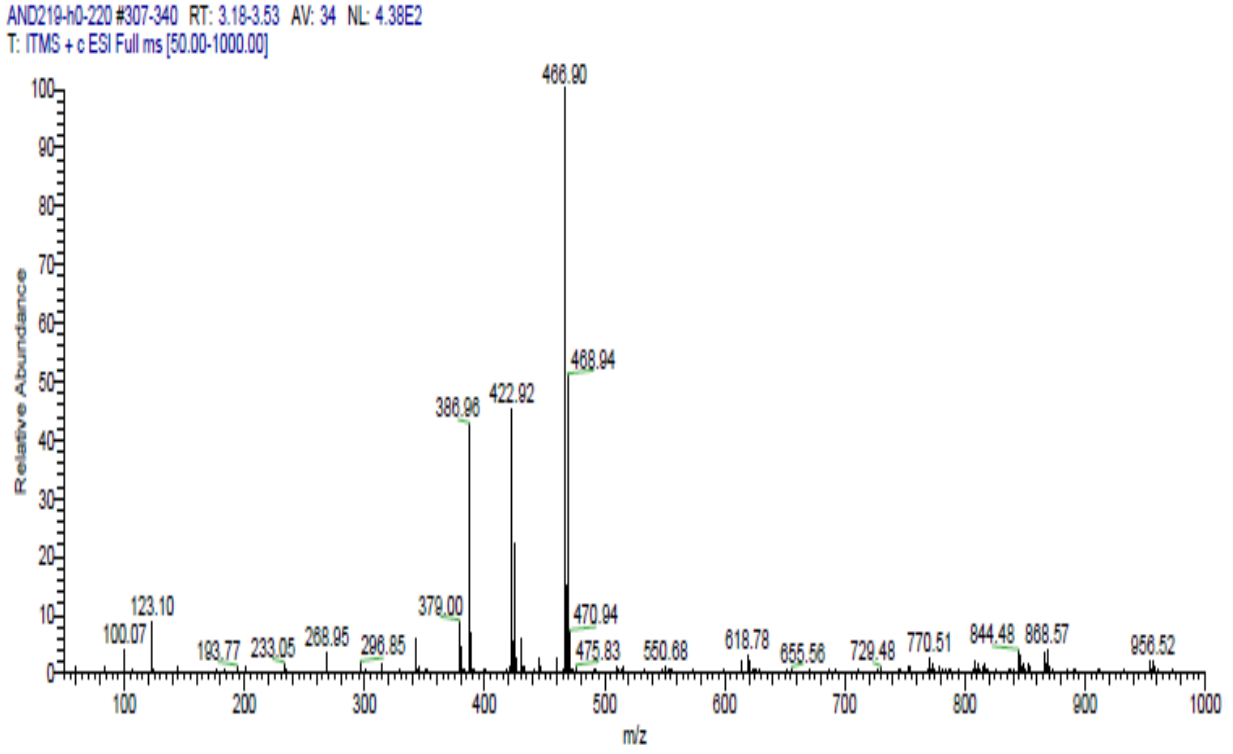

LC-MS, Method 2:

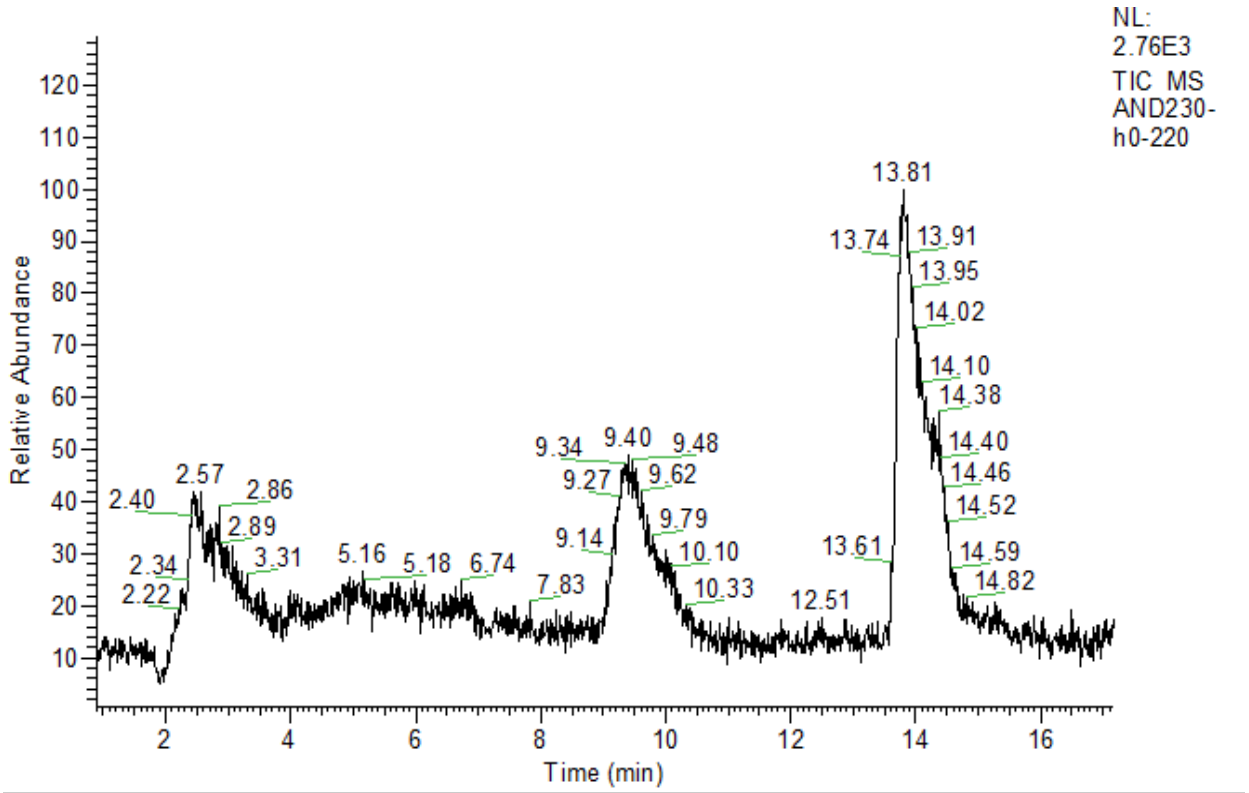

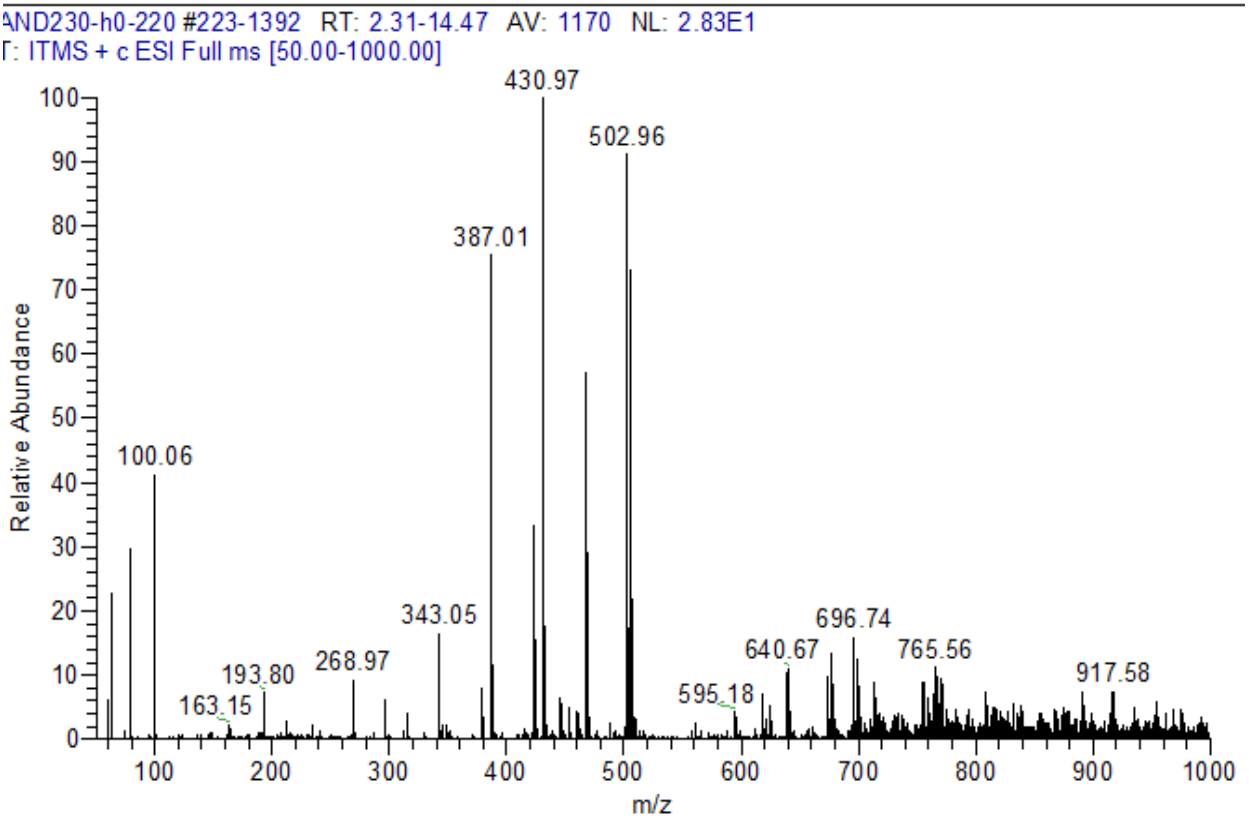

VITA

Ashley Nichole Dame was born to Lyndale and Margaret Dame in December 1988 in Lebanon, Missouri. She has one younger brother, Justin Dame, currently in Alaska. She graduated from Southwest Baptist University with a B.S. in Chemistry in 2010 and a M.S. in Inorganic Chemistry from the University of Missouri-Columbia. Ashley earned her PhD, in Radiochemistry, in the spring of 2017, under the direction of Dr. Silva Jurisson. She has taken a position at Oak Ridge National Lab (ORNL), working with the Nuclear Materials Processing Group within the Nuclear Security and Isotope Technology Division.